EXPLORING DESIGN STRATEGIES TO TUNE THE ELECTRONIC STRUCTURE AND ULTRAFAST DYNAMICS OF IRON(II) POLYPYRIDYL CHROMOPHORES

By

Lindsey Louise Jamula

A DISSERTATION

Submitted to
Michigan State University
in partial fulfillment of the requirements
for the degree of

Chemistry - Doctor of Philosophy

2013

ABSTRACT

EXPLORING DESIGN STRATEGIES TO TUNE THE ELECTRONIC STRUCTURE AND ULTRAFAST DYNAMICS OF IRON(II) POLYPYRIDYL CHROMOPHORES

By

Lindsey Louise Jamula

The overall goal of this research project is to develop low cost sensitizers for Dye-sensitized solar cells (DSSCs) by moving to first row transition metal-based chromophores, specifically iron(II) polypyridyl complexes. To be an effective sensitizer the MLCT state of a chromophore must be sufficiently long lived for injection into the semiconductor to occur. Unfortunately, iron(II) polypyridyl complexes intrinsically have short lived MLCT states due to ultrafast deactivation to lower lying ligand field states. The research has been developed to gain more understanding of the fundamental causes underlying the ultrafast processes. This study is highly collaborative within our group and the aim here has been along the synthetic front, providing the means through which we may begin to tackle this complicated problem.

Iron(II) polypyridyl complexes commonly possess a strained coordination environment through which orbital degeneracy is removed. The dense ligand field manifold that arises from the deviation from octahedral symmetry may be mediating the charge transfer to ligand field excited state deactivation. We set out to develop a highly symmetric iron(II) chromophore through which we may begin to investigate this theory. Our first efforts yielded a complex with a nearly perfect octahedral coordination environment that exhibits some exciting properties along with a significantly altered electronic structure.

A series of symmetric iron(II) polypyridyl complexes were prepared to evaluate the impact of symmetry and substituent effects on the electronic structure and the synthesis and characterization will be presented. We also made the first step toward implemeting such a chromophore in a DSSC by introducing anchoring groups to the periphery of the ligands through which it can bind to a metal oxide semiconductor. We have not yet developed a viable sensitizer for a TiO_2, however we have uncovered some promising possibilities and the future design strategies that are proposed that may bring us one step closer.

For my wonderful husband Michael

ACKNOWLEDGEMENTS

First of all I would like to thank my advisor Jim McCusker for all of the guidance and support he has provided throughout my graduate career. His enthusiasm for science is contagious and to be included amongst the talented scientists that make up the McCusker group has been a great pleasure. I would also like to thank my undergraduate advisor, Professor Sheila R. Smith at the University of Michigan-Dearborn, for her guidance and encouragement to pursue a graduate degree. She is an exceptional role model and presented a research opportunity that sparked my interest in inorganic chemistry and allowed me to develop the skills necessary to take on graduate research.

I would like to thank every member of the McCusker group, I am blessed to have had the opportunity to work with all of you. You have all contributed in some way to my success which I am grateful for, and consider you all friends and not just colleagues. Dong, thank you for sharing your synthetic expertise, your guidance has been invaluable. Allison, without your hard work and passion toward our concerted efforts, my project could not have gone anywhere. I am so very grateful for your friendship, support, and your talents that aided in our mutual success.

I would like to thank my entire family for their unwavering support and encouragement. I cannot put into words how important my family is to me and every bit of my success stems from their belief in me. Mom and Dad, you instilled the confidence in me to achieve anything I set out to do and I am so very grateful. Rob and Jessica, thanks for always looking out for your little sister and despite the fact that I now have more degrees than you, haha, I know my place in the hierarchy and will always look up

to the both of you. Granny, you are my role model and I strive to be as amazing as you are. Grandma and Grandpa, I could not have asked for better grandparents and I hope I make you proud.

To all of my extended family, I feel blessed to have all of you in my life. We cannot choose our relatives, however I somehow hit the jackpot with you and consider myself lucky to be part of this family. Speaking of luck, I also hit the jackpot when I met my husband. Mike, you have brought so much to my life, your love and support throughout this endeavor was essential and I appreciate you so much. You and Tyler Anne have brightened up my life enormously and I am so grateful for you both.

I want to acknowledge Brenda, my mentor and friend, for the great person you are and imparting your work ethic. Jenny, my oldest friend, for always being there through thick and thin. Lisa, my cohort in this prolonged adventure in graduate school, I could not have hung in there without you. You have become my closest friend and I am so appreciative for you. Rick, my friend and personal cupid, thank you for all of the fun outings and changing my life by introducing me to my husband. Kayla, a great friend who I can always count on. Drew, the most reliable person I have ever met, you are a great friend. Kate, Eileen, Jennie, Larry, Dani, Troy, Joel, Adam, Scott, and Brenna for all of the good times during, and after work that have made all these years in grad school bearable.

TABLE OF CONTENTS

LIST OF TABLES

LIST OF FIGURES

LIST OF SCHEMES

Chapter 1. Introduction to the Design of Iron(II)-Based Chromophores

1.1 Introduction

While global energy consumption is ever increasing, the world is failing to put the global energy system on a more sustainable path.[1] Society relies heavily on fossil fuels for our energy needs. 40% of energy consumption in the U.S. goes toward electric power production and with the current infrastructure in place and wide accessibility of coal, transitioning away from the current system will not be timely or easy.[2] The electric power sector also happens to be the leading source of CO_2 emissions in this country.[3] With increasing concerns over global climate change we must move toward renewable, carbon-neutral sources of energy. The sun is the most scalable among the available sources, providing enough energy in one day to supply the world's energy needs for one year.[4] Current photovoltaic technology is expensive and cannot compete cost effectively with fossil fuels, therefore solar energy lies at the bottom of the list of renewable energy sources in use today.

A cheaper alternative to the commercially available silicon based devices was developed in 1991 with the introduction of a nanocrystalline titanium dioxide (TiO_2) based dye-sensitized solar cell (DSSC) or Grätzel cell.[5] TiO_2 is a wide band gap semiconductor which cannot absorb or make use of visible light and is therefore sensitized with a chromophore chemically adsorbed to the surface. The TiO_2 based DSSC exhibited a 7% light harvesting efficiency. Dye-sensitization was not a new concept; the significant advance was the use of nanoparticles of TiO_2 which greatly increased the surface area of the semiconductor. The efficiency of single junction DSSCs

improved to approximately 11% where it has held steady for nearly twenty years, despite much efforts in research. Regardless of the low efficiency, the practicality of these devices lies in the prospect to utilize inexpensive materials for components of the cell.

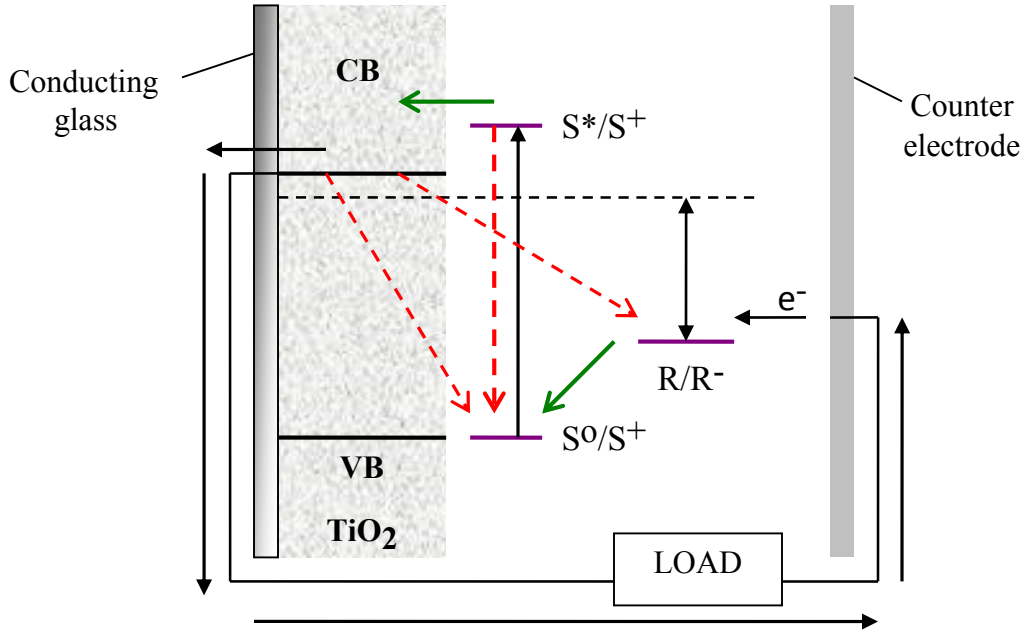

Figure 1-1. Diagram of the Grätzel cell. Green arrows represent forward processes that allow the cell to function regeneratively. The red dashed arrows represent processes that hinder cell function. For interpretation of the references to color in this and all other figures, the reader is referred to the electronic version of this dissertation.

The Grätzel cell is depicted in Figure 1-1. The chromophore is chemically bound to the TiO_2 semiconductor which is coated on an indium or fluorine doped tin oxide (FTO) substrate. Upon absorption of a photon, the sensitizer is promoted to an excited state that can inject an electron into the conduction band of TiO_2 causing the charge separation. Ideally, electrons will move through the nanocrystalline TiO_2 to the back contact and flow through the cell to the external load. Residual current will flow to the counter electrode then to the redox mediator in solution where it can re-reduce the

oxidized sensitizer. Unwanted processes also occur in the cell, such as charge recombination with the oxidized sensitizer or the redox couple.

A considerable amount of the research toward DSSC optimization has involved the sensitizer. The sensitizer must have high molar absorptivity in the solar spectrum and be able to bind strongly to the semiconductor. It must be able to undergo charge separation, with an excited state above the conduction band in order to inject an electron, and a low energy highest occupied molecular orbital (HOMO) to be reduced by the redox couple. The metal-to-ligand charge transfer (MLCT) excited states of d^6 coordination compounds, specifically ruthenium(II) polypyridyl chromophores, make them efficient for solar harvesting and sensitization of wide-bandgap semiconductors.[6] The "N3" and "black dye," shown in Figure 1-2, demonstrate good performance in DSSCs and highlight the charge separation capability of the dye. The polypyridyl ligands have low lying π^* molecular orbitals capable of accepting an electron upon excitation of the complex and the thiocyanates stabilize the charge on the ruthenium. The carboxylic acid group can form ester linkages to the TiO_2 resulting in strong binding with good electronic communication between the dye and semiconductor.

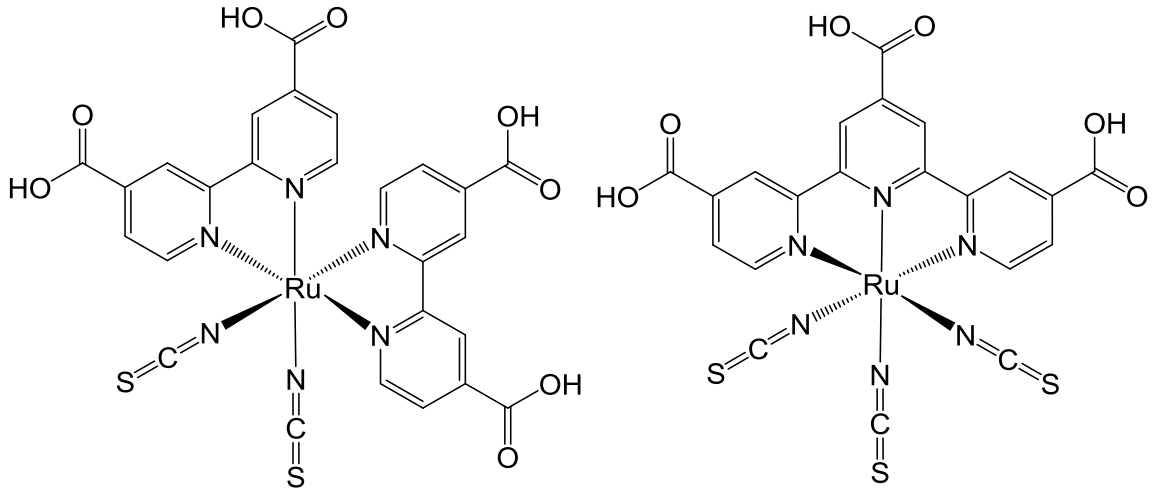

N3 **Black dye**

Figure 1-2. Structures of $[Ru(dcbpy)_2(NCS)_2]^{2+}$ (N3) and $[Ru(tcterpy)(NCS)_3]^{2+}$ (black dye).

The latest developments in structural design of ruthenium photosensitizers were recently reviewed.[7] The strategies employed are too numerous to describe here, but overall, variations on the standard N3 chromophore have led to much insight on achieving enhanced light absorption, extending absorption to the near-IR, enhancing stability, and the understanding of charge recombination. Despite the vast understanding gained, the best performing ruthenium chromophores to date are similar to the "Grätzel type" sensitizer.[8] Though these ruthenium chromophores have ideal properties for the sensitization of TiO_2, they are a costly component of the cell. Various alternatives have been investigated, including organic dyes, porphyrins, and phthalocyanines.[9] In 1998, Ferrere and Gregg reported the observation of a photocurrent from an iron(II) based chromophore, sparking our interest in an iron(II) sensitizer as an ideal substitute due to the abundance and low cost of first row metals.[10] The feasibility of utilizing such a chromophore is hindered by the intrinsic properties of first row transition metals.

Gaining a better understanding of the ultrafast relaxation dynamics of iron(II) complexes is critical to developing a viable chromophore for DSSCs. Moving away from ruthenium(II) based dyes may open the door to the replacement of another costly component of cell, the platinum counter electrode, by utilizing an alternate redox couple.

We know from ligand field theory that the d orbitals in a transition metal ion are degenerate. In the presence of an octahedral field, the d orbitals split into non-bonding (t_{2g}) and anti-bonding (e_g*) sets of orbitals. In second and third row transition metal complexes this octahedral splitting is large resulting in high energy anti-bonding orbitals regardless of the identity of the ligands. In first row transition metal complexes the octahedral splitting is not as great resulting in lower energy ligand field states that are more accessible, therefore the charge separation dynamics are much different.

In order to achieve a photocurrent in a DSSC, an excited state of a chromophore must lie above the conduction band of TiO_2 and must be sufficiently long lived for an electron to be injected into the semiconductor prior to relaxation to a lower lying state. In these ruthenium based chromophores, absorption of a photon results in a MLCT excited state; an electron is promoted from a metal based d orbital into a π* orbital of the ligand. As shown in Figure 1-3, the MLCT states are the lowest lying excited states, positioned above the conduction band of TiO_2, and are sufficiently long lived (ns) for injection to occur. In iron(II) complexes, photoexcitation results in promotion of an electron into an MLCT state followed by ultrafast relaxation into lower lying ligand field states and it is unclear as to whether efficient injection can occur.

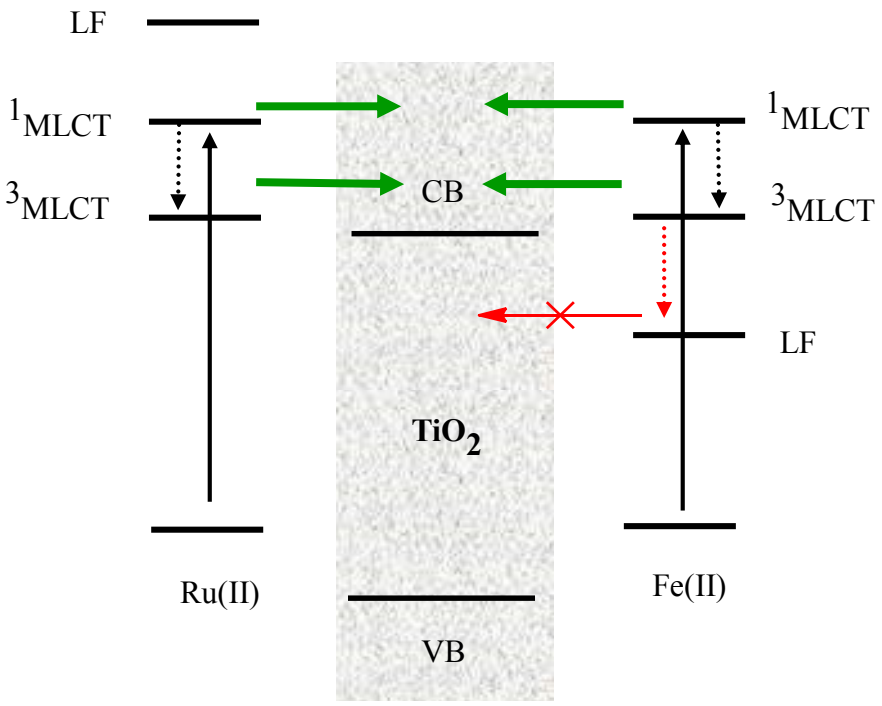

Figure 1-3. Representation of the excited states of the sensitizer and TiO_2.

The ligand field states in iron(II) complexes are metal based and thus have unfavorable electronic overlap with TiO_2, therefore injection from an upper lying excited state prior to any relaxation would be required. Lian and coworkers found evidence for electron injection from vibrationally hot excited states in ruthenium, iron, and rhenium complexes.[11] The focus of our research is to study the deactivation from the initially formed excited state in iron(II) complexes with the overall intention of slowing down the relaxation process to promote injection.

1.2 Relaxation Dynamics of Iron(II) Complexes

As mentioned above, we know from ligand field theory that the d orbitals in a transition metal ion are degenerate. In the presence of an octahedral field, the d orbitals

split into non-bonding (t_{2g}) and anti-bonding (e_g*) sets of orbitals. For d^4-d^7 first row transition metal ions, oxidation state of the metal and the ligand field strength will determine the ground state. In the presence of a strong ligand field, octahedral splitting is large and the low energy conformation is achieved by pairing spins, while in the presence of a weak field ligand, the high spin state is lower in energy. Iron(II) polypyridyls, such as tris(2,2'-bipyridine)iron(II) and bis(2,2':6',2"-terpyridine)-iron(II) complexes are approximated as possessing octahedral symmetry and exist in the low spin $^1A_1$ state, where there are six electrons in the t_{2g} nonbonding orbitals. In the $^5T_2$ high spin state, there are four electrons in the t_{2g} nonbonding orbitals and two in the e_g* σ-antibonding orbitals. The formation of the $^5T_2$ state is accompanied by a 0.2 Å elongation of the Fe-N bond. The occupancy of the $^1A_1$ and $^5T_2$ states are shown in Figure 1-4, along with a typical energy level diagram of octahedral iron(II) complexes. The diagram is general to the family of iron(II)-based systems with the ordering of the ligand field states as calculated from the Tanabe-Sugano diagram for d^6 octahedral complexes and is not quantitative with absolute energies.

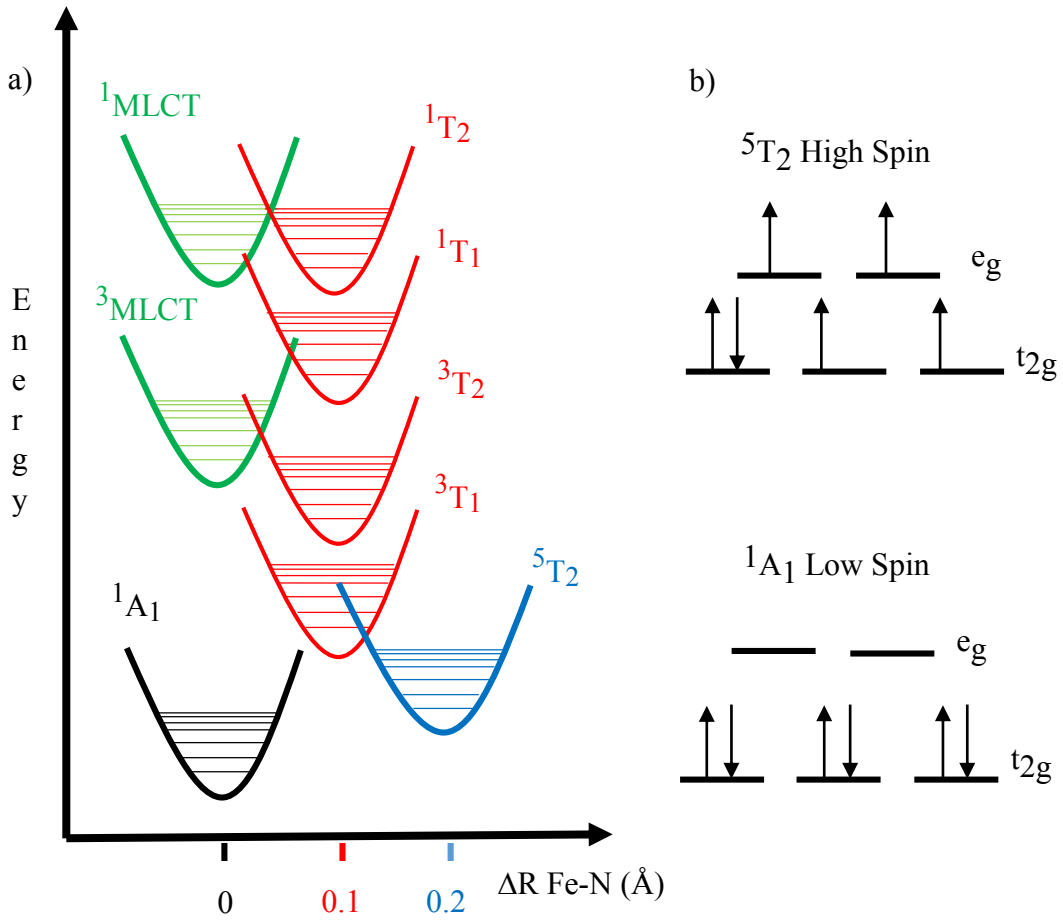

Figure 1-4. a) Typical potential energy level diagram of Fe(II) based complexes (adapted from reference 12 and references therein).[12] b) Occupancy of the ligand field split d orbitals in iron(II) complexes.

Iron(II) polypyridyls have been widely investigated chemically and photophysically. It is well established that upon photoexcitation, the low spin complex undergoes a metal to ligand charge transfer, followed by ultrafast deactivation to a long lived ligand field state. It has been shown that this long lived ligand field state is the $^5T_2$ state and ultrafast electronic absorption measurements reveal sub-picosecond dynamics associated with the formation of the $^5T_2$ state.[13] Further work using stimulated resonance Raman and femtosecond transient absorption experimentally verified that the

$^5T_2$ state is established in 200 fs.[14] The mechanism for the rapid conversion ($\Delta S = 2$) was thought to proceed via $^1A_1 \rightarrow {}^1MLCT \rightarrow {}^5T_2$. It has also been determined that rapid deactivation from the charge-transfer manifold occurs in less than 100 fs, which appears to be characteristic of the whole class of low spin iron(II) polypyridyl complexes.[15] Due to the short time scale, the mechanism mediating the deactivation to the transient $^5T_2$ state is still unclear. Much more is known about the conversion from the long lived excited state to ground state since the ligand field excited state lasts for hundreds of picoseconds to hundreds of nanoseconds, depending on the ligands. Also, the dynamics of iron(II) spin-crossover complexes have received a lot of attention in recent years, with much interest stemming from potential applications in molecular switches and display devices.[16–18]

Ultrafast optical studies by Chergui and coworkers have provided important mechanistic information on the excited state evolution of tris(2,2'-bipyridine)-iron(II).[12,19,20] The observation of two distinct emission features, along with other evidence, allowed them to conclude that the first event is ultrafast intersystem-crossing (ISC) from the ^1MLCT to the ^3MLCT (<30 fs) with strong mixing between the ^1MLCT and ^3MLCT states, followed by ISC to the $^5T_2$ state. A computational study by de Graaf et al. provided additional evidence for their findings from the analysis of the energy dependence of electronic states on the changes in geometry associated with the LS-HS spin state conversion.[21] Consequently, the currently recognized mechanism of excited state evolution for iron(II) polypyridyls is $^1A_1 \rightarrow {}^1MLCT \rightarrow {}^3MLCT \rightarrow {}^5T_2$.

1.3 Design Strategies Toward the Development of Iron(II)-Based Sensitizers

As mentioned above, a photocurrent has been observed from and iron(II)-based chromophore, specifically $[Fe(dcpby)_2(CN)_2]$ (Fe(2,2'-bipyridine-4,4'-dicarboxylic acid)$_2(CN)_2$).[10] As with other iron(II) polypyridyls, upon photoexcitation to a charge transfer state it undergoes ultrafast relaxation (<100 fs) to the long lived ligand field state that is localized on the metal. Electron injection is not possible from this ligand field state as there is unfavorable overlap and it lies below the conduction band of TiO_2.[11] Injection had to be occurring from an initially formed MCLT state and the quantum yield for injection was determined to be ~12% following excitation into the low energy charge transfer band.[22] We can think about this injection efficiency in terms of a competition of rates: the rate of injection versus rate of relaxation. Therefore, there are two approaches we could take toward developing a viable iron(II) sensitizer: 1) speed up the electron injection process, or 2) slow down the relaxation process.

The first approach is quite a tall order, as it seems that conditions are just right to promote injection. In $Fe(dcpby)_2(CN)_2$, the carboxylate anchoring groups are electron withdrawing and are located in the 4-position of the dye, which is along the transition dipole which should mediate the electron transfer process. Furthermore, carboxylate groups provide good electronic communication with the TiO_2 since there is orbital overlap between the extended π system of the carboxylate and the d orbitals of titanium. Recent theoretical work by Jakubikova and coworkers has shown that injection from this specific molecule will vary depending on the binding mode, but ranges between 0.3-7.3 ps through a carboxylate linker.[23] It is possible that alternate anchoring groups could decrease this rate, however we believed we had better chances taking on the second

approach of slowing down the relaxation rate, which has taken us down two distinct paths.

Our initial approach to investigate the mechanism of the ^{1}MLCT $\rightarrow$ $^5T_2$ deactivation was inspired by what is known for the $^1A_1 \leftrightarrow {}^5T_2$ spin state interconversion. It is well known that population of e_g* σ-antibonding orbitals results in an increase in metal – ligand bond length when a complex converts from the $^1A_1$ to the $^5T_2$ state. This observation leads to the possibility that spin state interconversion is coupled to the vibrational modes of the complex. The hypothesis originated from the work by Purcell and Vanquickenborne who established a connection between enantiomerization of d^6 complexes and spin state interconversion.[24,25] McCusker et al. proposed that torsional modes play an essential role in the kinetics of spin state interconversion between $^5T_2 \leftrightarrow {}^1A_1$ states and found evidence that suggests there is a correlation.[26] In attempts to determine a deactivating coordinate of the MLCT excited state, we set out to investigate the extent to which a torsional coordinate might modulate MLCT to ligand field kinetics by introducing steric bulk to the terminal rings of 2,2':6',2"-terpyridine (terpy) and preparing the bis-tridentate iron(II) complexes.[27] The terpy series yielded a lot of information on the correlation between charge transfer deactivation and ground state recovery, but did not significantly slow the charge transfer deactivation, therefore we set out on an alternative strategy.[28]

In general, iron(II) polypyridyls are approximated to possess octahedral symmetry, while in reality the ligand environments are commonly strained, reducing the coordination symmetry. Research from our collaborative efforts with Huse and coworkers has shown that varying chemical composition and ligand–field symmetry

influence the valence charge density of ground and excited states.[29–31] Symmetry effects could also influence the ultrafast dynamics of the charge transfer deactivation. Deviation from octahedral symmetry will remove the orbital degeneracy and increase the number of states shown in the energy diagram in Figure 1-4, and the increased density of states may be mediating the ultrafast relaxation. In an effort to minimize the number of these state that we believe to be mediating the deactivation, the goal of the present investigation was to introduce a more symmetrical coordination environment to an iron(II) center.

Most of the work presented herein stems from the second strategy, on moving toward a more symmetrical environment we stumbled on a molecule with some exciting properties. The symmetric coordination environment did not yield the anticipated effect of slowing down the charge transfer deactivation process, however it appeared to effect significant changes to the electronic structure. This observation led us down a new path of examining ways to tune the electronic structure even further through synthetic modification of the ligand system. There is a chance that this new system has presented us with the opportunity to make a first row transition metal complex behave more like a second row metal complex, which would have major implications for use in DSSCs. We have also taken the next step toward implementation of an iron(II)-based chromophore into a DSSC by installing anchoring groups to this new system.

Though much of our efforts have been focused on this new, ever evolving strategy, we have not abandoned our original approach of investigating vibrational modes. Following up on the terpy series, which involved one torsional coordinate, we were interested in locking the complex in a rigid ligand framework to minimize all movement: the torsional modes as well as the known Fe-N bond elongation that

accompanies the charge transfer to ligand field transition. In the last chapter I will introduce our current work along this front based on Lehn-type cryptand ligand systems.[32,33]

1.4 Contents of Dissertation

The focus of the research described in this dissertation involves the design, synthesis, and characterization of a series of highly symmetrical iron(II) polypyridyl complexes for the analysis of the influence of coordination environment and substituent effects on the electronic structure. Chapter 2 presents the preparation of a new iron(II) complex possessing nearly perfect octahedral symmetry. The interesting coordination chemistry of the highly versatile carbonyl bridged ligand is highlighted and discussed in detail. The new complex possesses some very exciting properties which are examined through a comparison with two pseudo-octahedral complexes. Design and synthetic efforts toward the preparation of an isostructural control molecule are also discussed.

Chapter 3 introduces the design of two additional symmetric iron(II) complexes. We set out to replace the carbonyl bridges with alternate functional groups in order to investigate whether the interesting properties discussed in Chapter 2 arise from the symmetrical geometry or from inductive effects from the bridging groups of the ligand. The development of the synthesis of the ligands and corresponding iron(II) complexes is discussed.

Chapter 4 lays the groundwork for an investigation into determining ways to effectively tune the energetics of the excited states of these new symmetric iron(II) complexes. The design of a series of molecules in which substituents are introduced to the periphery of the ligands in an effort to modulate the physical properties will be

presented. The first of this new series has been successfully prepared and will be discussed.

Chapter 5 moves the discussion away from the fundamentals from the previous chapters and moves toward the overall application of the new iron(II) chromophores. This section details the installation of anchoring groups through which these new chromophores may bind to a semiconductor. As a starting point we have successfully introduced the most commonly employed carboxylate anchoring group to our new ligand system and the synthesis and characterization will be discussed. A survey of other functional groups that may be utilized, along with proposed synthetic methods toward their development will be presented.

Chapter 6 introduces a new system that we have just begun to investigate. As a follow up to the study of the correlation of torsional modes with ultrafast deactivation that was described in my Masters Thesis, we set out to design iron(II) polypyridyl complexes with fixed cage ligand structures.[27] A Lehn-type cryptand was employed to prepare a tri-nuclear assembly which may possess interesting redox properties and the synthesis and preliminary characterization will be presented.

REFERENCES

REFERENCES

(1) International Energy Agency *World Energy Outlook, Executive Summary*; 2012.

(2) U.S. Energy Information Administration *Annual Energy Review*; 2012.

(3) Environmental Protection Agency *Inventory of U.S. Greenhouse Gas Emissions and Sinks: 1990-2011*; 2013.

(4) *Report of the Basic Energy Sciences Workshop on Solar Energy Utilization*; Department of Energy: Washington DC, 2005.

(5) O'Regan, B.; Grätzel, M. *Nature* **1991**, *353*, 737–740.

(6) Ardo, S.; Meyer, G. J. *Chemical Society Reviews* **2009**, *38*, 115–64.

(7) Yin, J.-F.; Velayudham, M.; Bhattacharya, D.; Lin, H.-C.; Lu, K.-L. *Coordination Chemistry Reviews* **2012**, *256*, 3008–3035.

(8) Nazeeruddin, M. K.; Kay, A.; Miiller, E.; Liska, P.; Vlachopoulos, N.; Gratzel, M.; Lausanne, C.-; April, R. **1993**, *115*, 6382–6390.

(9) Clifford, J. N.; Martínez-Ferrero, E.; Viterisi, A.; Palomares, E. *Chemical Society Reviews* **2011**, *40*, 1635–46.

(10) Ferrere, S.; Gregg, B. A. *Journal of the American Chemical Society* **1998**, *120*, 843–844.

(11) Asbury, J. B.; Wang, Y.-Q.; Hao, E.; Ghosh, H. N.; Lian, T. *Research on Chemical Intermediates* **2001**, *27*, 393–406.

(12) Cannizzo, a.; Milne, C. J.; Consani, C.; Gawelda, W.; Bressler, C.; van Mourik, F.; Chergui, M. *Coordination Chemistry Reviews* **2010**, *254*, 2677–2686.

(13) McCusker, J. K.; Walda, K. N.; Dunn, R. C.; Simon, J. D.; Madge, D.; Hendrickson, D. N. *J. Am. Chem. Soc.* **1993**, *115*, 298.

(14) Smeigh, A. L.; Creelman, M.; Mathies, R. A.; McCusker, J. K. *Journal of the American Chemical Society* **2008**, *130*, 14105–7.

(15) Juban, E. a.; Smeigh, A. L.; Monat, J. E.; McCusker, J. K. *Coordination Chemistry Reviews* **2006**, *250*, 1783–1791.

(16) Hauser, A.; Enachescu, C.; Daku, M. L.; Vargas, A.; Amstutz, N. *Coordination Chemistry Reviews* **2006**, *250*, 1642.

(17) Gütlich, P.; Koningsbruggen, P. J. Van; Renz, F. *Structure and Bonding* **2004**, *107*, 27–75.

(18) Halcrow, M. A. *Polyhedron* **2007**, *26*, 3523–3576.

(19) Gawelda, W.; Cannizzo, A.; Pham, V.-T.; Mourik, F. van; Bressler, C.; Chergui, M. *J. Am. Chem. Soc.* **2007**, *129*, 8199.

(20) Bressler, C.; Milne, C.; Pham, V.-T.; Elnahhas, a; van der Veen, R. M.; Gawelda, W.; Johnson, S.; Beaud, P.; Grolimund, D.; Kaiser, M.; Borca, C. N.; Ingold, G.; Abela, R.; Chergui, M. *Science (New York, N.Y.)* **2009**, *323*, 489–92.

(21) De Graaf, C.; Sousa, C. *Chemistry - A European Journal* **2010**, *16*, 4550–4556.

(22) Ferrere, S. *Chemistry of Materials* **2000**, *12*, 1083–1089.

(23) Bowman, D. N.; Blew, J. H.; Tsuchiya, T.; Jakubikova, E. *Inorganic Chemistry* [Online Early Access] DOI:10.1021/ic4007839 Publication Date (Web): July 9, 2013.

(24) Purcell, K. F. *Journal of the American Chemical Society* **1979**, *101*, 5147–5152.

(25) Vanquickenborne, L. G.; Pierloot, K. *Inorganic Chemistry* **1981**, *20*, 3673–3677.

(26) McCusker, J. K.; Rheingold, A. L.; Hendrickson, D. N. *Inorganic Chemistry* **1996**, *35*, 2100–2112.

(27) Jamula, L. L. Masters Thesis, Michigan State University, 2010.

(28) Brown, A. M. PhD Dissertation, Michigan State University, 2011.

(29) Huse, N.; Kim, T. K.; Jamula, L.; McCusker, J. K.; de Groot, F. M. F.; Schoenlein, R. W. *Journal of the American Chemical Society* **2010**, *132*, 6809–16.

(30) Huse, N.; Cho, H.; Hong, K.; Jamula, L.; Groot, F. M. F. De; Kim, T. K.; Mccusker, J. K.; Schoenlein, R. W. *Journal of Physical Chemistry Letters* **2011**, *2*, 880–884.

(31) Cho, H.; Strader, M. L.; Hong, K.; Jamula, L.; Gullikson, E. M.; Kim, T. K.; de Groot, F. M. F.; McCusker, J. K.; Schoenlein, R. W.; Huse, N. *Faraday Discussions* **2012**, *157*, 463.

(32) Rodriguez-Ubis, J.-C.; Alpha, B.; Plancherel, D.; Lehn, J.-M. *Helv. Chim. Acta* **1984**, *67*, 2264.

(33) De Mendoza, J.; Mesa, E.; Rodríguez-Ubis, J.-C.; Vázquez, P.; Vögtle, F.; Windscheif, P.-M.; Rissanen, K.; Lehn, J.-M.; Lilienbaum, D.; Ziessel, R. *Angewandte Chemie International Edition in English* **1991**, *30*, 1331–1333.

Chapter 2. Introducing a Highly Symmetric Coordination Environment to Iron(II)

2.1 Introduction

Ruthenium(II) polypyridyl complexes are commonly employed as chromophores in DSSCs. Though these ruthenium chromophores have ideal properties for the sensitization of TiO_2, they are a costly component of the cell. An iron(II) based chromophore is an ideal alternative due to the abundance and low cost of first row metals. The efficacy of an iron(II) chromophore is hindered by the ultrafast relaxation to ligand field states, which is in competition with injection into the conduction band of the semiconductor. In order to overcome this challenge, we are investigating the mechanism of the ultrafast deactivation with the ultimate goal of slowing down this process.

Our initial approach involved the introduction of steric bulk to the terminal rings of 2,2':6',2"-terpyridine (terpy) and preparation of the bis-tridentate iron(II) complexes to investigate a torsional deactivation pathway.[1] The steric tuning had a minimal effect on the relaxation rate leading us to pursue a new strategy.[2] The deviation from a truly octahedral coordination environment of the planar terpy ligands may be facilitating the deactivation to the lower lying ligand field states. Tris(2,2'-bipyridine)iron(II) ($[Fe(bpy)_3]^{2+}$) and bis(2,2':6',2"-terpyridine)iron(II) ($[Fe(terpy)_2]^{2+}$) are approximated to possess octahedral symmetry, but the strained ligands reduce the symmetry to D_3 and C_2, respectively. We propose that the reduced symmetry of these complexes may be mediating the charge transfer deactivation. Therefore, the goal of the present research is the design and preparation of highly symmetric iron(II) chromophores. In designing such a system, it is our intent to remove ligand restraints in order to achieve the desired

symmetry while still following the criteria necessary to develop a viable sensitizer for DSSCs.

To attain the desired symmetry the most obvious first choice would be Hexapyridineiron(II) ($[Fe(py)_6]^{2+}$), which is known and was structurally characterized nearly fifty years ago.[3] From the X-ray crystal structure investigation it becomes immediately apparent that this complex is not a viable option. The complex achieves the desired octahedral symmetry, however the Fe-N bond lengths are greater than 2.2 Å signifying a high spin ground state. Furthermore, the complex is off-white and is not stable in solution, losing a pyridine in exchange for a solvent molecule in acetonitrile.[4] Overall, high spin iron(II) complexes lack the stability and molar absorptivity necessary to meet the criteria for a sensitizer.

The inspiration for the molecule in this investigation arose from research efforts toward improving the photophysical properties of bis-tridentate ruthenium(II) complexes. $[Ru(terpy)_2]^{2+}$ has structural advantages over $[Ru(bpy)_3]^{2+}$ but suffers from poor excited state properties. The ^{3}MLCT of $[Ru(terpy)_2]^{2+}$ is relatively short lived (250 ps) and the complex has uncharacteristically weak emission at room temperature.[5] These anomalous features are attributed to the accessibility of the metal centered states. Unfavorable bite angles of the *mer* coordinated terpy leads to a weak ligand field which stabilizes the metal centered states, making them thermally accessible. There is much interest in the pursuit of a more octahedral coordination environment by expanding the bite angles to achieve a stronger ligand field and destabilize the metal centered states, rendering them less accessible.[6] Although our motivations for moving toward a more symmetrical

environment differ, ours being to collapse the ligand field manifold into more discrete states, the expansion of the bite angles of tridentate ligands is an ideal path to pursue.

Recent work by Schramm et al. introduced an octahedral ruthenium(II) polypyridyl complex with unprecedented photophysical properties.[7] The expansion of the coordination environment of a terpy-like ligand resulted in improved bite angles and the formation of a complex that has a significantly extended excited state lifetime, a higher room temperature quantum yield, and remains functional in aerated conditions. The synthesis of the ruthenium(II) complex is complicated by the nature of the ligand. Despite some synthetic hurdles that the preparation of the analogous iron(II) complex would potentially entail, it seemed an ideal choice for this investigation.

The ligand of interest in this study, 2,6-di(2-carboxypyridyl)pyridine (dcpp), was first introduced by Abarca et al. in 1998, while the coordination chemistry was not investigated until 2005.[8,9] The ligand is essentially an extended version of the widely studied and commercially available di(2-pyridyl)ketone (dpk), which has been known and well described in the literature since it was first prepared in the early 1950s.[10] Unlike the rigid terpy ligand, the expanded dcpp has the flexibility to coordinate in a more symmetrical environment (Figure 2-1).

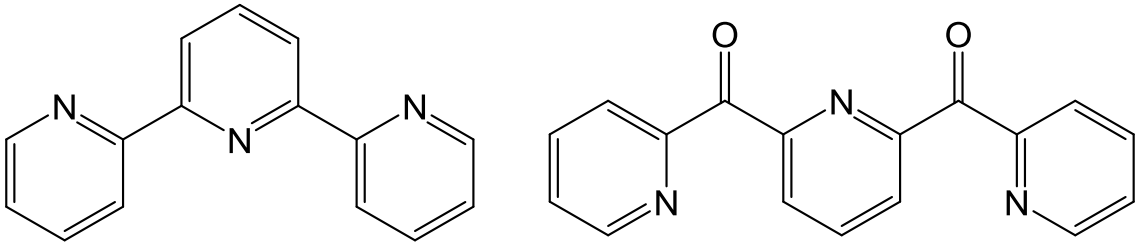

terpy **dcpp**

Figure 2-1. Structures of 2,2':6',2"-terpyridine (terpy) and 2,6-di(2-carboxypyridyl)-pyridine (dcpp).

The dcpp ligand is highly sensitive to reaction conditions, therefore it rarely remains intact upon coordination to a metal center. In most cases the highly reactive carbonyl bridge is transformed in solution resulting in a plethora of binding possibilities. The versatility of the ligand makes it attractive to a wide range of research areas, including the preparation of polynuclear clusters, single molecule magnets, and coordination polymers.[9]

While the reactivity of dcpp was of great concern at the outset of this study, the target octahedral iron complex, bis(2,6-di(2-carboxypyridyl)pyridine)iron(II) has been successfully prepared and thoroughly investigated. The consequences of moving toward more symmetrical coordination environment are examined through a comparison of the new iron(II) complex with the well-known pseudo-octahedral tris(2,2'-bipyridine)iron(II) and bis(2,2':6',2"-terpyridine)iron(II) complexes (Figure 2-2). The synthesis and characterization will be fully described here, while further discussion on the photophysics and implications were examined by Allison Brown in her PhD Dissertation.[2]

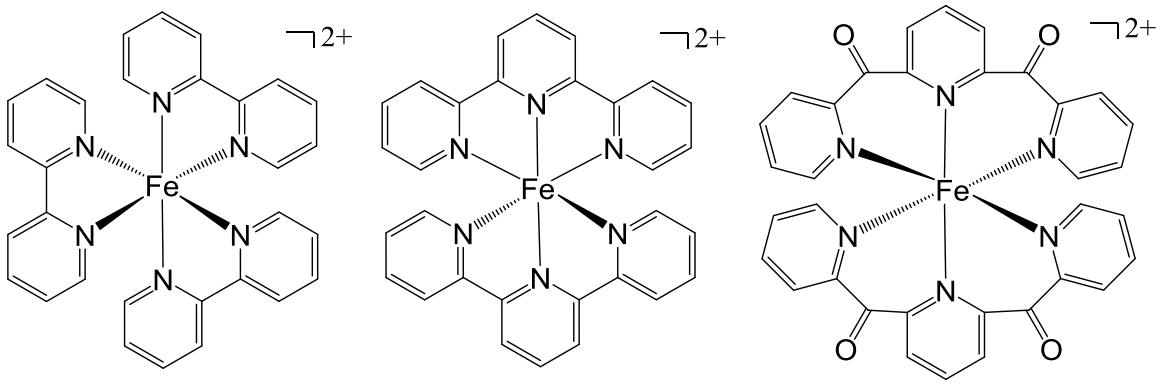

$[Fe(bpy)_3]^{2+}$ **$[Fe(terpy)_2]^{2+}$** **$[Fe(dcpp)_2]^{2+}$**

Figure 2-2. Structures of tris(2,2'-bipyridine)iron(II) $[Fe(bpy)_3]^{2+}$, bis(2,2':6',2"-terpyridine)iron(II) $[Fe(terpy)_2]^{2+}$, and bis(2,6-di(2-carboxypyridyl)pyridine)iron(II) $[Fe(dcpp)_2]^{2+}$.

In an effort to gain more insight on the properties of the new iron(II) complex, it is necessary to prepare a control molecule. An isostructural d^{10} molecule would aid in distinguishing properties that may be attributed to the complex from ligand based effects. Analysis of the ligand alone would be inadequate due to the free lone pairs on the nitrogen atoms as well as the vastly different arrangement that the dcpp assumes on upon coordination. Attempts to isolate either a zinc(II), gallium(III), or cadmium(II) analog have been unsuccessful thus far. Unlike with the complexation of the iron(II) compound, the reactivity of the dcpp appears to be detrimental to the formation of these complexes. Many different routes employing a variety of reagents and conditions were pursued and will be discussed.

2.2 Experimental

2.2.1 Synthesis

General. All chemicals were of reagent grade, purchased from Sigma-Aldrich, Alfa Aesar, Acros Organics, or Strem Chemicals and used as received unless otherwise noted. Solvents were purchased from Sigma-Aldrich, Jade Scientific, Spectrum, Mallinckrodt, EMD Chemical, or CCI and were purified using standard purification techniques.[11] All air-sensitive reactions were carried out under inert atmosphere by standard Schlenk techniques utilizing thoroughly deoxygenated solvents that were degassed by the freeze—pump—thaw method. ^{1}H NMR and ^{13}C NMR were recorded with Varian UnityPlus-300 MHz, Varian UnityPlus-500 MHz, and Agilent DDR2 500 MHz spectrometers. Ground state absorption spectra were obtained on a Varian Cary 50 spectrophotometer. IR spectra were obtained on a Mattson Galaxy 5000 FTIR.

Elemental analysis was obtained through the Analytical facilities at Michigan State University and Columbia Analytical Services (Tucson, AZ). Electrospray mass spectra (ESI-MS) were obtained from the staff of the MSU Mass Spectrometry Facility. The characterization data of previously unknown compounds are included in the appendix at the end of this chapter.

2,6-Di(2-methylenepyridyl)pyridine (dmpp). The compound was prepared according to the published procedure from 2-picoline (14.9 g, 160 mmol) and 2,6-difluoropyridine (2.30 g, 20 mmol).[12] The crude product was purified by vacuum distillation yielding a yellow oil. Yield: 4.96 g (95%). The oil does not crystallize upon standing as described in the literature until a KOH pellet is added to the product to dry it promoting crystallization. mp 46ºC. ^{1}H NMR (500MHz, $CDCl_3$) δ (ppm): 8.53 (ddd, 2H, 6-H of the pyridyl arms (py-a)), 7.56 (td, 2H, 4py-a), 7.50 (t, 1H, 4-H of the bridging pyridyl (py-b)), 7.23 (dt, 2H, 3py-a), 7.09 (dtd, 2H, 5py-a), 7.05 (d, 2H, 3/5py-b), 4.33 (s, 4H).

2,6-Pyridinedicarboxylate diethyl ester. The compound was prepared from 2,6-pyridinedicarboxylic acid (12.0 g, 71.8 mmol) according to the literature procedure.[13] The crude product is obtained as a colorless oil which does not readily crystallize. The product is precipitated by dissolution of the oil in minimal ethanol and flash freezing by submersion in liquid nitrogen. The solid must be filtered quickly to avoid melting/redissolution. Once in the solid form the compound may be recrystallized by dissolution in ethanol at room temperature and placing in the freezer. The hygroscopic solid must be stored in a vacuum desiccator to maintain integrity. Yield: 11.2 g (70%). ^{1}H NMR ($CDCl_3$), δ (ppm): 8.31 (d, 2H); 8.04 (t, 1H); 4.5 (q, 4H); 1.47 (t, 6H).

2,6-Di(2-carboxypyridyl)pyridine (dcpp). This compound was prepared via two different routes, by modification of previously published procedures.

Method A.[14] To a 100 mL round bottom flask equipped with a reflux condenser were added dmpp (0.510 g, 1.95 mmol), excess selenium dioxide (1.35 g, 12.2 mmol), and glacial acetic acid (50 mL) and the solution was refluxed for 8 hours. The reaction mixture was filtered hot through celite to remove selenium and the solvent evaporated in vacuo. The brown residue was dissolved in $CHCl_3$ and washed with saturated $NaHCO_3$ (aq). The product was purified by column chromatography on silica with 2% EtOH in $CHCl_3$ and recrystallized by dissolving by sonication in EtOAc at room temperature and adding hexanes till cloudy (~1:1) and cooling to 0^{o}C. Yield 0.176 g (30%).

Method B.[15] To a 250 mL round bottom air-free flask were added 2-bromopyridine (3.12 g, 19.7 mmol) and dry THF (~80 mL) via cannula. Under nitrogen, the solution was cooled to -78^{o}C in a dry ice/acetone bath. 1.6 M n-BuLi solution in hexanes (12.3 mL, 19.7 mmol) was added dropwise over 30 minutes and the solution stirred for an additional 30 minutes. To a separate air free flask was added diethyl 2,6-pyridinedicarboxylate (2.01 g, 8.96 mmol) and dry THF (~20 mL) and the solution transferred dropwise via 22 gauge cannula to the reaction mixture over 40 minutes. The solution was stirred for an additional 2 hours at -78^{o}C before quenching with methanol (20 mL) and allowing to warm to room temperature and stir overnight. 10% HCl (40 mL) was added and the organic layer removed. The acidic aqueous layer was washed with CH_2Cl_2 (1 x 50 mL) and then basified with 5 M NaOH. The basic aqueous layer was then extracted with CH_2Cl_2 (3 x 100 mL). The organic layer dried with $MgSO_4$, filtered, and evaporated. The crude product is fairly clean and purification is not

necessary, but may be purified as in *Method A*. Yield: 1.80 g (70%). mp 135.0-135.5. ^{1}H NMR ($(CD_3)_2CO$, 500 MHz) δ (ppm): 8.69 (ddd, 2H, 6py-a), 8.28 (t, 1H, 4py-b), 8.24 (d, 2H, 3/5py-b), 8.07 (dt, 2H, 3py-a), 7.95 (td, 2H, 4py-a), 7.57 (dtd, 2H, 5py-a).

$[Fe(dcpp)_2](PF_6)_2$. To an air free flask dcpp (0.585 g, 2.02 mmol) and deoxygenated 4:3 MeOH/H_2O (50 mL) via cannula were added. The solution was gently warmed (40°C) under nitrogen to promote dissolution. A separate air free flask was charged with 1 equivalent of $FeCl_2 \cdot 2H_2O$ (0.146 g, 0.897 mmol) and 4:3 MeOH/H_2O (20 mL). The Fe(II) solution was transferred via cannula to the ligand solution which immediately turned pale green then gradually darkened to deep blue. The reaction was allowed to stir for 18 hours at room temperature. A separate air free flask was charged with 4 equivalents of NH_4PF_6 (0.620 g, 3.80 mmol) and 4:3 MeOH/H_2O (15 mL) which was then transferred via cannula to the reaction mixture. The solution was concentrated by evaporation under a stream of N_2 yielding dark blue precipitate which was filtered and rinsed with H_2O. The crude product was dissolved in acetonitrile and the solution was washed with hexanes to remove grease. The acetonitrile solution was concentrated then purified by passage through a basic alumina column. The product was recrystallized by diethyl ether vapor diffusion into a 1:1 acetone/acetonitrile solution of the complex. Yield: 0.451 g (54%). ^{1}H NMR ($(CD_3)_2CO$, 500 MHz): δ (ppm) 8.75 (t, 2H, J = 7.6 Hz, 4py-b), 8.49 (d, 4H, J = 7.6 Hz, 3/5py-b), 8.34 (td, 4H, J = 7.8, 1.2 Hz, 4py-a), 8.19 (dd, 4H, J = 7.8, 1.7 Hz, 3py-a), 8.05 (dd, 4H, J = 5.9, 1.2 Hz, 6py-a), 7.49 (td, 4H, J = 5.9, 1.7 Hz, 5py-a). ^{13}C NMR ($(CD_3)_2CO$, 500 MHz): δ (ppm) 180.69, 160.92, 159.21, 159.08, 144.60, 140.93, 131.20, 128.96, 128.05. TOF-MS [ESI, *m/z* (rel int)]: 317.0

(100) $[C_{34}H_{22}N_6O_4Fe]^{2+}$, 779.1 (20) $\{[C_{34}H_{22}N_6O_4Fe](PF_6)\}^+$. IR (KBr, cm^{-1}): 1699.2 s, 1683.4 s, 1596.1 m, 1434.7 w, 1328.4 m, 1242.6 w, 986.2 w, 915.9 w, 836.5 br, 760.6 m, 667.9 w. Elemental Analysis for $C_{34}H_{22}N_6O_4FeP_2F_{12}\cdot CH_3OH$, Calculated: C, 43.96; H, 2.74; N, 8.78; Fe, 5.84. Found: C, 43.83; H, 2.73; N, 8.79; Fe, 5.80. UV-Vis (CH_3CN) $\lambda(\varepsilon(M^{-1}cm^{-1}))$: 354 nm (11000), 445 nm (2500), 513 nm (4600), 606 nm (6200).

$[Cd(dmpp)_2](PF_6)_2$. To a 50 mL Erlenmeyer flask were added dmpp (0.761 g, 2.91 mmol), $Cd(CH_3CO_2)_2$ (0.217 g, 0.941 mmol), and 1:1 EtOH/H_2O (20 mL) and the solution was allowed to stir overnight in the presence of air. 10 equivalents of NH_4PF_6 in H_2O was added and a beige precipitate formed. The product was filtered then recrystallized by ether diffusion into an acetone solution yielding white crystalline needles. Yield: 0.666 g (72%). ^1H NMR ($(CD_3)_2CO$, 500 MHz): δ (ppm) 8.23 (t, 2H, *J* = 7.8 Hz, 4py-b), 8.12 (td, 4H, *J* = 7.8, 1.7 Hz, 4py-a), 7.93 (dd, 8H, *J* = 7.8, 1.7 Hz, 3py-a, 3/5py-b), 7.70 (dq, 4H, *J* = 5.3, 1.0 Hz, 6py-a), 7.35 (td, 4H, *J* = 5.3, 1.0 Hz, 5py-a), 4.61 (d, 4H, *J* = 14.5 Hz), 4.43 (d, 4H, *J* = 14.5 Hz). ^{13}C NMR ($(CD_3)_2CO$, 500 MHz): δ 157.84, 157.66, 148.86, 142.36, 141.37, 126.39, 125.15, 124.60, 43.37. TOF-MS [ESI, *m/z* (rel int)]: 318.0 (25) $[C_{34}H_{22}N_6Cd]^{2+}$. IR (KBr, cm^{-1}): 1604.1 m, 1575.1 m, 1482.8 m, 1440.3 m, 1111.7 w, 1016.4 m, 842.2 br, 779.4 w. Elemental Analysis for $C_{34}H_{22}N_6CdP_2F_{12}$, Calculated: C, 44.54; H, 2.42; N, 9.17. Found: C, 44.01; H, 3.07; N, 9.06.

$[Cd(dcpp)_2]^{2+}$. Many routes have been employed to prepare this compound successfully; however, it could not be isolated in pure form.

Method A. $[Cd(dcpp)_2](PF_6)_2$ was prepared by modification of a literature procedure.[16] To a round bottom flask dcpp (0.101 g, 0.349 mmol), $Cd(NO_3)_2 \cdot 4H_2O$ (0.050 g, 0.162 mmol), and dry acetonitrile (30 mL) were added and the solution stirred for 6 hours. The solution was evaporated and the remaining solid dissolved in H_2O/MeOH and 4 equivalents of NH_4PF_6 were added yielding a sticky white solid. The solid was dissolved in acetonitrile and precipitated with ether, but instead of yielding a solid, a coagulated gel-like suspension forms. The gel is filtered yielding a flaky white solid that contains the desired product. TOF-MS [ESI, *m/z* (rel int)]: 346.0 (5) $[C_{34}H_{22}N_6O_4Cd]^{2+}$, 837.0 (5) $\{[C_{34}H_{22}N_6O_4Cd](PF_6)\}^+$.

Method B. $[Cd(dcpp)_2](PF_6)_2$. To a round bottom flask dcpp (0.120 g, 0.415 mmol), anhydrous $Cd(CH_3CO_2)_2$ (0.033 g, 0.143 mmol), and dry ethanol (20 mL) were added and the solution was warmed at 50°C overnight. 20 equivalents of NH_4PF_6 in 4 mL of ethanol were added and the solution concentrated yielding a thick gel-like solid as in Method A. The gel is filtered yielding a flaky white solid that contains the desired product. TOF-MS [ESI, *m/z* (rel int)]: 346.1 (10) $[C_{34}H_{22}N_6O_4Cd]^{2+}$, 837.0 (5) $\{[C_{34}H_{22}N_6O_4Cd](PF_6)\}^+$.

Method C. $[Cd(dcpp)_2](ClO_4)_2$. A 25 mL Erlenmeyer flask was charged with dcpp (0.0987 g, 0.341 mmol) and ethanol (3 mL). $Cd(ClO_4)_2 \cdot xH_2O$ (0.0369 g, 0.119 mmol) in 1 mL of ethanol was added dropwise with stirring. During addition solution becomes cloudy then coagulates forming a gel as in Method A. A flaky white solid is obtained that contains the desired product. TOF-MS [ESI, *m/z* (rel int)]: 346.0 (15) $[C_{34}H_{22}N_6O_4Cd]^{2+}$, 791.0 (20) $\{[C_{34}H_{22}N_6O_4Cd](ClO_4)\}^+$.

Method D. $[Cd(dcpp)_2](PF_6)_2$. A 125 mL Erlenmeyer flask was charged with $[Cd(dmpp)_2](PF_6)_2$, DMF (50 mL), and activated carbon. The reaction mixture was heated to 100°C and bubbled with air for 5 hours. The carbon was filtered and water was added to the filtrate to precipitate the product which was found to be a mixture of $[Cd(dcpp)_2](PF_6)_2$ and dcpp. TOF-MS [ESI, *m/z* (rel int)]: 346.1 (30) $[C_{34}H_{22}N_6O_4Cd]^{2+}$.

To date, all attempts to purify: column chromatography on silica, reverse phase silica, neutral alumina, basic alumina, and size-exclusion chromatography have been unsuccessful, therefore the pure product is yet to be isolated.

2,6-Di(2-ketalpyridyl)pyridine (dkpp). The protection of the carbonyls of dcpp was carried out by modification of a published procedure.[17] To a 100 mL round bottom flask equipped with a Dean-Stark trap was added dcpp (0.774 g, 2.68 mmol), freshly distilled ethylene glycol (2 mL), dry toluene (50 mL), and 3 drops of H_2SO_4. The reaction mixture was refluxed utilizing an oil bath for 6 days. Upon heating black residue forms in the flask, sticking to the sides. Heating to 120°C for 5 days resulted in no water collection in trap so warmed to 125°C on the last day, resulting in the removal of water. The toluene layer is poured into an Erlenmeyer flask and placed in the freezer to precipitate the product. Yield: 0.423 g, (42%). The black residue from reaction flask was dissolved in $CHCl_3$ and washed with 5% Na_2CO_3, and found to contain a mixture of unreacted dcpp, partially reacted monoketal, and the diketal product. TLC on silica (in CH_3CN or CH_2Cl_2) shows clear separation of the three compounds, but with the desired product remaining at the baseline no attempts were made to isolate it by column

chromatography. mp 177-178°C. ^{1}H NMR ($(CD_3)_2CO$, 500 MHz): δ 8.37 (d, 2H, *J* = 4.8 Hz, 6py-a), 7.79 (t, 1H, *J* = 7.7 Hz, 4py-b), 7.68 (td, 2H, *J* = 7.7 Hz, 4py-a), 7.60 (d, 2H, *J* = 7.9 Hz, 3/5py-b), 7.58 (d, 2H, *J* = 7.9 Hz, 3py-a), 7.20 (dtd, 2H, *J* = 4.8 Hz, 5py-a), 4.03 (dm, 8H, *J* = 4.4 Hz). ^{13}C NMR ($(CD_3)_2CO$, 500 MHz): δ 148.32, 136.12, 135.80, 135.57, 122.53, 121.15, 119.98, 109.99, 65.26. TOF-MS [ESI, *m/z* (rel int)]: 378.1 (100) $[C_{21}H_{19}N_3O_4]H^+$. IR (KBr, cm^{-1}): 3046.6 w, 2950.2 w, 2886.5 m, 1588.8 m, 1573.4 m, 1466.5 m, 1442.4 m, 1279.2 w, 1215.4 m, 1133.1 s, 1031.5 s, 992.2 s, 949.6 m, 834.5 m, 797.1 m, 762.5 m, 669.2 m.

2.2.2 Physical Measurements

X-ray Structure Determination. Single-crystal X-ray diffraction data for $[Fe(dcpp)_2](PF_6)_2$ was acquired at the X-ray Facility of Michigan State University. X-ray quality single crystals were obtained by slow diffusion of diethyl ether into an acetonitrile solution of the compound. A black block crystal with dimensions 0.15 × 0.15 × 0.08 mm was mounted on a Nylon loop using very small amount of paratone oil. Data were collected using a Bruker CCD (charge coupled device) based diffractometer equipped with an Oxford Cryostream low-temperature apparatus operating at 173 K. Data were measured using omega and phi scans of 0.5° per frame for 30 s. The total number of images was based on results from the program COSMO[18] where redundancy was expected to be 4.0 and completeness of 100% out to 0.83 Å. Cell parameters were retrieved using APEX II software[19] and refined using SAINT on all observed reflections. Data reduction was performed using the SAINT software[20] which corrects for Lp. Scaling and absorption corrections were applied using SADABS[21] multi-scan technique,

supplied by George Sheldrick. The structures are solved by the direct method using the SHELXS-97 program and refined by least squares method on F^2, SHELXL-97, which are incorporated in SHELXTL-PC V6.10.[22] Anisotropic thermal parameters were refined for all non-hydrogen atoms. Hydrogen atoms were localized in their calculation positions and refined by using the riding model.

Cyclic Voltammetry. Electrochemical measurements were carried out using a CH Instruments CH620D electrochemical analyzer to determine the $E_{1/2}$ for ligand reductions and metal oxidations of each complex. Solutions of the compounds were prepared in distilled CH_3CN containing NBu_4PF_6 (ca. 0.1 M) as the supporting electrolyte. A standard three-electrode setup was used with a platinum working electrode, carbon rod counter electrode, and a Ag/AgCl or $Ag/AgNO_3$ electrode as the reference. All measurements were made inside an inert atmosphere glovebox. Data was acquired at a scan rate of 100 mV s^{-1}. After data collection ferrocene was added to subsequent scans for reference.

2.2.3 Theoretical Calculations

Theoretical calculations were performed using Gaussian 03.[23] The initia4 geometry of the $[Fe(dcpp)_2]^{2+}$ molecule was obtained from the crystal structure data and subsequently optimized in two steps. The first optimization was performed using the density functional B3LYP with the 3-21G** basis set, followed by a second optimization using the B3LYP functional with the 6-31G* basis set. Optimizations were repeated using the polarizable continuum model (PCM) to account for solvent effects. Frequency calculations at the B3LYP/6-31G* level of theory were performed on the final optimized

structures to ensure that these geometries corresponded to global minima. Time-dependent DFT was used to calculate energies of excited states and obtain models of the molecular orbitals.

2.3 Results and Discussion

2.3.1 Synthesis of 2,6-Di(2-carboxypyridyl)pyridine

2,6-Di(2-carboxypyridyl)pyridine, dcpp, may be prepared by a variety of methods. It was first synthesized by Abarca et al. from a general strategy they developed to yield a series of potential helicating ligands from triazolopyridines.[8] Due to the wide interest in the fascinating coordination possibilities of this ligand, alternate routes have been developed.[7,15,24–26]

A clear starting point toward the development of the synthesis of $[Fe(dcpp)_2]^{2+}$ was to look to the route of the preparation of the ruthenium analog by Schramm et al.[7] Due to the nature of the ligand (vide infra), the complex could not be prepared by simply coordinating the ligand to the metal. Instead, the target molecule was obtained by simultaneous coordination/ligand oxidation from 2,6-di(2-methylenepyridyl)pyridine, dmpp. Therefore, it was an obvious choice to prepare the dmpp first, from which the dcpp may be prepared by a simple oxidation procedure.

A one step procedure for the preparation of dmpp, or tripyridinedimethane, was developed by Vedernikov et al.[27] The route involves lithiating 2,6-lutidine, creating a bis(nucleophile) to react with pyridine. The simple one step procedure yields impure crude products requiring tedious fractional distillation and results in only moderate yields. An improved method was developed by Dyker and Muth in 2004.[12] This

procedure involves the lithiation of 2-picoline, to be used as the nucleophile to react with 2,6-difluoropyridine. It is crucial to use at least a four-fold excess of the nucleophile, since the product has two acidic methylene bridges that each lead to consumption of one equivalent of the lithiated picoline. This optimized reaction was chosen and provided a 95% yield of the dmpp, as shown in Scheme 2-1. Dmpp is subsequently oxidized with selenium dioxide to dcpp.

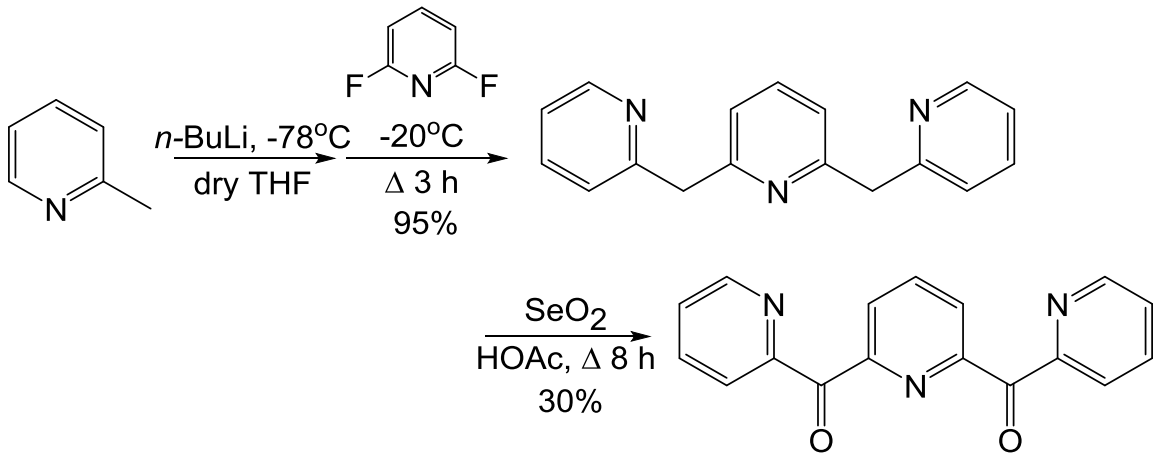

Scheme 2-1. Stepwise synthesis of 2,6-di(2-methylenepyridyl)pyridine (dmpp) and 2,6-di(2-carboxypyridyl)pyridine (dcpp).

The selenium dioxide oxidation, or Riley oxidation, is commonly employed in our lab for the oxidation of the active methyl groups on substituted bipyridyls. The method may be utilized to oxidize methyl groups to alcohols, and with excess oxidant will convert them to ketones. Though this route is convenient, selenium dioxide is not pleasant to work with; it readily sublimes, has a harsh, unpleasant odor, can burn the nose and throat upon exposure, and even result in garlic breath. Furthermore, much difficulty arises in removing the malodorous selenium byproducts completely while maintaining a decent yield. Overall, this method stinks, literally, and another route was pursued.

An alternate method for the preparation of dcpp was adapted from work by Goldsmith and Stack.[15] This convenient method involves the lithiation of 2-bromopyridine followed by nucleophilic attack of a diethyl ester of 2,6-pyridinedicarboxylate, as shown in Scheme 2-2. The reaction is relatively clean, requiring little effort in purification, and the product is obtained in 70% yield. This route is also preferential in that, by slight modifications to the starting materials, it allows for ease of functionalization to install anchoring groups and other structural modifications of the molecule, as will be discussed in later chapters of this dissertation.

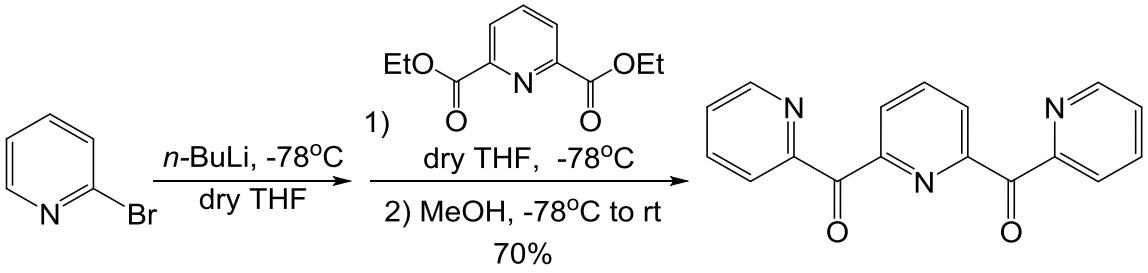

Scheme 2-2. Alternate synthesis of 2,6-di(2-carboxypyridyl)pyridine (dcpp).

2.3.2 Coordination Chemistry of 2,6-Di(2-carboxypyridyl)pyridine

The coordination chemistry of dcpp has been a hot topic in recent years. From the time the ligand properties were first investigated in 2005 to 2009 there were already 14 crystallographically established coordination modes of dcpp.[9,28] By introducing the carbonyl bridges, not only are there two new possible coordinating sites, the oxygen atoms, but the carbon of the carbonyl is highly susceptible to transformation resulting in various forms of the ligand.

One of the first things we learn in introductory organic chemistry is about the reactivity of carbonyl compounds, with organic texts referring to the addition of a nucleophile to a carbonyl group as the simplest of all organic reactions.[29] The concept is

introduced with the example of an aldehyde or ketone dissolved in water or alcohol, in which water acts a nucleophile and attacks the electrophilic carbonyl forming the hydrate, or *gem*-diol, and alcohol will produce a hemiacetal or hemiketal. As shown in Scheme 2-3, an equilibrium exists between a ketone and its hydrated form that usually lies far toward the ketone, however, special factors can shift the equilibrium more toward the hydrated form. In the case of dcpp, the electron withdrawing 2-pyridyl groups increase the electrophilicity of the carbonyl carbon which may shift this equilibrium more toward the hydrated form.

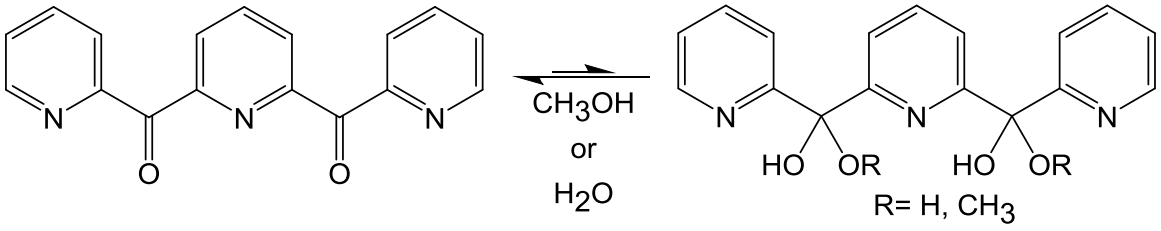

Scheme 2-3. Equilibrium of dcpp in water or methanol.

The hydrated or hemiketal forms of dcpp are not stable in the solid form and have not been isolated. In solution, evidence for the formation of the hemiketal can be seen in the ^{1}H NMR spectrum (Figure 2-3). Dcpp remains intact in deuterated acetone (shown), acetonitrile, or chloroform, but evidence of hemiketal formation appears in deuterated methanol. Quantitative NMR was not performed, but from integration of a standard ^{1}H NMR spectrum it appears that the equilibrium lies toward the ketone with a 4:1 ratio of ketone to hemiketal.

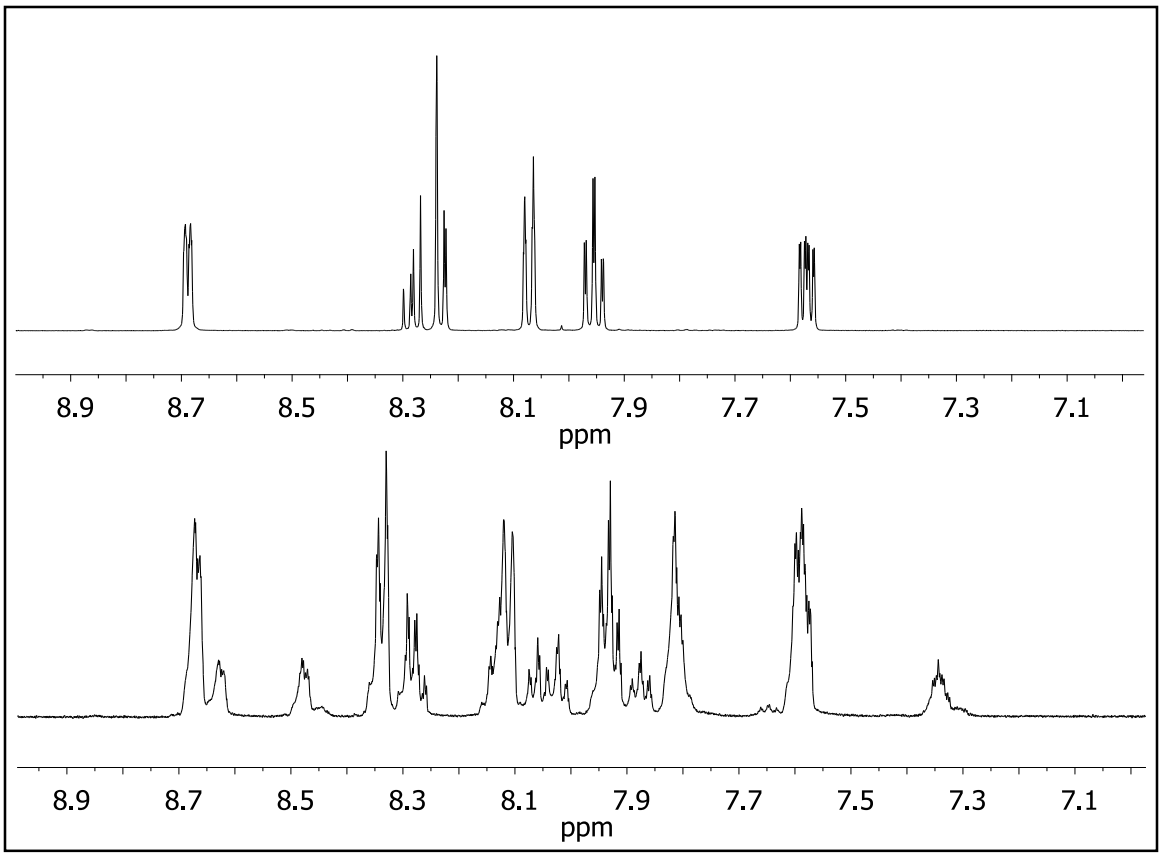

Figure 2-3. ^{1}H NMR of dcpp in $(CD_3)_2CO$ (top) and CD_3OD (bottom).

Coordination of the pyridyl nitrogen atoms to a metal ion may shift the equilibrium further toward the hydrated form. Donation of the nitrogen lone pair to the metal will increase polarization of the carbon-carbon bond between the pyridyl carbon and carbonyl carbon, making it more electrophilic. Also, a mechanism for metal promoted hydrolysis/solvolysis has been proposed based on a crystal structure study on Cu(II) dcpp complexes.[24] The planar dcpp wraps around the metal in a helical fashion and the nucleophilic solvent (H_2O or CH_3OH) is captured by the metal through a weak interaction forming a distorted quasi-octahedral structure. This coordination environment, together with the steric effect of the helical structure, dictates the

nucleophilic attack by the solvent. This mechanism has been termed metal-promoted, helical chelation-induced hydrolysis and asymmetric solvolysis.

Due to the reactivity of dcpp, small variations in stoichiometry, reaction conditions, and choice of solvent lead to different structures. It is unusual that the ligand remains intact upon coordination, and even more so in the presence of water or methanol.[9] This seems to be the case with the coordination chemistry of iron(III) and dcpp, as well as with the chemistry of iron(II) and di(2-pyridyl)ketone (dpk).[30–33] Since the motivation behind much of the research is the preparation of polynuclear clusters, single molecule magnets, and coordination polymers, in which hydrolysis of the ligand is preferred, it appears that not many attempts have been made to coordinate the ligand intact.

2.3.3 Synthesis of Bis(2,6-di(2-carboxypyridyl)pyridine)iron(II)

According to the work by Schramm et al. bis(2,6-di(2-carboxypyridyl)-pyridine)ruthenium(II) could not be prepared via coordination of the ligand to the metal.[7] The authors claim that neither working in the exclusion of air, nor higher temperatures, nor microwave heating could produce the target molecule. Though not explicitly stated, it is likely that the reactive carbonyl is problematic. The target molecule was obtained by simultaneous coordination/ligand oxidation from 2,6-di(2-methylenepyridyl)pyridine, dmpp, shown in Scheme 2-4. This simultaneous coordination/ligand oxidation has been found to occur in other Ru(II) polypyridyls with activated positions on the ligand back bone.[34]

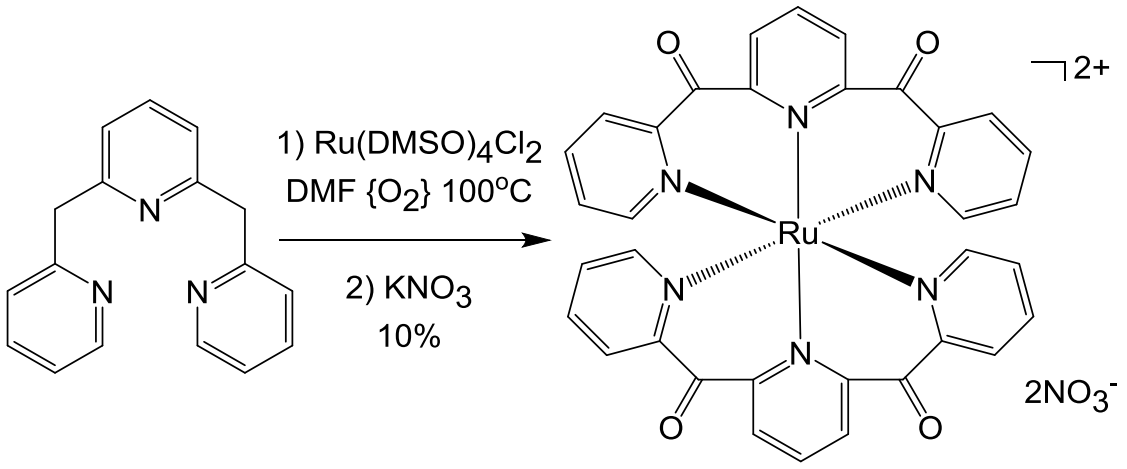

Scheme 2-4. Synthesis of $Ru(dcpp)_2](NO_3)_2$ (adapted from reference 3).

The iron(II) chemistry likely could not proceed by the same method, since Fe(II) in solution is highly susceptible to oxidation to Fe(III). Nevertheless, the method was attempted, to no avail. Identical conditions were utilized, as well as a few variations in solvent choice, temperatures, order of addition, and attempts to initially exclude oxygen. In all cases, there was no evidence of the desired product by ESI-MS. Also, the samples were paramagnetic by NMR, likely from the formation of Fe(III) compounds.

The standard route employed in our lab for the preparation of Fe(II) polypyridyl complexes is the addition of one equivalent of $FeCl_2 \cdot 2H_2O$ to two equivalents of ligand in methanol/water. The reasoning for the choice of solvent mixture is as follows: methanol for solubilizing the ligand, water for solubilizing the iron(II) reagent, and ease of isolation since the PF_6^- salt of the complex may be easily metathesized from this solvent mixture, which almost always is obtained in pure form upon filtration of the reaction mixture. Ignoring all precedence in the literature for this particular ligand system (vide supra), the standard route was attempted. $[Fe(dcpp)_2](PF_6)_2$ was

successfully prepared and the optimized reaction conditions produced a 54% yield of pure product (Scheme 2-5).

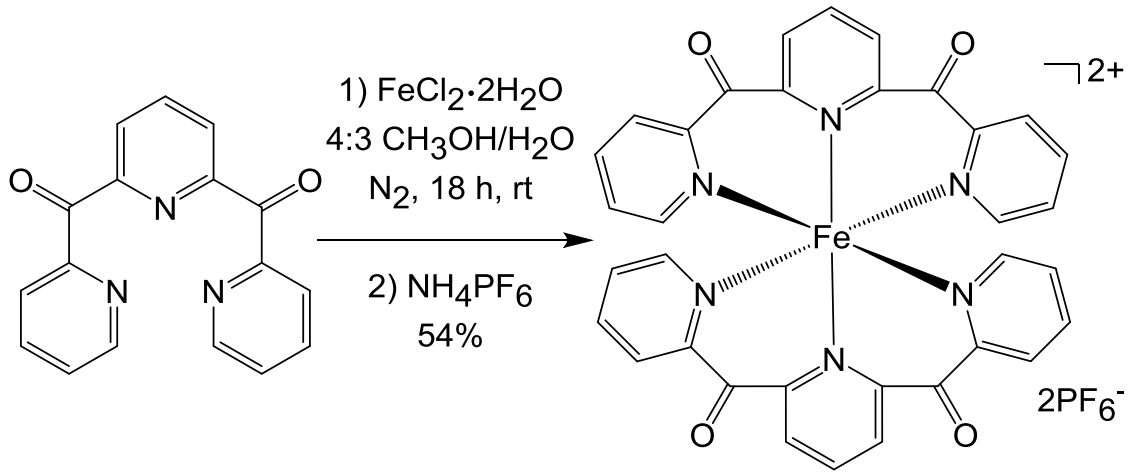

Scheme 2-5. Synthesis of $[Fe(dcpp)_2](PF_6)_2$.

Unlike with the preparation of most iron(II) polypyridyl complexes, which produce high yields of pure products right out of the gate, the formation of $[Fe(dcpp)_2]^{2+}$ is accompanied by formation of a byproduct. The reaction mixture initially turns green then darkens as the desired complex forms, and longer reaction times increase the yield of the desired product. Varying the ligand to metal ratio (i.e., 4:1, 3:1, 2:1) does not have a significant effect on product/byproduct formation, and it was determined that optimal yield is obtained from a slight excess of ligand (2.25:1 ratio). Presumably, the byproduct arises from hydrate or hemiketal formation, therefore an alternate solvent system may prevent the formation of the byproduct. However, since the byproduct and excess ligand may be easily removed by column chromatography, an alternate solvent system was not employed. The blue colored $[Fe(dcpp)_2]^{2+}$ may be purified by the same method as the Ru(II) analog, by silica gel chromatography with 20:1 acetonitrile/KNO_3 (aq). The excess ligand is eluted first followed by $[Fe(dcpp)_2]^{2+}$, while the byproduct remains on

the column. A better method for purification was found to be chromatography on basic alumina with acetonitrile. The alumina column runs much more quickly and retains the ligand and byproduct, with only the pure product being eluted. The product may then be recrystallized by diethyl ether vapor diffusion into a 1:1 acetone/acetonitrile.

The formation of this complex in water/methanol is a curiosity and requires further investigation. Since the focus of the current research is on the properties of the resulting complex, the reaction was not further analyzed, but an observation about the synthesis should be noted. Attempts to isolate $[Fe(dcpp)_2]Cl_2$ from the reaction were unsuccessful, yielding only the byproduct and unreacted ligand, metathesis to the PF_6^- salt was a must. I am uncertain of the reason behind this, is the counter ion that important? Is the formation affected by the change in pH upon adding an excess of the acidic NH_4PF_6 reagent? Alternate solvent systems, pH adjustments, and alternative counterions should be investigated.

2.3.4 Properties of Bis(2,6-di(2-carboxypyridyl)pyridine)iron(II)

Single crystals suitable for X-ray crystallography were obtained and the crystal structure solved by Dr. Dong Guo. As was the intended goal, an octahedral coordination environment is achieved with $[Fe(dcpp)_2]^{2+}$ and the crystal structure as shown in Figure 2-4. The crystallographic data is listed in Table 2-1 and selected geometric parameters are listed in Tables 2-2 and 2-3.

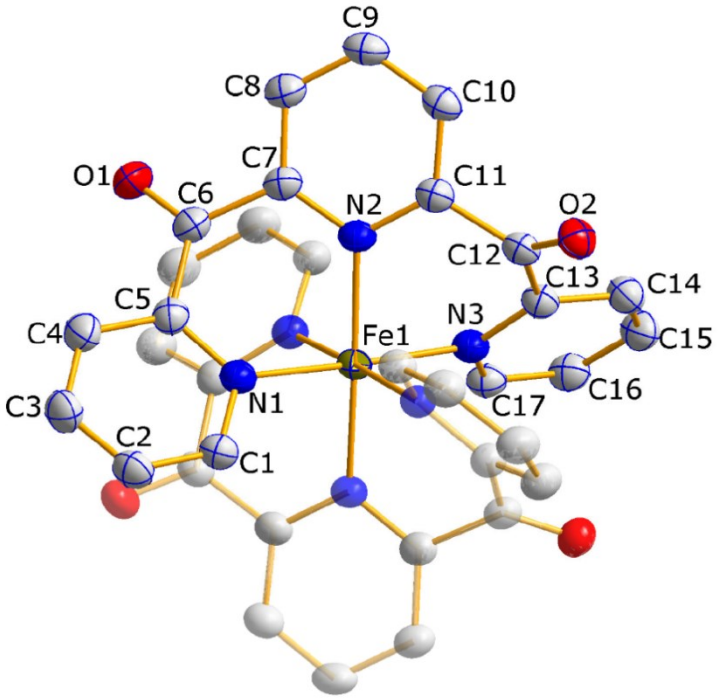

Figure 2-4. ORTEP Drawing of the cation of $[Fe(dcpp)_2]^{2+}$ obtained from single-crystal X-ray structure determination. Atoms are represented as 50% probability thermal ellipsoids. Hydrogen atoms and anions are omitted for clarity.

Table 2-1. Crystallographic data for $[Fe(dcpp)_2](PF_6)_2$.

$[Fe(dcpp)_2](PF_6)_2$ [a]			
Empirical formula	$C_{34}H_{22}F_{12}FeN_6O_4P_2$	ρ_{calc}mg/mm^3	1.816
Formula weight	924.37	μ/mm^{-1}	0.66
Temperature/K	173(2)	F(000)	1856
Crystal system	Orthorhombic	2θmax	56.6°
Space group	Pbcn	Reflections collected	21855
a/Å	14.5603 (3)	Independent reflections	4199
b/Å	15.4333 (3)	Reflections with $I > 2\sigma(I)$	3524
c/Å	15.0431 (3)	R(int)	0.072
Volume/Å^3	3380.39 (12)	R_1 [b]	0.047
Z	4	wR_2 [c]	0.133
		Goodness-of-fit on F^2	1.05

[a] Obtained with graphite monochromated Mo $K\alpha$ radiation (λ = 0.71073 Å) [b] $R_1 = \sum ||F_o| - |F_c|| / \sum |F_o|$. [c] $wR_2 = \{ \sum [w(F_o^2 - F_c^2)^2 / \sum [w(F_o^2)^2]\}^{1/2}$.

Table 2-2. Selected bond lengths from the X-ray crystal structure of $[Fe(dcpp)_2](PF_6)_2$.

Selected Bond Lengths (Å)	
Fe1—N2i	1.974 (2)
Fe1—N2	1.974 (2)
Fe1—N1	1.985 (2)
Fe1—N1i	1.985 (2)
Fe1—N3i	1.989 (2)
Fe1—N3	1.989 (2)
Symmetry code (i) $-x, y, -z+1/2$	

Table 2-3. Selected bond angles from the X-ray crystal structure of $[Fe(dcpp)_2](PF_6)_2$.

Selected Bond Angles (°)			
N2i—Fe1—N2	178.96 (8)	N1—Fe1—N3i	89.07 (7)
N2i—Fe1—N1	90.48 (7)	N1i—Fe1—N3i	177.63 (6)
N2—Fe1—N1	88.79 (6)	N2i—Fe1—N3	91.86 (6)
N2i—Fe1—N1i	88.79 (6)	N2—Fe1—N3	88.87 (6)
N2—Fe1—N1i	90.48 (7)	N1—Fe1—N3	177.63 (6)
N1—Fe1—N1i	90.61 (9)	N1i—Fe1—N3	89.07 (7)
N2i—Fe1—N3i	88.92 (9)	N3i—Fe1—N3	91.35 (9)
N2—Fe1—N3i	91.86 (6)	Symmetry code (i) $-x, y, -z+1/2$	

The flexibility of the dcpp ligand has allowed for improved bite angles around the metal center, coordinating in a helical fashion. A much more symmetrical environment is achieved as compared to the coordination environment of the rigid bpy and terpy ligands as shown in Figure 2-5.

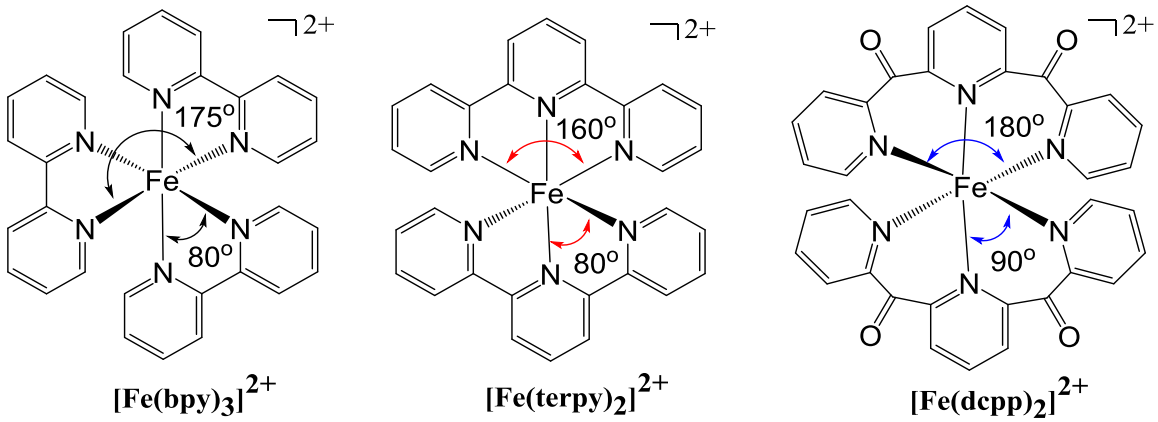

Figure 2-5. Structures of $[Fe(bpy)_3]^{2+}$, $[Fe(terpy)_2]^{2+}$, and $[Fe(dcpp)_2]^{2+}$ showing the coordination environment with approximate bond angles.

An important characteristic that a DSSC chromophore must possess is absorptivity in the visible region. Chromophores containing conjugated ligand systems, like bpy and terpy fit this criteria. The dcpp ligand is not conjugated in the normal sense of the word, but is cross-conjugated. A cross-conjugated compound is one in which there are three unsaturated groups, where two of them are conjugated to a third but are not conjugated to each other.[35] In the case of dcpp, the pyridyl rings are not conjugated to each other, but are each conjugated to the carbonyl groups. We were uncertain of the implications of this since cross-conjugated systems are considered to be much less able to promote electron delocalization than true conjugation, until recently that is. Recent theoretical investigations have found that the connectivity pattern in cross-conjugation will lead to enhanced electron delocalization effects for electronically excited states.[36]

From the optical absorption spectrum in Figure 2-6, we can see that the lack of a truly conjugated system is not detrimental to the molar absorptivity, and the oscillator strength was determined to be comparable for all three systems.[2] The sharp feature in the $[Fe(terpy)_2]^{2+}$ spectrum, that is not seen in the other two, arises from the delocalization

over the three rings, signifying that delocalization is in fact not extended across the entire dcpp ligand in the new complex. The red-shifted absorption maximum of the $[Fe(dcpp)_2]^{2+}$ is ideal for a sensitizer, as it covers more of the solar spectrum.

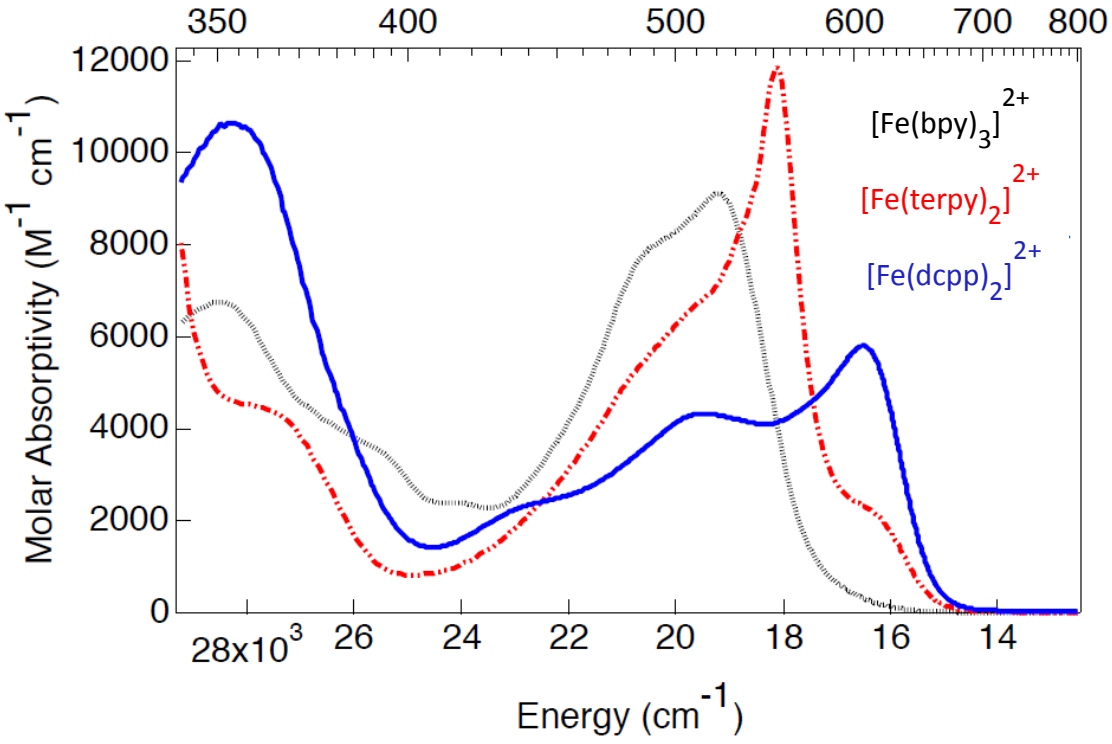

Figure 2-6. Ground state electronic absorption spectrum of $[Fe(bpy)_3]^{2+}$ (black), $[Fe(terpy)_2]^{2+}$ (red), and $[Fe(dcpp)_2]^{2+}$ (blue) in CH_3CN (collected by Allison Brown, adapted from reference 2).

When the dcpp ligand twists from its planar arrangement upon coordination the orbital overlap across the conjugated branches within one ligand will be disturbed. However, medium π-π stacking intramolecular interactions are observed between each ketone plane of one dcpp ligand and a peripheral pyridine ring of another dcpp ligand. The shortest inter-planar atom…atom separations and dihedral angles are 2.87 Å (19.3°) and 2.84 Å (18.8°) for the stacked pairs, respectively, with the center-to-center separations of these stacked pairs of 3.26 Å and 3.40 Å. The cooperative effects of inter-

ligand interactions might be a reason for the formation of the tight coordination of Fe(II) core.

Carbonyl lone pair (l.p.)—π interactions have recently been recognized as significant supramolecular bonding contacts by the scientific community.[37–41] The importance of these l.p.—π interactions were first recognized in biological macromolecules nearly twenty years ago, but this interaction was seemingly overlooked in small synthetic molecules as they have been rarely reported.[42] Mooibroek et al. performed a detailed analysis of the Cambridge Structure Database and found that these carbonyl l.p.—π interactions are not uncommon with nearly 6000 occurances.[39] The authors note that the majority of these contacts with benzene rings are weak and the incorporation of nitrogen into the ring strengthens this interaction. Electron deficiency of the pyridine ring clearly induces the formation of stronger l.p.—π interaction.

In the case of the $[Fe(dcpp)_2]^{2+}$, the π-acidic nature of the pyridine rings and metal coordination induced polarization both favor the carbonyl l.p.—π interaction. This is quite noteworthy since the metal coordination induced polarization is also known to facilitate nucleophilic addition at the carbonyl carbon in other complexes with the dcpp ligand. The formation of this particular molecule is likely aided by this l.p.—π interaction, stabilizing the carbonyl in addition to stabilizing the entire molecule.

From the crystal structure data of $[Fe(dcpp)_2]^{2+}$ we determined the distance (d) between the centroid of the terminal pyridine rings to the oxygen of the carbonyl bridges on the opposing ligand to be 3.351-3.365 Å. The carbonyl stacks with the pyridyl ring in a nearly planar arrangement with 18.8-19.3^{o} angle between planes. Preliminary DFT

calculations suggest the significant interligand π interactions, may facilitate delocalization over the entire molecule as shown in Figure 2-7.

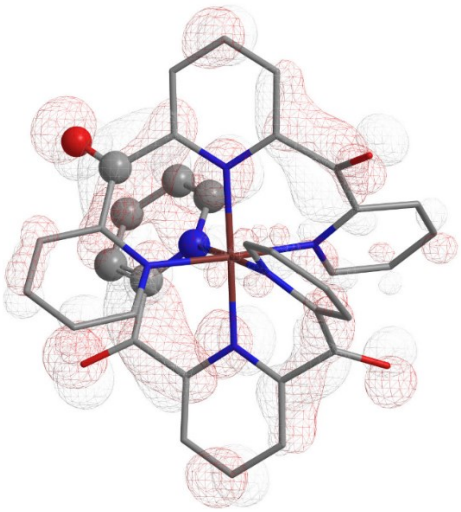

d (centroid to O) = 3.351 – 3.365 Å
ω (angle between planes) = 18.8-19.3°

Figure 2-7. Results from a TD-DFT calculation on $[Fe(dcpp)_2]^{2+}$ showing the interligand π stacking interaction between the carbonyl of one ligand with the pyridyl ring of the other. Also shown is the schematic of the structural parameters determined from the crystal structure used to characterize the l.p.—π contact.

The electrochemistry, photoluminescence investigation, and proposed effects of symmetry on ligand field strength are described in detail elsewhere, but in the interest of being thorough will also be mentioned here.[2] The electrochemistry of $[Fe(dcpp)_2]^{2+}$ was found to differ greatly from $[Fe(bpy)_2]^{2+}$ and $[Fe(terpy)_2]^{2+}$, with the oxidation and first reduction potentials being much more positive (Table 2-4). The electrochemical behavior is attributed to the electron withdrawing carbonyls along with better metal ligand overlap.

Table 2-4. Electrochemical potentials for the oxidation and first reduction of $[Fe(bpy)_3](PF_6)_2$, $[Fe(terpy)_2](PF_6)_2$, and $[Fe(dcpp)_2](PF_6)_2$, measured with $Ag/AgNO_3$ reference with 0.1 M $TBAPF_6$ electrolyte in acetonitrile, externally referenced to ferrocene (adapted from reference 2).

Compound	E 1 / 2 [ox]	E 1 / 2 [red]
$[Fe(bpy)_3]^{2+}$	0.665 V	-1.775 V
$[Fe(terpy)_2]^{2+}$	0.715 V	-1.675 V
$[Fe(dcpp)_2]^{2+}$	1.295 V	-0.965 V

There are four distinct reductions which are facilitated by the electron withdrawing carbonyls. The significant shift of the oxidation potential is consistent with the inductive influence of ligand substituents on the Fe(II)/Fe(III) redox couple, with more electron withdrawing groups leading to a more positive redox couple.[43] This inductive effect appears to be more significant as compared to substituted terpy ligands, likely due to enhanced metal ligand overlap and stronger π accepting capacity of the ligand, leading to larger ligand field splitting and stabilization of the t_{2g} set.

A stronger ligand field may be achieved by improving metal ligand orbital overlap by expanding the coordination environment. The lower energy of the ligand-based π*-orbitals leads to a better energetic match with the π-symmetry d-orbitals of the metal center, stabilizing the t_{2g} set. This allows us to propose the molecular orbital diagrams in Figure 2-8, depicting the effect that the structural differences have on the ligand field splitting.

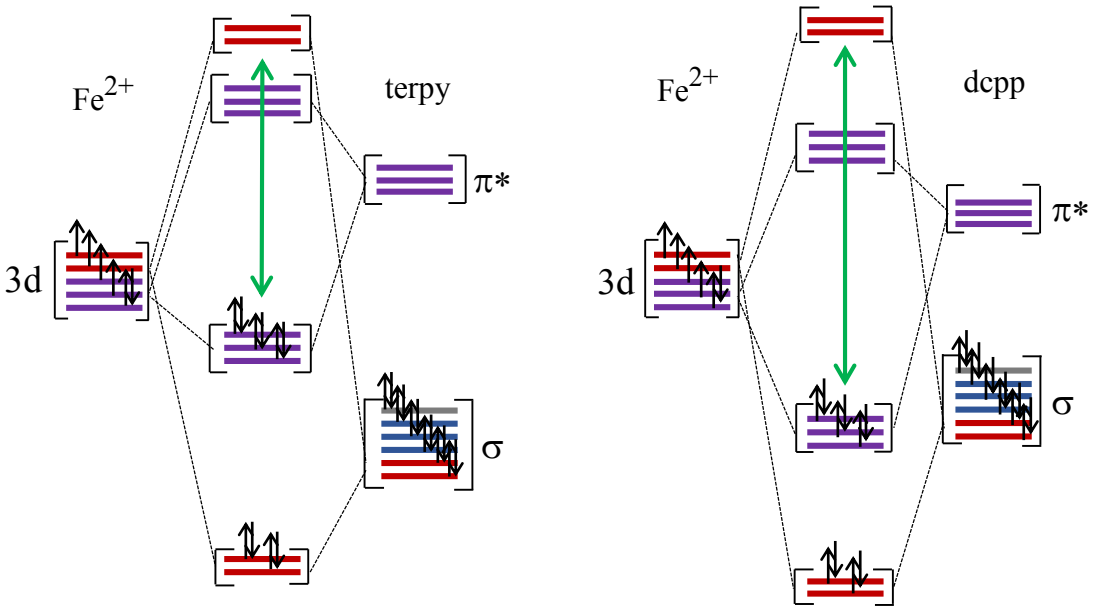

Figure 2-8. Proposed molecular orbital diagrams of $Fe(terpy)_2]^{2+}$ (left) and $Fe(dcpp)_2]^{2+}$ (right) showing effects of ligand orbital movement on ligand field splitting.

We are currently investigating whether we have increased the ligand field strength sufficiently to result in an inversion of the lowest energy excited states from the $^5T_2$ to $^3T_1$. Preliminary photoluminescence experiments have provided evidence for weak emission, suggesting that we may be accessing a triplet ligand field state. Weak emission was detected in a 9:2 butyronitrile/propionitrile glass at 80 K at 800 nm, which is at the limit of our detector so further evidence was required.[2] A solid-state emission experiment was performed by Christian Reber at the Université de Montréal who also found evidence of photoluminescence, with the presence of weak emission at low temperature centered around 700 nm. As for other possible sources of the photoluminescence, we cannot rule out the ^{3}MLCT state, an emissive impurity, or a ligand based effect. In order to narrow down the source of the emission, it is crucial to develop a control molecule.

2.3.5 Quest for a Control Molecule

In the review of the coordination chemistry of di(2-pyridyl)ketone (dkp) and 2,6-di(2-carboxypyridyl)pyridine (dcpp) the authors state "at the outset of our efforts we were aware that such ligands could not be incorporated in metal complexes in, e.g. aqueous or alcoholic reaction media."[9] I seem to have stumbled upon the exception to the rule with the coordination of iron(II) and was not optimistic to find a second when setting out to prepare a control analog.

The first choice for a control molecule is the zinc(II) analog. Being a first row transition metal as well as having a divalent charge would make it the most isostructural with the Fe(II) analog, while at the same time provide insight from the absence of d-d transitions. Coordination chemistry of Zn(II) with dcpp is unknown in the literature, but Zn(II) with dpk has been widely investigated in the context of polynuclear cluster chemistry.[9,44–46] Dpk is highly sensitive to the reaction media in reactions with zinc, and although rare, can remain intact in a reaction.[44] In most cases the carbonyl is hydrated, even by trace amounts of water in the solvent or in the starting materials.[45]

Many routes were attempted employing various Zn(II) reagents, solvents, and reaction conditions. Most of the zinc(II) reagents are hydrates, so even in the situations where dry solvent is used, the reaction fails to yield any of the desired product (by ESI-MS). The instance in the literature where the ligand remained intact was accomplished by adding $ZnCl_2$ to dkp in acetonitrile and layering in hexane/ether and allowing to sit. This method was attempted with $ZnCl_2$ and dcpp in the inert atmosphere dry box, and even under these dry, mild conditions there was no evidence of the desired product.

Coordination of 2,6-di(2-methylenepyridyl)pyridine, dmpp, to Zn(II) is possible but attempts to oxidize the ligand after coordination are too harsh and strip the ligand from the metal. After many fruitless attempts I changed direction toward the preparation of a gallium(III) analog.

Gallium is not technically a transition metal, but a post-transition metal, or poor metal, in the p-block of the periodic table with a common oxidation state of +3 which is d^{10}. A difference in oxidation state is not ideal, but due to the difficulty encountered with the Zn(II) chemistry, it was worth pursuing. The coordination chemistry of Ga(III) is rather unexplored, but medicinal applications have sparked more interest in the field. The survey of the literature by Bandoli et al. found only 17 homoleptic bis-tridentate Ga(III) compounds, with only 6 of these being meridionally bound.[47] Ga(III) not only binds to nitrogen, but readily coordinates to oxygen, also the tendency of Ga to form hydroxo-bridged dimers raised many concerns. Despite the apprehension, the wide availability and ease of preparation of anhydrous reagents made it worth a shot.

To avoid any of the hydration problems with the reactive carbonyl of dcpp and the propensity of the formation of hydroxo-bridges dimers of gallium, every effort was made to exclude water. Reactions utilizing the commercially available anhydrous gallium(III) isopropoxide, gallium(III)chloride, and gallium(III) iodide were attempted with no success. In exploring the literature, I stumbled upon an interesting gallium reagent that was used to prepare $[Ga(bpy)_3]^{3+}$.[48] The researchers found that the reaction of "GaI" with one equivalent of bpy in toluene unexpectedly led to the high yield formation of $[Ga(bpy)_3]I_3$. They found that presence of water led to the formation of gallium dimers,

but since water may easily be excluded from the reaction in toluene, this route was pursued.

"GaI" is a very interesting, easily prepared reagent, that was recently reviewed highlighting its versatility in organic synthesis and gallium cluster formation.[49] GaI appeared in the literature in 1955 and identity of its formulation has been redetermined numerous times.[50–53] The currently accepted formulation is a mixture of sub-iodides and predominately exists as the mixed valence salt $[(Ga^{+})_2][Ga_2I_6^{2-}]$. The reagent is simply prepared by sonication of elemental gallium and iodine in toluene at 30°C. "GaI" is used in disproportionation reactions in which gallium(III) complexes form, accompanied by the deposition of elemental gallium which may be easily removed from the reaction.[48,54] Unfortunately, attempts to prepare $[Ga(dcpp)_2]^{3+}$ employing "GaI" have failed.

One last ditch effort with the gallium chemistry was based off of the work by Manessi et al.[55] They prepared the only known homoleptic, bis-tridentate gallium(III) complex in which the ligand coordinates strictly through nitrogens. They utilized $(Et_4N)[GaCl_4]$ which is simply prepared from Et_4NCl and $GaCl_3$ in ethanol to synthesize the target molecule. An analogous method was attempted for the preparation $[Ga(dcpp)_2]^{3+}$, but not surprisingly, has also failed to yield any of the desired product.

Looking back at the hydration behavior of dkp it is important to note that metals in high oxidation states facilitate the hydration while low oxidation states hinder it.[56] This may be why Ga(III) has been difficult. A second point to note is that the hydration behavior is attributed to steric strain imposed on the carbonyl carbon upon complexation. The small size of Zn(II) and Ga(III) may be contributing to the transformation of the ketone in dcpp. Investigating other options for a control molecule, we thought about

cadmium(II). We were hesitant to move to second row transition metals, but since the larger size may alleviate some of the strain it was a viable option.

Finally, the quest for a control molecule began to yield some positive results, $[Cd(dcpp)_2]^{2+}$ has been successfully prepared under a variety of conditions (Scheme 2-6). Reactions employing $Cd(NO_3)_2 \cdot 4H_2O$, anhydrous $Cd(CH_3CO_2)_2$ and $Cd(ClO_4)_2 \cdot xH_2O$ in either acetonitrile or ethanol have produced the target molecule. As was the case with the iron(II) analog, the reaction is plagued by byproduct formation. Cd(II) ions are used to prepare metal organic coordination polymers and from the ESI-MS it appears that polymerization may be occurring.[57,58] To date, all attempts to purify the complex have been unsuccessful. Avoiding hydrated Cd(II) reagents and alcohol or aqueous solvents would be preferable, but we encounter solubility issues with anhydrous reagents in anhydrous solvents, and attempts to prepare the complex under these conditions have not produced results.

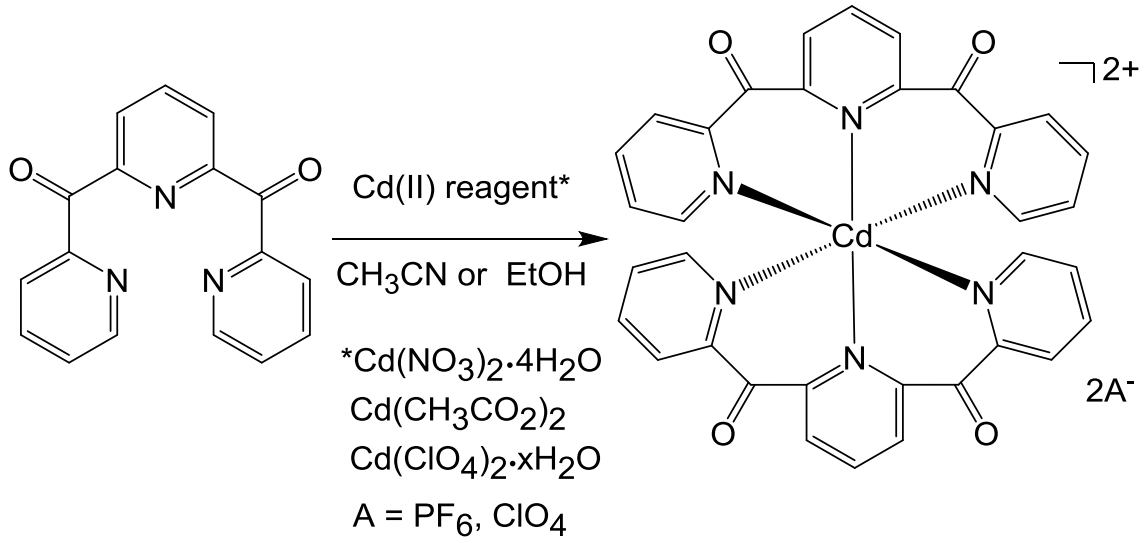

Scheme 2-6. Synthesis of $[Cd(dcpp)_2]^{2+}$.

An alternate course of action toward the preparation of $[Cd(dcpp)_2]^{2+}$ was to synthesize it by the route of Schramm et al. by simultaneous coordination/ligand oxidation (vide supra). Air must not be an efficient oxidant in this case since $[Cd(dmpp)_2]^{2+}$ forms with no evidence of $[Cd(dcpp)_2]^{2+}$. The synthesis of $[Cd(dmpp)_2](PF_6)_2$ was adjusted to allow for cleaner isolation and was prepared in 72% yield according to Scheme 2-7. Our current efforts are now directed at oxidizing the ligand after complexation.

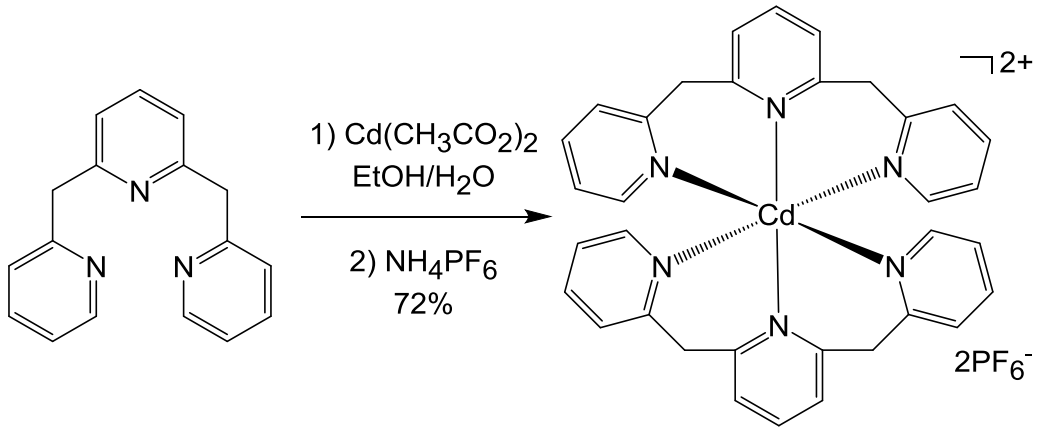

Scheme 2-7. Synthesis of $[Cd(dmpp)_2](PF_6)_2$.

A variety of oxidation procedures have been attempted with little success. The selenium dioxide catalyzed procedure that was used to prepare the dcpp ligand was found to be too harsh as it strips the ligand from the metal center. Mild sodium periodate mediated procedures have also been attempted, but led to the same result.[59,60] Air would be the ideal oxidant, but prolonged heating in DMF while being bubbled with air resulted in no change, signifying the need for a catalyst. Auto-oxidation of carbon acids can be achieved utilizing potassium *t*-butoxide as a catalyst, but again this would likely wreak havoc on the metal complex.[61] Looking into other options for a catalyst, we thought

about activated carbon. Activated carbon is commonly employed as a catalyst support, but it actually possesses catalytic activity on its own due to the surface oxides and structure. I attempted the same procedure of heating in DMF while bubbling with air, but this time in the presence of activated carbon, and achieved the best result to date (Scheme 2-8). This seems to be the most promising route as the major products are the desired complex and dcpp, without evidence of the high mass byproducts that were formed in the previous methods. Efforts are ongoing with this reaction to find the right temperature conditions to limit the degradation of the metal complex.

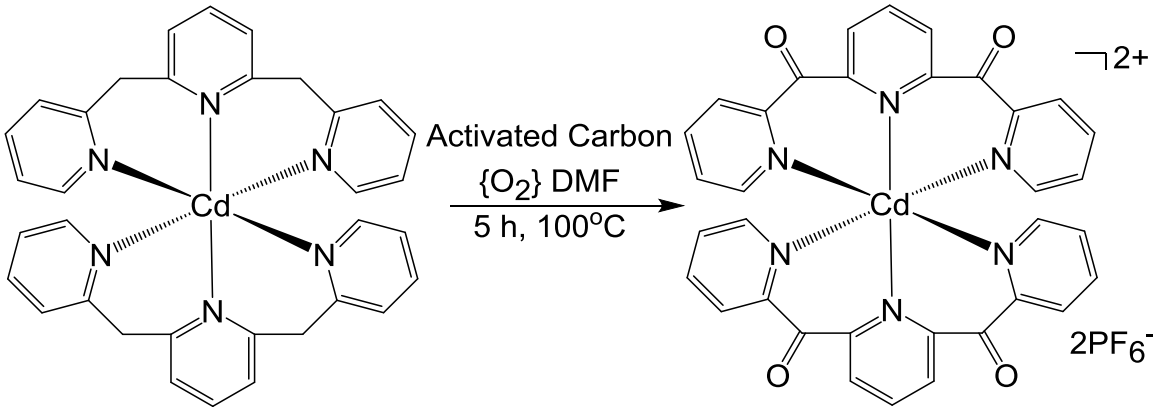

Scheme 2-8. Synthesis of $[Cd(dcpp)_2](PF_6)_2$ via oxidation of $[Cd(dmpp)_2](PF_6)_2$.

A new approach with the cadmium(II) chemistry that we are just beginning to look at involves protection of the carbonyl. Protection of the carbonyl groups of dcpp is readily achieved by the traditional route of acid catalyzed ketalization as shown in Scheme 2-8.[17] Much higher yields are common with this chemistry and will likely be achieved in due course, but to date this reaction was performed only once, suffered from incomplete conversion, and yet to be optimized.

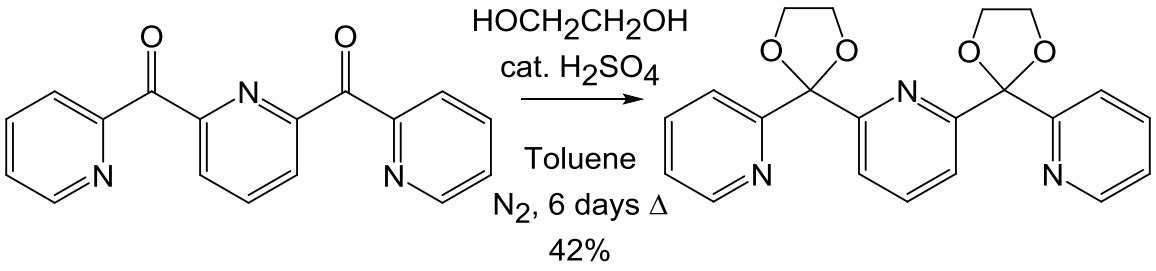

Scheme 2-9. Synthesis of 2,6-di(2-ketalpyridyl)pyridine (dkpp).

Initially there was much reluctance toward pursuing protection chemistry since deprotection commonly employs harsh hydrolytic conditions.[17,62] Also, sterics of a protected ligand may present an issue to complex formation, but researchers have found that the ketal protected dkp can coordinate to Cu(II), Co(II), Ni(II), and Pd(II), so hopefully this will not be an issue.[63,64] If the protected dkpp ligand can even bind, it is crucial that the complex remain intact upon deprotection so mild conditions are necessary. Mild deprotection methods have recently been developed that are much more promising for this chemistry.[65–68] To date, the coordination of dkpp to Cd(II) is yet to be attempted, but if successful, a promising deprotection method developed by Sun et al. will be pursued.[65] Deprotection is achieved under extremely mild conditions by catalytic iodine in acetone that can provide high yields in just minutes under neutral conditions.[65]

2.4 Concluding comments

A highly symmetric iron(II) polypyridyl complex with some very exciting properties has been successfully prepared. Unexpectedly, the coordination of the highly reactive of 2,6-di(2-carboxypyridyl)pyridine ligand to iron(II) proceeds smoothly in aqueous solution, against all precedence in the literature. The resulting complex provides

a good starting point toward the investigation of the effect of geometry on the ultrafast dynamics of iron(II) polypyridyls. Though we have not achieved the overall goal of slowing down the charge transfer deactivation to the ligand field state,[2] we may have developed an iron(II) complex with a strong enough ligand field to achieve inversion of the lowest energy excited state. The pursuit for a control molecule is ongoing and necessary to gain more information on this system.

APPENDIX

APPENDIX

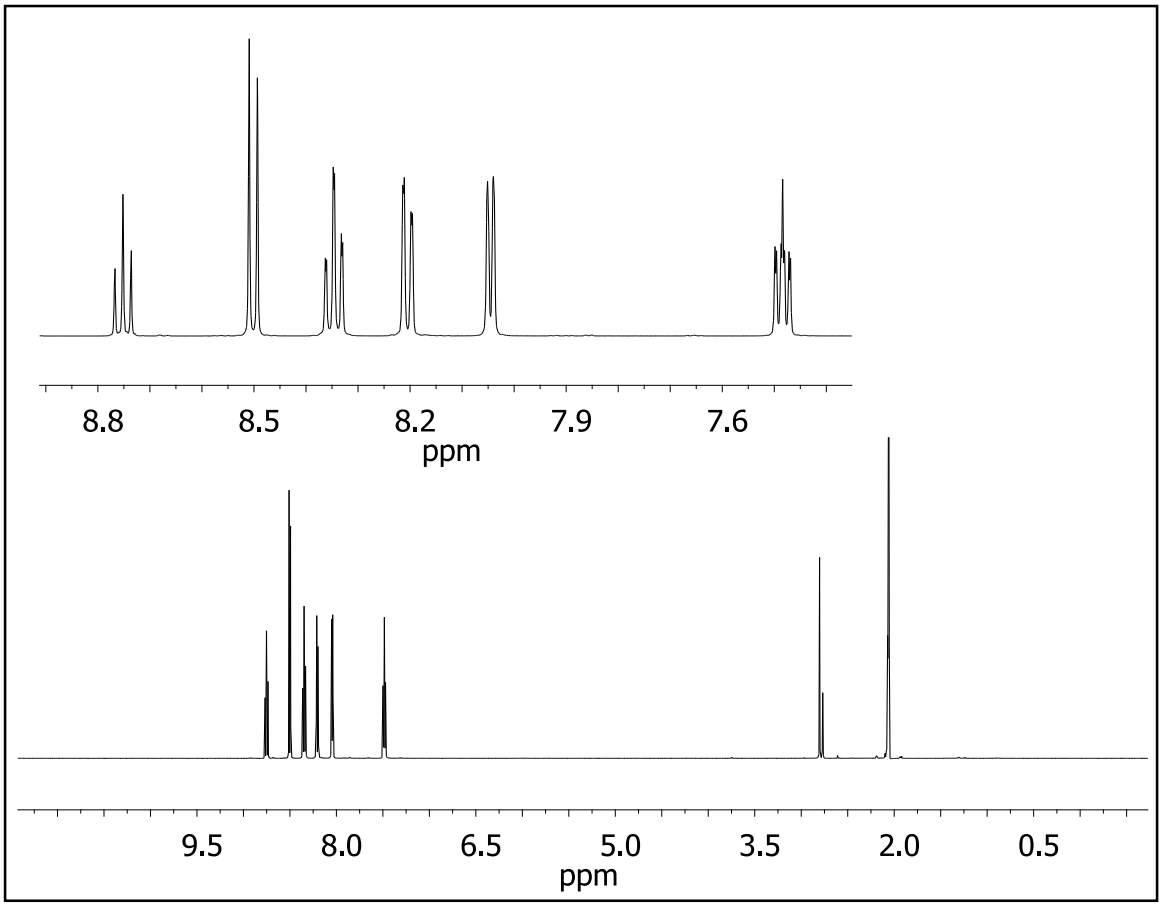

Figure 2-9. ^{1}H NMR spectrum of $[Fe(dcpp)_2](PF_6)_2$ in $(CD_3)_2CO$.

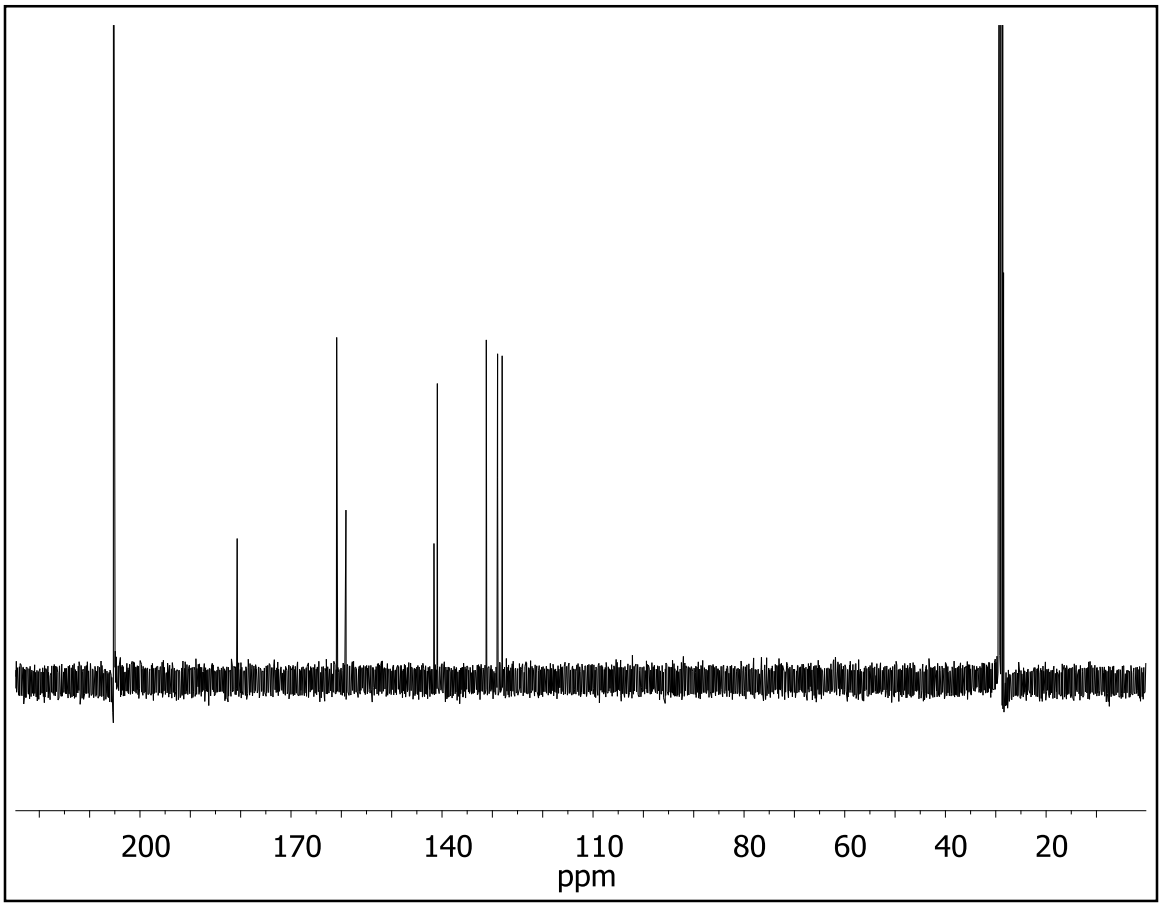

Figure 2-10. ^{13}C NMR spectrum of $[Fe(dcpp)_2](PF_6)_2$ in $(CD_3)_2CO$.

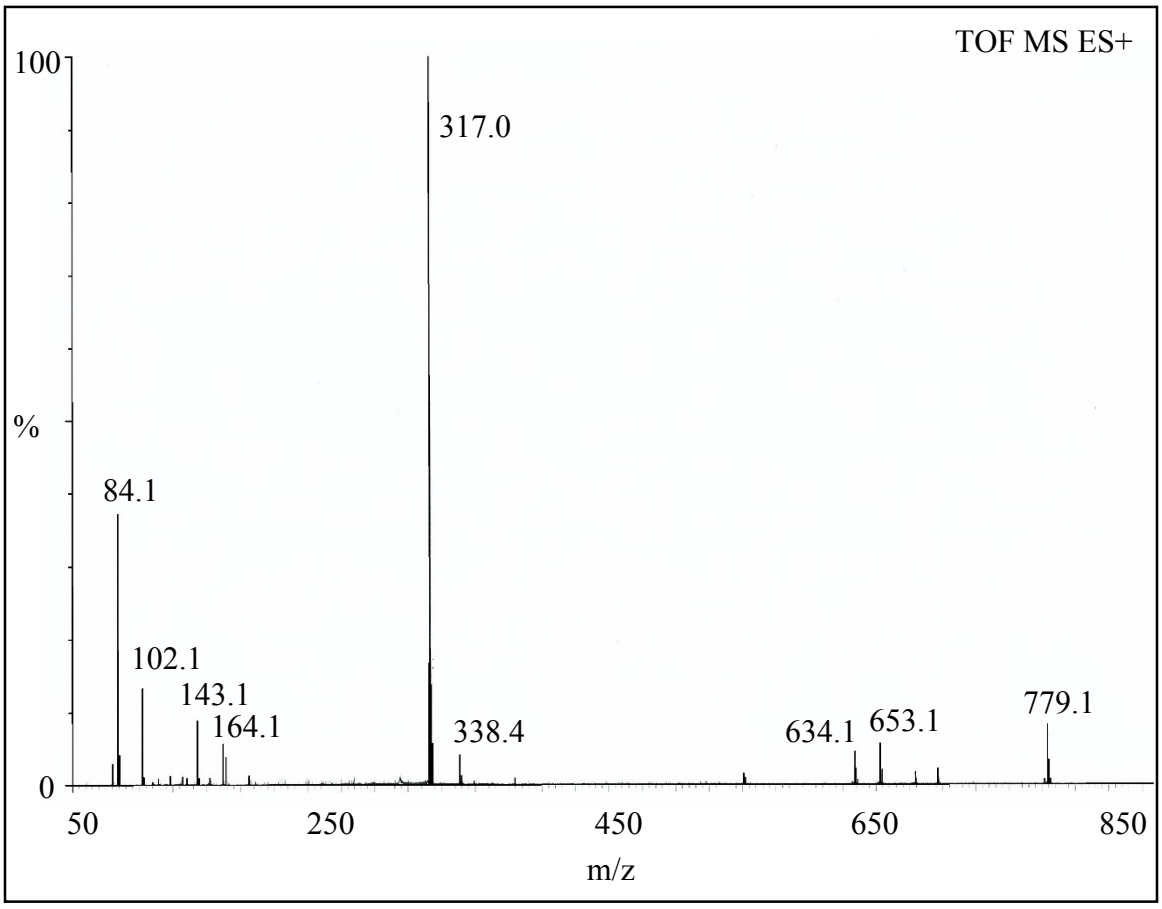

Figure 2-11. ESI-MS $[Fe(dcpp)_2](PF_6)_2$.

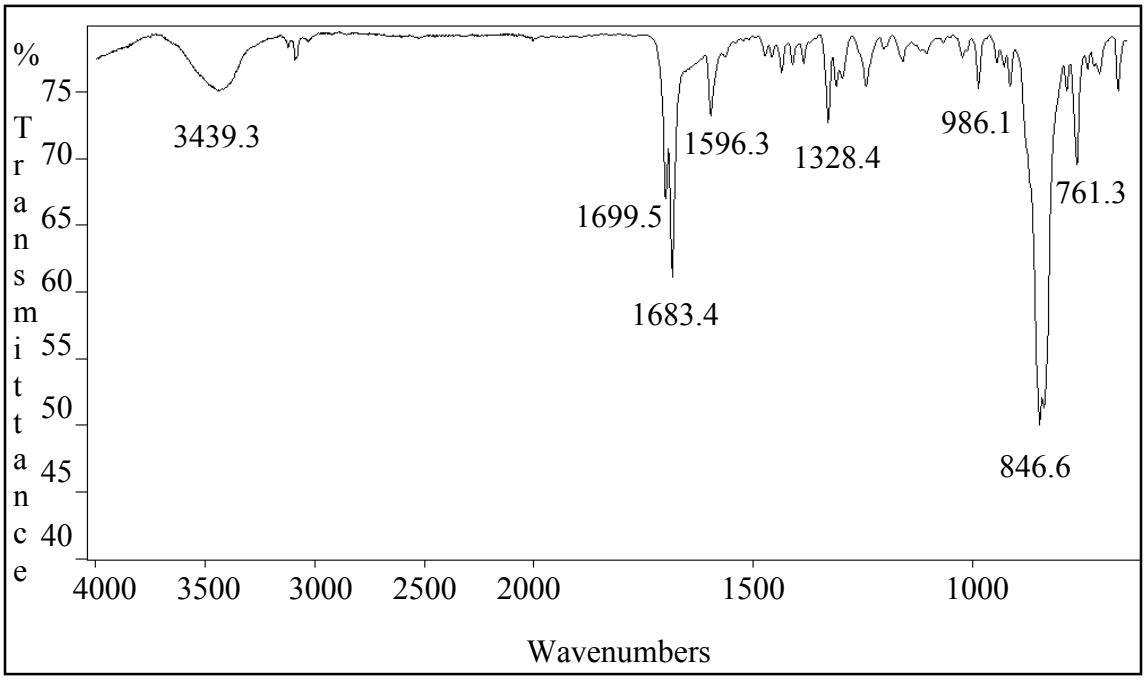

Figure 2-12. IR spectrum of $[Fe(dcpp)_2](PF_6)_2$

Table 2-5. Geometric parameters for the X-ray crystal structure of $[Fe(dcpp)_2](PF_6)_2$.

Bond Lengths (Å)			
Fe1—N2	1.9737 (17)	C8—H8A	0.9300
Fe1—N2i	1.9738 (17)	C9—C10	1.384 (3)
Fe1—N1i	1.9844 (15)	C9—H9A	0.9300
Fe1—N1	1.9845 (15)	C10—C11	1.388 (3)
Fe1—N3	1.9893 (15)	C10—H10A	0.9300
Fe1—N3i	1.9893 (15)	C11—C12	1.502 (3)
O1—C6	1.213 (2)	C12—C13	1.493 (3)
O2—C12	1.211 (2)	N3—C17	1.353 (2)
N1—C1	1.346 (3)	N3—C13	1.359 (2)
N1—C5	1.358 (2)	C13—C14	1.389 (3)
C1—C2	1.385 (3)	C14—C15	1.389 (3)
C1—H1A	0.9300	C14—H14A	0.9300
C2—C3	1.375 (3)	C15—C16	1.385 (3)
C2—H2A	0.9300	C15—H15A	0.9300
C3—C4	1.386 (3)	C16—C17	1.380 (3)
C3—H3A	0.9300	C16—H16A	0.9300
C4—C5	1.387 (3)	C17—H17A	0.9300
C4—H4A	0.9300	P1—F1	1.5783 (14)
C5—C6	1.499 (3)	P1—F2	1.5910 (16)
N2—C11	1.351 (2)	P1—F5	1.5960 (14)
N2—C7	1.359 (2)	P1—F3	1.6043 (16)
C6—C7	1.503 (3)	P1—F6	1.6152 (14)
C7—C8	1.387 (3)	P1—F4	1.6156 (14)
C8—C9	1.385 (3)		
Bond Angles (o)			
N2—Fe1—N2i	178.96 (8)	C10—C9—C8	118.4 (2)
N2—Fe1—N1i	90.48 (7)	C10—C9—H9A	120.8
N2i—Fe1—N1i	88.79 (6)	C8—C9—H9A	120.8
N2—Fe1—N1	88.79 (6)	C9—C10—C11	119.12 (18)
N2i—Fe1—N1	90.48 (7)	C9—C10—H10A	120.4
N1i—Fe1—N1	90.61 (9)	C11—C10—H10A	120.4
N2—Fe1—N3	88.87 (6)	N2—C11—C10	123.31 (17)
N2i—Fe1—N3	91.86 (6)	N2—C11—C12	119.35 (16)
N1i—Fe1—N3	89.07 (7)	C10—C11—C12	117.13 (16)
N1—Fe1—N3	177.63 (6)	O2—C12—C13	122.36 (17)
N2—Fe1—N3i	91.86 (6)	O2—C12—C11	121.24 (17)
N2i—Fe1—N3i	88.87 (6)	C13—C12—C11	115.58 (15)
N1i—Fe1—N3i	177.63 (6)	C17—N3—C13	117.05 (15)
N1—Fe1—N3i	89.07 (7)	C17—N3—Fe1	122.23 (12)
N3—Fe1—N3i	91.35 (9)	C13—N3—Fe1	120.63 (12)
C1—N1—C5	117.25 (16)	N3—C13—C14	123.05 (18)
C1—N1—Fe1	121.21 (13)	N3—C13—C12	118.69 (15)
C5—N1—Fe1	120.94 (13)	C14—C13—C12	117.92 (16)

Table 2-5 (cont'd)

N1—C1—C2	122.75 (18)	C15—C14—C13	118.65 (18)
N1—C1—H1A	118.6	C15—C14—H14A	120.7
C2—C1—H1A	118.6	C13—C14—H14A	120.7
C3—C2—C1	119.43 (19)	C16—C15—C14	118.68 (18)
C3—C2—H2A	120.3	C16—C15—H15A	120.7
C1—C2—H2A	120.3	C14—C15—H15A	120.7
C2—C3—C4	118.72 (19)	C17—C16—C15	119.53 (19)
C2—C3—H3A	120.6	C17—C16—H16A	120.2
C4—C3—H3A	120.6	C15—C16—H16A	120.2
C3—C4—C5	118.95 (19)	N3—C17—C16	122.83 (17)
C3—C4—H4A	120.5	N3—C17—H17A	118.6
C5—C4—H4A	120.5	C16—C17—H17A	118.6
N1—C5—C4	122.54 (18)	F1—P1—F2	91.46 (9)
N1—C5—C6	119.61 (16)	F1—P1—F5	91.42 (8)
C4—C5—C6	117.68 (17)	F2—P1—F5	90.78 (9)
C11—N2—C7	116.81 (17)	F1—P1—F3	90.33 (9)
C11—N2—Fe1	121.34 (12)	F2—P1—F3	178.01 (9)
C7—N2—Fe1	121.65 (12)	F5—P1—F3	90.02 (8)
O1—C6—C5	120.26 (17)	F1—P1—F6	179.03 (9)
O1—C6—C7	119.44 (18)	F2—P1—F6	89.01 (8)
C5—C6—C7	119.75 (16)	F5—P1—F6	89.42 (7)
N2—C7—C8	122.65 (17)	F3—P1—F6	89.18 (8)
N2—C7—C6	120.20 (17)	F1—P1—F4	90.54 (8)
C8—C7—C6	117.13 (17)	F2—P1—F4	89.67 (9)
C9—C8—C7	119.58 (18)	F5—P1—F4	177.98 (8)
C9—C8—H8A	120.2	F3—P1—F4	89.47 (9)
C7—C8—H8A	120.2	F6—P1—F4	88.62 (7)
N1—C1—C2	122.6 (3)	C13—C14—C15	118.6 (2)
N1—C1—H1A	118.7	C13—C14—H14A	120.7
C2—C1—H1A	118.7	C15—C14—H14A	120.7
C3—C2—C1	119.3 (3)	C16—C15—C14	119.0 (3)
C3—C2—H2A	120.3	C16—C15—H15A	120.5
C1—C2—H2A	120.3	C14—C15—H15A	120.5
C2—C3—C4	119.1 (3)	C15—C16—C17	119.5 (3)
C2—C3—H3A	120.5	C15—C16—H16A	120.2
C4—C3—H3A	120.5	C17—C16—H16A	120.2
C3—C4—C5	118.7 (3)	N3—C17—C16	122.7 (2)
C3—C4—H4A	120.6	N3—C17—H17A	118.6
C5—C4—H4A	120.6	C16—C17—H17A	118.6
N1—C5—C4	122.7 (2)	O6A—P1—O5A	91.35 (13)
N1—C5—C6	119.7 (2)	O6A—P1—O2A	91.40 (11)
C4—C5—C6	117.5 (2)	O5A—P1—O2A	90.54 (12)
C11—N2—C7	116.7 (2)	O6A—P1—O4A	90.39 (13)
C11—N2—Fe1	121.29 (17)	O5A—P1—O4A	178.14 (13)

Table 2-5 (cont'd)

C7—N2—Fe1	121.81 (17)	O2A—P1—O4A	90.09 (12)
O1—C6—C5	120.0 (2)	O6A—P1—O3A	90.56 (12)
O1—C6—C7	119.9 (2)	O5A—P1—O3A	89.83 (13)
C5—C6—C7	119.5 (2)	O2A—P1—O3A	178.00 (11)
N2—C7—C8	122.8 (2)	O4A—P1—O3A	89.49 (12)
N2—C7—C6	120.3 (2)	O6A—P1—O1A	179.04 (13)
C8—C7—C6	116.8 (2)	O5A—P1—O1A	89.22 (12)
C9—C8—C7	119.6 (3)	O2A—P1—O1A	89.36 (10)
C9—C8—H8A	120.2	O4A—P1—O1A	89.03 (12)
C7—C8—H8A	120.2	O3A—P1—O1A	88.68 (10)

Symmetry codes: (i) $-x, y, -z+1/2$.

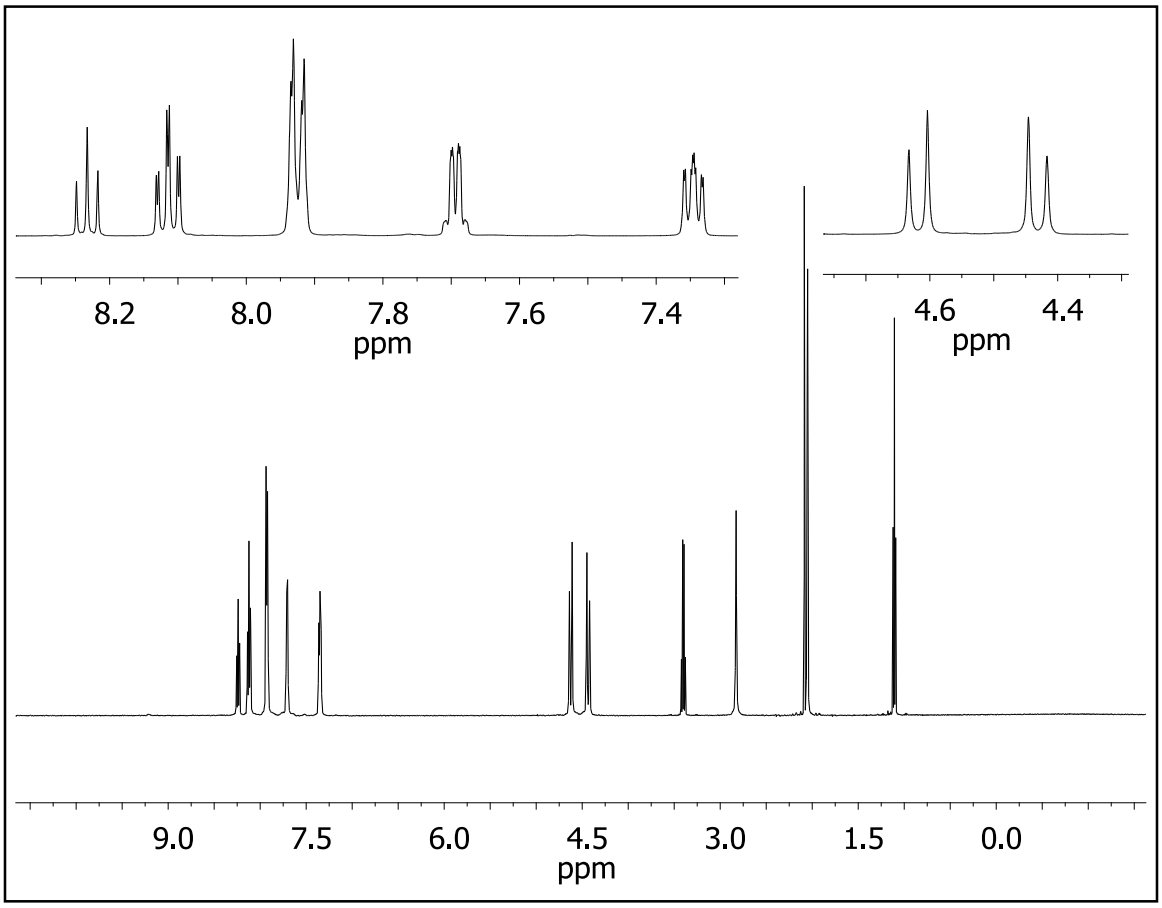

Figure 2-13. ^{1}H NMR spectrum of $[Cd(dmpp)_2](PF_6)_2$ in $(CD_3)_2CO$.

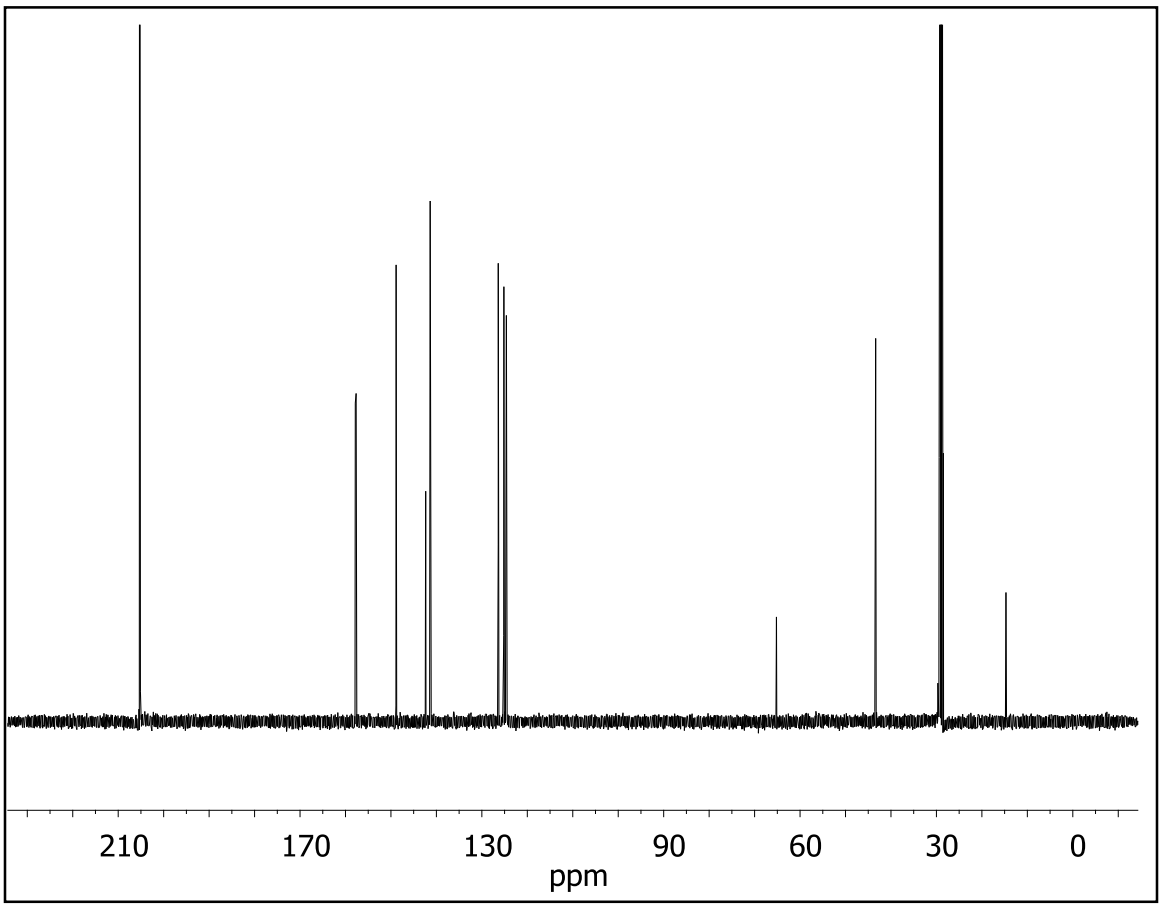

Figure 2-14. ^{13}C NMR spectrum of $[Cd(dmpp)_2](PF_6)_2$ in $(CD_3)_2CO$.

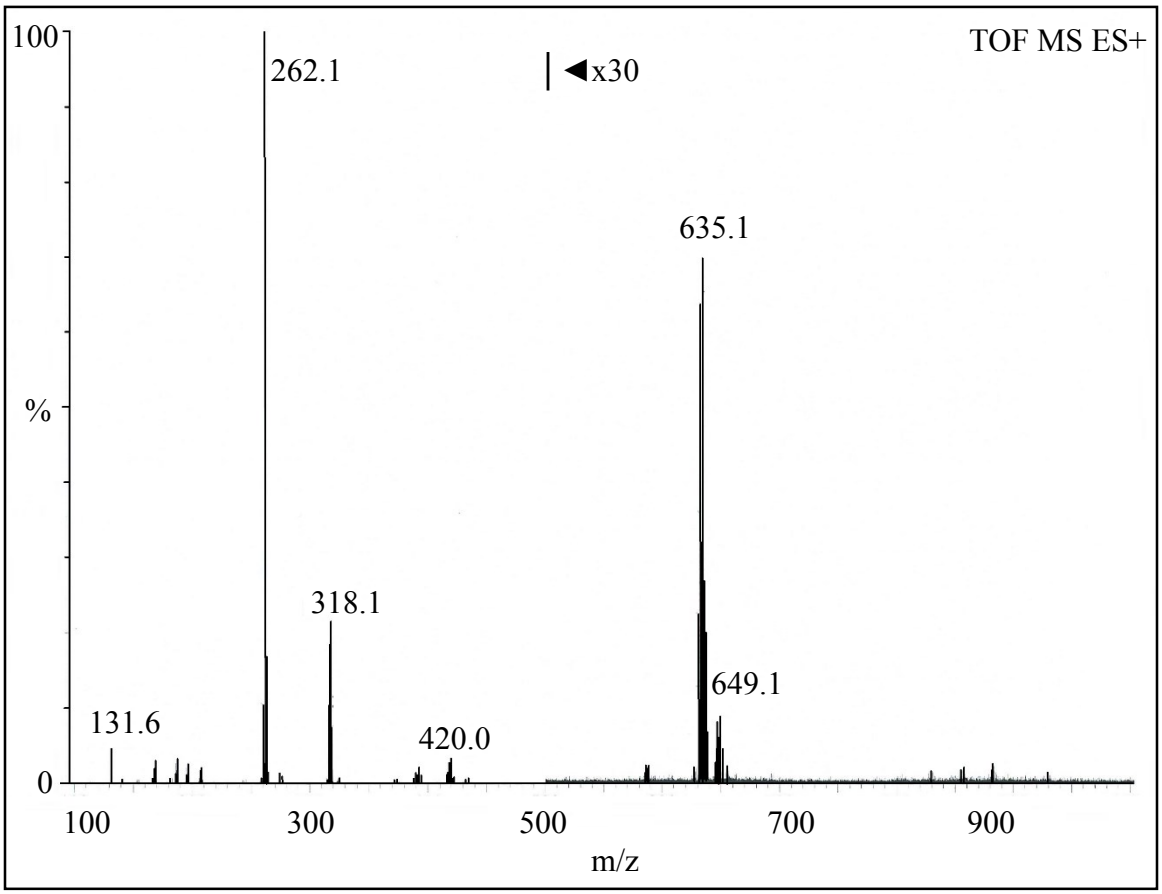

Figure 2-15. ESI-MS of $[Cd(dmpp)_2](PF_6)_2$.

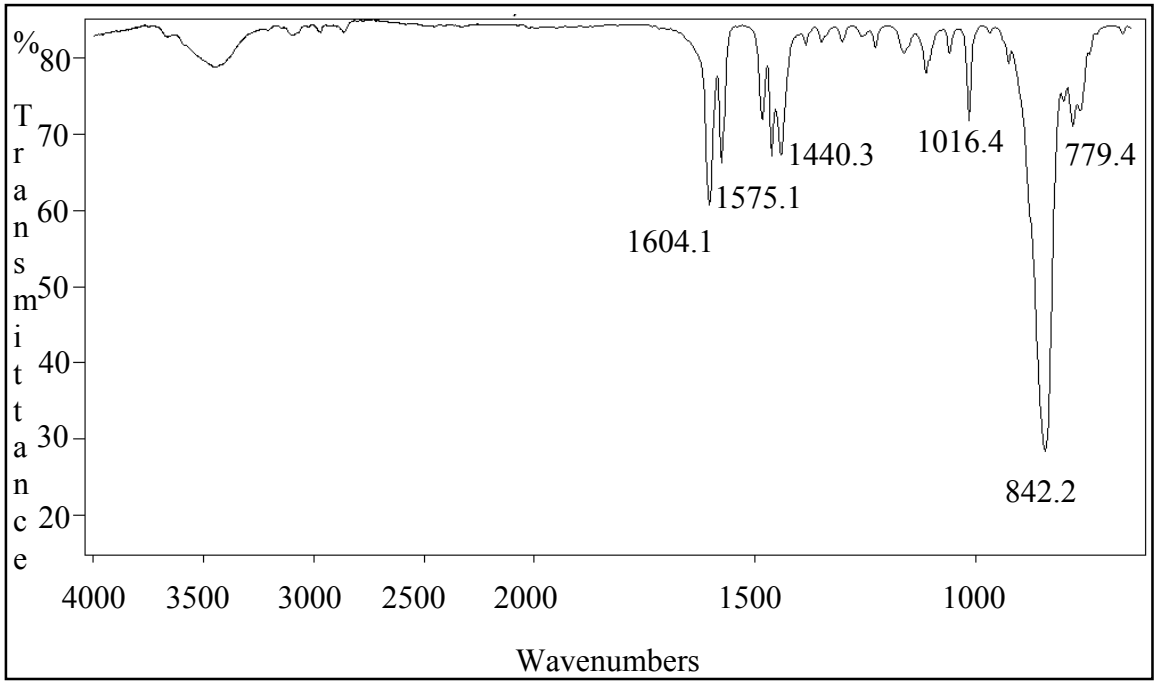

Figure 2-16. IR spectrum of $[Cd(dmpp)_2](PF_6)_2$.

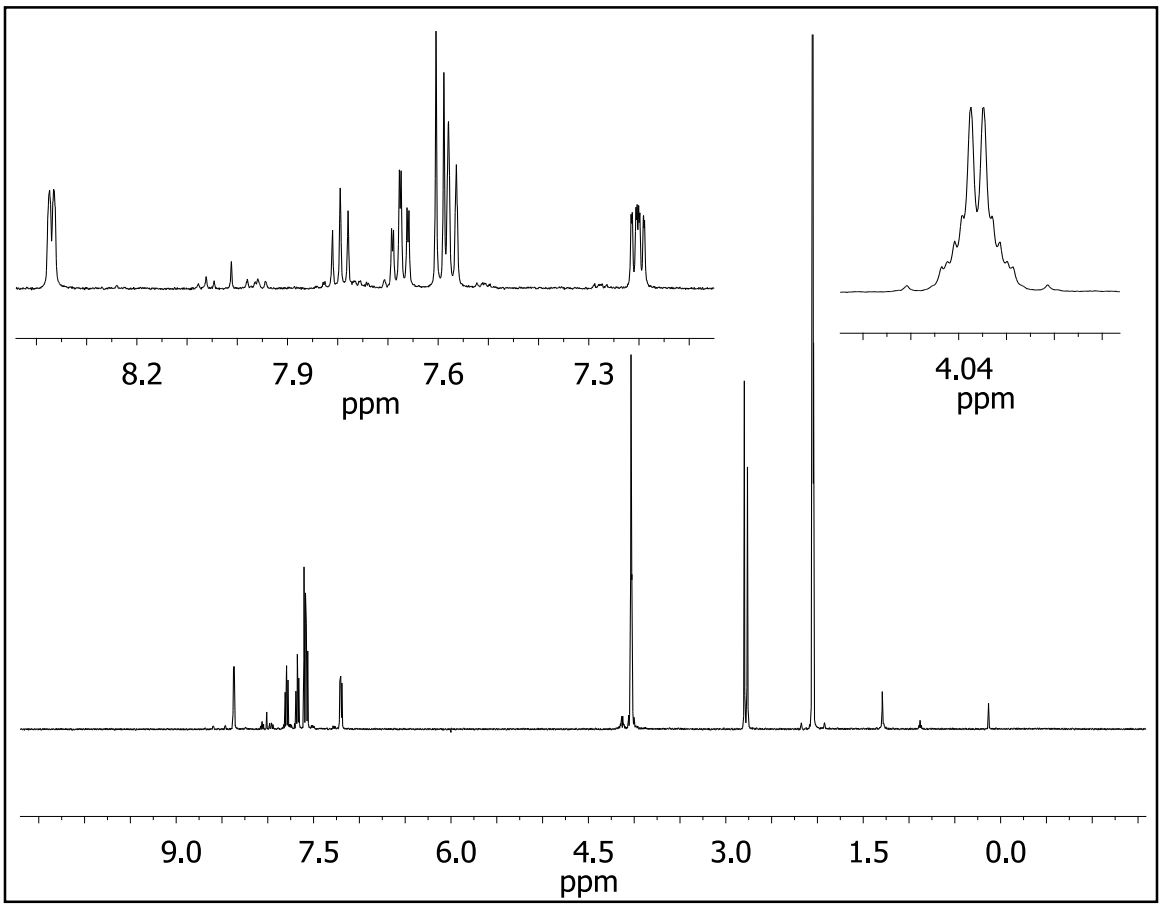

Figure 2-17. ^{1}H NMR spectrum of 2,6-di(2-ketalpyridyl)pyridine (dkpp) in $(CD_3)_2CO$. Following recrystallization the spectrum is less resolved, therefore the spectrum of the crude material is shown.

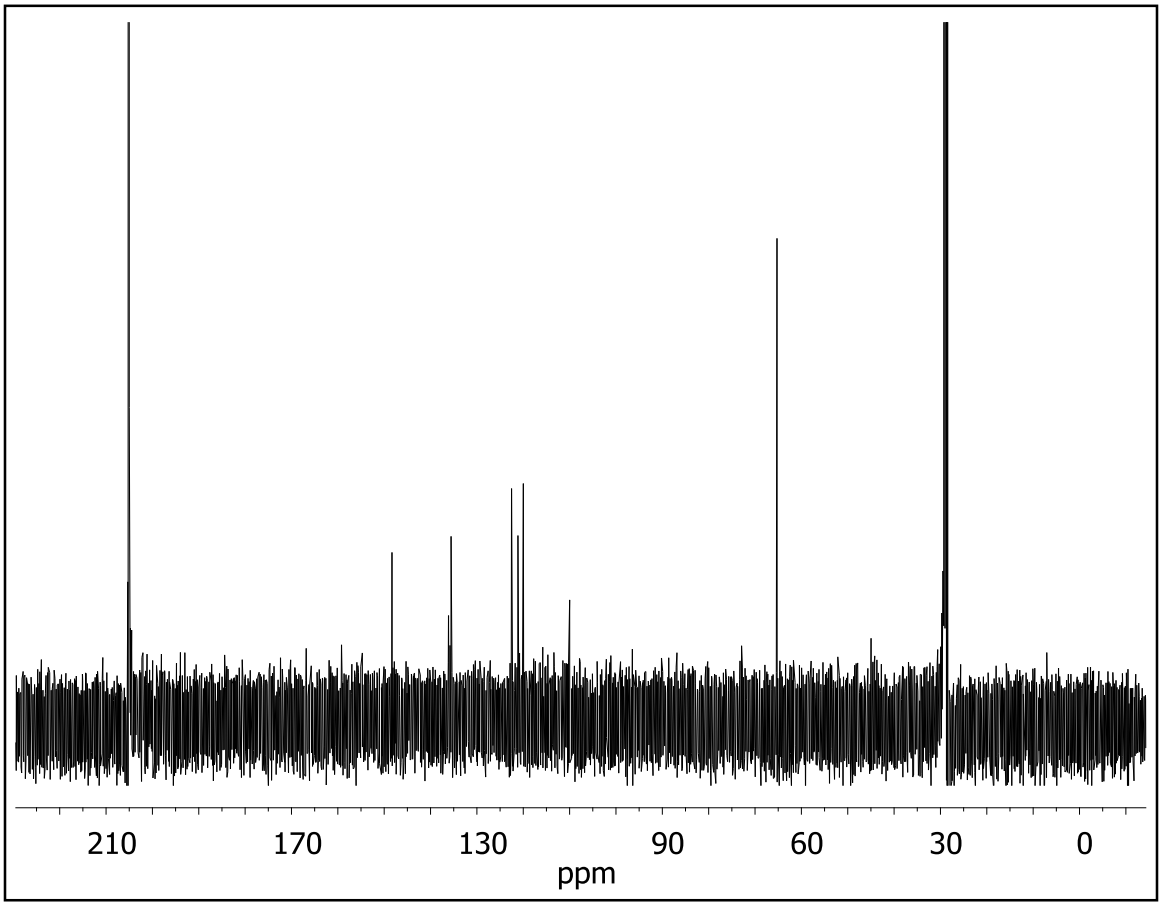

Figure 2-18. ^{13}C NMR spectrum of 2,6-di(2-ketalpyridyl)pyridine (dkpp) in $(CD_3)_2CO$.

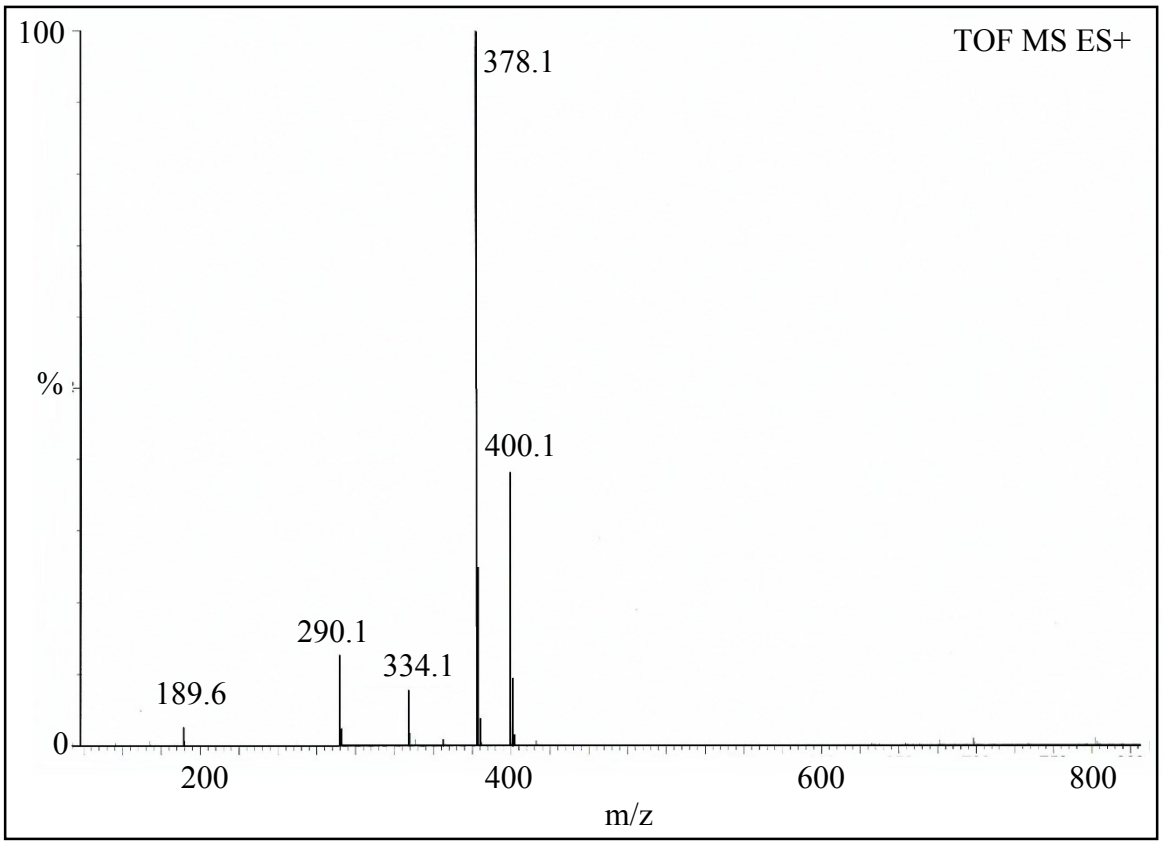

Figure 2-19. ESI-MS of 2,6-di(2-ketalpyridyl)pyridine (dkpp).

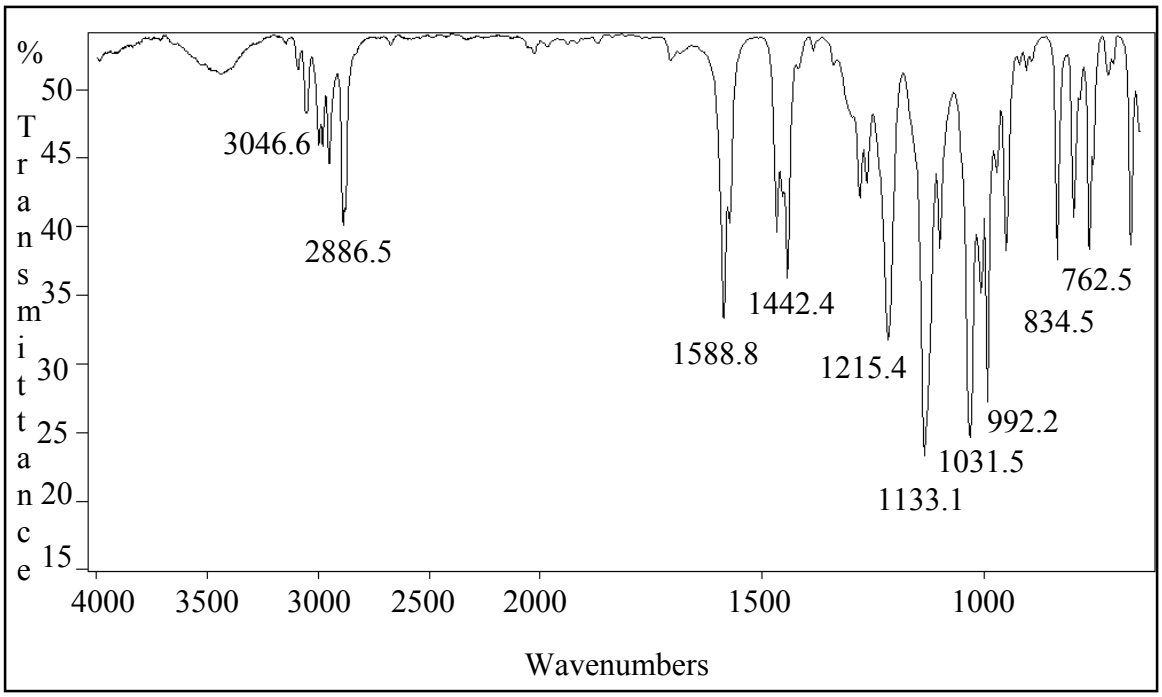

Figure 2-20. IR spectrum of 2,6-di(2-ketalpyridyl)pyridine (dkpp).

REFERENCES

REFERENCES

(1) Jamula, L. L. Masters Thesis, Michigan State University, 2010.

(2) Brown, A. M. PhD Dissertation, Michigan State University, 2011.

(3) Doedens, R.; Dahl, L. *Journal of the American Chemical Society* **1966**, *88*, 4847–4855.

(4) McGhee, L.; Siddique, R. M.; Winfield, J. M. *Journal of the Chemical Society, Dalton Transactions* **1988**, 1309.

(5) Sauvage, J.; Collin, J.; Chambron, J.; Guillerez, S. *Chemical Reviews* **1994**, *94*, 993–1019.

(6) Hammarström, L.; Johansson, O. *Coordination Chemistry Reviews* **2010**, *254*, 2546–2559.

(7) Schramm, F.; Meded, V.; Fliegl, H.; Fink, K.; Fuhr, O.; Qu, Z.; Klopper, W.; Finn, S.; Keyes, T. E.; Ruben, M. *Inorganic Chemistry* **2009**, *48*, 5677–84.

(8) Abarca, B.; Ballesteros, R.; Elmasnaouy, M. *Tetrahedron* **1998**, *54*, 15287–15292.

(9) Stamatatos, T. C.; Efthymiou, C. G.; Stoumpos, C. C.; Perlepes, S. P. *European Journal of Inorganic Chemistry* **2009**, 3361–3391.

(10) De Jonge, A. P.; den Hertog, H. J.; Wibaut, J. P. *Recueil des Travaux Chimiques des Pays-Bas et de la Belgique* **1951**, *70*, 989–996.

(11) Perrin, D. D.; Armarego, W. L. F. *Purification of Laboratory Chemicals, 3rd ed.*; Pergamon Press: New York, 1988.

(12) Dyker, G.; Muth, O. *European Journal of Organic Chemistry* **2004**, 4319–4322.

(13) Soutif, J.-C. J.-C.; Doan, N. T. H. H.; Montembault, V. *European Polymer Journal* **2006**, *42*, 126–132.

(14) Newkome, G. R.; Joo, Y. J.; Evans, D. W.; Fronczek, F. R.; Baker, G. R. *The Journal of Organic Chemistry* **1990**, *55*, 5714–5719.

(15) Goldsmith, C. R.; Stack, T. D. P. *Inorganic Chemistry* **2006**, *45*, 6048–55.

(16) Yan, C.; Chen, Q.; Chen, L.; Feng, R.; Shan, X.; Jiang, F.; Hong, M. *Australian Journal of Chemistry* **2011**, *64*, 104.

(17) Newkome, G. R.; Taylor, H. C. R.; Fronczek, F. R.; Delord, T. J. *The Journal of Organic Chemistry* **1984**, *49*, 2961–2971.

(18) COSMO V1.58, Software for the CCD Detector Systems for Determining Data Collection Parameters **2008**.

(19) APEX2 V2008.5-0, Software for the CCD Detector System **2008**.

(20) SAINT V 7.34 Software for the Integration of CCD Detector System **2008**.

(21) SADABS V2.008/2 Program for absorption corrections using Bruker-AXS CCD based on the method of Robert; Blessing, R. H. *Acta Cryst.* **1995**, *A51*, 33–38.

(22) Sheldrick, G. M. *Acta Cryst.* **2008**, *A64*, 112–122.

(23) Frisch, M. J.; Trucks, G. W.; Schlegel, H. B.; Scuseria, G. E.; Robb, M. A.; Cheeseman, J. R.; J. A. Montgomery, J.; Vreven, T.; Kudin, K. N.; Burant, J. C.; Millam, J. M.; Iyengar, S. S.; Tomasi, J.; Barone, V.; Mennucci, B.; Cossi, M.; Scalmani, G.; Rega, N.; Petersson, G. A.; Nakatsuji, H.; Hada, M.; Ehara, M.; Toyota, K.; Fukuda, R.; Hasegawa, J.; Ishida, M.; Nakajima, T.; Honda, Y.; Kitao, O.; Nakai, H.; Klene, M.; Li, X.; Knox, J. E.; Hratchian, H. P.; Cross, J. B.; Adamo, C.; Jaramillo, J.; Gomperts, R.; Stratmann, R. E.; Yazyev, O.; Austin, A. J.; Cammi, R.; Pomelli, C.; Ochterski, J. W.; Ayala, P. Y.; Morokuma, K.; Voth, G. A.; Salvador, P.; Dannenberg, J. J.; Zakrzewski, V. G.; Dapprich, S.; Daniels, A. D.; Strain, M. C.; Farkas, O.; Malick, D. K.; Rabuck, A. D.; Raghavachari, K.; Foresman, J. B.; Ortiz, J. V; Cui, Q.; Baboul, A. G.; Clifford, S.; Cioslowski, J.; Stefanov, B. B.; Liu, G.; Liashenko, A.; Piskorz, P.; Komaromi, I.; Martin, R. L.; Fox, D. J.; Keith, T.; Al-Laham, M. A.; Peng, C. Y.; Nanayakkara, A.; Challacombe, M.; Gill, P. M. W.; Chen, B. J. W.; Wong, M. W.; Gonzalez, C.; Pople, J. A. Gaussian 03, Revision D.01 **2004**.

(24) Chen, X.-D.; Mak, T. C. W. *Inorganica Chimica Acta* **2005**, *358*, 1107–1112.

(25) Abarca, B.; Ballesteros, R.; Chadlaoui, M. *ARKIVOC* **2008**, *2008*, 73–83.

(26) Goldsmith, C. R.; Jonas, R. T.; Stack, T. D. P. *Journal of the American Chemical Society* **2002**, *124*, 83–96.

(27) Vedernikov, A. N.; Huffman, J. C.; Caulton, K. G. *Inorganic Chemistry* **2002**, *41*, 6244–6248.

(28) Chen, X.-D.; Mak, T. C. W. *Journal of Molecular Structure* **2005**, *748*, 183–188.

(29) Clayden, J.; Greeves, N.; Warren, S.; Peter Wothers *Organic Chemistry*; Oxford University Press: New York, 2001.

(30) Chen, X.-M. X.-D.; Du, M.; He, F.; Mak, T. C. W. *Polyhedron* **2005**, *24*, 1047–1053.

(31) Georgopoulou, A. N.; Sanakis, Y.; Raptopoulou, C. P.; Psycharis, V.; Boudalis, A. K. *Polyhedron* **2009**, *28*, 3251–3256.

(32) Boudalis, A. K.; Donnadieu, B.; Nastopoulos, V.; Clemente-Juan, J. M.; Mari, A.; Sanakis, Y.; Tuchagues, J.-P. J.-P.; Perlepes, S. P. *Angewandte Chemie (International ed. in English)* **2004**, *43*, 2266–70.

(33) Boudalis, A. K.; Sanakis, Y.; Clemente-Juan, J. M.; Donnadieu, B.; Nastopoulos, V.; Mari, A.; Coppel, Y.; Tuchagues, J.-P.; Perlepes, S. P. *Chemistry - A European Journal* **2008**, *14*, 2514–26.

(34) Rau, S.; Schwalbe, M.; Losse, S.; Görls, H.; McAlister, C.; MacDonnell, F. M.; Vos, J. G. *European Journal of Inorganic Chemistry* **2008**, *2008*, 1031–1034.

(35) Phelan, N. F.; Orchin, M. *Journal of Chemical Education* **1968**, *45*, 633–637.

(36) Limacher, P. a.; Lüthi, H. P. *Wiley Interdisciplinary Reviews: Computational Molecular Science* **2011**, *1*, 477–486.

(37) Egli, M.; Sarkhel, S. *Accounts of Chemical Research* **2007**, *40*, 197–205.

(38) Wan, C.-Q.; Chen, X.-D.; Mak, T. C. W. *CrystEngComm* **2008**, *10*, 475.

(39) Mooibroek, T. J.; Gamez, P.; Reedijk, J. *CrystEngComm* **2008**, *10*, 1501.

(40) Kumar Seth, S.; Dey, B.; Kar, T.; Mukhopadhyay, S. *Journal of Molecular Structure* **2010**, *973*, 81–88.

(41) Quiñonero, D.; Estarellas, C.; Frontera, A.; Deyà, P. M. *Chemical Physics Letters* **2011**, *508*, 144–148.

(42) Egli, M.; Gessner, R. V. *Proc. Natl. Acad. Sci. U. S. A.* **1995**, *92*, 180–184.

(43) Chambers, J.; Eaves, B.; Parker, D.; Claxton, R.; Ray, P. S.; Slattery, S. J. *Inorganica Chimica Acta* **2006**, *359*, 2400–2406.

(44) Katsoulakou, E.; Lalioti, N.; Raptopoulou, C. P.; Terzis, A.; Manessi-Zoupa, E.; Perlepes, S. P. *Inorganic Chemistry Communications* **2002**, *5*, 719–723.

(45) Katsoulakou, E.; Bekiari, V.; Raptopoulou, C. P.; Terzis, A.; Lianos, P.; Manessi-Zoupa, E.; Perlepes, S. P. *Spectrochimica Acta. Part A, Molecular and Biomolecular Spectroscopy* **2005**, *61*, 1627–38.

(46) Lalioti, N.; Raptopoulou, C. P.; Terzis, A.; Aliev, A. E.; Gerothanassis, I. P.; Manessi-Zoupa, E.; Perlepes, S. P. *Angewandte Chemie* **2001**, *113*, 3311–3314.

(47) Bandoli, G.; Dolmella, a; Tisato, F.; Porchia, M.; Refosco, F. *Coordination Chemistry Reviews* **2009**, *253*, 56–77.

(48) Baker, R. J.; Jones, C.; Kloth, M.; Mills, D. P. *New Journal of Chemistry* **2004**, *28*, 207.

(49) Baker, R. J.; Jones, C. *Dalton Transactions* **2005**, 1341–8.

(50) Corbett, J. D.; McMullan, R. K. *Journal of the American Chemical Society* **1955**, 77.

(51) Wilkinson, M., Worrall, I. J., . *Journal of Organometallic Chemistry* **1975**, *93*, 39.

(52) Gerlach, C.; Hönle, W.; Simon, A. *Z. Anorg. Allg. Chem.* **1982**, 7.

(53) Green, M. L. H.; Mountford, P.; Smout, G. J.; Speel, S. R. *Polyhedron* **1990**, *9*, 2763–2765.

(54) Jurca, T.; Dawson, K.; Mallov, I.; Burchell, T.; Yap, G. P. a; Richeson, D. S. *Dalton Transactions* **2010**, *39*, 1266–72.

(55) Manessi, A.; Papaefstathiou, G. S.; Raptopoulou, C. P.; Terzis, A.; Zafiropoulos, T. F. *Journal of Inorganic Biochemistry* **2004**, *98*, 2052–62.

(56) Knight, J. C.; Amoroso, A. J.; Edwards, P. G.; Prabaharan, R.; Singh, N. *Dalton Transactions* **2010**, *39*, 8925–36.

(57) Gou, L.; Zhang, B.; Hu, H.-M.; Chen, X.-L.; Wang, B.-C.; Wu, Q.-R.; Qin, T.; Tang, Z.-X. *Journal of Molecular Structure* **2008**, *889*, 244–250.

(58) Wu, Q.-R.; Wang, J.-J.; Hu, H.-M.; Wang, B.-C.; Wu, X.-L.; Fu, F.; Li, D.-S.; Yang, M.-L.; Xue, G.-L. *Inorganic Chemistry Communications* **2010**, *13*, 715–719.

(59) Shaikh, T. M. A.; Emmanuvel, L.; Sudalai, A. *The Journal of Organic Chemistry* **2006**, *71*, 5043–6.

(60) Tabatabaeian, K.; Mamaghani, M.; Mahmoodi, N. O.; Khorshidi, a. *Catalysis Communications* **2008**, *9*, 416–420.

(61) Neumann, R.; Sasson, Y. *The Journal of Organic Chemistry* **1984**, *49*, 1282–1284.

(62) Newkome, G. R.; Taylor, H. C. R. *The Journal of Organic Chemistry* **1979**, *44*, 1362–1363.

(63) Newkome, G. R.; Gupta, V. K.; Taylor, H. C. R.; Fronczek, F. R. *Organometallics* **1984**, *3*, 1549–1554.

(64) Newkome, G. R.; Taylor, H. C. R.; Fronczek, F. R.; Gupta, V. K. *Inorganic Chemistry* **1986**, *25*, 1149–1154.

(65) Sun, J.; Dong, Y.; Cao, L.; Wang, X.; Wang, S.; Hu, Y. *The Journal of Organic Chemistry* **2004**, *69*, 8932–4.

(66) Das, S.; Borah, R.; Devi, R.; Thakur, A. *Synlett* **2008**, 2741–2762.

(67) Kumar, D.; Kumar, R.; Chakraborti, A. *Synthesis* **2008**, 1249–1256.

(68) Olson, M. E.; Carolan, J. P.; Chiodo, M. V.; Lazzara, P. R.; Mohan, R. S. *Tetrahedron Letters* **2010**, *51*, 3969–3971.

Chapter 3. Development of Symmetric Analogs to Investigate the Influence of the Bridging Group

3.1 Introduction

The development of the highly symmetric $[Fe(dcpp)_2]^{2+}$ provided a nice starting point to our investigation. Introducing a nearly perfect octahedral coordination environment appears to give rise to fascinating properties. The drastic difference in physical properties and seemingly significant increase in ligand field strength as compared to other known iron(II) polypyridyls led us to design analogs to uncover more information.

The motivation behind the design of the next set of molecules is two-fold. First, the development of a control molecule is crucial, as an isostructural d^{10} molecule would aid in distinguishing properties that may be attributed to the complex from ligand based effects. The highly reactive carbonyl has proven to be problematic in the coordination chemistry of Zn(II), Ga(III), and Cd(II), it is therefore in our best interest to develop a ligand system in which we replace the carbonyl groups with a less reactive bridging group to allow for more accessibility to a control molecule. Second, can the characteristics be attributed strictly to the enhanced geometry or are they more a result of the identity of the ligand? The electron withdrawing carbonyl groups in the ligand seemingly have a substantial impact on the properties of the complex so we set out to prepare ligands with alternate bridging groups to investigate this further.

As described in Chapter 1, an important characteristic that a DSSC sensitizer must possess is absorptivity in the visible region. Chromophores containing conjugated ligand systems fit this criteria, and we found in the investigation of 2,6-di(2-

carboxypyridyl)pyridine (dcpp) that a cross-conjugated ligand fits as well. In an effort to investigate the importance of the carbonyl bridge, while still retaining the optical properties, it was pertinent to maintain the cross-conjugation. Also, the π interaction of the carbonyl groups with the facing pyridyl rings appears to be essential to achieving the overall geometry of the complex, therefore it was in our best interest to preserve this aspect of the structure.

We set out to prepare analogs that we presumed would be isostructural with $[Fe(dcpp)_2]^{2+}$ and allow us to differentiate between the effects of the ligand arrangement and substituent effects. Two ideal choices for this investigation involve replacing the carbonyl bridging groups with imine and vinylidene functional groups, shown in Figure 3-1. By systematically moving away from the more electronegative oxygen to nitrogen then to carbon should allow us to distinguish between the effects of inductive stabilization of the π* orbitals of the ligand and interligand interactions.

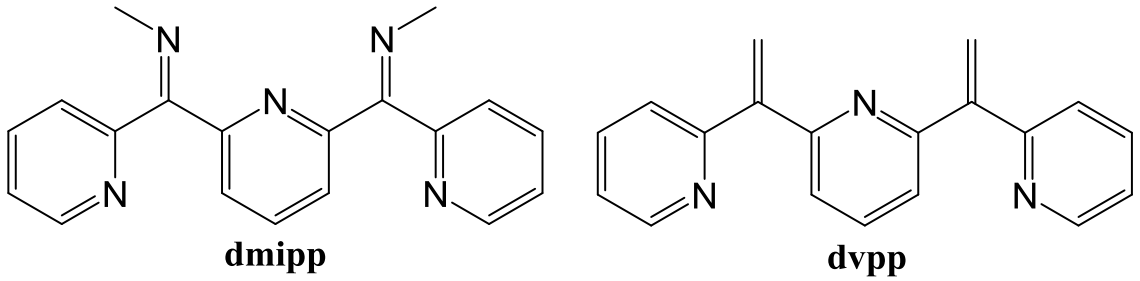

Figure 3-1. Structures of 2,6-di(2-(*N*-methylimine)pyridyl)pyridine (dmipp) and 2,6-di(2-vinylidenepyridyl)pyridine (dvpp).

The simplest imine that may be introduced is a primary ketamine (>C=N-H), but an imine bearing an alkyl group (>C=N-CH_3), or Schiff base, would be more stable and is more synthetically accessible and was therefore chosen. As for the carbon analog, vinylidene (>C=CH_2), or 1,1-ethenediyl, was chosen for its simplicity and is also

synthetically accessible. The ligands 2,6-di(2-(*N*-methylimine)pyridyl)pyridine (dmipp) and 2,6-di(2-vinylidene-pyridyl)pyridine (dvpp) were prepared, and as with dcpp, have the flexibility to coordinate in a symmetrical environment.

Concern was raised at the outset of this study that the geometric differences in these functional groups may interfere with the ability to achieve an isostructural analog. Using the X-ray crystal structure of $[Fe(dcpp)_2]^{2+}$ as a starting point, geometry optimizations of the desired complexes were obtained and indicate that the differences should not hinder coordination and will likely yield isostructural molecules as shown in Figure 3-2.

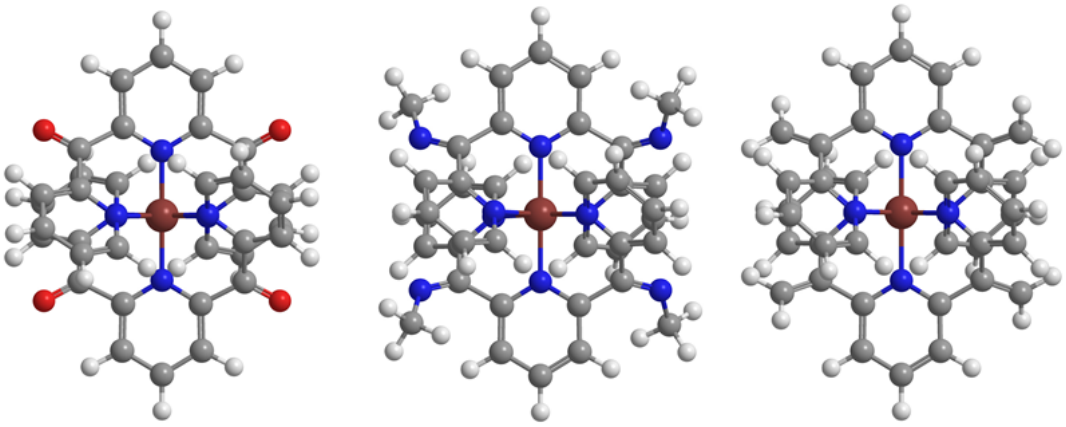

Figure 3-2. Optimized Structures of $[Fe(dcpp)_2](PF_6)_2$ (left), $[Fe(dmipp)_2](PF_6)_2$ (center), and $[Fe(dvpp)_2](PF_6)_2$ (right).

Additional apprehension at the beginning of this investigation involves the Schiff base analog. First, imines are usually unstable and are easily hydrolyzed to the carbonyl. Furthermore, with the installation of two additional nitrogens we are introducing potential coordination sites. Unfortunately, attempts to prepare $[Fe(dmipp)_2]^{2+}$ in the desired coordination environment have failed, instead the dmipp ligand coordinates through the

central pyridyl ring and the imine nitrogens. The synthetic efforts toward the preparation of this analog will be discussed, along with future strategies to overcome the problem. Fortunately, the dvpp analog presented no such issue and was successfully prepared, and the synthesis and characterization will be discussed. The properties were examined and a comparison with $[Fe(dcpp)_2]^{2+}$ will be presented.

The absence of the highly reactive carbonyl in the dvpp ligand renders it less susceptible to hydrolysis. This allows for more ease in the preparation of a control molecule and the $[Zn(dvpp)_2]^{2+}$ complex has been prepared. This analog may be useful in our continuing efforts in the quest for a control molecule for the $[Fe(dcpp)_2]^{2+}$.

3.2 Experimental

3.2.1 Synthesis

General. All chemicals were of reagent grade, purchased from Sigma-Aldrich, Alfa Aesar, Acros Organics, or Strem Chemicals and used as received unless otherwise noted. Solvents were purchased from Sigma-Aldrich, Jade Scientific, Spectrum, Mallinckrodt, EMD Chemical, or CCI and were purified using standard purification techniques.[1] All air-sensitive reactions were carried out under inert atmosphere by standard Schlenk techniques utilizing thoroughly deoxygenated solvents that were degassed by the freeze—pump—thaw method. ^{1}H NMR and ^{13}C NMR were recorded with Varian UnityPlus-300 MHz, Varian UnityPlus-500 MHz, and Agilent DDR2 500 MHz spectrometers. Ground state absorption spectra were obtained on a Varian Cary 50 spectrophotometer. IR spectra were obtained on a Mattson Galaxy 5000 FTIR. Elemental analysis was obtained through the Analytical facilities at Michigan State

University. Electrospray mass spectra (ESI-MS) were obtained from the staff of the MSU Mass Spectrometry Facility. The characterization data of previously unknown compounds are included in the appendix at the end of this chapter.

2,6-Di(2-(*N*-methylimine)pyridyl)pyridine (dmipp). This compound was prepared by modification of previously published procedures.[2,3] A 200 mL round bottom flask equipped with a Dean-Stark trap was charged with dcpp (0.165 g, 0.569 mmol), methylamine in methanol (2 mL, 2.0 M, 4.00 mmol), dry methanol (10 mL), and dry benzene (30 mL). The solution was refluxed for 72 hours under N_2, and the solvent subsequently evaporated to yield a dark green oil. The oil appears to be a mixture of three products (by TLC and NMR), but attempts to purify resulted in hydrolysis, therefore the crude oil product is used as-is in the subsequent reaction.

$[Fe(dmipp)_2](PF_6)_2$. The crude dmipp (0.180 g, 0.569 mmol) from the previous reaction is dissolved in dry MeOH (~10 mL). The brown solution is transferred to a second air-free flask containing $(NH_4)_2Fe(SO_4)_2 \cdot 6H_2O$ (0.0555 g, 0.142 mmol) which turns dark blue immediately. The reaction was stirred for 30 min at rt and NH_4PF_6 (0.100 g, 0.617 mmol) was added. Diethyl ether (10 mL) was added and the solution placed in the freezer. After 18 hours no precipitate had formed so the solution was concentrated and water added and the blue/purple product filtered. Crude Yield: 0.1047 g (76%). The crude product contains at least five compounds that may be separated by column chromatography on neutral alumina with acetonitrile. The first band to elute was intense purple and determined to be $[Fe(dmipp)_2](PF_6)_2$ coordinated through the imine groups and central pyridine ring. Subsequent fractions did not correspond to the correct mass (according to ESI-MS) and were increasingly paramagnetic by NMR. There was no

evidence of the product in the desired coordination mode. Characterization of $[Fe(dmipp)_2](PF_6)_2$ coordinated through the imine groups: ^{1}H NMR ($(CD_3)_2CO$, 500 MHz): δ (ppm) 8.93 (ddd, 4H, *J* = 4.8, 1.6, 1.0 Hz, 6py-a (pyridyl arm)), 8.55 (t, 2H, *J* = 8.0 Hz, 4py-b (bridging pyridyl)), 8.40 (d, 4H, *J* = 8.0 Hz, 3py-b), 8.18 (td, 4H, *J* = 7.8, 1.7 Hz, 4py-a), 7.95 (dt, 4H, *J* = 7.8, 1.0 Hz, 6py-a), 7.75 (dtd, 4H, *J* = 4.8, 1.0 Hz, 5py-a), 2.75 (s, 12H, N-CH_3). ^{13}C NMR $(CD_3)_2CO$, 500 MHz): δ (ppm) 175.0, 160.4, 150.9, 147.8, 137.8, 137.1, 128.4, 126.3, 125.7, 40.8. TOF-MS [ESI, *m/z* (rel int)]: 343.1 (100) $[C_{38}H_{34}N_{10}Fe]^{2+}$, 831.2 (15) $\{[C_{38}H_{34}N_{10}Fe](PF_6)\}^+$. IR (KBr, cm^{-1}): 1588.3 m, 1585.0 m, 1465.1 w, 1384.1 m, 1336.0 m, 1152.5 w, 1118.4 w, 1071.8 w, 840.4 br, 757.9 m.

2,6-Di(2-vinylidenepyridyl)pyridine (dvpp). The target molecule was prepared analogously to 2,2'-vinylidenedipyridine according to the procedure by Summers et al.[4] from dcpp (1.999 g, 6.91 mmol). The brown crude oil was purified by silica gel chromatography with acetonitrile as the eluent. The bright yellow band is collected (Rf = 0.32), which immediately begins to darken after leaving the column and upon evaporation yields the dark red oil product. Yield 0.688 g (35%). The pure product should be stored in the dark and used fairly quickly (within days), as it polymerizes to a tacky, insoluble orange solid. ^{1}H NMR ($(CD_3)_2CO$, 500 MHz): δ 8.61 (ddd, 2H, *J* = 4.8, 1.8, 1.0 Hz, 6py-a), 7.81 (t, 1H, *J* = 7.8 Hz, 4py-b), 7.77 (td, 2H, *J* = 7.7, 1.8 Hz, 4py-a), 7.50 (dt, 2H, *J* = 7.9, 1.0 Hz, 3py-a), 7.44 (d, 2H, *J* = 7.8 Hz, 3/5py-b), 7.31 (td, 2H, *J* = 4.8, 1.0 Hz, 5py-a), 6.10 (d, 2H, *J* = 1.8 Hz), 6.05 (d, 2H, *J* = 1.8 Hz). ^{13}C NMR ($(CD_3)_2CO$, 500 MHz): δ 157.60, 157.03, 148.99, 148.87, 136.84, 136.14, 123.04,

122.47, 121.80, 119.39. TOF-MS [ESI, *m/z* (rel int)]: 286.2 (20) $[C_{19}H_{15}N_3]H^+$, 571.4 (100) $2[C_{19}H_{15}N_3]H^+$.

$[Fe(dvpp)_2](PF_6)_2$. To an air-free flask dvpp (0.163 g, 0.570 mmol) and deoxygenated 1:1 MeOH/H_2O (30 mL) via cannula were added. The solution was gently warmed (40°C) under nitrogen to promote dissolution of the oil. A separate air-free flask was charged with $(NH_4)_2Fe(SO_4)_2 \cdot 6H_2O$ (0.0690 g, 0.176 mmol) and 1:1 MeOH/H_2O (20 mL). The Fe(II) solution was transferred via cannula to the ligand solution which immediately turned red, darkening quickly to deep brown. The reaction was allowed to stir for 2 hours at room temperature. A separate air-free flask was charged with 20 equivalents of NH_4PF_6 (0.605 g, 3.73 mmol) and 1:1 MeOH/H_2O (10 mL) which was then transferred via cannula to the reaction mixture. The solution was concentrated by evaporation under a stream of N_2 yielding brown precipitate which was filtered and rinsed with H_2O. The crude product was dissolved in acetonitrile and the solution was washed with hexanes to remove grease. The acetonitrile solution was concentrated then purified by passage through a basic alumina column. Two distinct bands form, a red band followed by green band. The product (red band) eluted first and may be recrystallized by slow evaporation of methanol or by diethyl ether vapor diffusion into a 1:1 acetone/methanol solution of the complex. Yield: 0.0822 g (51%). ^{1}H NMR ($(CD_3)_2CO$, 500 MHz): δ 8.31 (t, 2H, *J* = 7.9 Hz, 4py-b), 8.03 (d, 4H, *J* = 7.9 Hz, 3/5py-b), 7.99 (td, 4H, *J* = 7.7, 1.4 Hz, 4py-a), 7.81 (d, 4H, *J* = 7.7, 0.7 Hz, 3py-a), 7.30 (d, 4H, *J* = 5.9, 0.7 Hz, 6py-a), 7.05 (td, 4H, *J* = 5.9, 1.4 Hz, 5py-a), 5.69 (s, 4H), 5.44 (s, 4H). ^{13}C NMR ($(CD_3)_2CO$, 500 MHz): δ 162.60, 162.32, 158.14, 144.18, 139.67, 138.87,

125.57, 124.75, 124.11, 123.16. TOF-MS [ESI, *m/z* (rel int)]: 313.1 (100) $[C_{38}H_{30}N_6Fe]^{2+}$, 771.1 (1) $\{[C_{38}H_{30}N_6Fe](PF_6)\}^{+}$. IR (KBr, cm^{-1}): 3100.0 w, 1594.8 m, 1566.5 m, 1478.8 s, 1436.6 m, 1384.8 m, 1287.1 w, 1164.4 m, 1091.3 w, 1021.0 w, 960.5 m, 842.3 br, 759.9 s. Elemental Analysis for $C_{38}H_{30}N_6FeP_2F_{12}$, Calculated: C, 49.80; H, 3.30; N, 9.17. Found: C, 49.42; H, 3.29; N, 8.99. UV-Vis (CH_3CN) λ(ε($M^{-1}cm^{-1}$)): 281 nm (33000), 384 nm (7700), 445 nm (6800), 491 nm (7000).

$[Zn(dvpp)_2](PF_6)_2$. The compound was prepared by modification of a literature procedure.[5] To a 50 mL Erlenmeyer flask was added dvpp (0.0389 g, 0.136 mmol) and $CHCl_3$ (6 mL). To a separate flask was added $Zn(CH_3CO_2)_2 \cdot 2H_2O$ (0.0123 g, 0.0560 mmol) and MeOH (5 mL). The Zn solution was transferred to the ligand solution by pipet and allowed to stir for 30 min. NH_4PF_6 (0.0600 g, 0.368 mmol) was dissolved in methanol and added to the reaction mixture. Diethyl ether was added to precipitate the peach product. The product was recrystallized by slow evaporation of a methanol solution yielding colorless plate crystals. Yield: 0.0341 g (66%). ^1H NMR ($(CD_3)_2CO$, 500 MHz): δ 8.36 (t, 2H, *J* = 7.9 Hz, 4py-b), 8.15 (td, 4H, *J* = 7.8, 1.5 Hz, 4py-a), 7.95 (d, 4H, *J* = 7.9 Hz, 3/5py-b), 7.93 (dd, 4H, *J* = 5.4, 0.7 Hz, 6py-a), 7.86 (d, 4H, *J* = 7.9 Hz, 3py-a), 7.49 (td, 4H, *J* = 6.5, 0.7 Hz, 5py-a), 5.66 (s, 4H), 5.57 (s, 4H). ^{13}C NMR ($(CD_3)_2CO$, 500 MHz): δ 157.30, 157.24, 148.43, 142.67, 142.31, 141.26, 126.92, 125.77, 125.07, 124.66. TOF-MS [ESI, *m/z* (rel int)]: 317.1 (2) $[C_{38}H_{30}N_6Zn]^{2+}$.

3.2.2 Physical Measurements

X-ray Structure Determination. Single-crystal X-ray diffraction data was acquired at the X-ray facility of Michigan State University by Dr. Richard J. Staples. Data were collected as described in Chapter 2 of this dissertation.

Cyclic Voltammetry. Electrochemical measurements were carried out using a CH Instruments CH620D electrochemical analyzer to determine the $E_{1/2}$ for ligand reductions and metal oxidations of each complex. Solutions of the compounds were prepared in distilled CH_3CN containing NBu_4PF_6 (ca. 0.1 M) as the supporting electrolyte. A standard three-electrode setup was used with a platinum working electrode, carbon rod counter electrode, and Ag/AgCl or $Ag/AgNO_3$ electrode as the reference. All measurements were made inside an inert atmosphere glovebox. Data was acquired at a scan rate of 50 mV s^{-1}. After data collection ferrocene was added to subsequent scans for reference.

3.2.3 Theoretical Calculations

Geometry Optimizations. The initial geometries of the molecules were generated using SPARTAN or GaussView, or from crystal structure coordinates when available, and subsequently optimized in two steps.[6,7] The first optimization was performed using the density functional B3LYP with the 3-21G** basis set, followed by a second optimization using the B3LYP functional with the 6-31G* basis set. Frequency calculations at the B3LYP/6-31G* level of theory were performed on the final optimized structures to ensure that these geometries corresponded to global minima.

3.3 Results and Discussion

3.3.1 Significance of the π Interaction in Achieving the Preferred Geometry

Our pursuit to prepare $[Fe(dcpp)_2]^{2+}$ by the method of simultaneous ligand oxidation/coordination, that was described in Chapter 2, was complicated by the oxidation of iron(II) from the presence of oxygen. Therefore, efforts were made to exclude oxygen and obtain the methylene-bridged coordination compound $[Fe(dmpp)_2]^{2+}$, as shown in Scheme 3-1. After many attempts there was never any evidence of the desired complex by ESI-MS. By ^1H NMR the various samples are paramagnetic leading to the presumption that this complex may be similar to the hexakispyridyl complex $[Fe(py)_6]^{2+}$. The absence of the carbonyl bridge results in a weaker ligand field that cannot stabilize the low spin state, therefore the $Fe(dmpp)_2]^{2+}$ is likely high spin and unstable in solution.

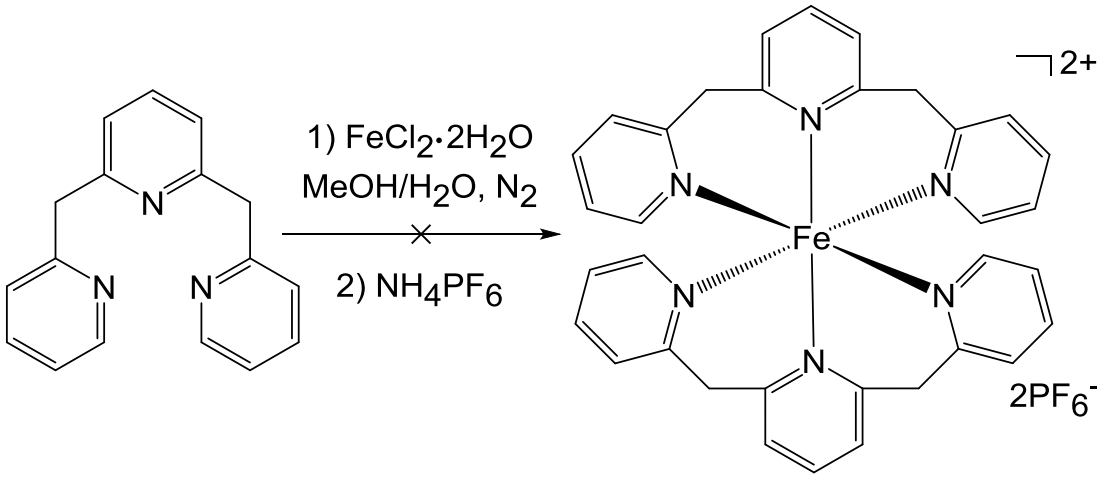

Scheme 3-1. Attempted synthesis of $[Fe(dmpp)_2](PF_6)_2$.

As discussed in Chapter 2, the π interaction of the carbonyl oxygen with the facing pyridyl rings appears to be essential to achieving the overall geometry of the

$[Fe(dcpp)_2]^{2+}$ complex. Introducing the imine and vinylidene bridges should allow for a similar π interaction. In the detailed analysis of the Cambridge Structure Database that was described in Chapter 2, the authors found that carbonyl lone pair (l.p.)—π interactions are quite common with nearly 6000 occurrences.[8] They also found many cases of imine groups with nitrogen l.p.—π interactions, with over 1000 hits, but on average, this interaction is notably weaker than the carbonyl interaction. No l.p.-π interaction is possible with the vinylidene bridge, but the more commonly known π-π stacking interaction may be present.

We normally think of π-stacking as the non-covalent interaction occurring between aromatic moieties, with an example of this in the stacking of benzene rings. The presumption that aromaticity is a requirement for π-stacking has recently been in question. Computational studies have suggested that stronger interactions may be achieved between benzene and a non-aromatic moiety than between two benzene rings, with π localization stabilizing the stacking interaction.[9] This suggests that the blanket phrase describing π-interactions as "aromatic interactions" is a misleading term and should be more generally defined. Furthermore, a recent review by Martinez and Iverson brings the use of the terms "π-stacking" and "π–π interactions" into question, finding that they are also overused in the literature and do not accurately describe the forces that drive non-covalent association between molecules.[10]

With the recent debate over terminology and continually evolving research on noncovalent interactions I am hesitant to suggest what interaction could exist.[9–12] I can only presume that the installation of a vinylidene bridging group may introduce sufficient

stabilization to allow for complex formation to occur, whether it be a result of the cross-conjugation in the ligand or through a so-called "π–π interaction."

3.3.2 Synthesis and Coordination of 2,6-Di(2-(*N*-methylimine)pyridyl)pyridine

Imines are known to be unstable and are easily hydrolyzed to the carbonyl. In general, imines that are formed from ketones and primary amines are only stable enough to isolate if the carbon or nitrogen bears an aromatic substituent. The target molecule dmipp bears the pyridyl substituents on the imine carbons which we hoped would be sufficient to stabilize the imine. Furthermore, if coordination with an iron(II) center could occur in the desired conformation, the l.p.-π interaction with the nitrogen of the imine and the facing pyridyl rings could further stabilize the imines.

Dmipp has been successfully prepared under various conditions according to the general method shown in Scheme 3-2. In all cases, dry solvent must be used and water should be removed from the reaction as it is formed. For imine formation in general, an acid catalyst is added to speed up the reaction, with optimal pH 4-6. Below pH 4 too much of the amine is protonated for the reaction to proceed and above pH 6 the proton concentration is too low to allow for the protonation of the OH leaving group in the dehydration step. The acid catalyst is not necessarily required and with more rigorous heating and longer reaction time the reaction may still proceed.

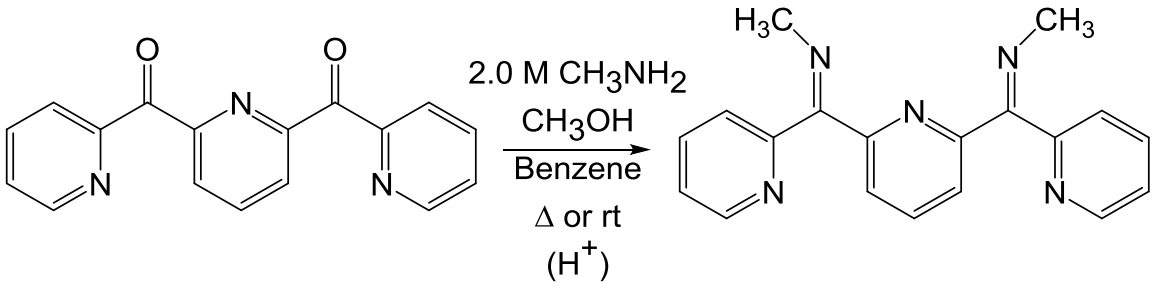

Scheme 3-2. General synthetic scheme for the preparation of 2,6-di(2-(*N*-methyl-imine)pyridyl)pyridine (dmipp).

Initially, a route described by Yorke et al. was adapted for the preparation of dmipp.[13] Amberlyst-15 was employed as the acid catalyst in the reaction, which was refluxed for 72 hours utilizing a Dean-Stark trap for water removal. There is evidence of product formation, but it could not be isolated cleanly so alternate routes were pursued. The acid catalyst was not required in this alternative procedure, which was also refluxed for 72 hours with a Dean-Stark trap, with no obvious difference in conversion.[2,3] As with the previous method, product purification was problematic.

A third procedure was pursued in which the compound may be prepared via vapor diffusion. The method by Thienthong et al. was described as a simplified procedure by which imines may be prepared quantitatively, requiring little or no work-up or purification.[14] The reaction is carried out in an H-tube in which one arm is charged with a volatile amine while the other arm contains the ketone and complete conversion can be achieved in 24-48 hours by simple vapor diffusion. The authors investigated many ketones and found that the reaction is assisted by a hydrogen bonding interaction with the oxygen of the carbonyl and may proceed neat if a hydroxyl group is present in the starting ketone. If no OH group is present, a small amount of dry methanol may be added to the ketone and the reaction proceeds quantitatively. This method was attempted

utilizing a "cow" type distillation receiver. One arm was charged with 20 mL of 2.0 M CH_3NH_2 in methanol and a second arm was charged with dcpp, 1 mL of dry methanol, and a stir bar. The apparatus was sealed and the ketone suspension was stirred for 24 hours with no noticeable change, after another 48 hours the ketone had completely solubilized and turned yellow, signifying that conversion to the imine had occurred. As with the two previous procedures the oil product was found to be a mixture, with some of the starting dcpp remaining as well as some partially converted product in with the desired product. Allowing the reaction to proceed longer may produce better yield, but to date this was not attempted.

By all routes, the preparation of the imine yields a mixture. The imine product is susceptible to hydrolysis and therefore any attempt to purify by recrystallization or column chromatography has proven to be difficult, resulting in reversion to dcpp. Coordination of the dmipp ligand to iron(II) could stabilize the imine groups, possibly allowing for cleaner separation of the compounds with less chance of hydrolysis, therefore, the crude oil product was used without purification in the coordination reaction. As anticipated, the reaction yielded a mixture of products due to the presence of partially and unconverted dcpp in the ligand mixture, but could be easily separated by column chromatography on neutral alumina. As predicted, coordination of the dmipp ligand to iron(II) stabilized the imine groups, unfortunately it was achieved by coordination of the imine nitrogens instead of the desired pyridyl coordination as shown in Scheme 3-3.

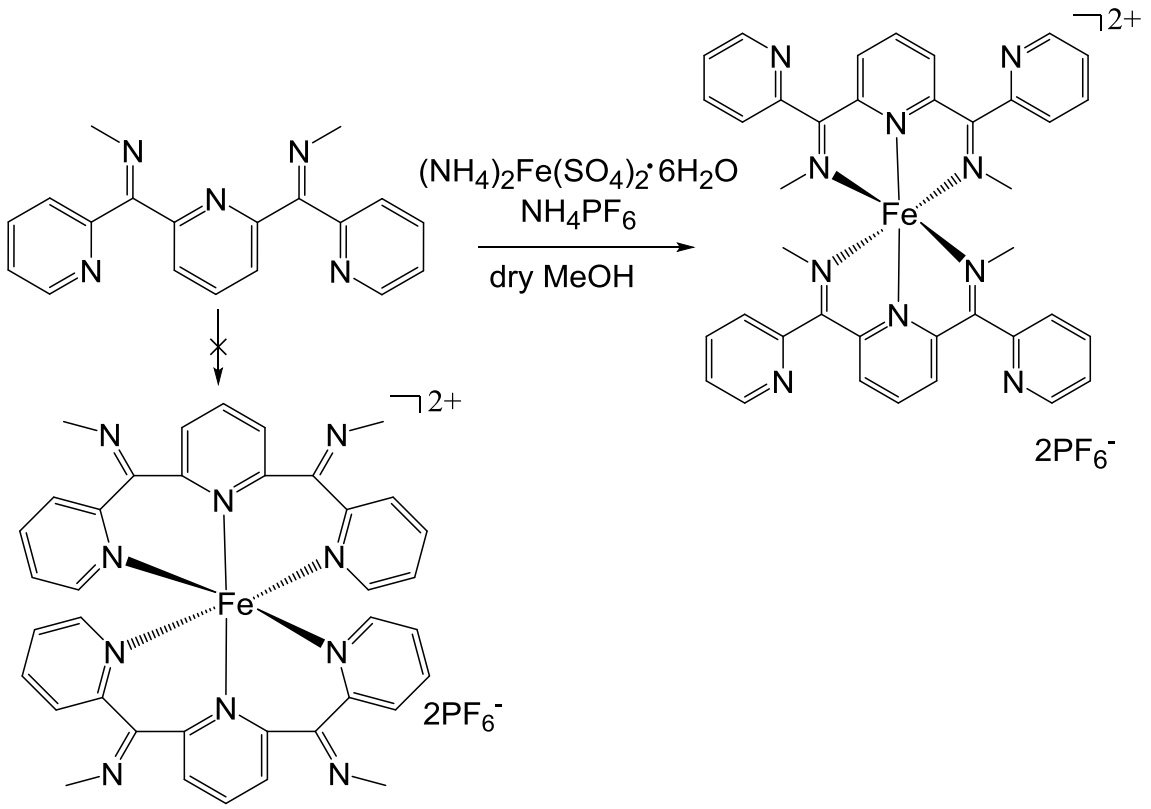

Scheme 3-3. Attempted preparation of the desired $[Fe(dmipp)_2]^{2+}$ resulting in the alternate coordination mode.

I was unable to obtain crystals suitable for X-ray crystal structure determination to verify the alternate coordination mode, but from ground state electronic absorption and ^1H NMR data it became clear that the desired complex was not achieved. $[Fe(dmipp)_2]^{2+}$ was not previously known, but iron(II) complexes possessing similar ligand systems that coordinate through imine groups are known and have been well characterized.[15–18] The ground state absorption spectrum for $Fe(dmipp)_2]^{2+}$ in acetonitrile is nearly identical to those published for similar compounds (Figure 3-3). Toma and coworkers performed calculations to identify the features in the absorption spectrum: the peaks at 600 nm and 485 nm are metal to ligand charge transfer (MLCT)

bands arising from $d_{xy} \rightarrow \pi^*$ and d_{xz}, $d_{yz} \rightarrow \pi^*$, respectively, and the weak band at 700 nm is attributed to a low energy ligand field transition.[16,17] The consistency of features in the $[Fe(dmipp)_2]^{2+}$ absorption spectrum with the literature reports provides strong evidence of the coordination mode.

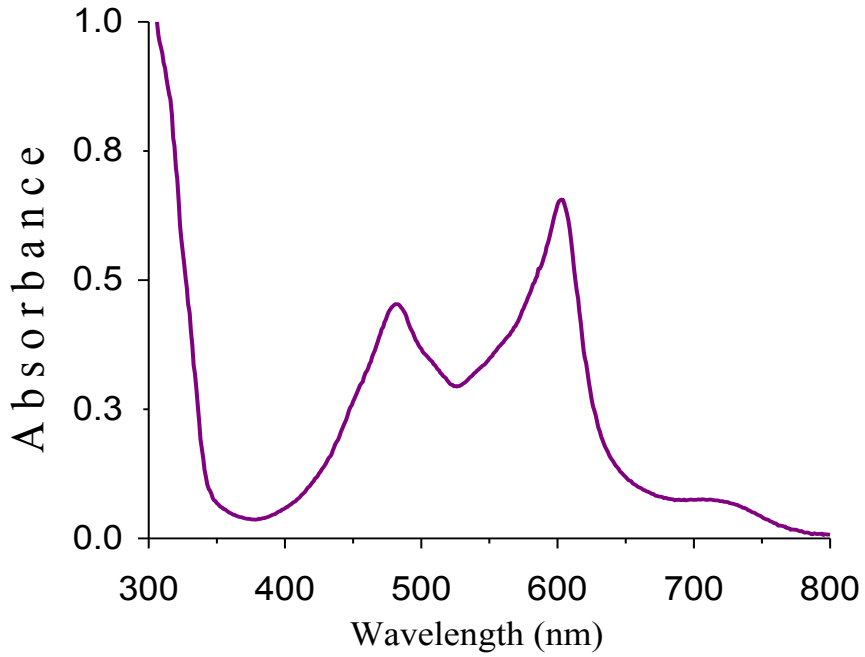

Figure 3-3. Ground state absorption spectrum of $[Fe(dmipp)_2]^{2+}$.

A second, more crucial piece of evidence is obtained from the ^1H NMR spectrum of the complex. Upon coordination of polypyridyl ligands to a metal center there is a drastic shift of the 6-position protons, which is well known in terpyridine chemistry.[19,20] The 6-position protons on the terminal rings of polypyridyl are the least shielded protons in the free ligand and therefore their signal appears far downfield. A free ligand is oriented in an *anti* arrangement to avoid strain between the lone pairs on the pyridyl nitrogens, and upon coordination the pyridyls reorient into a *syn* arrangement causing the

observed upfield shift of the 6-position protons. These protons are influenced by the metal-ligand bond as well as the close proximity to the adjacent ligand. We observe a shift of the other protons as well, but it is usually not as drastic as with the 6-position. This characteristic shift can be seen in the ^{1}H NMR spectra of dcpp and $[Fe(dcpp)_2]^{2+}$, shown in Figure 3-4. Since a clean ^{1}H NMR spectrum of the dmipp ligand has not been obtained, I cannot make the same comparison with the $[Fe(dmipp)_2]^{2+}$ spectrum; however the 6-position protons in the complex appear far downfield signifying that they are not affected by coordination to the metal (Figure 3-5) providing more evidence for the alternate coordination mode.

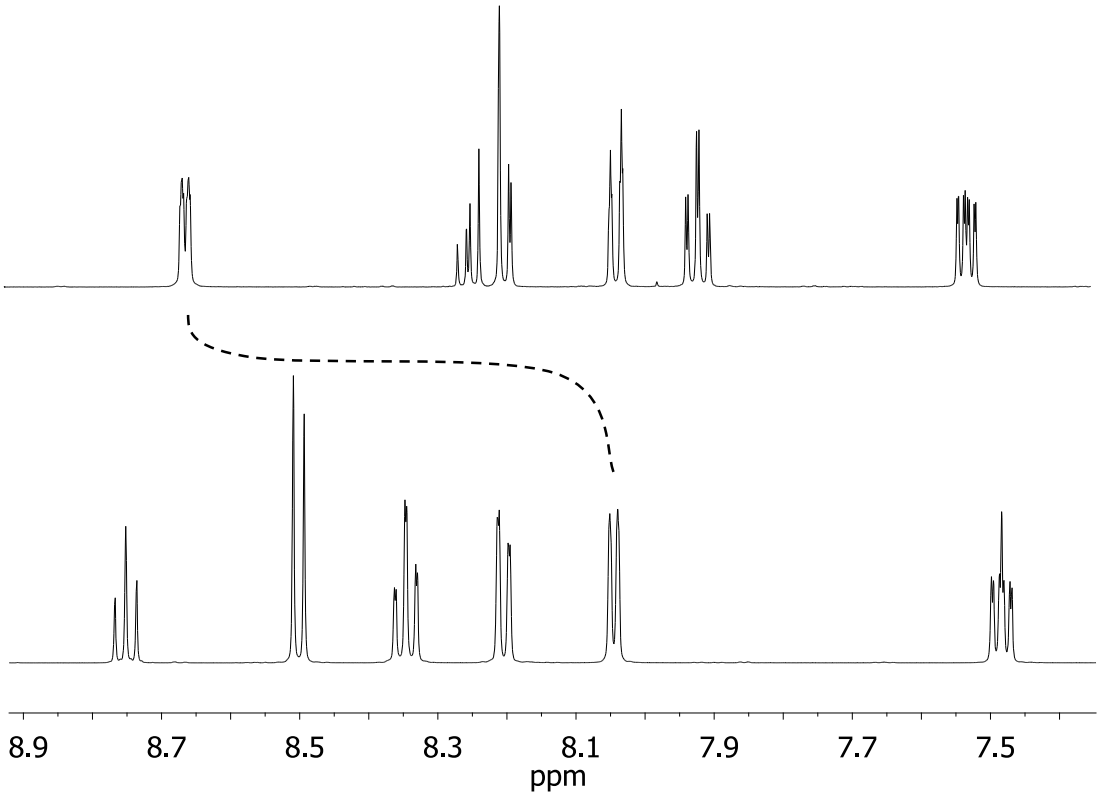

Figure 3-4. Characteristic shift of the 6-position protons shown by comparison of the ^{1}H NMR ($(CD_3)_2CO$) of the dcpp ligand (top) and $[Fe(dcpp)_2]^{2+}$ complex (bottom).

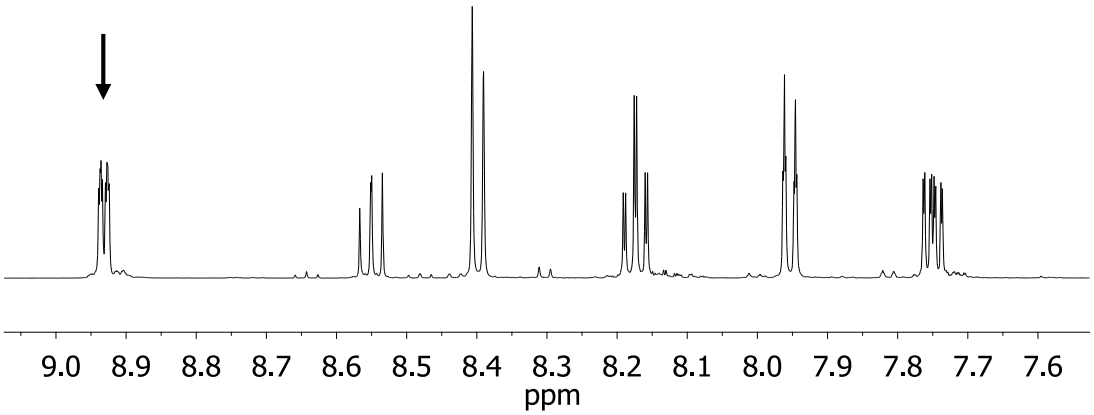

Figure 3-5. ^{1}H NMR ($(CD_3)_2CO$) of the $[Fe(dmipp)_2]^{2+}$ complex, note the chemical shift of the 6-position protons far downfield.

Since the imine complex does not possess the desired conformation it is not useful for the current investigation. We are currently pursuing the installation of a bulkier R group to the imine nitrogen in an effort to prevent binding at these sites. First on deck is the reaction of dcpp with t-butylamine. *t*-Butylamine is much less volatile than methylamine which may lead to more difficulty in obtaining the product and more rigorous conditions are likely necessary. Another possibility that has been considered is attempting the imine formation with the ligand already bound to the Fe(II) center. The chances of this route producing results is highly unlikely, since the $[Fe(dcpp)_2]^{2+}$ appears to be extremely stable. Furthermore, the carbonyls are stabilized by the l.p.-π interaction with the pyridyl rings likely rendering them unreactive.

3.3.3 Synthesis and Coordination of 2,6-Di(2-vinylidenepyridyl)pyridine

2,6-Di(2-vinylidenepyridyl)pyridine (dvpp) was not previously known, however is readily synthetically accessible since olefination reactions are quite commonplace with

a wide variety of options available. With 2,6-di(2-carboxypyridyl)pyridine (dcpp) already in hand it was fairly easy to develop the chemistry for the dvpp ligand. The Wittig reaction was employed and dvpp was prepared analogously to 2,2'-vinyldipyridine.[4,21] The product was purified by column chromatography and elutes as a yellow oil that quickly darkens to red upon standing. The product was used immediately in the subsequent coordination reaction, as shown in Scheme 3-4.

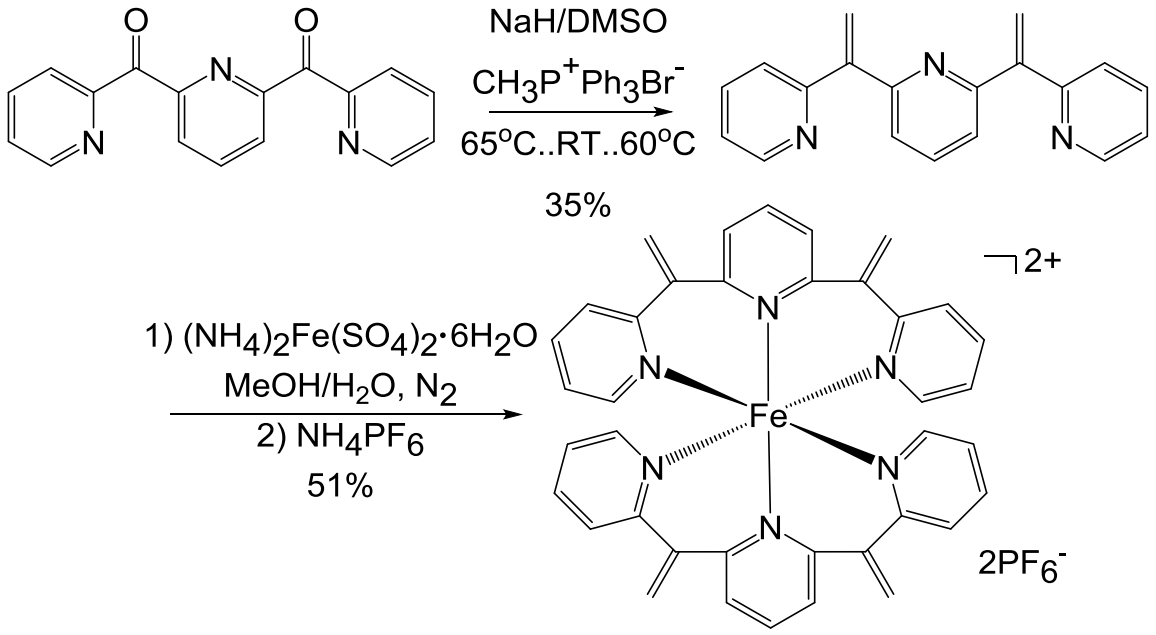

Scheme 3-4. Synthesis of 2,6-di(2-vinylidenepyridyl)pyridine (dvpp) and $[Fe(dvpp)_2]^{2+}$.

The dvpp product contained a small amount of partially converted ligand in which one carbonyl remains intact while the other was converted to the olefin. The presence of this impurity became apparent in the subsequent formation of the iron(II) complex. It is possible that this is a byproduct of the reaction that is carried through the silica column purification, despite much care being taken in isolation and clear separation by TLC. It is also possible that it may be occurring during the purification, as it is known that olefins

can undergo oxidative cleavage on silica in the presence of light and air.[22,23] When repeating this reaction, much more care was taken to exclude light during the workup and purification. However, if the impurity is carried through to the coordination reaction it may be easily removed during purification of the Fe(II) complex.

The product of the coordination reaction was obtained as a brown solid which was easily separated into two distinct products by column chromatography on basic alumina. The first band is red and is determined by ESI-MS to be the pure intended product. The second band is dark green and according to ESI-MS is two mass units too heavy signifying that it contains one carbonyl. Also, there is a carbonyl stretch in the IR spectrum of this green byproduct.

3.3.3 Properties of Bis(2,6-di(2-vinylidenepyridyl)pyridine)iron(II)

Single crystals of $[Fe(dvpp)_2](PF_6)_2$ suitable for X-ray crystallography were obtained by slow evaporation of a methanol solution of the complex. The crystal structure of $[Fe(dvpp)_2]^{2+}$ was solved and found to possess an octahedral coordination environment isostructural with the $[Fe(dcpp)_2]^{2+}$, shown in Figure 3-6. The crystallographic data is listed in Table 3-1 and selected geometric parameters are listed in Tables 3-2 and 3-3. With an isostructural analog in hand we can now investigate the source of the seemingly unique properties of the $[Fe(dcpp)_2]^{2+}$ complex.

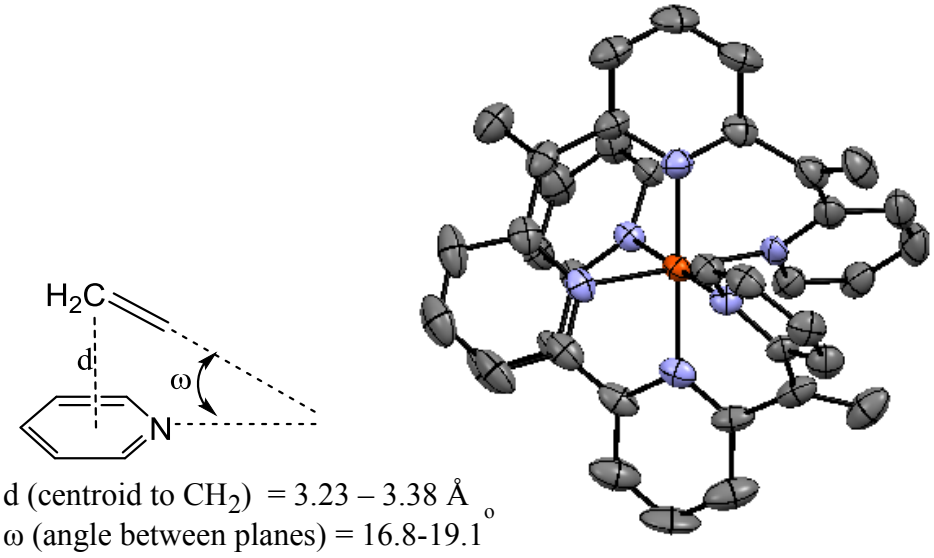

Figure 3-6. ORTEP drawing of the cation of $[Fe(dvpp)_2]^{2+}$ obtained from single-crystal X-ray structure determination. Atoms are represented as 50% probability thermal ellipsoids. Hydrogen atoms and anions are omitted for clarity. Also shown is the schematic of the structural parameters determined from the crystal structure used to characterize the π—π interaction.

Table 3-1. Crystallographic data for $[Fe(dvpp)_2](PF_6)_2$.

$[Fe(dvpp)_2](PF_6)_2$ [a]			
Empirical formula	$C_{38}H_{30}F_{12}FeN_6P_2$	ρ_{calc}mg/mm^3	1.563
Formula weight	916.47	μ/mm^{-1}	4.746
Temperature/K	173.01	F(000)	3712
Crystal system	Orthorhombic	2θ range	65.1° to 134.7°
Space group	Pbca	Reflections collected	19560
a/Å	13.5610 (3)	Independent reflections	5468
b/Å	22.4737 (5)	*R*(int)	0.1978
c/Å	25.5597 (5)	Final R indexes [I>=2σ (I)]	R_1 [b] = 0.0884 wR_2 [c] = 0.1911
Volume/Å^3	7789.7 (3)	Final R indexes [all data]	R_1 = 0.1659 wR_2 = 0.2363
Z	8	Goodness-of-fit on F^2	1.017

[a] Obtained with graphite monochromated Cu *K*α radiation (λ = 1.54178 Å) [b] $R_1 = \sum ||F_o| - |F_c|| / \sum |F_o|$. [c] $wR_2 = \{ \sum [w(F_o^2 - F_c^2)^2 / \sum [w(F_o^2)^2]\}^{1/2}$.

Table 3-2. Selected bond lengths from the X-ray crystal structure of $[Fe(dvpp)_2](PF_6)_2$.

Selected Bond Lengths (Å)	
Fe1—N1	1.988 (6)
Fe1—N2	1.989 (6)
Fe1—N3	1.998 (6)
Fe1—N4	1.986 (6)
Fe1—N5	1.990 (6)
Fe1—N6	1.996 (5)

Table 3-3. Selected bond angles from the X-ray crystal structure of $[Fe(dvpp)_2](PF_6)_2$.

Bond Angles (°)			
N2—Fe1—N5	179.5 (3)	N4—Fe1—N3	92.8 (2)
N2—Fe1—N4	89.4 (2)	N1—Fe1—N3	179.0 (2)
N5—Fe1—N4	90.5 (2)	N2—Fe1—N6	90.4 (2)
N2—Fe1—N1	89.0 (2)	N5—Fe1—N6	89.7 (2)
N5—Fe1—N1	90.3 (2)	N4—Fe1—N6	179.5 (2)
N4—Fe1—N1	87.9 (2)	N1—Fe1—N6	92.5 (2)
N2—Fe1—N3	90.2 (2)	N3—Fe1—N6	86.6 (2)
N5—Fe1—N3	90.4 (2)		

In order to compare the two analogs and determine the influence of the bridging groups we first need to look to what is known about substituent inductive effects. The effects of electron withdrawing and donating substituents in the 4-position of terpyridine on photophysical and electrochemical properties of ruthenium(II) complexes have been investigated.[24] Introducing any substituent to the 4-position of terpyridine in a Ru(II) complex results in a red shift of the MLCT. Electron withdrawing substituents are known to stabilize both the π^* (LUMO) and t_{2g} orbitals (HOMO), while electron donating substituents destabilize them. The substituent effects of 4-substituted terpy ligands on iron(II) redox properties have also been investigated.[25] The research shows that there is a linear increase in the Fe(II/III) couple as a function of increasing electron withdrawing nature of the substituents. This inductive influence is greater with Fe(II)

than for Co(II) and is attributed to the stronger iron(II)-terpy binding strength. In our case, the influence may be even more pronounced due to enhanced metal-ligand overlap from the octahedral environment.

In the optical absorption spectrum, shown in Figure 3-7, we can see that the dvpp analog possesses molar absorptivity in the visible region, as is key for use in dye sensitization, but is significantly blue-shifted in comparison to the dcpp analog. Since the metal-ligand overlap is comparable in the two systems it appears that the substituent effect of the bridging groups has a significant impact on the optical properties. Consistent with the what is known in the literature, the electron withdrawing carbonyl groups lower the energy of the π^* (LUMO) and t_{2g} orbitals (HOMO), while the electron donating vinylidene groups destabilize them. From the lower energy MLCT it appears that the stabilization of the t_{2g} is more pronounced in the dcpp analog compared to the destabilization of the t_{2g} in the dvpp, which we attribute to the better energy match of the π orbitals of the metal and ligand that was proposed in Chapter 2 (Figure 2-8).

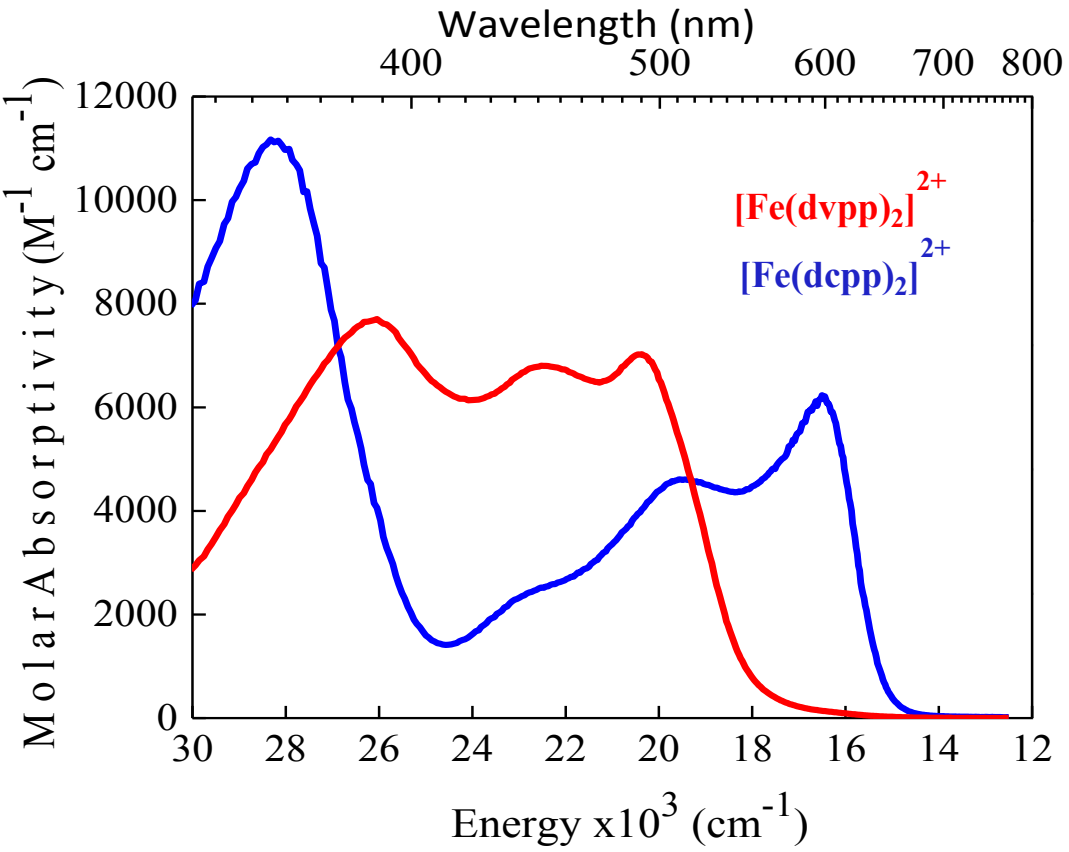

Figure 3-7: Ground state electronic absorption spectrum of $[Fe(dvpp)_2]^{2+}$ (red), and $[Fe(dcpp)_2]^{2+}$ (blue) in CH_3CN.

The electrochemical potentials of the $Fe(dvpp)_2]^{2+}$ were measured by cyclic voltammetry and the first oxidation and reduction potentials are listed in Table 3-4. The more negative reduction potential is attributed to the electron donating vinylidene bridges making the ligand harder to reduce. In comparison to the $[Fe(dcpp)_2]^{2+}$ complex, the less positive oxidation potential is consistent with the inductive influence of ligand substituents on the Fe(II/III) redox couple. The redox potentials are more in line with $[Fe(bpy)_3]^{2+}$ and it appears that any stabilization gained by moving toward a more symmetric geometry is countered by the inductive effect of the electron donating vinylidene bridges.

Table 3-4. Electrochemical potentials for the oxidation and first reduction of $[Fe(bpy)_3](PF_6)_2$, $[Fe(terpy)_2](PF_6)_2$, $[Fe(dvpp)_2](PF_6)_2$, and $[Fe(dcpp)_2](PF_6)_2$, measured with Ag/NO_3 or Ag/AgCl reference with 0.1 M $TBAPF_6$ electrolyte in acetonitrile, externally referenced to ferrocene.

Compound	$E_{1/2}$ [ox]	$E_{1/2}$ [red]
$[Fe(bpy)_3]^{2+}$	0.665 V	-1.775 V
$[Fe(terpy)_2]^{2+}$	0.715 V	-1.675 V
$[Fe(dvpp)_2]^{2+}$	0.640 V	-1.840 V
$[Fe(dcpp)_2]^{2+}$	1.295 V	-0.965 V

The isostructural analog $[Fe(dvpp)_2]^{2+}$ has provided some insight into the unique characteristics of $[Fe(dcpp)_2]^{2+}$ and it is clear that the electron withdrawing carbonyl groups have a significant impact on the properties. The photophysical investigation into the ultrafast dynamics of this analog is currently underway. It seems that we have two compounds at far ends of the spectrum and it would be ideal to obtain an analog somewhere in the middle, so efforts will continue toward developing an imine analog.

3.3.4 Continuing Quest for a Control Molecule

A motive behind the design of analogs of $[Fe(dcpp)_2]^{2+}$ was to remove the reactive carbonyl bridges in order to have easier access to a control molecule. The $[Fe(dvpp)_2]^{2+}$ does not possess the exciting properties that the dcpp analog has, but a control molecule could still prove to be useful. The zinc(II) analog may be easily prepared by a simple procedure of adding a Zn(II) salt to the dvpp ligand and stirring for 30 minutes. The product is precipitated from the reaction with ether yielding fairly clean product which can simply be recrystallized by ether diffusion.

With $[Zn(dvpp)_2]^{2+}$ in hand, our efforts are now turning toward back toward $[Zn(dcpp)_2]^{2+}$ by oxidizing the olefin groups after coordination. As discussed in Chapter 2, after many efforts to oxidize the methylene bridges in $[Cd(dmpp)_2]^{2+}$ we have yet to find the right conditions, most being too harsh and stripping the ligand from the metal center. We may have better luck finding mild conditions by which we may oxidize the vinylidene bridges. A promising possibility is the use of photochemistry, as it has been shown that olefins can undergo oxidative cleavage on silica gel in the presence of light and air.[22,23]

The ESI-MS data on this molecule is worrisome; though the product is present, it is drastically overshadowed by many other peaks, possibly signifying instability. Hopefully, the $[Zn(dvpp)_2]^{2+}$ is sufficiently stable to handle oxidative conditions and remain intact. If it proves to be unstable, it should be just as simple to prepare the Cd(II) analog which might be more stable toward oxidative conditions. Efforts are continuing toward a control molecule for $[Fe(dcpp)_2]^{2+}$.

3.4 Concluding Comments

Our efforts to develop a symmetric analog was achieved with the design and preparation of $[Fe(dvpp)_2]^{2+}$. This molecule provided a nice contrast to the $[Fe(dcpp)_2]^{2+}$ and allowed us to investigate the inductive effects of the bridging group of the ligand. With only two analogs in hand we can only postulate, nevertheless, it appears that the unique characteristics of the $[Fe(dcpp)_2]^{2+}$ can be attributed to the inductive effects from the electron withdrawing carbonyl groups. However, these inductive effects

are presumably heightened by the enhanced geometry. Work is ongoing toward the preparation of the imine analog to gain more information.

The other motive for this work was to develop an analog that would allow for more access to a control molecule. This also came to fruition, but since the $[Fe(dvpp)_2]^{2+}$ analog does not possess the same exciting characteristics, the $[Zn(dvpp)_2]^{2+}$ is not very useful to us as-is. We are currently in pursuit of methodology by which we may oxidize the olefin groups to carbonyls to achieve the desired $[Zn(dcpp)_2]^{2+}$.

APPENDIX

APPENDIX

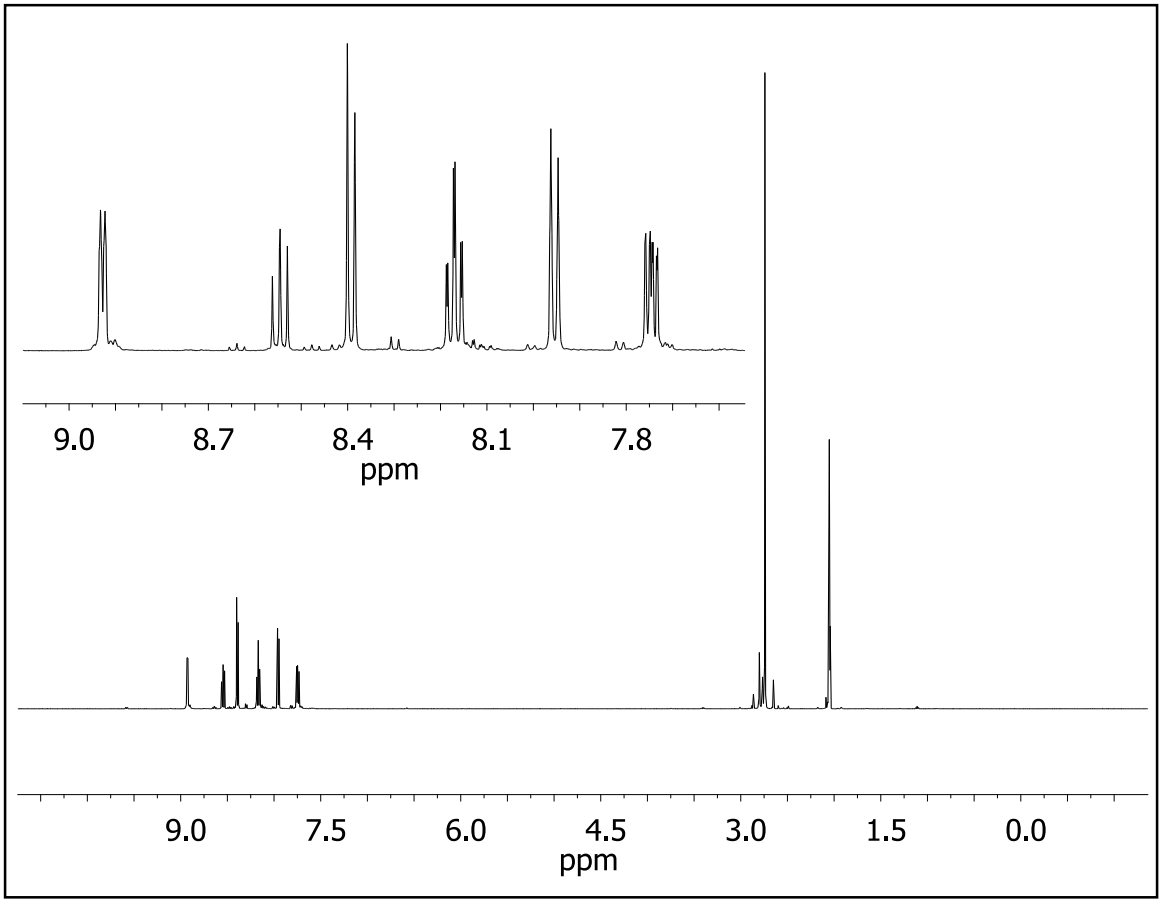

Figure 3-8. ^{1}H NMR of $[Fe(dmipp)_2](PF_6)_2$ in $(CD_3)_2CO$.

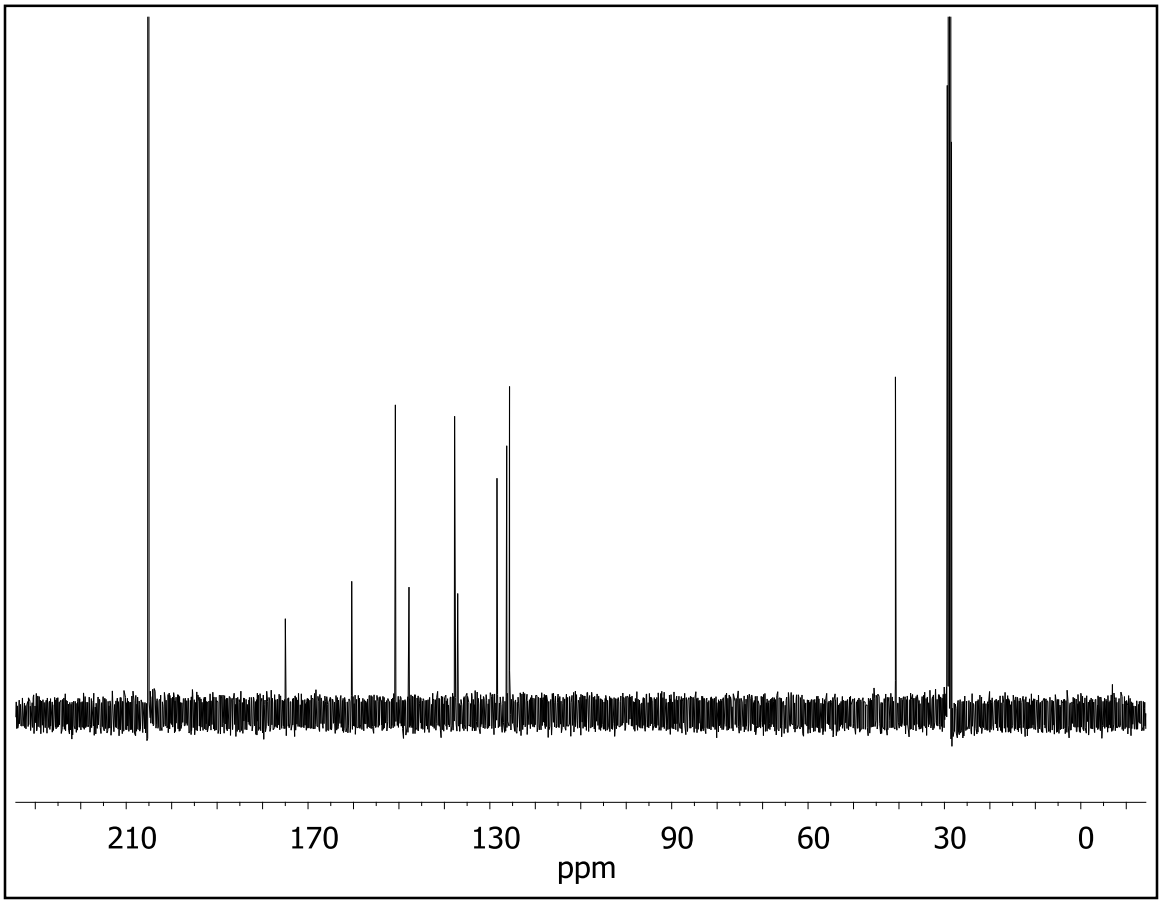

Figure 3-9. ^{13}C NMR of $[Fe(dmipp)_2](PF_6)_2$ in $(CD_3)_2CO$.

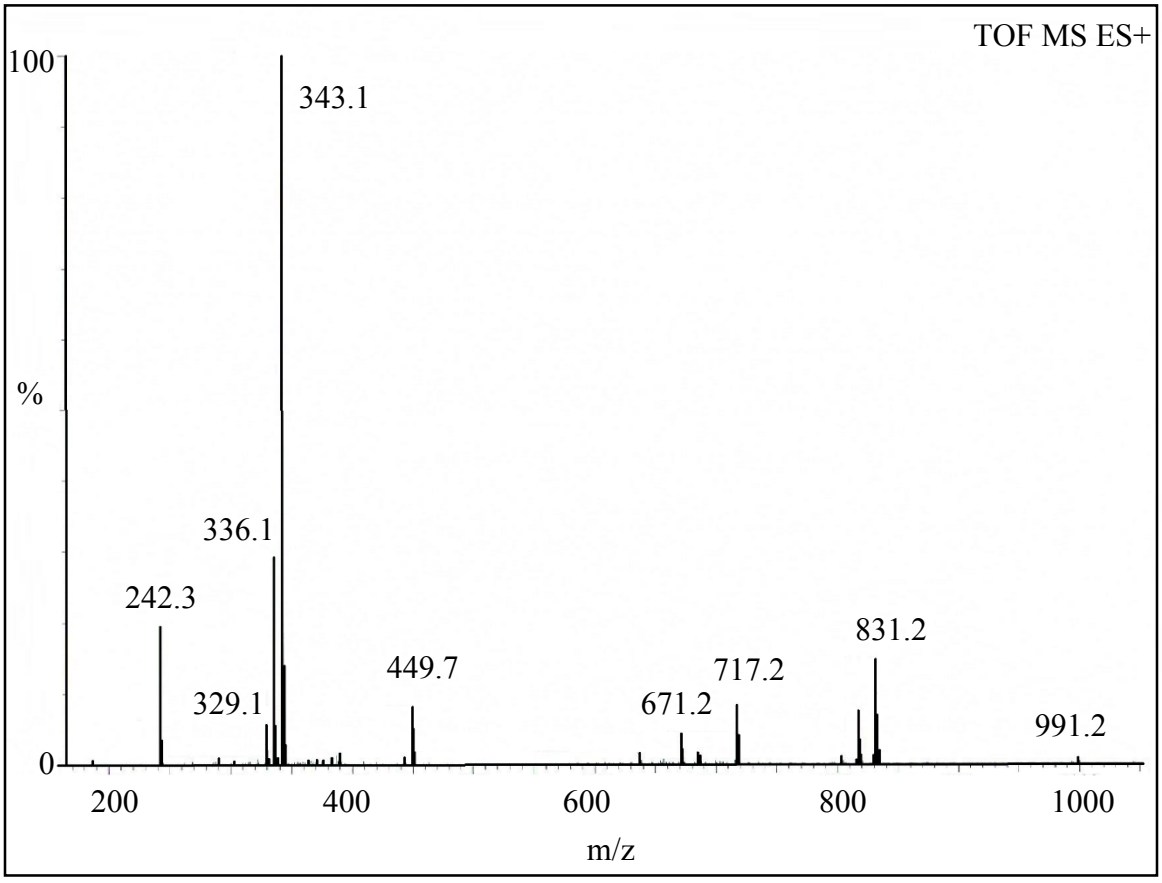

Figure 3-10. ESI-MS of $[Fe(dmipp)_2](PF_6)_2$

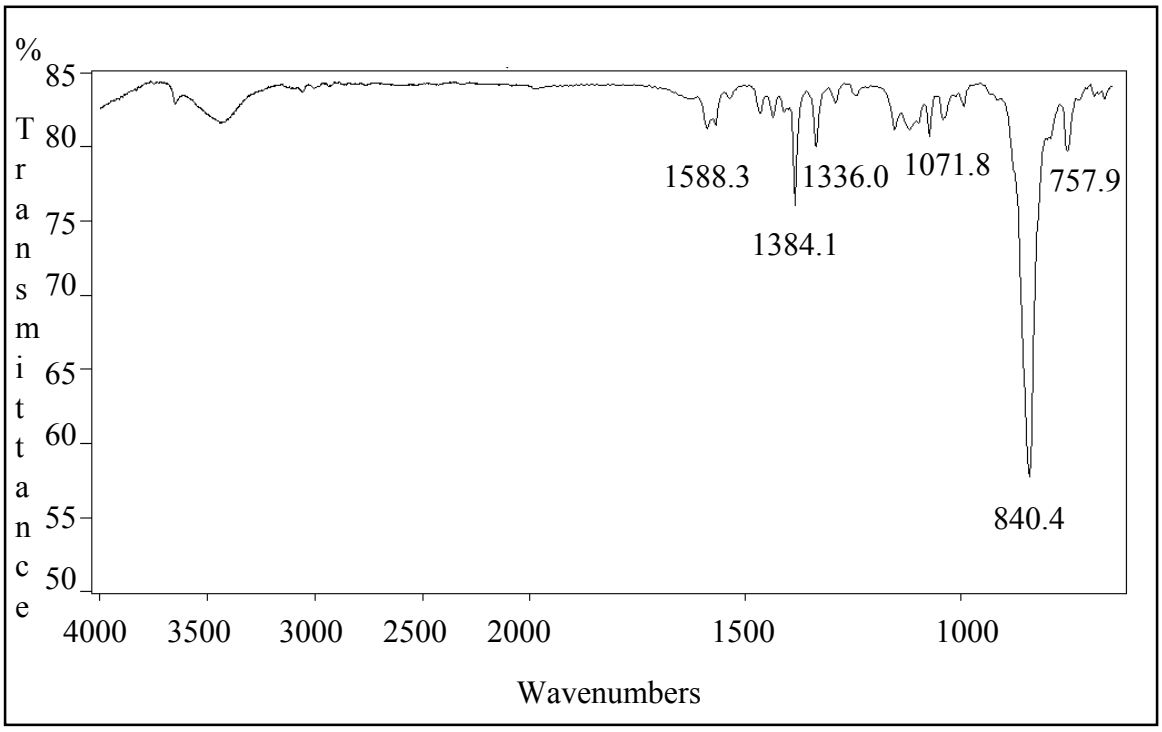

Figure 3-11. IR of $[Fe(dmipp)_2](PF_6)_2$

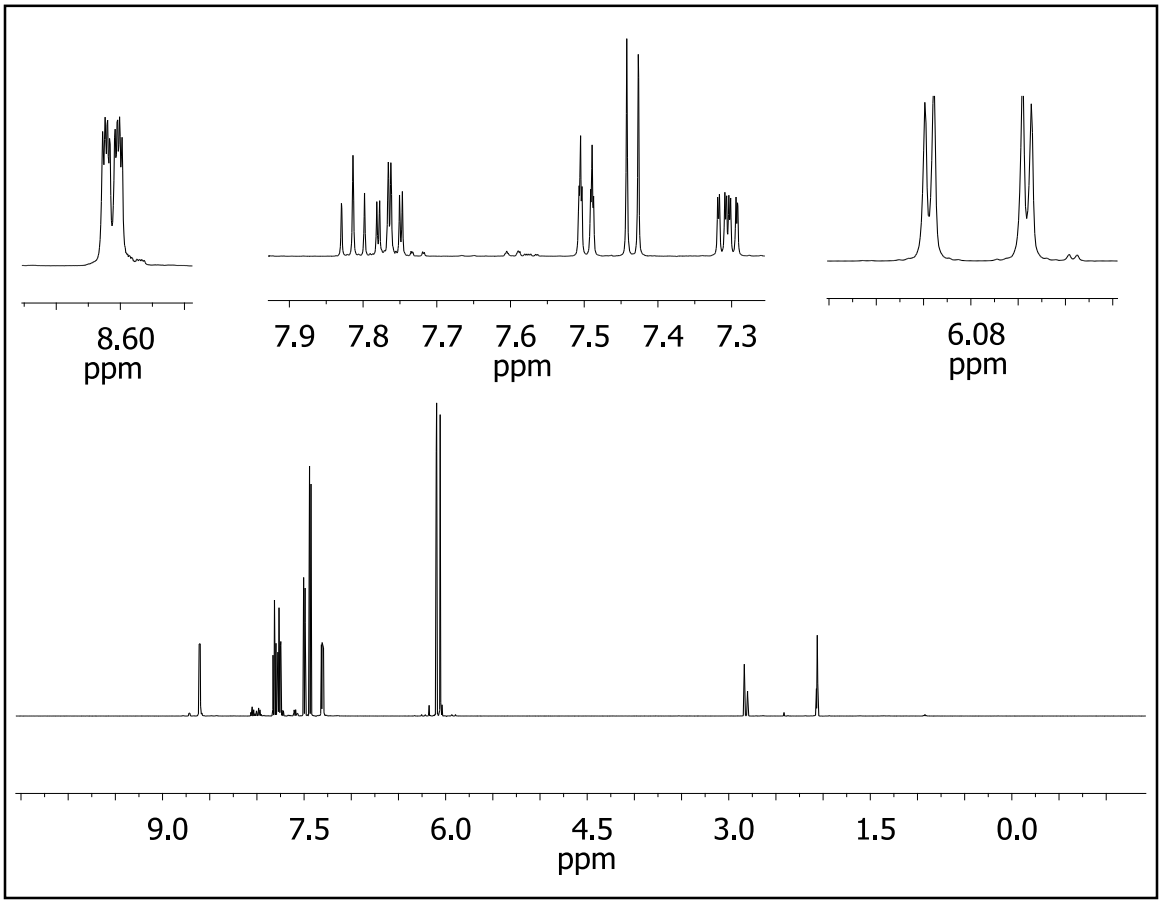

Figure 3-12. ^{1}H NMR of 2,6-di(2-vinylidenepyridyl)pyridine (dvpp) in $(CD_3)_2CO$.

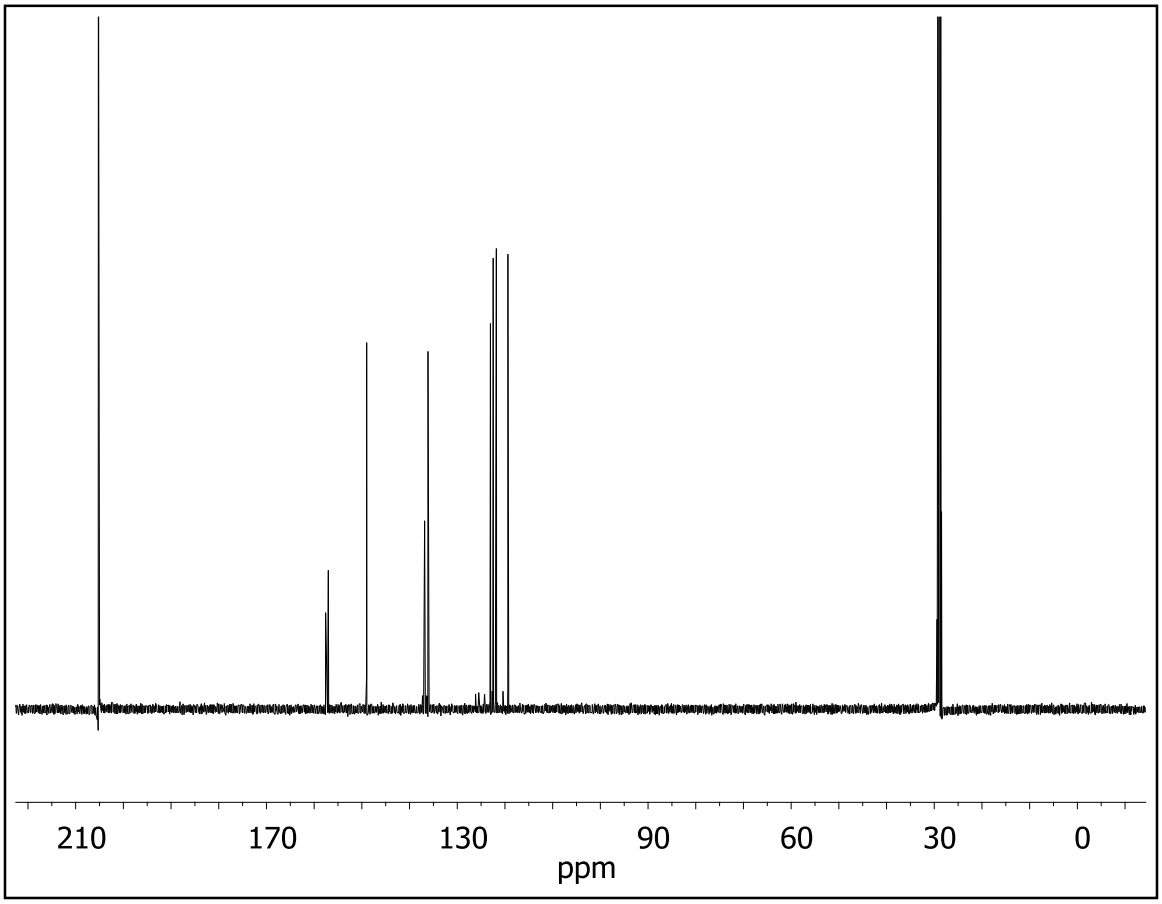

Figure 3-13. ^{13}C NMR of 2,6-di(2-vinylidenepyridyl)pyridine (dvpp) in $(CD_3)_2CO$.

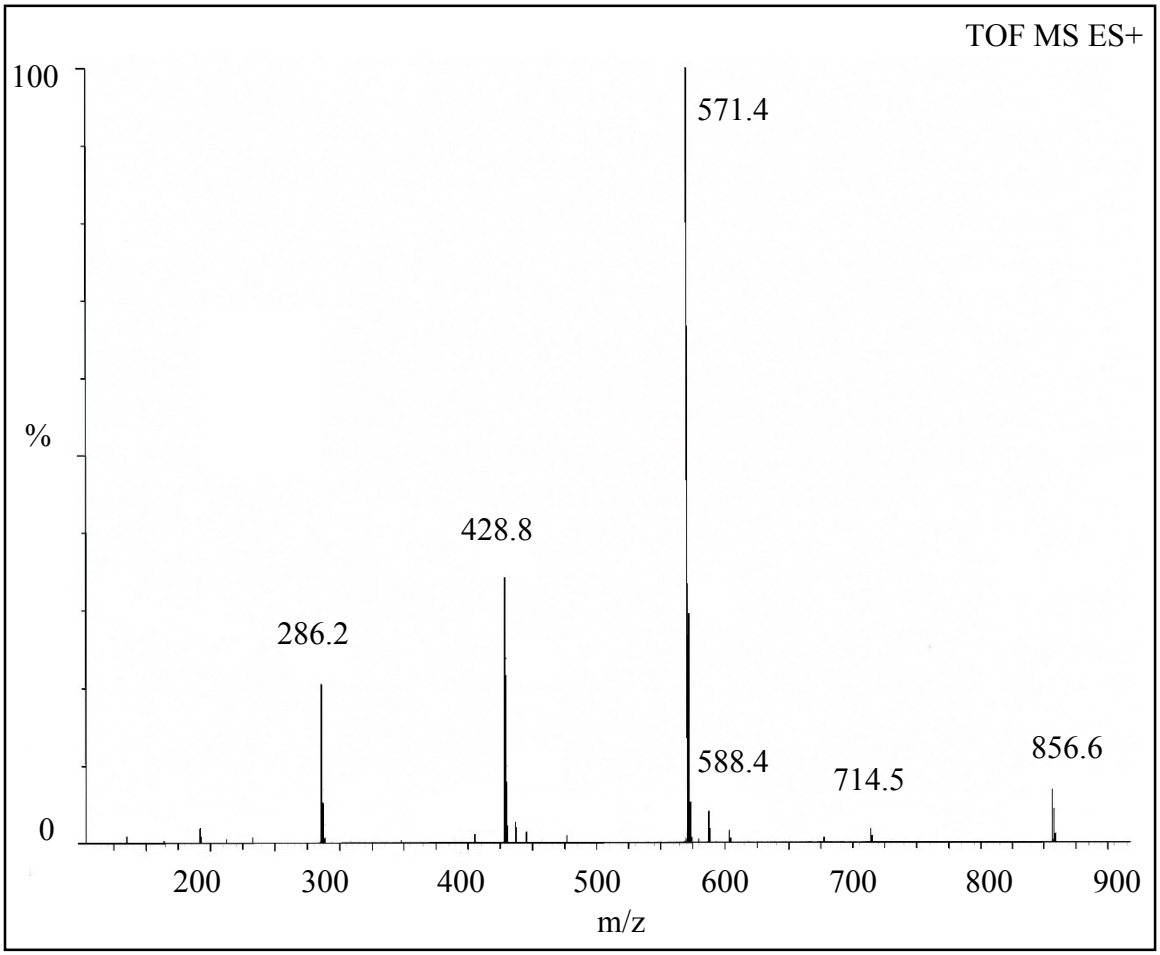

Figure 3-14. ESI-MS of 2,6-di(2-vinylidenepyridyl)pyridine dvpp.

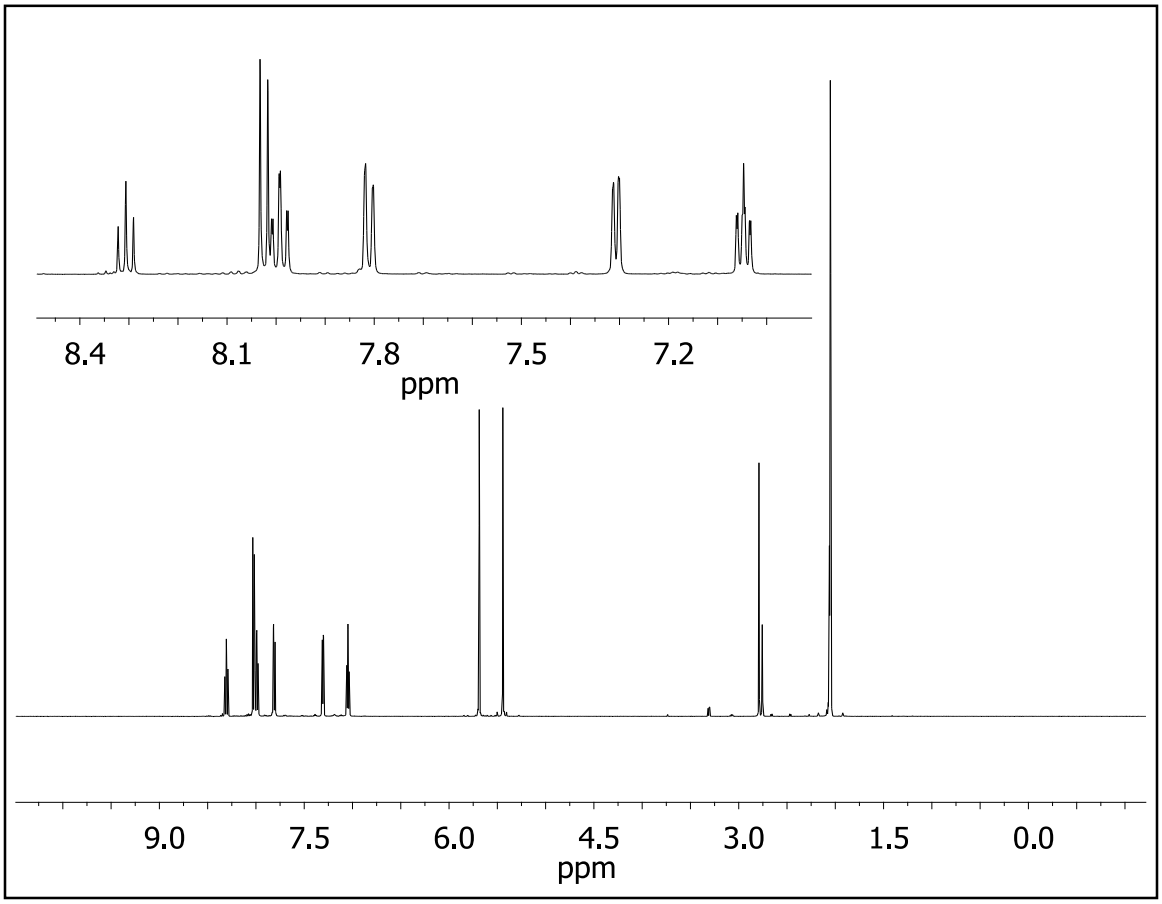

Figure 3-15. ^{1}H NMR of $[Fe(dvpp)_2](PF_6)_2$ in $(CD_3)_2CO$.

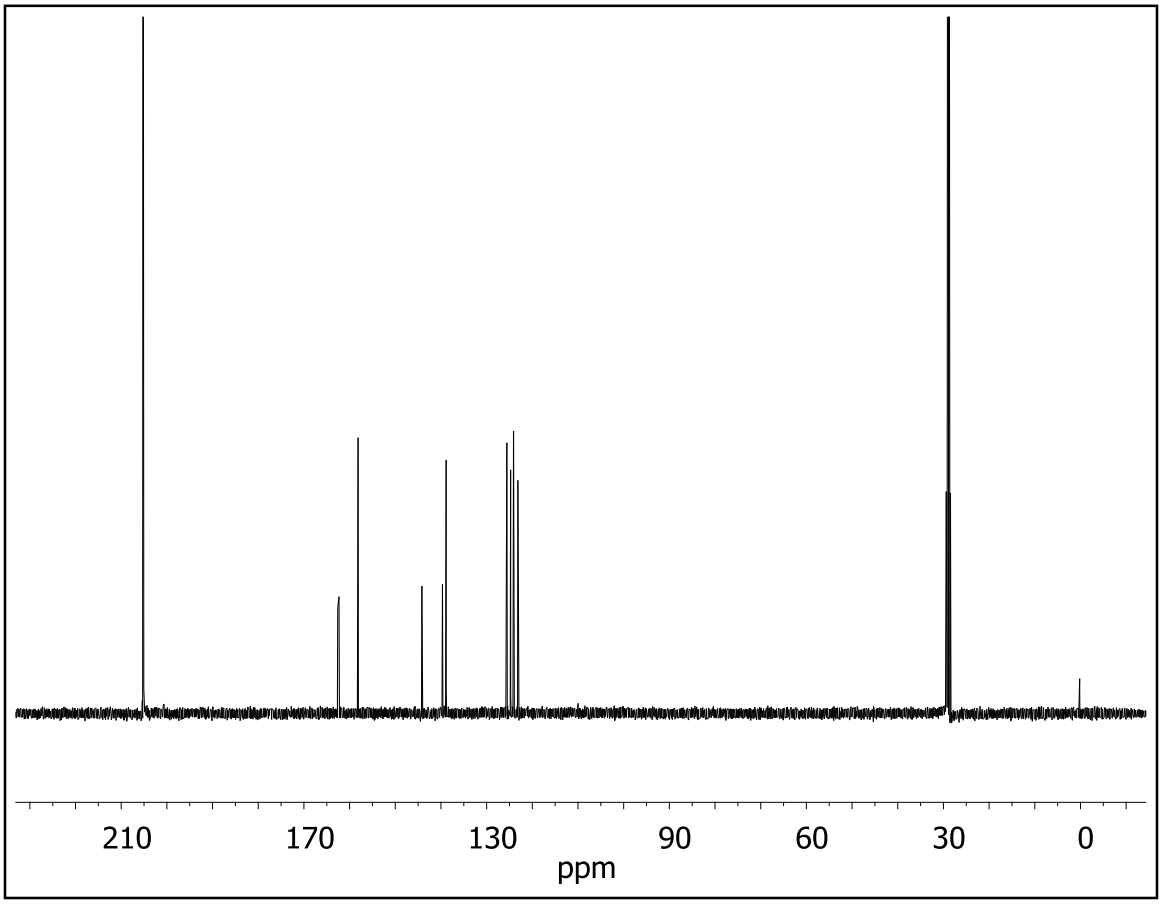

Figure 3-16. ^{13}C NMR of $[Fe(dvpp)_2](PF_6)_2$ in $(CD_3)_2CO$.

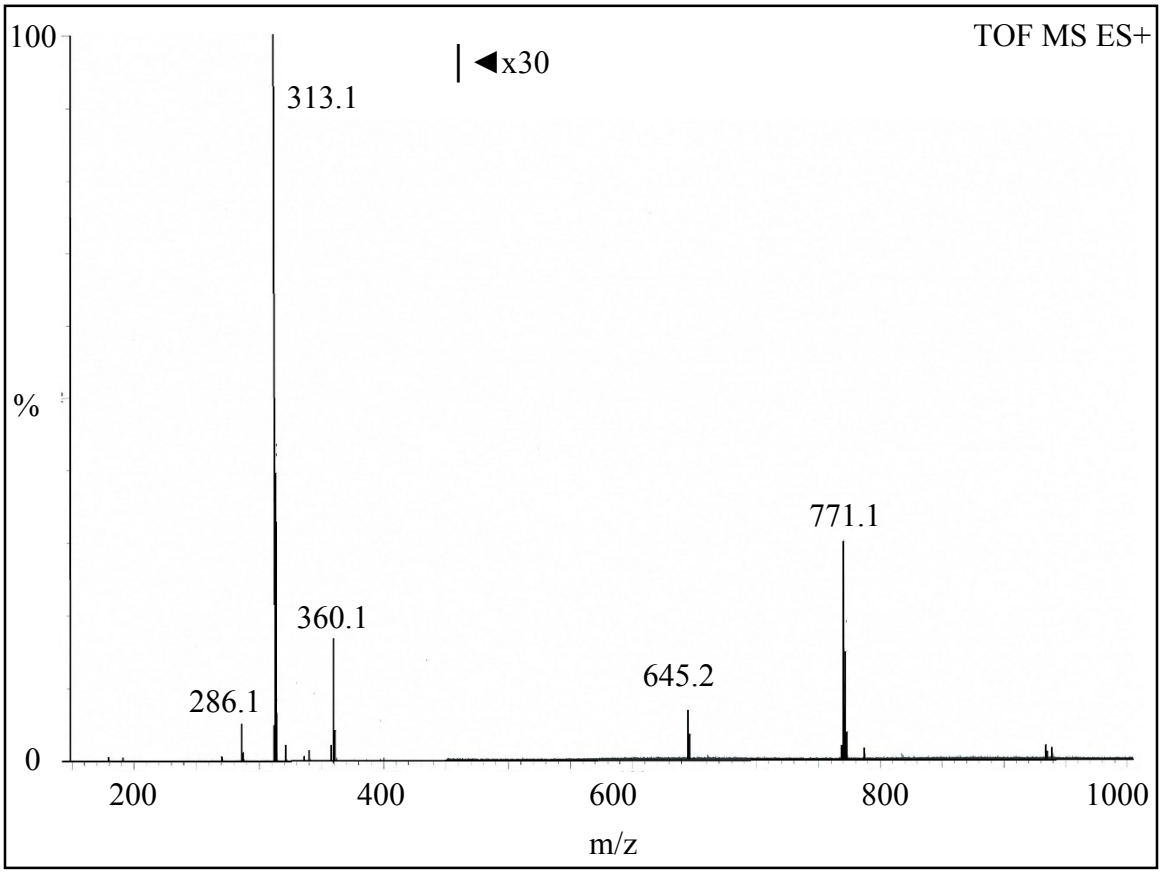

Figure 3-17. ESI-MS of $[Fe(dvpp)_2](PF_6)_2$.

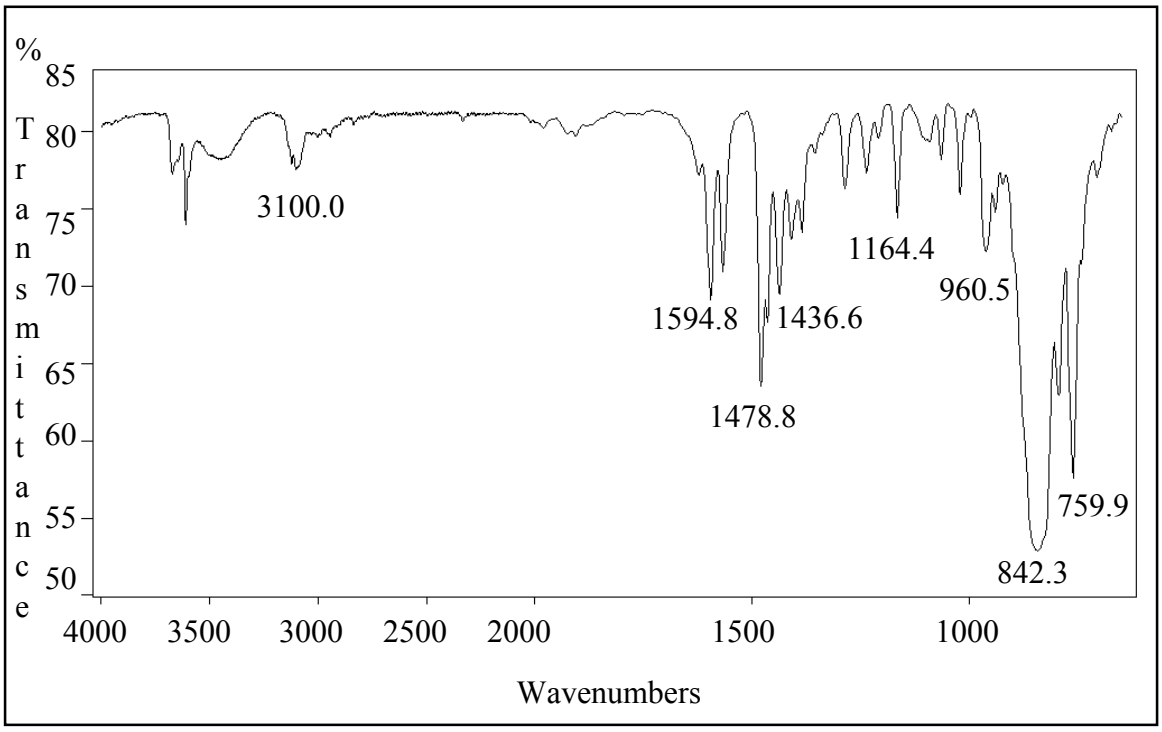

Figure 3-18. IR of $[Fe(dvpp)_2](PF_6)_2$.

Table 3-5. Geometric parameters for the X-ray crystal structure of $[Fe(dvpp)_2](PF_6)_2$.

Bond Lengths (Å)					
Fe1	N1	1.988(6)	C16	C17	1.387(14)
Fe1	N2	1.989(6)	C17	C18	1.365(14)
Fe1	N3	1.998(6)	C18	C19	1.359(12)
Fe1	N4	1.986(6)	C20	C21	1.377(12)
Fe1	N5	1.990(6)	C21	C22	1.385(18)
Fe1	N6	1.996(5)	C22	C23	1.395(18)
N1	C1	1.363(10)	C23	C24	1.402(12)
N1	C5	1.345(10)	C24	C25	1.498(13)
N2	C8	1.326(11)	C25	C26	1.316(14)
N2	C12	1.366(11)	C25	C27	1.472(12)
N3	C15	1.348(10)	C27	C28	1.378(12)
N3	C19	1.364(10)	C28	C29	1.357(16)
N4	C20	1.361(11)	C29	C30	1.373(16)
N4	C24	1.354(11)	C30	C31	1.396(12)
N5	C27	1.376(10)	C31	C32	1.503(13)
N5	C31	1.338(10)	C32	C33	1.319(13)
N6	C34	1.358(11)	C32	C34	1.481(13)
N6	C38	1.360(11)	C34	C35	1.395(13)
C1	C2	1.365(12)	C35	C36	1.367(17)
C2	C3	1.389(13)	C36	C37	1.371(16)
C3	C4	1.371(13)	C37	C38	1.370(12)
C4	C5	1.389(11)	P1	F1	1.616(16)
C5	C6	1.498(11)	P1	F2	1.552(14)
C6	C7	1.361(14)	P1	F3	1.517(12)
C6	C8	1.464(13)	P1	F4	1.578(11)
C8	C9	1.408(13)	P1	F5	1.585(12)
C9	C10	1.37(2)	P1	F6	1.594(14)
C10	C11	1.35(2)	P2	F7	1.539(12)
C11	C12	1.395(13)	P2	F8	1.553(10)
C12	C13	1.494(14)	P2	F9	1.542(9)
C13	C14	1.319(13)	P2	F10	1.628(10)
C13	C15	1.480(11)	P2	F11	1.623(8)
C15	C16	1.366(12)	P2	F12	1.587(9)

Bond Angles (o)							
N1	Fe1	N2	89.0(2)	C18	C19	N3	122.6(6)
N1	Fe1	N3	179.0(2)	N4	C20	C21	123.6(9)
N1	Fe1	N5	90.3(2)	C20	C21	C22	118.0(9)
N1	Fe1	N6	92.5(2)	C21	C22	C23	120.4(7)
N2	Fe1	N3	90.2(2)	C22	C23	C24	117.8(10)
N2	Fe1	N5	179.3(3)	N4	C24	C23	122.5(8)
N2	Fe1	N6	90.4(2)	N4	C24	C25	118.4(6)
N4	Fe1	N1	87.9(2)	C23	C24	C25	119.0(8)

Table 3.5 (cont'd).

N4	Fe1	N2	89.4(2)	C26	C25	C24	120.4(8)
N4	Fe1	N3	92.8(2)	C26	C25	C27	121.1(8)
N4	Fe1	N5	90.5(2)	C27	C25	C24	118.2(7)
N4	Fe1	N6	179.5(2)	N5	C27	C25	119.7(6)
N5	Fe1	N3	90.4(2)	N5	C27	C28	120.7(7)
N5	Fe1	N6	89.7(2)	C28	C27	C25	119.7(7)
N6	Fe1	N3	86.8(2)	C29	C28	C27	120.6(8)
C1	N1	Fe1	120.9(5)	C28	C29	C30	119.3(7)
C5	N1	Fe1	122.4(4)	C29	C30	C31	119.2(8)
C5	N1	C1	116.5(6)	N5	C31	C30	121.7(8)
C8	N2	Fe1	121.8(5)	N5	C31	C32	119.2(7)
C8	N2	C12	118.4(7)	C30	C31	C32	119.2(7)
C12	N2	Fe1	119.7(6)	C33	C32	C31	119.4(8)
C15	N3	Fe1	121.9(5)	C33	C32	C34	121.8(8)
C15	N3	C19	117.5(6)	C34	C32	C31	118.6(6)
C19	N3	Fe1	120.5(5)	N6	C34	C32	117.9(6)
C20	N4	Fe1	121.1(5)	N6	C34	C35	120.6(8)
C24	N4	Fe1	121.0(5)	C35	C34	C32	121.5(8)
C24	N4	C20	117.5(6)	C36	C35	C34	120.5(8)
C27	N5	Fe1	120.1(5)	C35	C36	C37	118.7(7)
C31	N5	Fe1	121.4(5)	C38	C37	C36	119.6(8)
C31	N5	C27	118.6(6)	N6	C38	C37	122.7(8)
C34	N6	Fe1	121.4(5)	F2	P1	F1	92.9(15)
C34	N6	C38	117.8(6)	F2	P1	F4	92.9(13)
C38	N6	Fe1	120.5(5)	F2	P1	F5	175.4(17)
N1	C1	C2	123.9(7)	F2	P1	F6	89.7(14)
C1	C2	C3	118.7(7)	F3	P1	F1	88.7(11)
C4	C3	C2	118.4(7)	F3	P1	F2	95.5(16)
C3	C4	C5	120.0(7)	F3	P1	F4	97.2(12)
N1	C5	C4	122.2(7)	F3	P1	F5	88.9(11)
N1	C5	C6	117.0(6)	F3	P1	F6	174.3(11)
C4	C5	C6	120.7(7)	F4	P1	F1	171.3(9)
C7	C6	C5	118.5(8)	F4	P1	F5	87.7(6)
C7	C6	C8	123.0(8)	F4	P1	F6	85.0(8)
C8	C6	C5	118.3(7)	F5	P1	F1	86.0(8)
N2	C8	C6	119.7(6)	F5	P1	F6	85.9(8)
N2	C8	C9	121.6(8)	F6	P1	F1	88.6(9)
C9	C8	C6	118.7(8)	F7	P2	F8	98.3(11)
C10	C9	C8	119.4(10)	F7	P2	F9	90.7(10)
C11	C10	C9	119.5(8)	F7	P2	F10	173.5(13)
C10	C11	C12	119.7(9)	F7	P2	F11	89.1(9)
N2	C12	C11	121.4(9)	F7	P2	F12	92.3(11)
N2	C12	C13	119.9(7)	F8	P2	F10	87.4(9)
C11	C12	C13	118.7(7)	F8	P2	F11	172.4(10)

Table 3.5 (cont'd).

C14	C13	C12	121.3(8)	F8	P2	F12	92.3(8)
C14	C13	C15	120.0(9)	F9	P2	F8	86.3(9)
C15	C13	C12	118.5(6)	F9	P2	F10	86.5(7)
N3	C15	C13	117.9(6)	F9	P2	F11	95.5(8)
N3	C15	C16	121.8(7)	F9	P2	F12	176.8(8)
C16	C15	C13	120.2(6)	F11	P2	F10	85.3(5)
C15	C16	C17	120.0(7)	F12	P2	F10	90.5(8)
C18	C17	C16	118.4(8)	F12	P2	F11	85.5(5)
C19	C18	C17	119.7(8)				

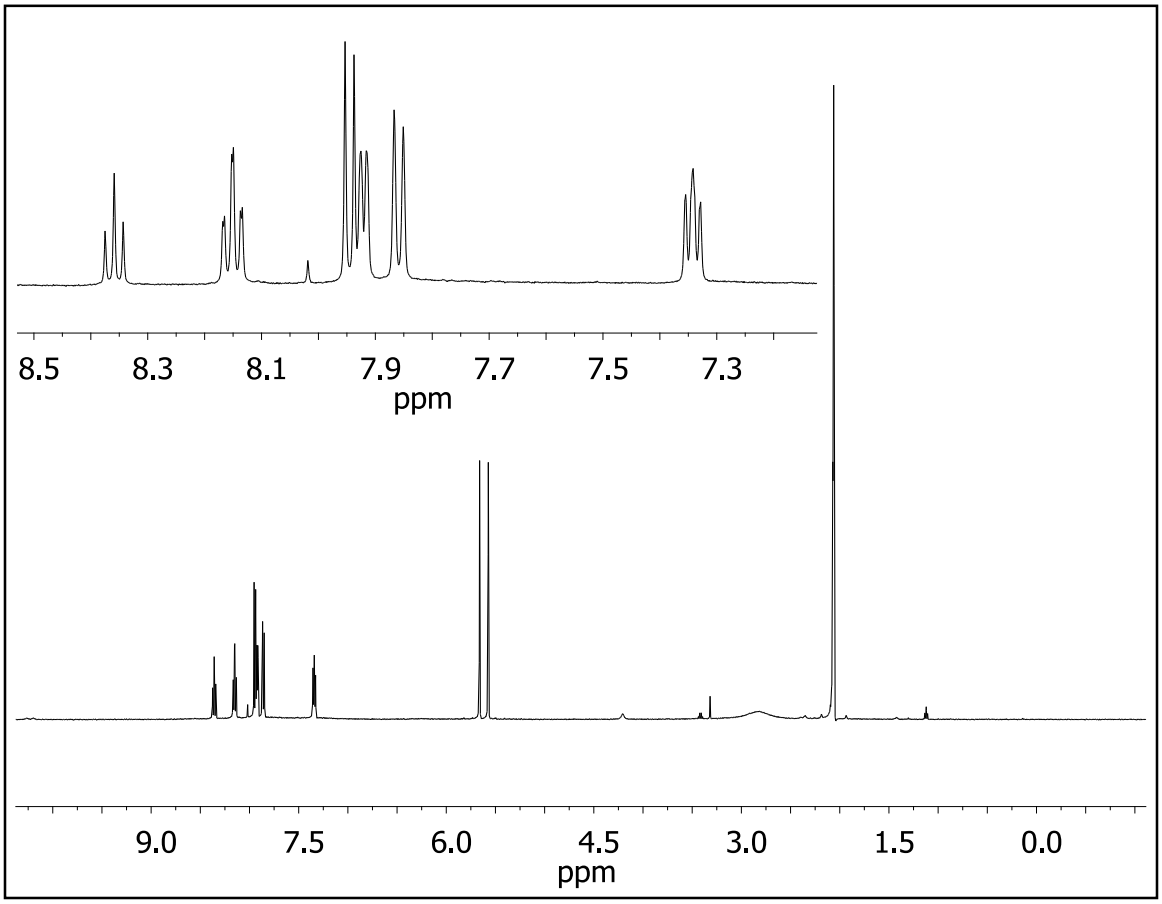

Figure 3-19. ^{1}H NMR of $[Zn(dvpp)_2](PF_6)_2$ in $(CD_3)_2CO$.

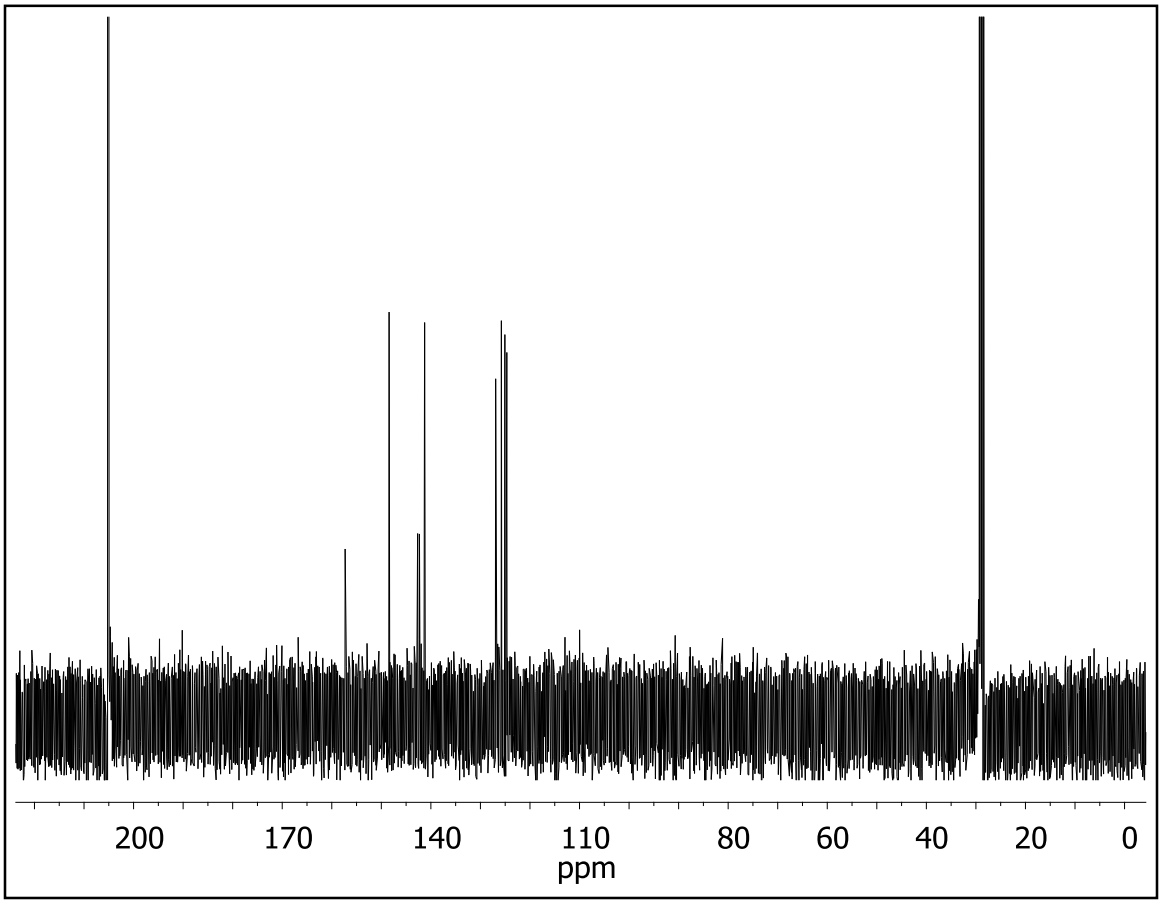

Figure 3-20. ^{13}C NMR of $[Zn(dvpp)_2](PF_6)_2$ in $(CD_3)_2CO$.

REFERENCES

REFERENCES

(1) Perrin, D. D.; Armarego, W. L. F. *Purification of Laboratory Chemicals, 3rd ed.*; Pergamon Press: New York, 1988.

(2) Flores-Chávez, B.; Martínez-Ortega, B. A.; Alvarado-Rodríguez, J. G.; Andrade-López, N. *Journal of Chemical Crystallography* **2005**, *35*, 451–456.

(3) Andrade-López, N.; Hanna, T. a.; Alvarado-Rodríguez, J. G.; Luqueño-Reyes, A.; Martínez-Ortega, B. a.; Mendoza-Espinosa, D. *Polyhedron* **2010**, *29*, 2304–2310.

(4) Summers, G. .; Ndawuni, M. .; Summers, C. . *Polymer* **2001**, *42*, 397–402.

(5) Hofmeier, H.; Hoogenboom, R.; Wouters, M. E. L.; Schubert, U. S. *Journal of the American Chemical Society* **2005**, *127*, 2913–21.

(6) SPARTAN 5.0 ed.; Wavefunction Inc.: Irvine, CA, **1997**.

(7) Frisch, M. J.; Trucks, G. W.; Schlegel, H. B.; Scuseria, G. E.; Robb, M. A.; Cheeseman, J. R.; J. A. Montgomery, J.; Vreven, T.; Kudin, K. N.; Burant, J. C.; Millam, J. M.; Iyengar, S. S.; Tomasi, J.; Barone, V.; Mennucci, B.; Cossi, M.; Scalmani, G.; Rega, N.; Petersson, G. A.; Nakatsuji, H.; Hada, M.; Ehara, M.; Toyota, K.; Fukuda, R.; Hasegawa, J.; Ishida, M.; Nakajima, T.; Honda, Y.; Kitao, O.; Nakai, H.; Klene, M.; Li, X.; Knox, J. E.; Hratchian, H. P.; Cross, J. B.; Adamo, C.; Jaramillo, J.; Gomperts, R.; Stratmann, R. E.; Yazyev, O.; Austin, A. J.; Cammi, R.; Pomelli, C.; Ochterski, J. W.; Ayala, P. Y.; Morokuma, K.; Voth, G. A.; Salvador, P.; Dannenberg, J. J.; Zakrzewski, V. G.; Dapprich, S.; Daniels, A. D.; Strain, M. C.; Farkas, O.; Malick, D. K.; Rabuck, A. D.; Raghavachari, K.; Foresman, J. B.; Ortiz, J. V; Cui, Q.; Baboul, A. G.; Clifford, S.; Cioslowski, J.; Stefanov, B. B.; Liu, G.; Liashenko, A.; Piskorz, P.; Komaromi, I.; Martin, R. L.; Fox, D. J.; Keith, T.; Al-Laham, M. A.; Peng, C. Y.; Nanayakkara, A.; Challacombe, M.; Gill, P. M. W.; Chen, B. J. W.; Wong, M. W.; Gonzalez, C.; Pople, J. A. Gaussian 03, Revision D.01 **2004**.

(8) Mooibroek, T. J.; Gamez, P.; Reedijk, J. *CrystEngComm* **2008**, *10*, 1501.

(9) Bloom, J. W. G.; Wheeler, S. E. *Angewandte Chemie (International ed. in English)* **2011**, *50*, 7847–9.

(10) Martinez, C. R.; Iverson, B. L. *Chemical Science* **2012**, *3*, 2191.

(11) Raju, R. K.; Bloom, J. W. G.; An, Y.; Wheeler, S. E. *Chemphyschem : A European Journal of Chemical Physics and Physical Chemistry* **2011**, *12*, 3116–30.

(12) Quiñonero, D.; Estarellas, C.; Frontera, A.; Deyà, P. M. *Chemical Physics Letters* **2011**, *508*, 144–148.

(13) Yorke, J.; Dent, C.; Decken, A.; Xia, A. *Inorganic Chemistry Communications* **2010**, *13*, 54–57.

(14) Thienthong, N.; Bergman, Y. E.; Perlmutter, P. *Synthetic Communications* **2009**, *39*, 2683–2693.

(15) Clark, R. J. H.; Turtle, P. C.; Strommen, D. P.; Streusand, B.; Kincaid, J.; Nakamoto, K. *Inorganic Chemistry* **1977**, *16*, 84–89.

(16) Kuwabara, I. H.; Comninos, F. C. M.; Pardini, V. L.; Viertler, H.; Toma, H. E. *Electrochimica Acta* **1994**, *39*, 2401–2406.

(17) Toma, H. E.; Kuwabara, I. H.; Faria, D. L. A. de *J. Braz. Chem. Soc.* **1996**, *7*, 391–394.

(18) Scott, J.; Gambarotta, S.; Korobkov, I.; Budzelaar, P. H. M. *Journal of the American Chemical Society* **2005**, *127*, 13019–29.

(19) Schubert, U. S.; Hofmeire, H.; Newkome, G. R. *Modern Terpyridine Chemistry*; Wiley-VCH, 2006.

(20) Jamula, L. L. Masters Thesis, Michigan State University, 2010.

(21) Eckhard, I.; Summers, L. *Australian Journal of Chemistry* **1974**, *27*, 2511.

(22) Shim, S. C.; Aronovitch, C.; Mazur, Y. *The Journal of Organic Chemistry* **1985**, *50*, 149–150.

(23) Sigman, M. E.; Barbas, J.; Corbett, S.; Chen, Y.; Ivanov, I.; Dabestani, R. *Journal of Photochemistry and Photobiology A: Chemistry* **2001**, *138*, 269–274.

(24) Maestri, M.; Armaroli, N.; Balzani, V.; Constable, E. C.; Thompson, A. M. W. C. *Inorganic Chemistry* **1995**, *34*, 2759–2767.

(25) Chambers, J.; Eaves, B.; Parker, D.; Claxton, R.; Ray, P. S.; Slattery, S. J. *Inorganica Chimica Acta* **2006**, *359*, 2400–2406.

Chapter 4. Tuning the Energetics of Excited States by Synthetic Modification of the Ligand System

4.1 Introduction

Our intentions for moving toward a more symmetric coordination environment were to collapse the ligand field manifold into discrete states to gain more understanding into the charge transfer to ligand field deactivation pathway. We achieved the desired geometry with the first molecule that we pursued and it was found to possess some exciting properties. The observation of weak emission from this fascinating new molecule has led us in a new direction. We believe that we may have introduced a strong enough ligand field to iron(II) to achieve inversion of the lowest energy excited states. If we have in fact been able to tune the energies of the lower excited states why couldn't we do the same to the higher energy levels and achieve inversion of a charge transfer excited state with a ligand field state.

We propose that the emission arises from the $^3T_1$ state ($t_{2g}^5\ e_g^1$) which will possess a different geometry than the $^1A_1$ (t_{2g}^6) ground and ^{1}MLCT excited states. The $^1A_1$ to ^{1}MLCT absorption maximum is at 605 nm while the emission feature is centered around 700 nm, which corresponds to an energy separation of ~2200 cm^{-1}. Considering the displacement of the potential energy surfaces from the difference in geometry, the zero point energy difference is likely even smaller. We propose that by making synthetic modifications to the ligand it may be possible to achieve inversion of the $^3T_1$ state with ^{3}MLCT state. As described in the introductory chapter, a major shortfall of iron(II) polypyridyls for use in DSSCs is that upon excitation to the MLCT the molecules undergo ultrafast deactivation to lower lying ligand field states. If we can prepare an iron(II)

complex with a charge transfer state as the lowest energy excited state it would open the door to great possibility for replacing Ru(II) sensitizers in DSSCs.

In order to achieve inversion of the excited states, we have to determine ways to stabilize the MLCT and destabilize the ligand field states. Tuning the energy of the ^{3}MLCT has been widely investigated for Ru(II) polypyridyls so we looked to this research for inspiration.[1–6] The introduction of electron withdrawing groups is known to lower the energy of the MLCT state, which is apparent in our new $[Fe(dcpp)_2]^{2+}$ molecule. The symmetry and inductive effects of the carbonyl groups in $[Fe(dcpp)_2]^{2+}$ have led to stabilization of the metal t_{2g} and ligand π^* orbitals as is evident in the electrochemistry (Chapter 2). From this trend, one possibility is that we could add more electron withdrawing substituents to lower the energy even further. Yet one must proceed with caution as too many electron withdrawing substituents may lower the basicity of the nitrogens and cause difficulty with the formation of the complex.

Among many other possibilities, one stands out as a promising strategy: the introduction of phenyl substituents to increase delocalization. Introducing a phenyl substituent, specifically p-tolyl, to terpy in Ru(II) complexes has been shown to stabilize the ^{3}MLCT by 1100 cm^{-1} relative to the ^{3}MLCT of the unsubstituted analog.[7] As for achieving the destabilization of the ligand field states, the introduction of a tolyl substituent could lead to an inductive increase in the basicity of the polypyridine, increasing the σ-donor strength which may have the effect of increasing the ligand field splitting and destabilizing the ligand field excited states.

We set out to prepare a series of molecules by introducing phenyl substituents to the 2,6-di(2-carboxypyridyl)pyridine (dcpp) ligand. The first molecule in the series has

been successfully prepared and will be described. Additional design strategies to achieve the excited state inversion will also be proposed.

4.2 Experimental

4.2.1 Synthesis

General. All chemicals were of reagent grade, purchased from Sigma-Aldrich, Alfa Aesar, Acros Organics, Strem Chemicals, or TCI Chemical and used as received unless otherwise noted. Solvents were purchased from Sigma-Aldrich, Jade Scientific, Spectrum, Mallinckrodt, EMD Chemical, or CCI and were purified using standard purification techniques.[8] All air-sensitive reactions were carried out under inert atmosphere by standard Schlenk techniques utilizing thoroughly deoxygenated solvents that were degassed by the freeze—pump—thaw method. ^{1}H NMR and ^{13}C NMR were recorded with Varian UnityPlus-300 MHz, Varian UnityPlus-500 MHz, and Agilent DDR2 500 MHz spectrometers. Ground state absorption spectra were obtained on a Varian Cary 50 spectrophotometer. IR spectra were obtained on a Mattson Galaxy 5000 FTIR. Elemental analysis was obtained through the Analytical facilities at Michigan State University. Electrospray mass spectra (ESI-MS) were obtained from the staff of the MSU Mass Spectrometry Facility. The characterization data of previously unknown compounds are included in the appendix at the end of this chapter.

***p*-Tolylboronic acid.** The compound was prepared according to the literature procedure from p-bromotoluene (7.19 g, 42.0 mmol) and purified by recrystallization from dissolution in hot toluene and adding hexanes and allowing it to slowly cool.[9] Yield: 5.71 g (57%). ^{1}H NMR (500MHz, $CDCl_3$) δ (ppm): 8.14 (d, 2H), 7.33 (d, 2H), 2,46 (s, 3H).

4-Hydroxypyridine-2,6-dicarboxylate diethyl ester. The compound was prepared from chelidamic acid (9.80 g, 3.98 mmol) according to a patent procedure.[10] The product was obtained as a tacky white sold which is recrystallized by dissolving in hot ethanol and adding hexanes till cloudy and placing in freezer. Yield: 7.07 g (61%). ^{1}H NMR (500MHz, $(CD_3)_2CO$) δ (ppm): 7.59 (s, 2H), 4.39 (q, 4H), 1.37 (t, 6H).

4-(Trifluoromethylsulfonyloxy)pyridine-2,6-dicarboxylate diethyl ester. The compound was prepared by modification of previously published procedures.[10,11] A 250 mL air-free round bottom flask equipped with an addition funnel was charged with 4-hydroxypyridine-2,6-dicarboxylate diethyl ester (4.14 g, 17.3 mmol) and dry CH_2Cl_2 (40 mL) and cooled to -78^{o}C in a dry ice/acetone bath. Once cool, dry pyridine was slowly added via syringe (2.5 mL, 2.45 g, 30.9 mmol). To the addition funnel was added CH2Cl2 (25 mL) and trifluoromethanesulfonic anhydride (3.71 mL, 6.22 g, 22.1 mmol), which is added dropwise to the reaction mixture over 15 minutes. The reaction was allowed to warm to room temperature over 2 hours and water was added to quench the reaction. The layers were separated and the water layer extracted with EtOAc (3 x 150 mL). The organic layers were combined, dried with $MgSO_4$, filtered and evaporated. The product may be used without purification or may be purified by recrystallization from 3:1 EtOAc/Hexanes. Yield: 6.06 g (94%). ^{1}H NMR (500MHz, $(CDCl_3)$ δ (ppm): 8.17 (s, 2H), 4.52 (q, 4H), 1.47 (t, 6H).

4-*p*-Tolylpyridine-2,6-dicarboxylate diethyl ester. The compound was prepared by modification of previously published procedures.[10,12] To a 250 mL round bottom flask was added 4-(trifluoromethylsulfonyloxy)pyridine-2,6-dicarboxylate diethyl ester (1.54 g, 4.14 mmol), *p*-tolylboronic acid (0.648 g, 4.77 mmol), $Pd(PPh_3)_4$ (0.380 g, 0.329 mmol, 8

mol%), *N,N*-diisopropylethylamine (DIPEA, 'Hünig's Base') (1.6 mL, 9.19 mmol) and dry dimethylformamide (~60 mL) and the reaction was stirred at 90-100°C overnight in the dark. The solvent was removed by vacuum distillation. The remaining brown/green solid was taken up in EtOAc (100 mL) and washed with H_2O (2 x 100 mL) and once with saturated NaCl (aq), dried with $MgSO_4$, filtered and evaporated. The crude reaction product may be purified by column chromatography on silica gel with 2% EtOAc in CH_2Cl_2. The product glows on silica under longwave UV so the column may be monitored by UV lamp. The unreacted triflate and boronic acid elute first followed by the product. The product may be recrystallized by dissolving in ethanol and adding hexanes and cooling to 0°C. Yield: 0.565 g (44%). ^{1}H NMR (($CDCl_3$, 500 MHz): δ 8.51 (s, 2H), 7.68 (d, 2H, J = 8.0 Hz), 7.36 (d, 2H, J = 8.0 Hz), 4.53 (q, 4H, J = 7.1 Hz), 2.45 (s, 3H), 1.49 (t, 6H, J = 7.1 Hz). ^{13}C NMR (($CDCl_3$, 500 MHz): δ 194.57, 164.94, 158.04, 150.86, 149.16, 130.11, 126.99, 125.23, 62.43, 21.32, 14.26. TOF-MS [ESI, *m/z* (rel int)]: 314.1 (100) $[C_{18}H_{19}NO_4]H^+$, 336.1 (20) $[C_{18}H_{19}NO_4]Na^+$, 649.3 (15) $2[C_{18}H_{19}NO_4]Na^+$. IR (KBr, cm^{-1}): 2976.7 w, 1717.0 s, 1600.7 m, 1377.9 m, 1345.7 s, 1257.4 s, 1140.5 m, 1069.7 m, 1023.5 m, 909.5 w, 830.3 m, 781.0 m, 745.6 w.

2,6-Di(2-carboxypyridyl)-4-*p*-tolylpyridine (dcptp). The compound was prepared analogously to dcpp by modification of the published procedure.[13] To a 250 mL round bottom air-free flask was added 2-bromopyridine (0.563 g, 3.57 mmol) and dry THF (~50 mL) via cannula. Under nitrogen, the solution was cooled to -78°C in a dry ice/acetone bath. 1.6 M n-BuLi solution in hexanes (2.2 mL, 3.52 mmol) was added dropwise over 15 minutes and the solution stirred for an additional 30 minutes. To a

separate air free flask was added 4-*p*-tolylpyridine-2,6-dicarboxylate diethyl ester (0.505 g, 1.61 mmol) and dry THF (~20 mL) and the solution transferred dropwise via 22 gauge cannula to the reaction mixture over 30 minutes. The solution was stirred for an additional 30 minutes at -78°C before quenching with methanol (4 mL) and allowing to warm to room temperature and stir overnight. To promote the separation of layers, hexanes (10 mL) was added followed by the addition of 10% HCl (20 mL) and the organic layer removed. The acidic aqueous layer was washed with CH_2Cl_2 (1 x 25 mL) and then basified with 5 M NaOH. The basic aqueous layer was then extracted with CH_2Cl_2 (3 x 50 mL). The organic layer dried with $MgSO_4$, filtered, and evaporated. The product was purified by column chromatography on silica with 2% EtOH in $CHCl_3$ and recrystallized by dissolution in minimal CH_2Cl_2 at room temperature and adding equal parts EtOAc and hexanes and allowing to stand. Yield 0.292 g (48%). mp 173-174°C. ^{1}H NMR ($(CD_3)_2CO$, 500 MHz): δ 8.72 (ddd, 2H, *J* = 4.7, 1.5, 1.0 Hz, 6py-a (pyridyl arm)), 8.47 (s, 2H, 3/5py-b (bridging pyridyl)), 8.13 (dt, 2H, *J* = 7.8, 1.0 Hz, 3py-a), 7.99 (td, 2H, *J* = 7.8, 1.7 Hz, 4py-a), 7.90 (d, 2H, *J* = 8.0, 1.7 Hz, Ph), 7.61 (dtd, 2H, *J* = 7.8, 4.7, 1.0 Hz, 5py-a), 7.44 (d, 2H, *J* = 8.0, Ph), 2.45 (s, 3H). ^{13}C NMR ($CDCl_3$, 500 MHz): δ 192.04, 153.89, 153.69, 150.54, 149.25, 140.22, 136.37, 133.08, 130.09, 127.11, 126.35, 126.19, 124.83, 21.33. TOF-MS [ESI, *m/z* (rel int)]: 380.1 (100) $[C_{24}H_{17}N_3O_2]H^+$, 402.1 (5) $[C_{24}H_{17}N_3O_2]Na^+$, 781.3 (5) $2[C_{24}H_{17}N_3O_2]Na^+$. IR (KBr, cm^{-1}): 3057.6 w, 1684.6 s, 1590.8 m, 1354.7 s, 1302.7 m, 1237.2 m, 1151.3 w, 1095.7 w, 1048.9 w, 1019.3 m, 991.1 m, 958.9 m, 903.8 w, 821.2 m, 764.7 m, 683.0 m. Elemental Analysis for $C_{24}H_{17}N_3O_2$, Calculated: C, 75.98; H, 4.52; N, 11.07. Found: C, 75.22; H, 4.36; N, 11.00.

$[Fe(dcptp)_2](PF_6)_2$. To an air-free flask dcptp (0.115 g, 0.302 mmol) and deoxygenated EtOH (50 mL) via cannula were added. The solution was warmed (50°C) under nitrogen to promote dissolution. A separate air-free flask was charged with $(NH_4)_2Fe(SO_4)_2 \cdot 6H_2O$ (0.0608 g, 0.155 mmol). The ligand solution was transferred via cannula to the flask containing the iron(II) salt. The reaction was warmed to 70°C and allowed to stir for 18 hours. After ~2 hours of warming the solution began to darken to an olive green color and gradually darkened to intense blue and allowed to heat overnight. A separate air-free flask was charged with 8 equivalents of NH_4PF_6 (0.202 g, 1.24 mmol) and H_2O (4 mL) which was then added via syringe to the reaction mixture. The solution was concentrated by evaporation under a stream of N_2 and water was added yielding dark blue precipitate which was filtered and rinsed with H_2O. The crude product was dissolved in acetonitrile and the solution was washed with hexanes to remove grease. The acetonitrile solution was concentrated then purified by passage through a basic alumina column. Yield: 0.0381 g (23%). ^{1}H NMR ($(CD_3)_2CO$, 500 MHz): δ (ppm) 8.75 (s, 4H, 3/5py-b), 8.37 (t, 4H, J = 7.8, 1.1 Hz, 4py-a), 8.20 (d, 4H, J = 7.8, 1.0 Hz, 3py-a), 8.16 (d, 4H, J = 5.8, 1.0 Hz, 5py-a), 8.06 (d, 4H, J = 8.3 Hz, Ph), 7.50 (t, 4H, J = 7.8, 5.8, 1.0 Hz, 5py-a), 7.49 (d, 4H, J = 8.3 Hz, Ph), 2.46 (s, 6H). ^{13}C NMR ($(CD_3)_2CO$, 500 MHz): δ (ppm) 180.91, 160.94, 159.41, 159.31, 142.32, 141.89, 140.92, 131.06, 130.49, 129.01, 128.00, 127.48, 127.27, 20.48. TOF-MS [ESI, *m/z* (rel int)]: 407.0 (15) $[C_{48}H_{34}N_6O_4Fe]^{2+}$, 959.1 (5) $\{[C_{48}H_{34}N_6O_4Fe](PF_6)\}^+$. UV-Vis ($CH_3CN$) λ(ε($M^{-1}cm^{-1}$)): 339 nm (21600), 381 nm (15500), 445 nm (2400), 515 nm (4000), 626 nm (8400).

4.2.2 Physical Measurements

Cyclic Voltammetry. Electrochemical measurements were carried out using a CH Instruments CH620D electrochemical analyzer to determine the $E_{1/2}$ for ligand reductions and metal oxidations of each complex. Solutions of the compounds were prepared in distilled CH_3CN containing NBu_4PF_6 (ca. 0.1 M) as the supporting electrolyte. A standard three-electrode setup was used with a platinum working electrode, carbon rod counter electrode, and a Ag/AgCl electrode as the reference. All measurements were made inside an inert atmosphere glovebox. Data was acquired at a scan rate of 50 mV s^{-1}. After data collection, ferrocene was added to subsequent scans for reference.

4.3 Results and Discussion

4.3.1 Design of the π-Extended Ligand System

The goal of the present investigation is to achieve stabilization of a charge transfer state and destabilization of the ligand field excited states of the symmetric iron(II) polypyridyl complex $[Fe(dcpp)_2]^{2+}$. Inspired by the work of Damrauer and coworkers (vide supra), we set out to introduce *p*-tolyl substituents to the pyridyl rings of 2,6-di(2-carboxypyridyl)pyridine (dcpp).[7]

It is well known that extending the conjugation of polypyridyl ligand can effectively lower the energy of the charge transfer state. A straightforward example of this of this is evident in the comparison of bpy and terpy. Delocalization over three ring in terpy compared to just two rings in bpy leads to a lower energy charge transfer. Introducing phenyl substituents allows for further delocalization and effectively lowers the LUMO or π* orbitals of the ligand. The choice of the *p*-tolyl substituent as opposed to an

unsubstituted phenyl is two-fold. First, the electron donating methyl group on the phenyl will make the functional group slightly electron donating which may have the effect of increasing the σ-donor strength of the ligand, possibly destabilizing ligand field excited states. Second, the methyl group will allow for further functionalization, i.e. installation of an anchoring group which is essential for application as a sensitizer in DSSCs.

It has been shown that a single substituent on the central ring of terpy can have a significant impact on the properties, therefore we chose to first introduce a single substituent to the central ring of dcpp.[4,14] Further synthetic elaboration will be pursued in due course with the installation of substituents to the terminal pyridyl rings. Since the dcpp ligand system differs from other polypyridyls in that it is cross-conjugated, it will be interesting to see the effects of extending the conjugation of a single ring versus all rings. If the *p*-tolyl substituent on the central pyridyl ring can produce the desired effect of stabilization of the charge transfer state, can it then be further stabilized by the introduction of *p*-tolyl groups on the terminal rings? Or do the presence of the cross-conjugated bridges inhibit any cumulative stabilization?

As mentioned above, an added benefit of the tolyl group is the possible enhancement of the σ-donor strength and destabilization of the ligand field states. We propose another analog by which we can target this separately, by introducing electron donating alkyl groups to the 5-position of the terminal pyridyl rings. If we could achieve stabilization of the MLCT through the *p*-tolyl substituent on the central ring and destabilization of the ligand field states through enhanced σ-donation from the terminal rings, this would be ideal.

Taking a step back, and looking at the big picture, the preparation of heteroleptic Ru(II) complexes is well known and provides much opportunity to tune the photophysical properties. For instance, heteroleptic complexes carrying an electron withdrawing group and an electron donating group on the two separate ligands always show lower emission energies than the parent homoleptic complexes because the π^* orbital of the accepting ligand is stabilized while the donating ligand destabilizes the metal centered t_{2g} orbitals.[4] Iron(II) complexes are much more labile, therefore heteroleptic compounds are extremely difficult to obtain. Using the cross-conjugation to our advantage, if we can in fact achieve the desired result of tuning the excited states by inducing different effects from varying the substituents on the terminal rings versus the central ring, we are essentially working with a heteroleptic-like iron(II) complex without the synthetic complications. We are just beginning to investigate the possibilities with this ligand system and only time will tell, but on top of the unique properties of $[Fe(dcpp)_2]^{2+}$ that were discussed Chapter 2, the synthetic possibilities with this type of ligand could prove to be very exciting.

4.3.2 Synthesis and Coordination of 2,6-Di(2-carboxypyridyl)-4-*p*-tolylpyridine

The transformation of the bridging groups of 2,6-di(2-carboxypyridyl)pyridine (dcpp), described in the previous chapter, was easily achieved from a one-step reaction directly from dcpp. The installation of functional groups to the pyridyl rings is not as straightforward, but from a retrosynthetic analysis of the preparation of dcpp it becomes clear that we may introduce functional groups to the terminal rings and/or the central ring independently prior to the final reaction step (Scheme 4-1). The accessibility of various analogs through this route makes it highly desirable.

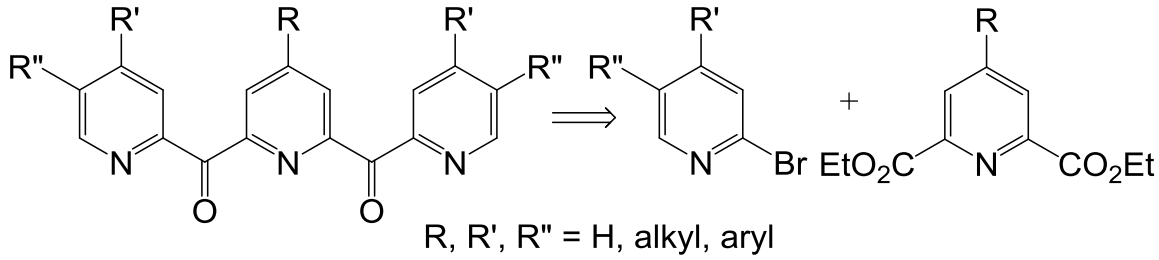

Scheme 4-1. Retrosynthetic analysis of substituted 2,6-di(2-carboxypyridyl)pyridine.

All of the desired analogs in this investigation possess the *p*-tolyl substituent on the central ring, therefore we pursued this starting material first. 4-*p*-Tolylpyridine-2,6-dicarboxylate diethyl ester was not previously described in the literature, but similar structures exist and based on literature methods the target compound can be readily attained through Suzuki coupling as shown in Scheme 4-2.[10,12,15–17]

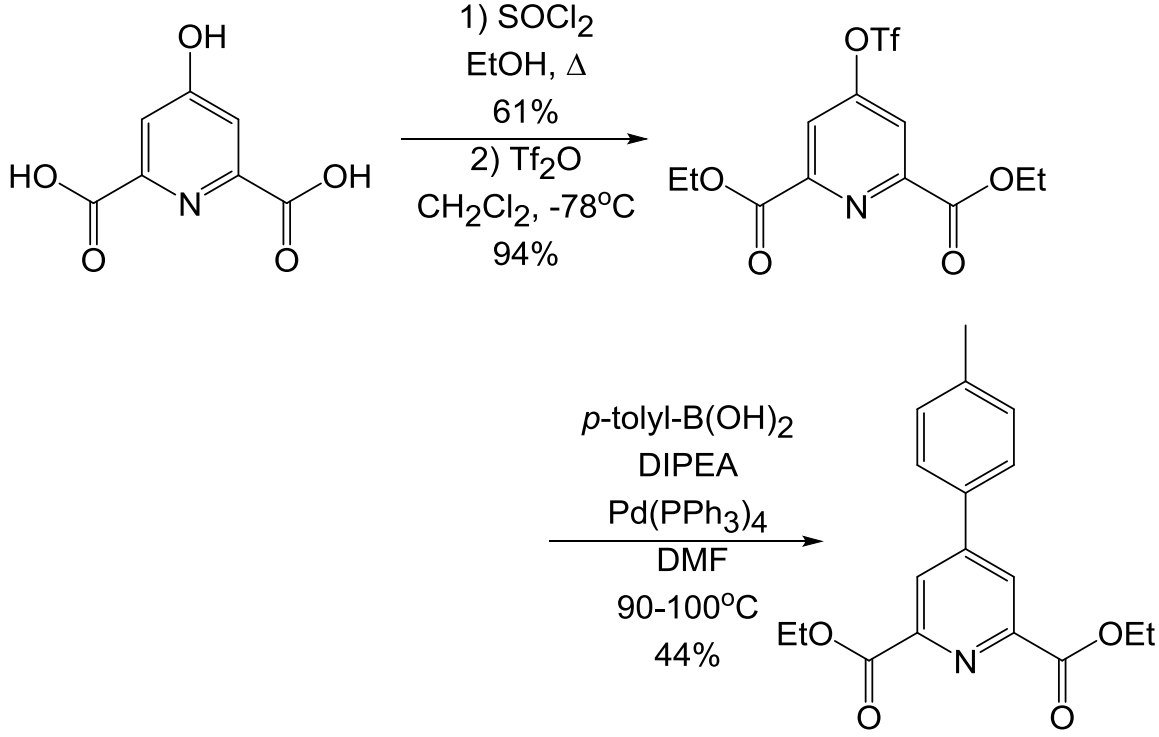

Scheme 4-2. Preparation of 4-*p*-tolylpyridine-2,6-dicarboxylate diethyl ester.

The first step of the synthesis required the esterification of chelidamic acid. This reagent is commercially available and was initially purchased at over $40/gram. The reagent was used sparingly, due to the high expense, and the ester was prepared via the standard sulfuric acid catalyzed Fischer esterification in ethanol. At this small scale the yield of this reaction was very poor so the alternate esterification through the acyl chloride was attempted, resulting in better yield. To have any hope of obtaining the final target molecule, the high expense, scale, and yield of the first reaction left much to be desired and this whole reaction scheme was almost abandoned. Luckily, TCI Chemical sells the same reagent at higher purity for $6/gram, and at larger scale the yield was much improved.

Since organotriflates may be readily obtained from phenols, and the boronic acid reagent is easily prepared from 4-bromotoluene, the Suzuki coupling route was an obvious choice. The coupling reaction requires extremely dry conditions and despite my best efforts to exclude water, the reaction suffered from lower than expected yields, achieving only 44%. The reaction was undertaken during humid spring and summer months and since most of the reagents and solvent are hygroscopic the reaction seemed to be adversely affected. With the central pyridyl ring in hand, the first ligand for this study was prepared analogously to dcpp in 48% yield, as show in Scheme 4-3.

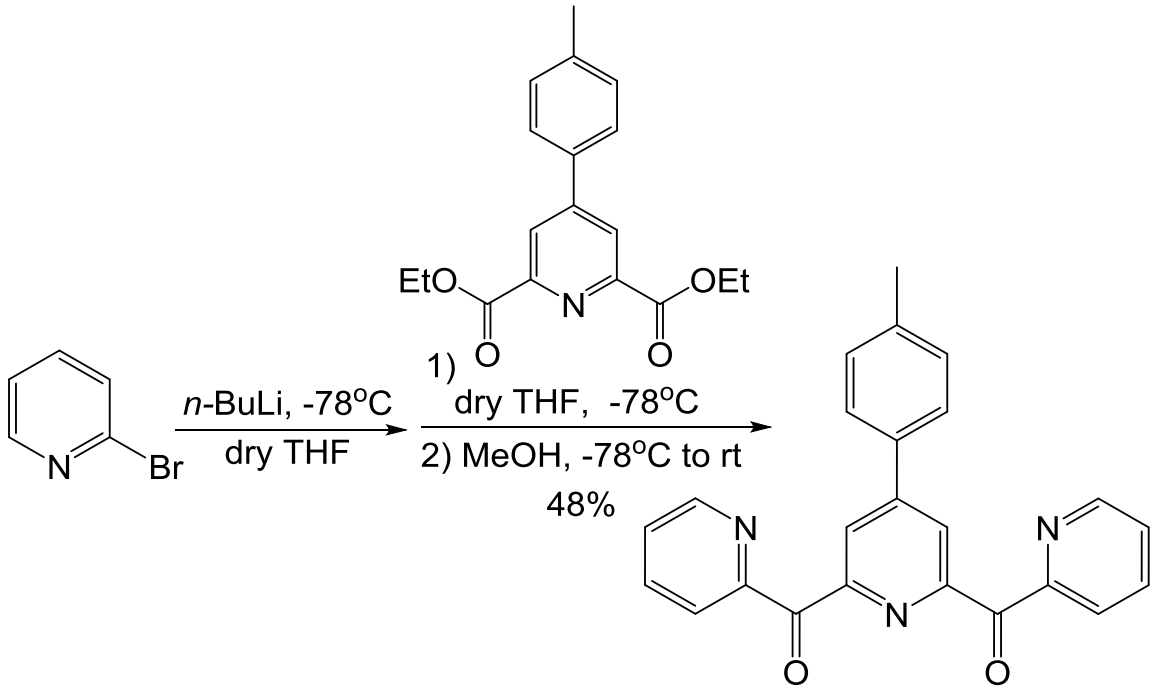

Scheme 4-3. Preparation of 2,6-di(2-carboxypyridyl)-4-*p*-tolylpyridine (dcptp).

The reaction has only been completed once, therefore the 48% yield is acceptable for a first attempt. It is truly a shame that we have only just begun to embark on this investigation, because there is no doubt that, with just a little more time, the two other desired analogs would be in hand (Figure 4-1). The procedure would be the same with the only difference being the 2-bromopyridine starting material. 2-bromo-5-methylpyridine is commercially available, while the 2-bromo-4-*p*-tolylpyridine may be prepared by a simple palladium catalyzed coupling reaction of 2-bromo-4-iodopyridine with a Grignard reagent of toluene.[18]

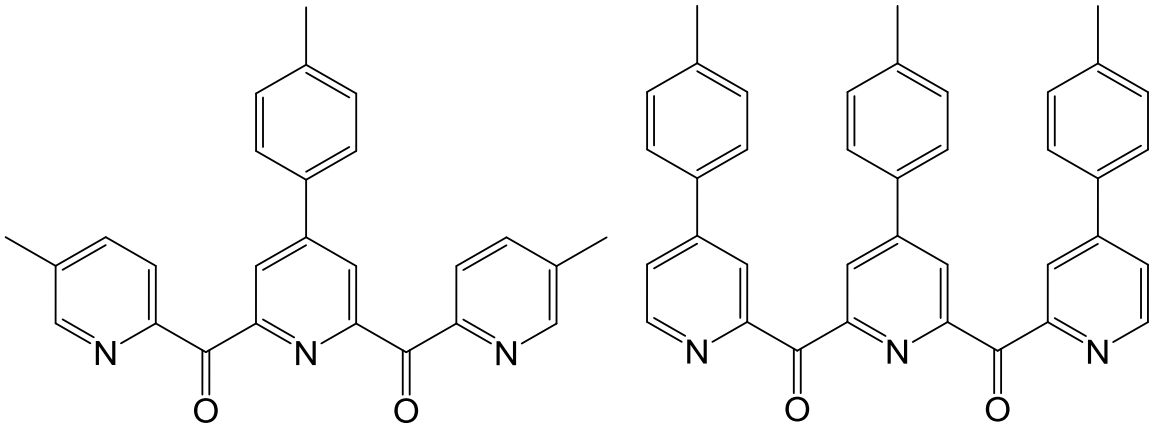

Figure 4-1. Structures of desired analogs of 2,6-di(2-carboxypyridyl)-4-*p*-tolylpyridine.

With dcptp we may begin to look at the effect of extending the π-system of the dcpp ligand. $[Fe(dcptp)_2]^{2+}$ has been successfully prepared, albeit by a slightly different procedure that the other iron(II) complexes described in this dissertation. The standard procedure of adding an iron(II) salt to a slight excess of ligand in methanol and water does not work for this system. The *p*-tolyl substituent leads to solubility issues in this solvent mixture and despite longer reaction times and prolonged heating, there was no color change or other evidence of a reaction taking place and only unreacted ligand was recovered from the reaction. Instead the product was obtained by reaction in ethanol by heating to just under the boiling point for 24 hours. Again, unreacted ligand was recovered from the reaction, but the product was present in 23% yield, shown in Scheme 4-4. Longer reaction times or bringing to reflux may prove to increase the yield, but to date the reaction has yet to be optimized.

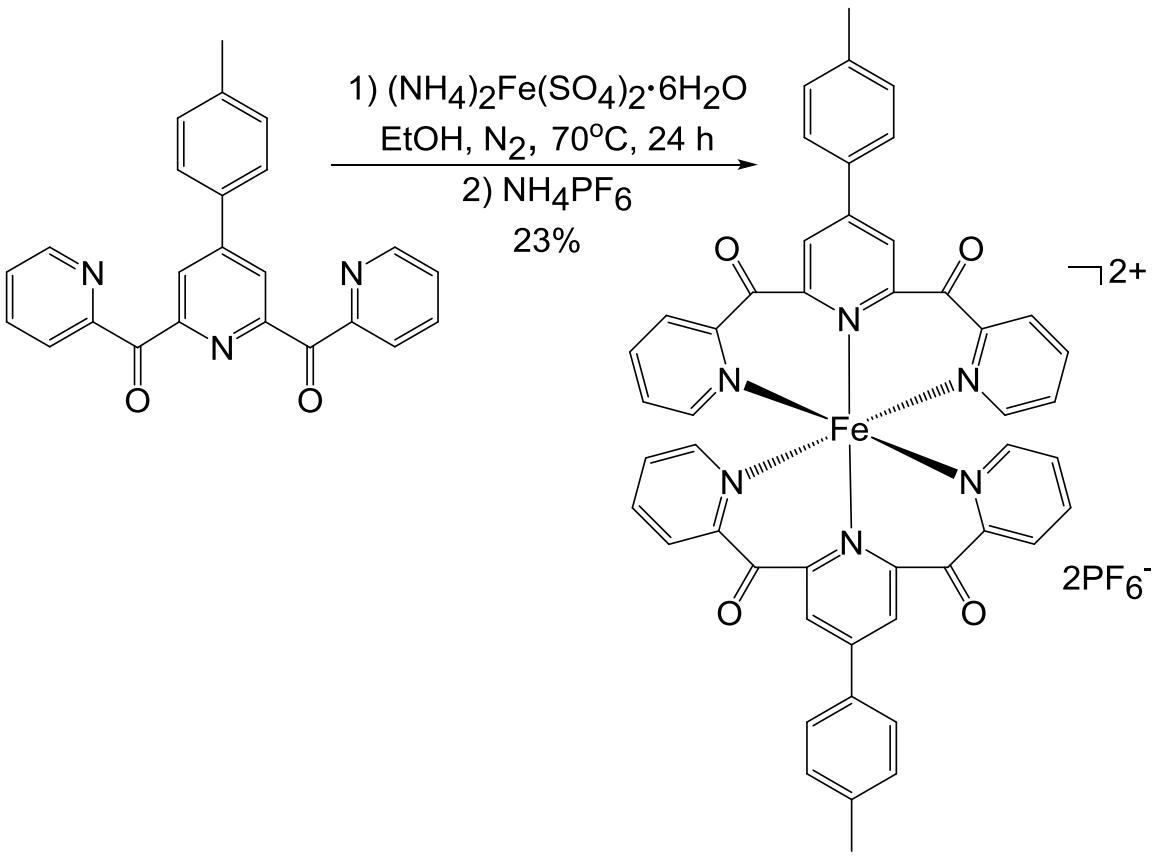

Scheme 4-4. Preparation of $[Fe(dcptp)_2](PF_6)_2$.

4.3.3 Preliminary Investigation into the Effects of Extending the π-System

With the successful preparation of $[Fe(dcptp)_2]^{2+}$ we can begin to investigate the effect of extending the π-system. Since only one analog has been obtained we can only compare the properties to $[Fe(dcpp)_2]^{2+}$ leaving many questions unanswered, however it is a good starting point. From the optical absorption spectrum, shown in Figure 4-2, we can see that the introduction of a *p*-tolyl group to the 4-position of the central pyridyl ring leads to a red-shifted absorption maximum and an increase in the MLCT oscillator strength, consistent with what is known for *p*-tolyl substituents on Ru(II) terpy chromophores.[4,7]

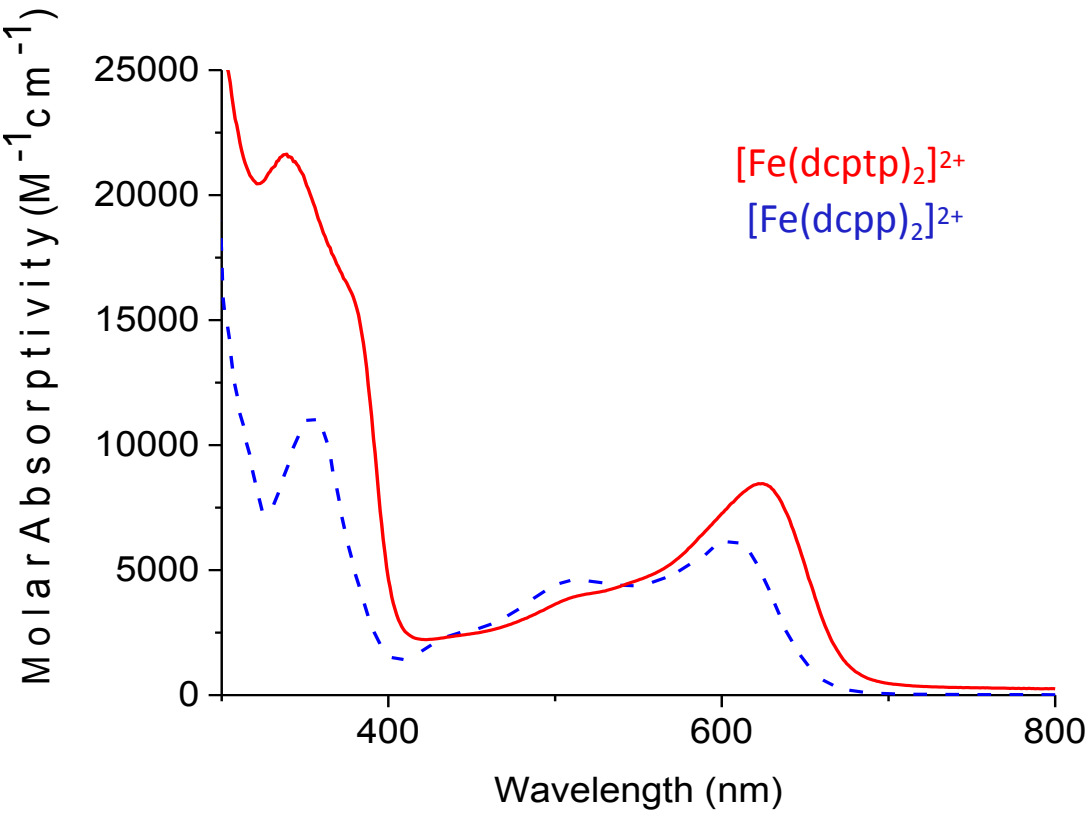

Figure 4-2. Ground state electronic absorption spectrum of $[Fe(dcpp)_2](PF_6)_2$ (blue dashed) and $[Fe(dcptp)_2](PF_6)_2$ (red solid) in acetonitrile.

The electrochemical potentials of $[Fe(dcptp)_2]^{2+}$ were measured by cyclic voltammetry and as with $[Fe(dcpp)_2]^{2+}$ there are four distinct ligand reductions attributed to the presence of the four electron withdrawing carbonyl bridges. The oxidation and first reduction potentials are listed in Table 4-1, along with the potentials of $[Fe(dcpp)_2]^{2+}$ for comparison. The *p*-tolyl substituent induces a negative 95 mV shift in the oxidation potential signifying destabilization of the metal t_{2g} orbitals. The first reduction potential is essentially unchanged as the negative 10 mV shift of the first reduction potential is within

error of the experiment, but could indicate a slight destabilization of the LUMO π* level of the ligand.

Table 4-1. Electrochemical potentials for the oxidation and first reduction of $[Fe(dcpp)_2](PF_6)_2$ and $[Fe(dcptp)_2](PF_6)_2$, measured with Ag/AgCl reference with 0.1 M $TBAPF_6$ electrolyte in acetonitrile, externally referenced to ferrocene.

Compound	$E_{1/2}$ [ox]	$E_{1/2}$ [red]
$[Fe(dcpp)_2]^{2+}$	1.295 V	-0.965 V
$[Fe(dcptp)_2]^{2+}$	1.200 V	-0.975 V

The electrochemistry is consistent with the work by Maestri et al. who found that electron donating substituents on Ru(II)terpy complexes destabilize both the HOMO and LUMO, and the HOMO t_{2g} levels are destabilized more than the LUMO π* levels.[4] We tend to think of *p*-tolyl substituent as an electron acceptor because of the lower energy MLCT that arises. However, the electron-rich ring acts as a donating group as it leads to an increase in the basicity of the nitrogens which makes the removal of one electron from the metal t_{2g} orbital easier, as the resulting Fe(III) can interact more strongly with the donating ligands.[4,7] The overall effect is a smaller HOMO-LUMO gap and lower energy MLCT.

From this data it appears that we are on the right track as the introduction of single tolyl substituent to the central ring of the ligands has led to a lower energy MLCT and slight destabilization of the metal t_{2g} orbitals. It will be interesting to see the effect of introducing the additional substituents to the ligands that were shown in Figure 4-1.

4.3.4 Alternative Strategies to Tune the Energetics of Excited States

As mentioned above, one of the strategies to lower the energy of the MLCT state is through the introduction of electron withdrawing groups to the periphery of the ligands. Initially, there was hesitation along this front as too many electron withdrawing substituents may lower the basicity of the nitrogens and cause difficulty with the formation of the complex. However, in our efforts toward the overall goal of developing a viable sensitizer, we set out to install substituents through which we may achieve attachment to metal oxide substrates. As will be discussed in the next chapter, we have successfully installed electron withdrawing carboxylate groups to the terminal rings of the dcpp ligand and prepared the iron(II) complexes, however there are complications with characterization of these analogs and we have yet to determine the effect of these substituents. Though we cannot use these specific analogs in this present investigation, the apprehension toward this strategy is lessened and this may be a feasible approach to lower the MLCT state.

Another approach that is gaining a lot of attention in recent years for Ru(II) dyes is cyclometallated complexes in which a pyridyl ring is replaced with a phenyl ring. Substituting a nitrogen with an anionic carbon, or strong σ-donor, results in a considerable decrease in the ^{3}MLCT energy.[2] The metal based HOMO is significantly destabilized while the LUMO π* is destabilized by a smaller extent resulting in the lower MLCT. These cyclometallating ligands allow for manipulation of both the ground and excited states through installation of substituents on the phenyl ring.[19] The Ru(II) cyclometallated complexes are all heteroleptic in which only one pyridyl group has been replaced with a

phenyl, therefore, much difficulty would likely arise in introducing this type of ligand to an iron(II) center, as iron(II) complexes are much more labile.

A more synthetically accessible strategy to introduce an anionic carbon would be through the use of N-heterocyclic carbenes, in which the chemistry with iron(II) is known.[20] An exciting new report was recently published in which an iron(II) N-hetercyclic carbene complex achieves a prolonged ^{3}MLCT lifetime.[21] The anionic carbene ligands show greater σ-donor character compared to terpy, significantly destabilizing the $^5T_2$ ligand field state, however, the LUMO is also destabilized resulting in higher energy charge transfer states. If we may combine the strategies mentioned above to stabilize the charge transfer state with the enhanced σ-donation from an anionic carbene ligand to destabilize the ligand field state we may be able to achieve inversion of the excited states of an iron(II) chromophore.

4.4 Concluding Comments

Efforts to modulate the energetics of the excited states of a symmetric iron(II) complex through synthetic means has been initiated with the preparation of an analog of $[Fe(dcpp)_2]^{2+}$ possessing an extended π-system. The 2,6-di(2-carboxypyridyl)-4-*p*-tolylpyridine (dcptp) ligand was readily obtained through adaptation from known methods and achieved through an analogous procedure for the preparation of the unsubstituted dcpp. The coordination chemistry of dcptp by our standard procedure was complicated by the solubility characteristics of the ligand, however, $[Fe(dcptp)_2]^{2+}$ was successfully obtained by implementing more rigorous conditions. The increased delocalization that is achieved through extending the conjugation of the central ring of dcpp has resulted in stabilization

of the MLCT and destabilization of the metal centered t_{2g} orbitals as is evident in the optical absorption and electrochemical data. This investigation is in its infancy and additional characterization is necessary to determine the impact of these changes on the excited state dynamics. Further synthetic elaboration, involving the introduction of substituents to the terminal rings of dcpp has been proposed, and should provide us more information on the viability of the current strategy to effectively tune the excited state energetics of iron(II) chromophores.

APPENDIX

APPENDIX

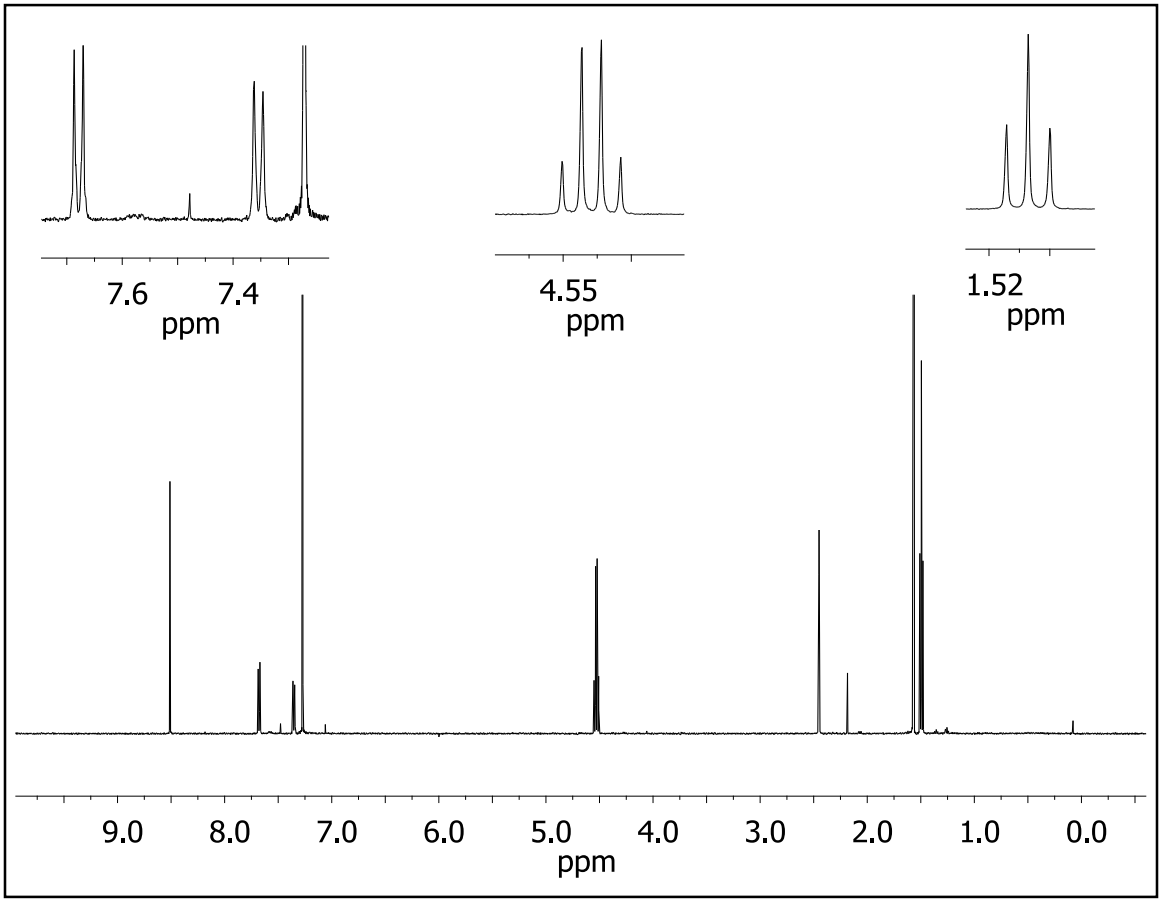

Figure 4-3. ^{1}H NMR of 4-*p*-tolylpyridine-2,6-dicarboxylate diethyl ester in $CDCl_3$.

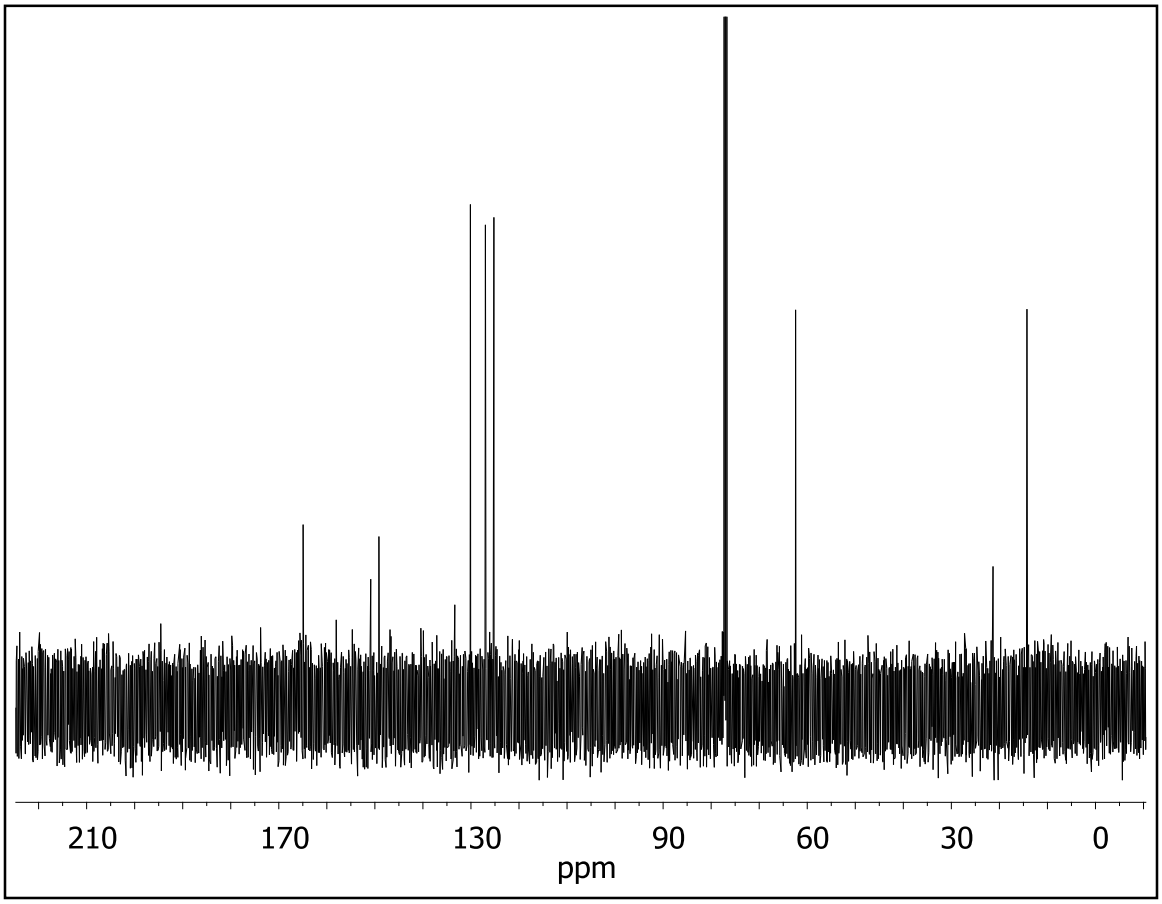

Figure 4-4. ^{13}C NMR of 4-*p*-tolylpyridine-2,6-dicarboxylate diethyl ester in $CDCl_3$.

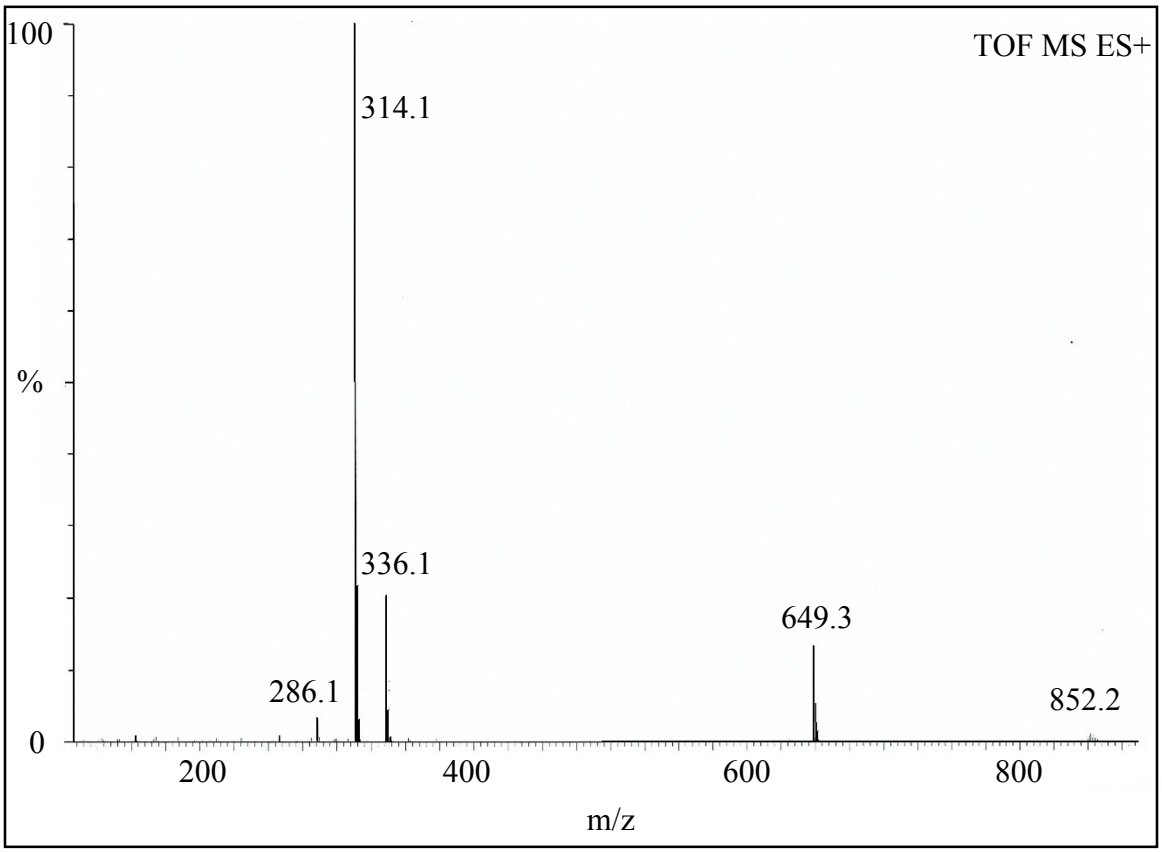

Figure 4-5. ESI-MS of 4-*p*-tolylpyridine-2,6-dicarboxylate diethyl ester.

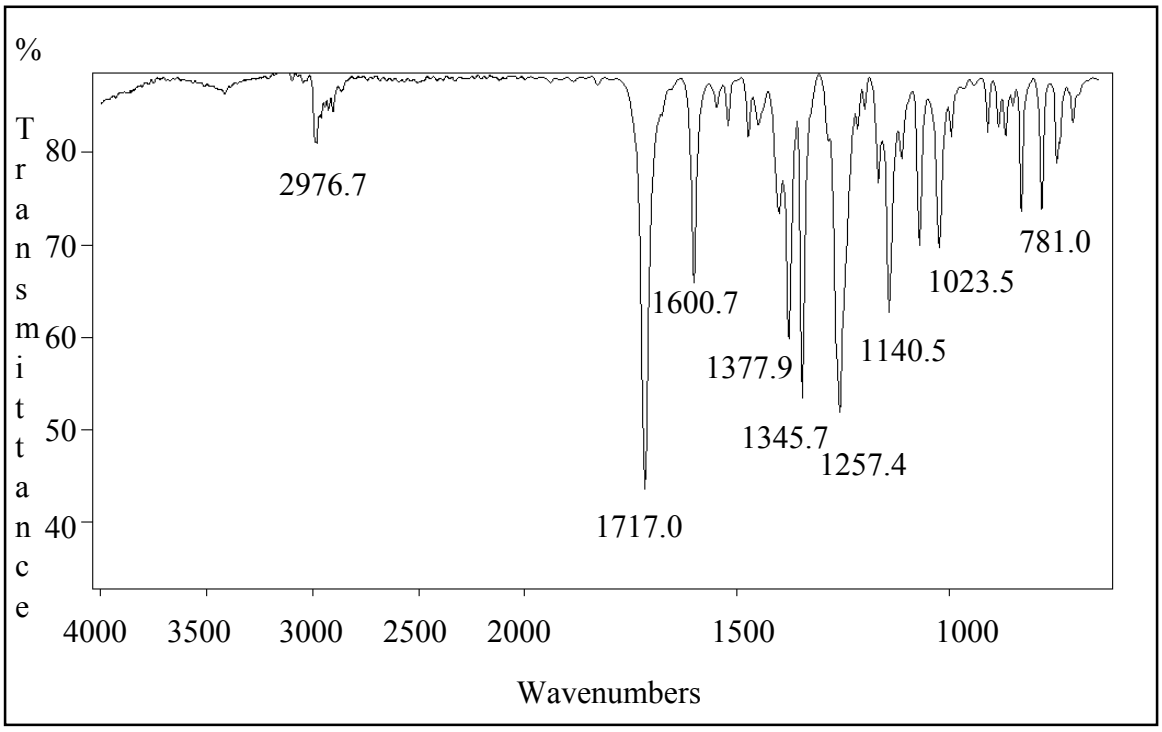

Figure 4-6. IR of 4-*p*-tolylpyridine-2,6-dicarboxylate diethyl ester.

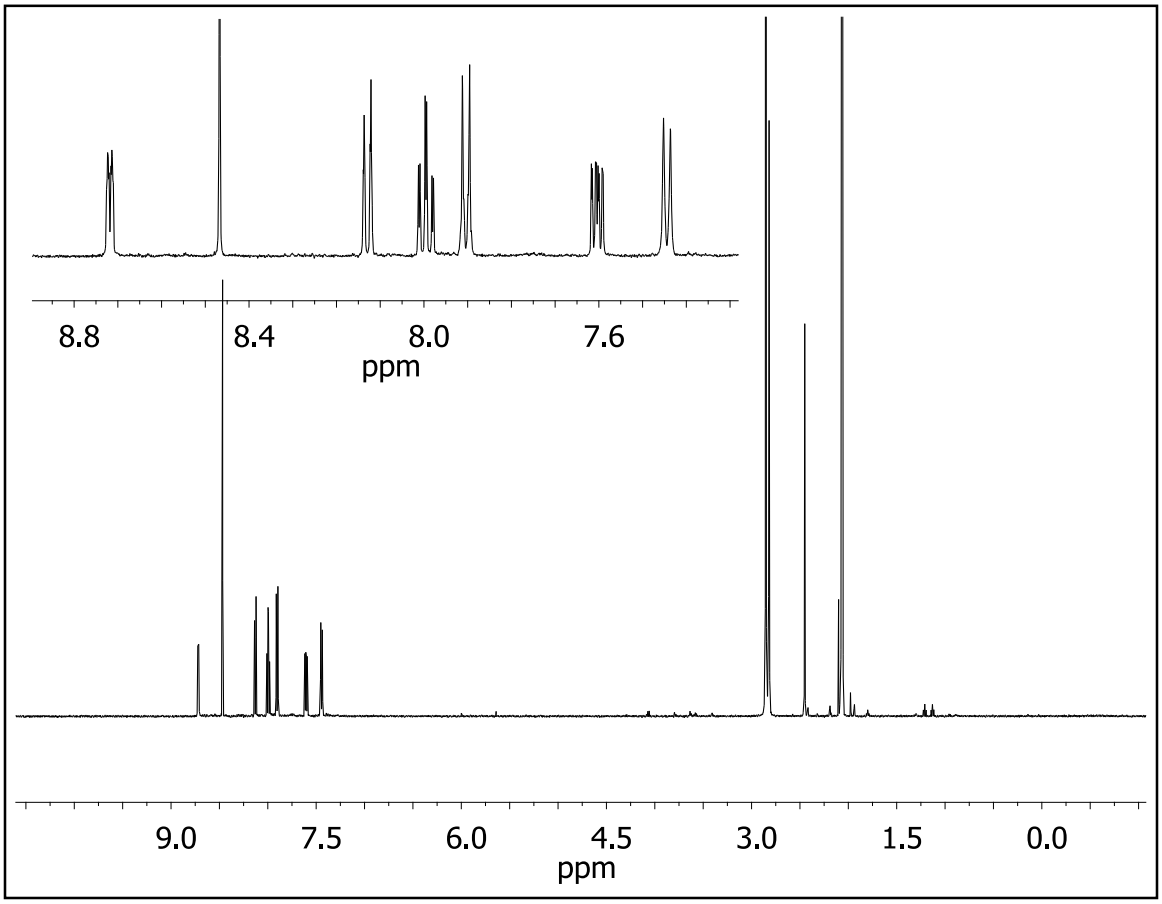

Figure 4-7. ^{1}H NMR of 2,6-di(2-carboxypyridyl)-4-*p*-tolylpyridine (dcptp) in $(CD_3)_2CO$.

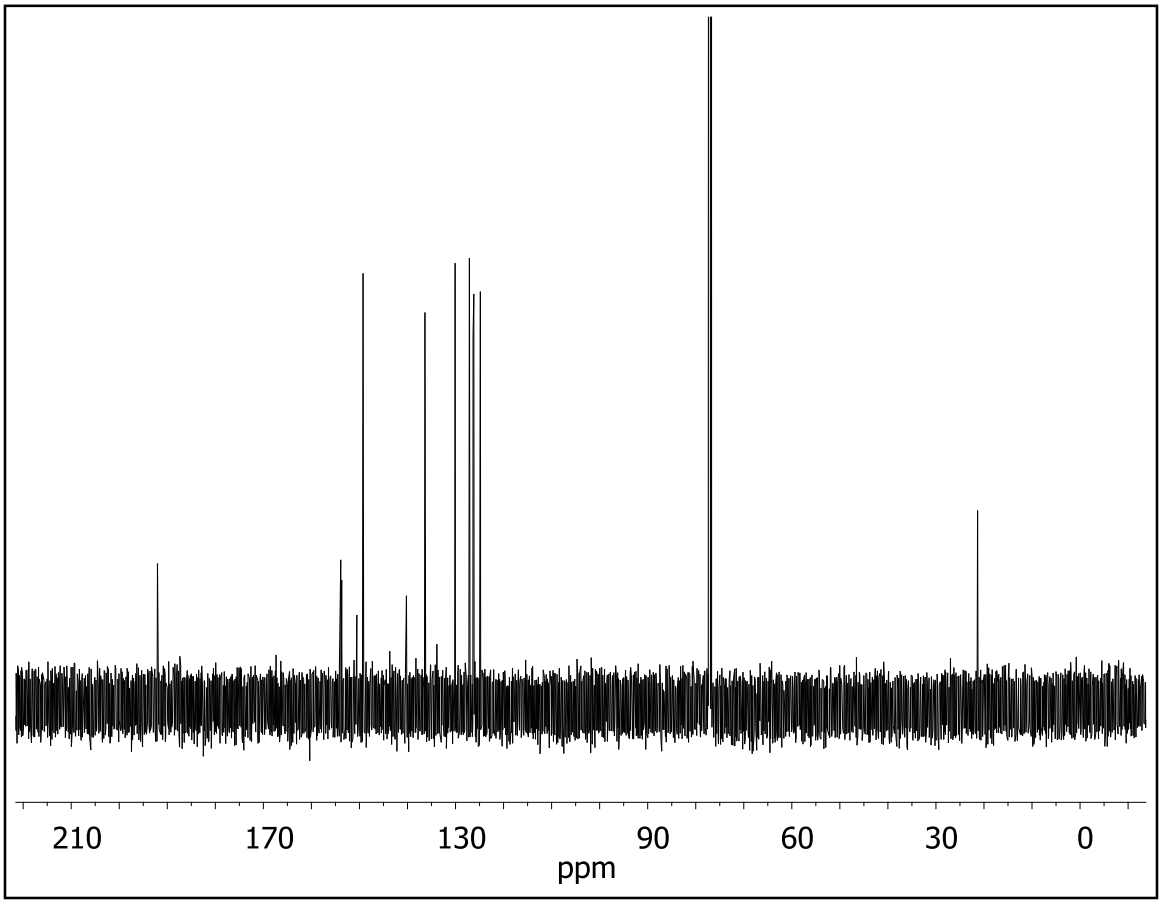

Figure 4-8. ^{13}C NMR of 2,6-di(2-carboxypyridyl)-4-*p*-tolylpyridine (dcptp) in $CDCl_3$.

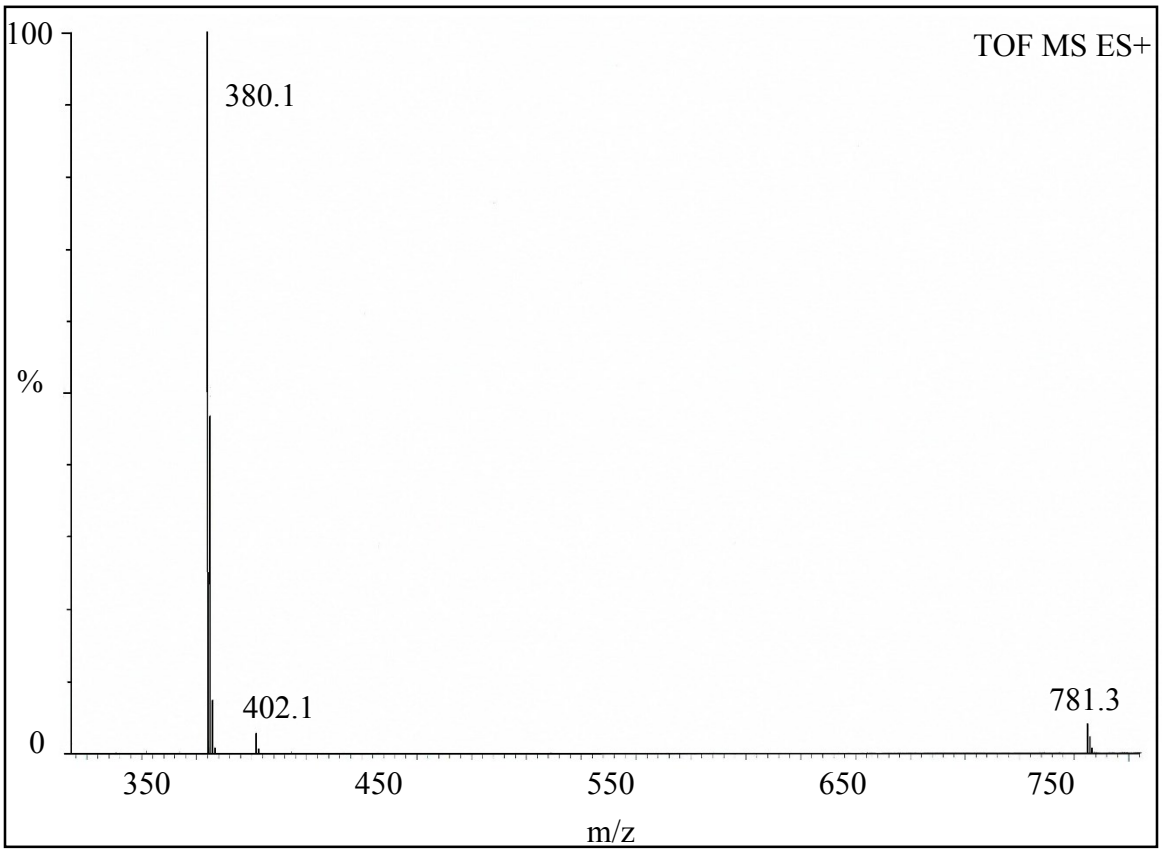

Figure 4-9. ESI-MS of 2,6-di(2-carboxypyridyl)-4-*p*-tolylpyridine (dcptp).

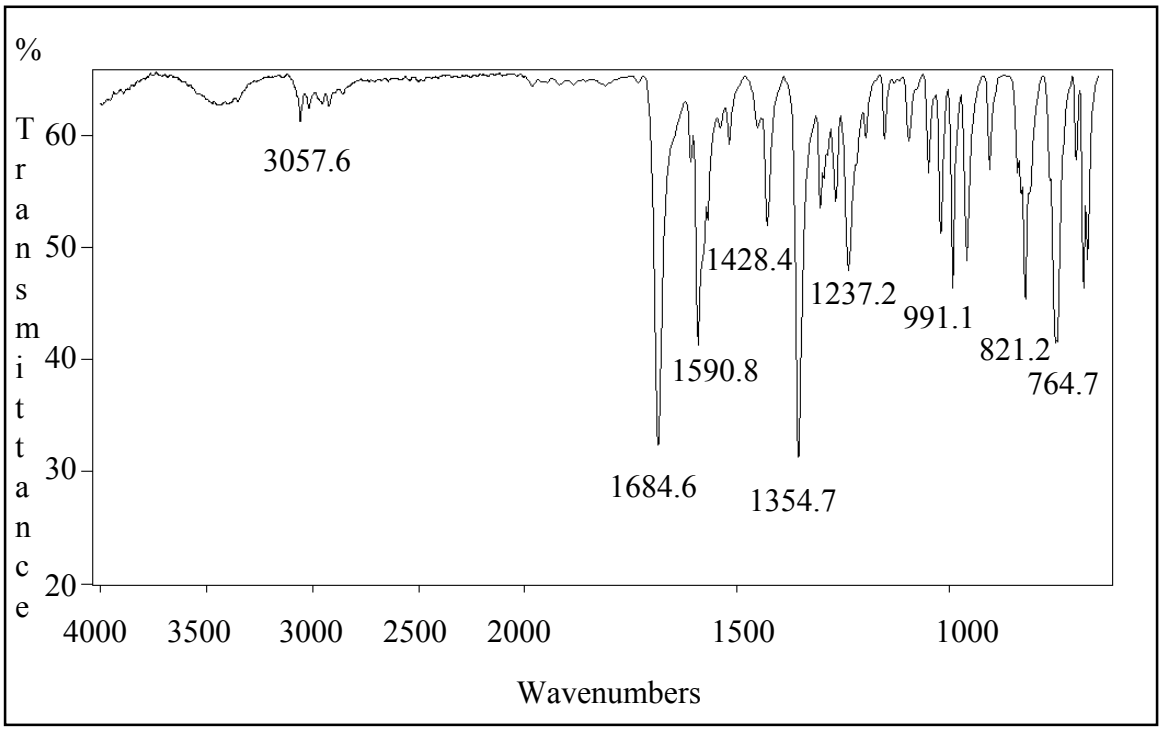

Figure 4-10. IR of 2,6-di(2-carboxypyridyl)-4-*p*-tolylpyridine (dcptp).

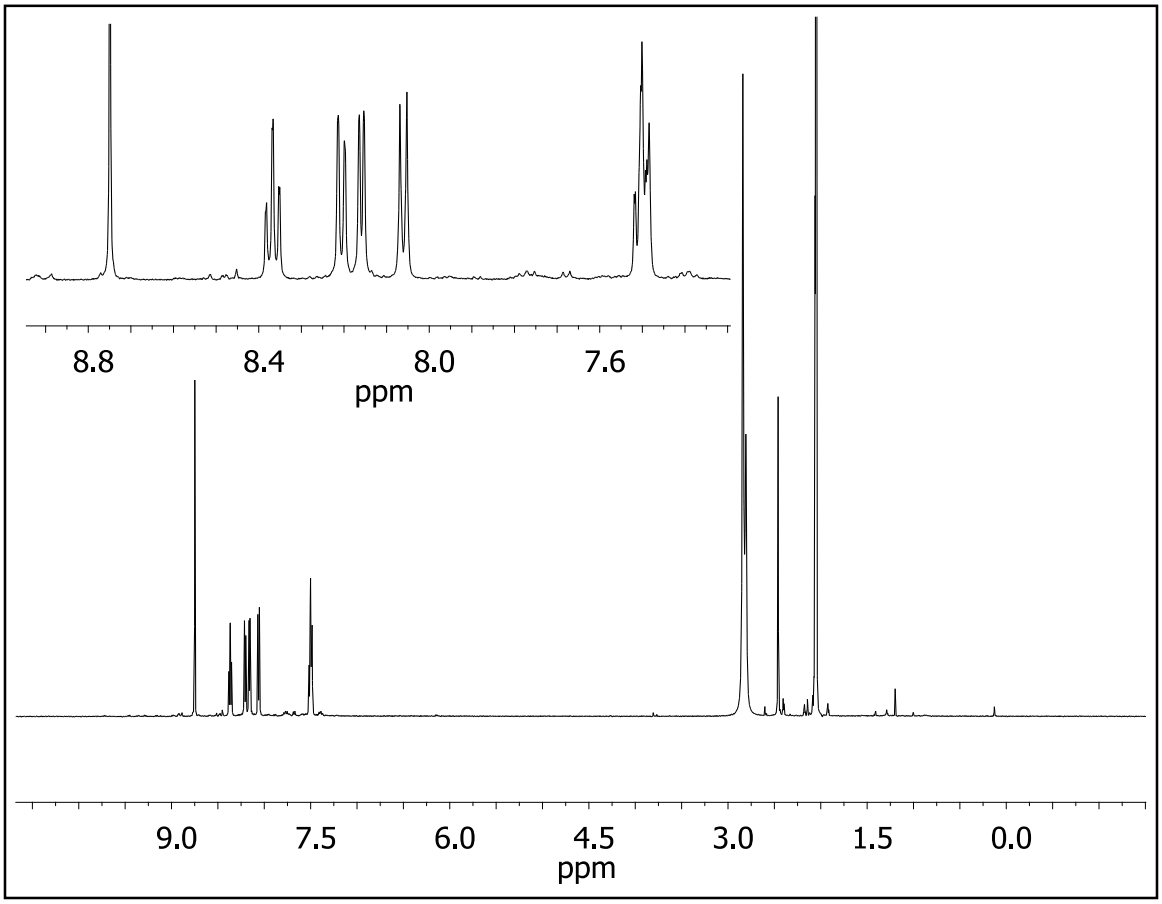

Figure 4-11. ^{1}H NMR of $[Fe(dcptp)_2](PF_6)_2$ in $(CD_3)_2CO$.

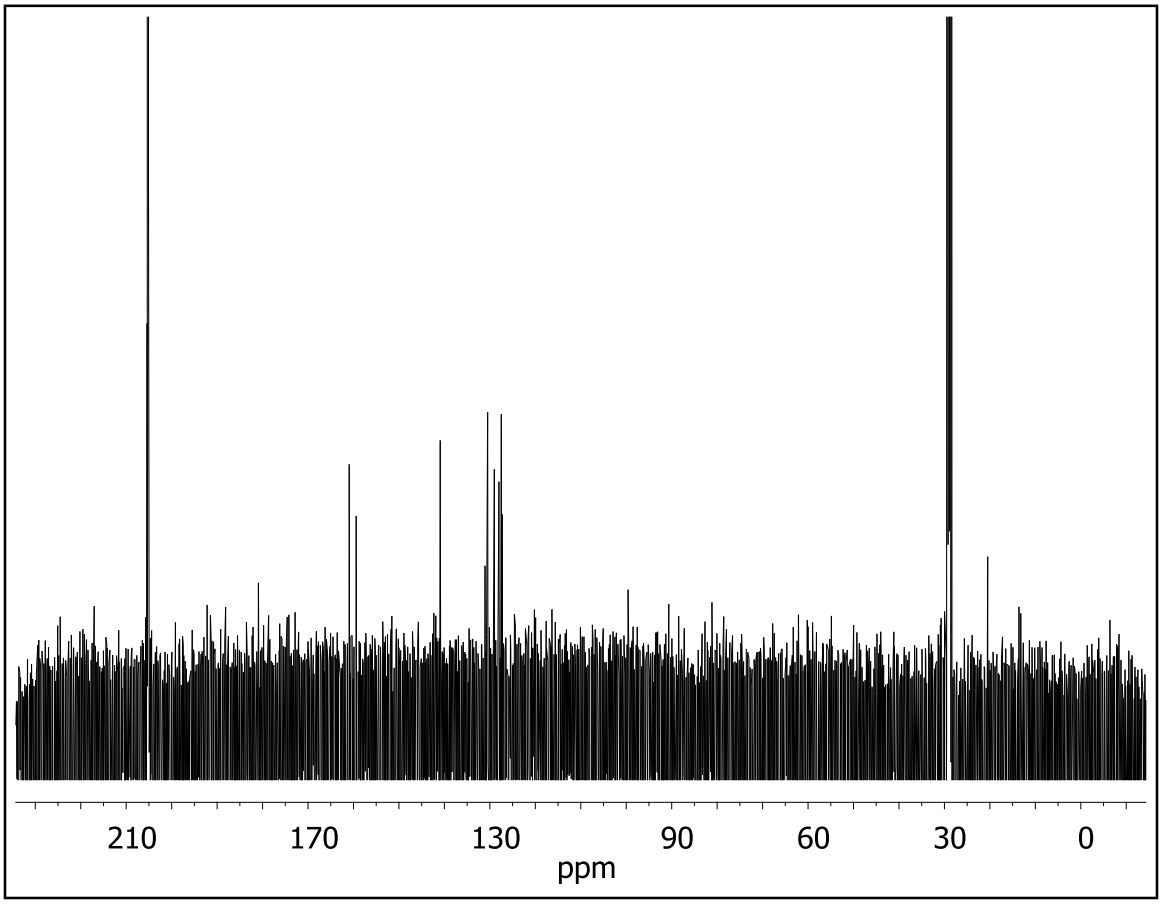

Figure 4-12. ^{13}C NMR of $[Fe(dcptp)_2](PF_6)_2$ in $(CD_3)_2CO$.

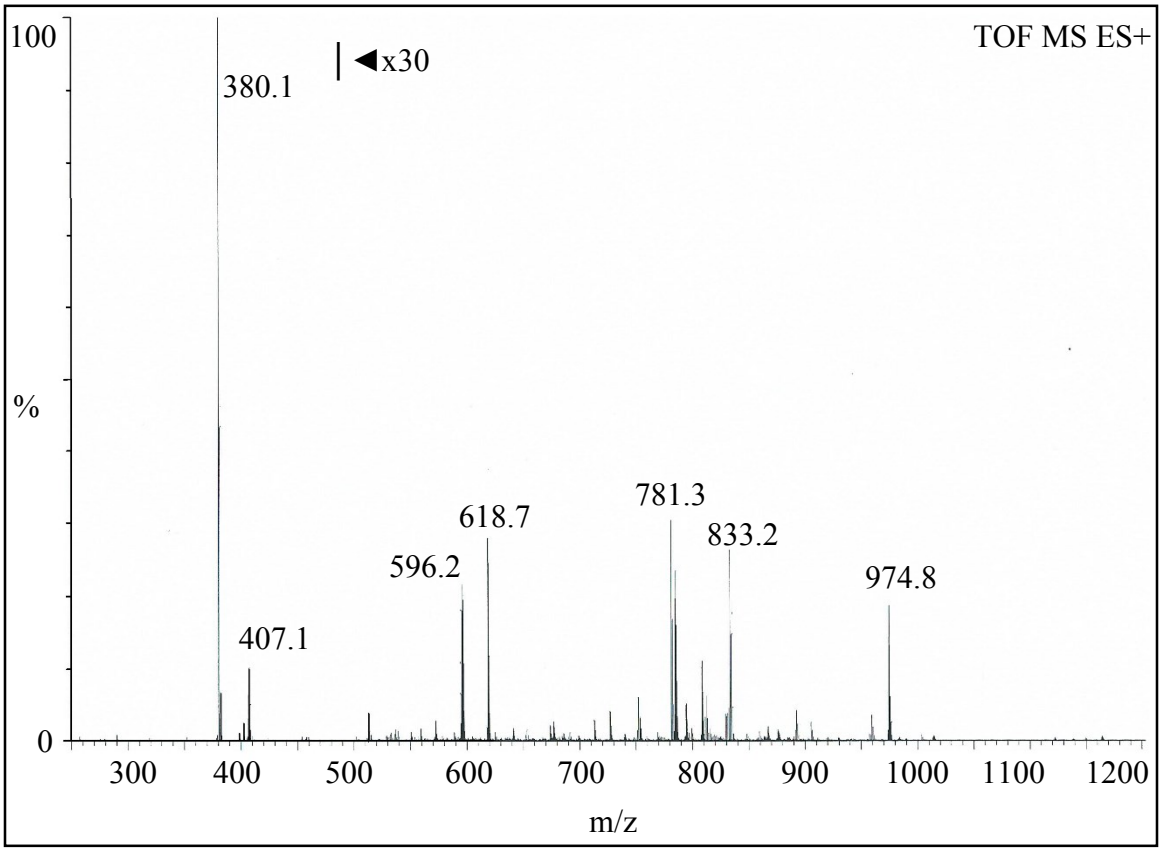

Figure 4-13. ESI-MS of $[Fe(dcptp)_2](PF_6)_2$.

REFERENCES

REFERENCES

(1) Juris, A.; Balzani, V.; Barigelletti, F.; Campagna, S.; Belser, P.; Von Zelewsky, A. *Coordination Chemistry Reviews* **1988**, *84*, 85–277.

(2) Hammarström, L.; Johansson, O. *Coordination Chemistry Reviews* **2010**, *254*, 2546–2559.

(3) Abrahamsson, M.; Lundqvist, M. J.; Wolpher, H.; Johansson, O.; Eriksson, L.; Bergquist, J.; Rasmussen, T.; Becker, H.-C.; Hammarström, L.; Norrby, P.-O.; Akermark, B.; Persson, P. *Inorganic Chemistry* **2008**, *47*, 3540–8.

(4) Maestri, M.; Armaroli, N.; Balzani, V.; Constable, E. C.; Thompson, A. M. W. C. *Inorganic Chemistry* **1995**, *34*, 2759–2767.

(5) Damrauer, N. H.; Boussie, T. R.; Devenney, M.; McCusker, J. K. *Journal of the American Chemical Society* **1997**, *119*, 8253–8268.

(6) Constable, E. C.; Housecroft, C. E.; Thompson, A. C.; Passaniti, P.; Silvi, S.; Maestri, M.; Credi, A. *Inorganica Chimica Acta* **2007**, *360*, 1102–1110.

(7) Hewitt, J. T.; Vallett, P. J.; Damrauer, N. H. *The Journal of Physical Chemistry A* **2012**, *116*, 11536–47.

(8) Perrin, D. D.; Armarego, W. L. F. *Purification of Laboratory Chemicals, 3rd ed.*; Pergamon Press: New York, 1988.

(9) White, J. R.; Price, G. J.; Schiffers, S.; Raithby, P. R.; Plucinski, P. K.; Frost, C. G. *Tetrahedron Letters* **2010**, *51*, 3913–3917.

(10) Belanger, D. B.; Siddiqui, M. A.; Curran, P. J.; Hamann, B.; Zhao, L.; Reddy, P. A. P.; Tadikonda, P. K.; Shipps Jr., G. W.; Mansoor, U. F. Novel JNK Inhibitors. WO 2008/082487 A2, 2008.

(11) Wu, W.; Kong, H.-K.; Li, H.; Ho, Y.-M.; Gao, Y.; Hao, J.; Murphy, M. B.; Lam, M. H.-W.; Wong, K.-L.; Lee, C.-S. *European Journal of Organic Chemistry* **2011**, *2011*, 5054–5060.

(12) Pouessel, J.; Abada, S.; Le Bris, N.; Elhabiri, M.; Charbonnière, L. J.; Tripier, R. *Dalton transactions (Cambridge, England : 2003)* **2013**, *42*, 4859–72.

(13) Goldsmith, C. R.; Stack, T. D. P. *Inorganic Chemistry* **2006**, *45*, 6048–55.

(14) Chambers, J.; Eaves, B.; Parker, D.; Claxton, R.; Ray, P. S.; Slattery, S. J. *Inorganica Chimica Acta* **2006**, *359*, 2400–2406.

(15) Xu, M.; Chen, C. Z.; Wan, P. *Journal of Photochemistry and Photobiology A: Chemistry* **2008**, *198*, 26–33.

(16) Ghoshal, A.; Sarkar, A.; Manickam, G.; Kumaran, R.; Jayashankaran, J. *Synlett* **2010**, *2010*, 1459–1462.

(17) Ohe, T.; Miyaura, N.; Suzuki, A. *The Journal of Organic Chemistry* **1993**, *58*, 2201–2208.

(18) LI, X.-H.; LIU, Z.-Q.; LI, F.-Y.; DUAN, X.-F.; HUANG, C.-H. *Chinese Journal of Chemistry* **2007**, *25*, 186–189.

(19) Bomben, P. G.; Robson, K. C. D.; Koivisto, B. D.; Berlinguette, C. P. *Coordination Chemistry Reviews* **2012**, *256*, 1438–1450.

(20) Hashimoto, T.; Urban, S.; Hoshino, R.; Ohki, Y.; Tatsumi, K.; Glorius, F. *Organometallics* **2012**, *31*, 4474–4479.

(21) Liu, Y.; Harlang, T.; Canton, S. E.; Chábera, P.; Suárez-Alcántara, K.; Fleckhaus, A.; Vithanage, D. a.; Göransson, E.; Corani, A.; Lomoth, R.; Sundström, V.; Wärnmark, K. *Chemical Communications* **2013**, *1*, 6412–6414.

Chapter 5. Functionalization of an Iron(II) Chromophore for Attachment to Metal Oxide Substrates

5.1 Introduction

The molecules presented in this dissertation have provided us with the opportunity to investigate the photophysical properties of symmetric iron(II) polypridyls. Though we have yet to achieve a prolonged charge transfer state lifetime, we are pursuing another aspect of the research toward the overall goal of implementing an iron(II) chromophore into a DSSC. The complexes presented thus far are not suitable for dye sensitization as they do not possess the means to bond to the semiconductor surface. To achieve efficient injection we must first install anchoring groups.

Dye sensitization may be achieved by physisorption or chemisorption, but early work by Gratzel and coworkers showed the incident photon to current efficiency is improved 30-fold from the introduction of anchoring groups providing the ability to bind to the semiconductor.[1] The most widely employed anchor is the carboxylate functional group, as it has been shown to bind to TiO_2 with good stability and provide strong electronic communication.[2,3] The relative ease of installation of carboxylic acid groups make it a clear front runner for this investigation. However, research into alternative anchoring groups has been a hot topic in recent years and alternate possibilities will be pursued in due course.[4–12]

Inorganic chromophores, specifically d^6 coordination compounds, are ideal sensitizers as they can undergo a metal to ligand charge transfer (MLCT) upon absorption of a photon creating a charge separated state. The presence of carboxylate groups on the periphery of the ligand allow for attachment to the semiconductor. Carboxylate groups are

ideal anchors for sensitization of TiO_2 as there is optimal overlap of the d-orbital of titanium with the extended π system of the carboxylate group, as shown in Figure 5-1. Also shown is the multiple binding modes that are possible with carboxylate groups. Researchers have found that initial binding involves one carboxylate linkage followed by stronger bidentate or bridging modes due the rotational freedom of the molecule allowing for immediate capture of another carboxylate group by a neighboring Ti atom.[3,13]

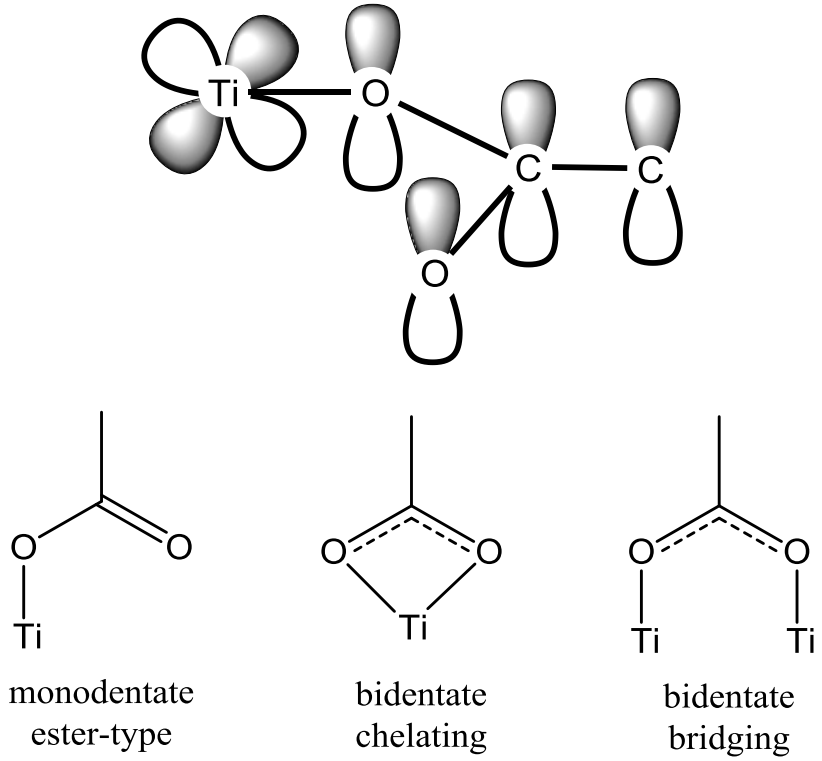

Figure 5-1. Depiction of the three possible binding modes of the carboxylate group to the titanium dioxide semiconductor, along with the orbital diagram for ester-type binding mode (adapted from references 2 and 14).[2,14]

The bpy and terpy ligands that are commonly employed bear multiple carboxylate groups and their planar structure allows for binding at multiple sites. Research has also shown that higher conversion efficiencies are obtained when there are numerous anchoring groups as in the "N3" and "black dye" that were described in Chapter 1. The 2,6-(2-

carboxypyridyl)pyridine (dcpp) ligand, on the other hand, is not planar since upon coordination to the metal center it takes on a helical arrangement. Though it is synthetically feasible to introduce carboxylate groups to all three rings of dcpp, the helical conformation of the dye molecule may hinder binding through multiple sites. If we functionalize the central ring, binding is possible through only one site, on the other hand if we functionalize the terminal rings, binding may be possible through both ligands to a TiO_2 nanoparticle. To determine if the functionalization of the terminal rings of dcpp would be sterically feasible a geometry optimization was performed.

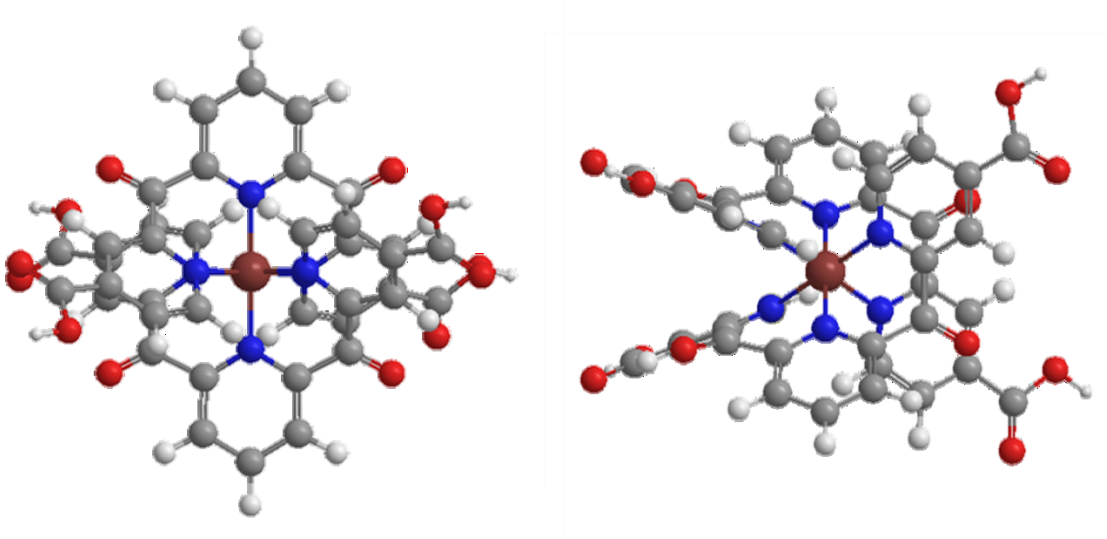

Figure 5-2. Optimized structure of bis(2,6-di(2-carboxy(4-pyridylcarboxylicacid))-pyridine)iron(II), $[Fe(dcpap)_2](PF_6)_2$, shown in two orientations for clarity.

The optimized structure, shown in Figure 5-2, shows that the carboxylate groups should not interfere with the carbonyl bridge lone pair-π interaction or the coordination environment of the dcpp ligand to the iron(II) center, therefore we set out to prepare an analog of dcpp that would allow for anchoring to a semiconductor surface. The carboxylic acid functionalized ligand and corresponding iron(II) complex have been successfully prepared and will be discussed. Carboxylic acids are known to be insoluble in most

solvents, therefore the ethyl ester analog of the ligand and complex have also been prepared. Future work toward the installation of alternative anchoring groups will also be presented.

5.2 Experimental

5.2.1 Synthesis

General. All chemicals were of reagent grade, purchased from Sigma-Aldrich, Alfa Aesar, Acros Organics, or Strem Chemicals and used as received unless otherwise noted. Solvents were purchased from Sigma-Aldrich, Jade Scientific, Spectrum, Mallinckrodt, EMD Chemical, or CCI and were purified using standard purification techniques.[15] All air-sensitive reactions were carried out under inert atmosphere by standard Schlenk techniques utilizing thoroughly deoxygenated solvents that were degassed by the freeze—pump—thaw method. ^{1}H NMR and ^{13}C NMR were recorded with Varian UnityPlus-300 MHz, Varian UnityPlus-500 MHz, and Agilent DDR2 500 MHz spectrometers. Ground state absorption spectra were obtained on a Varian Cary 50 spectrophotometer. IR spectra were obtained on a Mattson Galaxy 5000 FTIR. Elemental analysis was obtained through the Analytical facilities at Michigan State University. Electrospray mass spectra (ESI-MS) were obtained from the staff of the MSU Mass Spectrometry Facility. The characterization data of previously unknown compounds are included in the appendix at the end of this chapter.

2,6-Di(2-carboxy(4-methylpyridyl))pyridine (dcmpp). The compound was prepared analogously to 2,6-di(2-carboxypyridyl)pyridine (dcpp) by modification of the published procedure.[16] To a 250 mL round bottom air-free flask was added 2-bromo-4-

methylpyridine (4.87 g, 28.3 mmol) and dry THF (~120 mL) via cannula. Under nitrogen, the solution was cooled to -78°C in a dry ice/acetone bath. 1.6 M n-BuLi solution in hexanes (17.7 mL, 28.3 mmol) was added dropwise over 20 minutes and the solution stirred for an additional 30 minutes. To a separate air-free flask was added diethyl 2,6-pyridinedicarboxylate (3.00 g, 13.5 mmol) and dry THF (~20 mL) and the solution transferred dropwise via 22 gauge cannula to the reaction mixture over 30 minutes. The solution was stirred for an additional 30 minutes at -78°C before quenching with methanol (30 mL) and allowed to warm to room temp and stir overnight. 10% HCl (60 mL) was added and the organic layer removed. The acidic aqueous layer was washed with CH_2Cl_2 (1 x 100 mL) and then basified with 5 M NaOH. The basic aqueous layer was then extracted with CH_2Cl_2 (3 x 100 mL). The organic layer dried with $MgSO_4$, filtered, and evaporated. The product was purified by column chromatography on silica with 2% EtOH in $CHCl_3$ and recrystallized by dissolution in EtOAc at room temp and adding equal parts hexanes and cooling to 0°C. Yield 2.56 g (60%). mp 174-175°C. ^{1}H NMR ($(CD_3)_2CO$, 500 MHz): δ 8.50 (d, 2H, *J* = 4.9 Hz, 6py-a (pyridyl arm)), 8.24 (t, 1H, *J* = 7.8 Hz, 4py-b (bridging pyridyl)), 8.17 (d, 2H, *J* = 7.8 Hz, 3/5py-b), 7.87 (s, 2H, *J* = 0.7 Hz, 3py-a), 7.40 (d, 2H, *J* = 4.9, 0.7 Hz, 5py-a), 2.42 (s, 6H). ^{13}C NMR ($(CD_3)_2CO$ 500 MHz): δ 192.84, 154.41, 154.15, 148.76, 147.93, 137.42, 127.18, 126.20, 125.19, 20.04. TOF-MS [ESI, *m/z* (rel int)]: 318.1 (100) $[C_{19}H_{15}N_3O_2]H^+$, 340.1 (20) $[C_{19}H_{15}N_3O_2]Na^+$, 657.2 (20) $2[C_{19}H_{15}N_3O_2]Na^+$. IR (KBr, cm^{-1}): 3045.2 w, 1682.9 s, 1596.9 s, 1571.1 w, 1478.5 w, 1408.6 w, 1288.4 m, 1200.4 m, 1170.6 m, 1050.5 m, 994.5 w, 855.2 m, 773.4 m, 668.7 m.

Elemental Analysis for $C_{19}H_{15}N_3O_2$, Calculated: C, 71.91; H, 4.76; N, 13.24. Found: C, 71.42; H, 4.71; N, 13.08.

2,6-Di(2-carboxy(4-pyridylcarboxylicacid))pyridine (dcpap). The compound was prepared by modification of a literature procedure.[17] In a 100 mL beaker dcmpp (1.01 g, 3.17 mmol) was dissolved in conc. H_2SO_4 (50 mL) and cooled to 0°C in a NaCl ice bath. CrO_3 (1.89 g, 18.9 mmol) was finely ground and added in small portions over 1 hour. The dark green solution was warmed to 70-80°C for 2 hours then allowed to stir at room temperature overnight. The solution was poured over 300 mL of ice and the pH raised by slow addition of 5 M NaOH (~100-150 mL) until the product precipitates (pH ~2-3). Filtering the pasty white solid may be time consuming and can clog a fritted filter. To overcome this issue the suspension was first allow settle and most of the supernatant decanted off. Using a fine fritted filter the product was gravity filtered, once a substantial layer of product covers the frit a vacuum was applied by aspirator and the product may then be easily filtered without clogging the frit. The product was washed with water until the rinse was no longer green. The product was recrystallized by suspending in H_2O (~25 mL) and 1 M NaOH added until fully dissolved. 10% HCl was added to precipitate the product which was filtered as before and dried in a vacuum dessicator. Yield: 1.04 g (87%). ^{1}H NMR ($(CD_3)_2SO$, 500 MHz): δ (ppm) 8.82 (d, 2H, J = 4.9, 0.7 Hz, 6py-a), 8.29 (t, 1H, J = 6.8 Hz, 4py-b), 8.29 (s, 2H, 3py-a), 8.24 (d, 2H, J = 6.8, 1.6 Hz, 3/5py-b), 7.97 (dd, 2H, J = 4.9, 1.6 Hz, 5py-a). ^{13}C NMR ($(CD_3)_2SO$, 500 MHz): δ (ppm) 192.20, 165.87, 154.77, 153.48, 150.63, 139.42, 138.82, 127.64, 125.99, 123.90. TOF-MS [ESI, *m/z* (rel int)]: 376.1 (100) $\{[C_{19}H_{11}N_3O_6]-H+\}^-$. IR (KBr, cm^{-1}): 3444.0 br, 3090.4 w, 1712.6 s,

1686.7 s, 1606.0 w, 1465.2 m, 1327.7 s, 1295.7 s, 1266.3 s, 1237.7 s, 1186.5 m, 1087.3 w, 1013.4 m, 963.6 m, 885.7 w, 827.5 w, 760.8 m, 707.6 w, 672.2 m.

$[Fe(dcpap)_2](PF_6)_2$. An air-free flask was charged with dcpap (0.118 g, 0.313 mmol), H_2O (20 mL), and 1 M NaOH (0.62 mL, 0.620 mmol). The solution was bubble degassed with nitrogen for 20 minutes. A separate air-free flask was charged with of $(NH_4)_2Fe(SO_4)_2 \cdot 6H_2O$ (0.0587 g, 0.150 mmol) and H_2O (8 mL). The Fe(II) solution was transferred via cannula to the ligand solution which immediately turned brown then deep purple. The reaction was allowed to stir for 1 hour at room temperature. 0.1 M HPF_6 (12 mL, 1.20 mmol) was added and the solution cooled in the refrigerator (~2-8^{o}C). The dark purple precipitate was filtered and rinsed with H_2O. The crude product was dissolved in methanol and filtered to remove unreacted ligand. Diethyl ether was added to the filtrate to precipitate the pure product. Yield: 0.0345 g (21%). ^{1}H NMR (CD_3OD, 500 MHz): δ (ppm) 8.69 (t, 2H, *J* = 7.8 Hz, 4py-b), 8.52 (s, 4H, *J* = 1.6 Hz, 3py-a), 8.48 (d, 4H, *J* = 7.8, Hz, 3/5py-b), 7.92 (d, 4H, *J* = 5.9 Hz, 6py-a), 7.80 (dd, 4H, *J* = 5.9, 1.6 Hz, 5py-a). ^{13}C NMR (CD_3OD, 500 MHz): δ (ppm) 180.13, 161.86, 160.06, 158.09, 142.74, 141.93, 131.29, 127.31, 126.40, 126.38. TOF-MS [ESI, *m/z* (rel int)]: 405.0 (55) $[C_{38}H_{22}N_6O_{12}Fe]^{2+}$, 955.0 (2) $\{[C_{38}H_{22}N_6O_{12}Fe](PF_6)\}^+$. IR (KBr, cm^{-1}): 3427.1 br, 3091.8 w, 1725.1 s, 1696,1 s, 1611.5 w, 1383.9 w, 1297.3 w, 1237.0 m, 1084.1 w, 1015.1 w, 842.1 s, 765.6 m, 669.0 m. Elemental Analysis for $C_{38}H_{22}N_6O_{12}FeP_2F_{12} \cdot 5H_2O$, Calculated: C, 38.34; H, 2.71; N, 7.06. Found: C, 38.53; H, 2.70; N, 7.02.

2,6-Di(2-carboxy(4-pyridylcarboxylate ethyl ester))pyridine (dcpep). Dcpap (1.02 g, 2.71 mmol) and dry EtOH (20 mL) were added to a 100 mL round bottom flask.

The suspension was cooled in an ice bath and $SOCl_2$ (2 mL, 27.5 mmol) was added dropwise and the reaction stirred at room temperature overnight under nitrogen. The reaction mixture was vacuum distilled to remove solvent. The residue was dissolved in $CHCl_3$ and washed with 1 M NaOH then water. The organic layer was dried with Na_2SO_4, filtered, and evaporated leaving a faint yellow oil. The oil may be purified by dissolving in acetone/hexanes and cooling to 0°C. The precipitated product was filtered but immediately reverts to a colorless oil in the filter. Yield: 1.14 g (97%). ^{1}H NMR ($CDCl_3$, 500 MHz): δ (ppm) 8.83 (d, 2H, *J* = 4.9 Hz, 6py-a), 8.55 (s, 2H, 3py-a), 8.34 (d, 2H, *J* = 7.8 Hz, 3/5py-b), 8.14 (t, 1H, *J* = 7.8 Hz, 4py-b), 7.95 (dd, 2H, *J* = 4.9, 1.4 Hz, 5py-a), 4.41 (q, 4H, *J* = 7.1 Hz), 1.40 (t, 6H, *J* = 7.1 Hz). ^{13}C NMR ($CDCl_3$, 500 MHz): δ (ppm) 191.33, 164.34, 154.75, 153.13, 149.86, 138.38, 137.88, 127.45, 125.22, 124.50, 62.07, 14.16. TOF-MS [ESI, *m/z* (rel int)]: 434.1 (100) $[C_{23}H_{19}N_3O_6]H^+$.

$[Fe(dcpep)_2](PF_6)_2$. To an air-free flask dcpep (0.311 g, 0.718 mmol) and deoxygenated MeOH (30 mL via cannula) were added. The solution was gently warmed (40°C) under nitrogen to promote dissolution of the oil. A separate air-free flask was charged with $(NH_4)_2Fe(SO_4)_2 \cdot 6H_2O$ (0.121 g, 0.310 mmol). The ligand solution was transferred via cannula to the flask containing the iron(II) salt. The reaction was allowed to stir for 18 hours at room temperature. The solution turned pale brown but never darkens. A separate air-free flask was charged with NH_4PF_6 (0.375 g, 2.30 mmol) and MeOH (10 mL) which was transferred via cannula to the reaction mixture. The pale brown solution was concentrated by evaporation under a stream of N_2 resulting in a dark colored film coating the flask. The crude oily product was taken up with water and filtered. The product

was dissolved in acetonitrile and purified by passage through a neutral alumina column. The product was recrystallized by diethyl ether vapor diffusion into an acetonitrile solution of the complex. Yield: 0.0230 g (6%). ^{1}H NMR ($(CD_3)_2CO$, 500 MHz): δ (ppm) 8.87 (t, 2H, *J* = 7.8 Hz, 4py-b), 8.60 (d, 4H, *J* = 7.8 Hz, 3/5py-b), 8.51 (s, 4H, *J* = 1.7 Hz, 3py-a), 8.32 (d, 4H, *J* = 5.9 Hz, 6py-a), 7.87 (dd, 4H, *J* = 5.9, 1.7 Hz, 5py-a), 4.50 (q, 8H, *J* = 7.1 Hz), 1.40 (t, 12H, *J* = 7.1 Hz).

5.2.2 Physical Measurements

X-ray Structure Determination. Single-crystal X-ray diffraction data was acquired at the X-ray facility of Michigan State University. X-ray quality single crystals were obtained by slow diffusion of diethyl ether into an acetonitrile solution of the compound. Data were collected as described in Chapter 2 of this dissertation.

Cyclic Voltammetry. Electrochemical measurements were carried out using a CH Instruments CH620D electrochemical analyzer to determine the $E_{1/2}$ for ligand reductions and metal oxidations of each complex. Solutions of the compounds were prepared in distilled CH_3CN containing NBu_4PF_6 (ca. 0.1 M) as the supporting electrolyte. A standard three-electrode setup was used with a platinum working electrode, carbon rod counter electrode, and a Ag/AgCl or Ag/AgNO3 electrode as the reference. All measurements were made inside an inert atmosphere glovebox. Data was acquired at a scan rate of 50 mV s^{-1}. After data collection, ferrocene was added to subsequent scans for reference.

5.2.3 Theoretical Calculations

Geometry Optimizations. The initial geometries of the molecules were generated using SPARTAN or GaussView, or from crystal structure coordinates when available, and subsequently optimized in two steps.[18,19] The first optimization was performed using the density functional B3LYP with the 3-21G** basis set, followed by a second optimization using the B3LYP functional with the 6-31G* basis set. Frequency calculations at the B3LYP/6-31G* level of theory were performed on the final optimized structures to ensure that these geometries corresponded to global minima.

5.3 Results and Discussion

5.3.1 Installation of Anchoring Groups to 2,6-Di(2-carboxypyridyl)pyridine

Carboxylic acid groups may be readily introduced to aromatic methyl groups through various means, therefore we first need to introduce methyl substituents. From the retrosynthetic analysis of dcpp, that was described in the previous chapter, we may independently introduce functional groups to the terminal rings and/or central ring of dcpp prior to the final reaction step. Therefore, we may readily adapt the method by which we had previously prepared dcpp and the *p*-tolyl analog to introduce methyl groups to the rings. 2-Bromo-4-methylpyridine is commercially available, and quite expensive, but it may be readily obtained in high yield via bromination of 2-amino-4-methylpyridine.[20] With the starting materials readily accessible 2,6-di(2-carboxy(4-methylpyridyl))pyridine (dcmpp) was conveniently prepared via the standard route shown in Scheme 5-1.

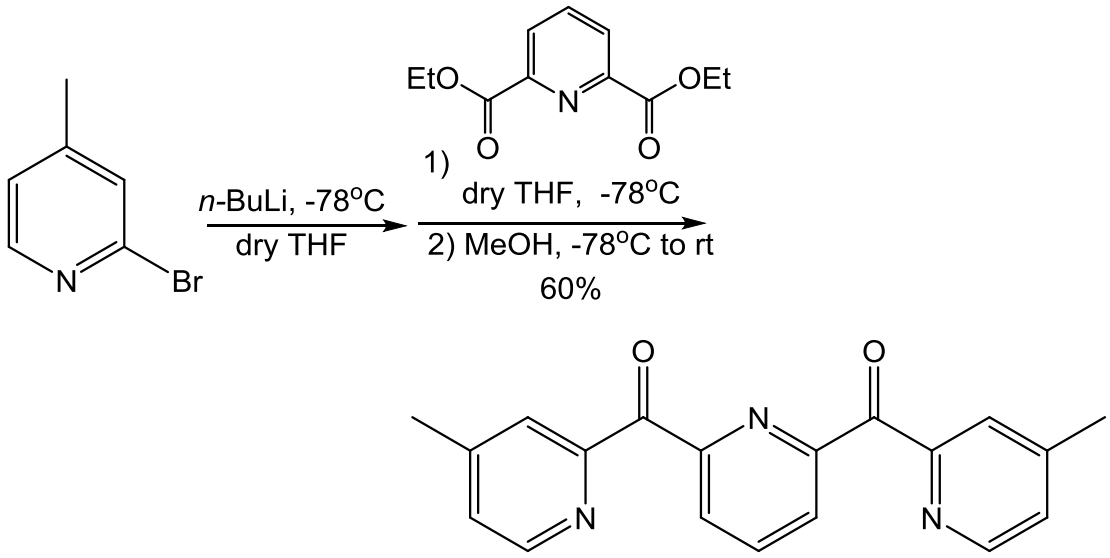

Scheme 5-1. Preparation of 2,6-di(2-carboxy(4-methylpyridyl))pyridine (dcmpp).

The standard method we use in our lab for the introduction of carboxylic acid functional groups to bpy ligands is the chromic acid oxidation, or variation of Jones oxidation.[17] The reaction requires harsh conditions and toxic reagents, but is highly efficient for the transformation of aromatic methyl groups. The method involves the preparation of chromic acid in situ from chromium trioxide and concentrated sulfuric acid. The route is convenient for bpy reagents as the carboxylic acid product is easily precipitated from the reaction with water. We set out to prepare 2,6-di(2-carboxy(4-pyridylcarboxylicacid))pyridine (dcpap) by the same method and found that the carboxylic acid product from the reaction of dcmpp does not precipitate when water is added, and the carbonyl bridges are likely hydrated under these conditions. Attempts were made to extract the product into various solvents to no avail. I attempted to neutralize the reaction mixture in an effort to make extraction easier, but as soon as the pH was raised slightly the product readily precipitated from the reaction and was isolated in 87% yield (Scheme 5-2).

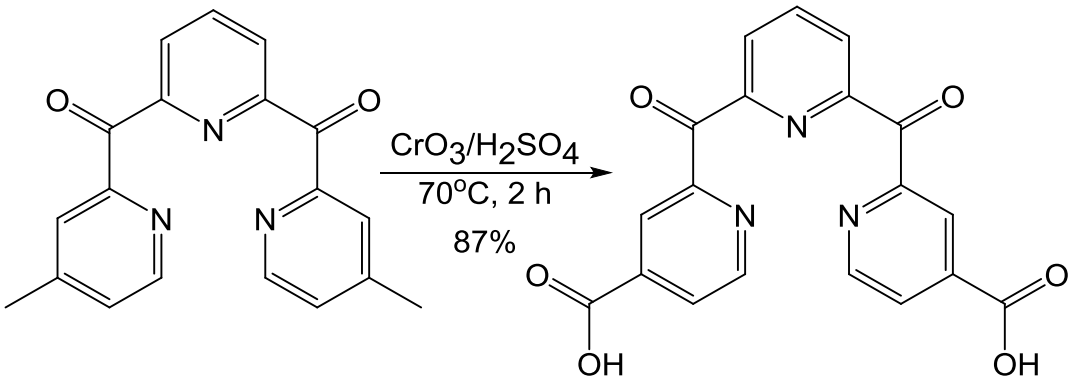

Scheme 5-2. Preparation of 2,6-di(2-carboxy(4-pyridylcarboxylicacid))pyridine (dcpap).

The diethyl ester of the ligand was prepared to allow for easier characterization. It was first prepared by Fischer esterification in low yield. As with the chelidamic acid described in Chapter 4, the yield was much improved by utilizing thionyl chloride in ethanol and the product obtained in 97% yield, shown in Scheme 5-3. The workup proved to be slightly difficult in that the product may not be obtained as a solid. Various attempts were made to crystallize the product and it would precipitate in cold solution, but as soon as it was filtered it reverts to oil, seemingly severely hygroscopic. It is funny that I set out to make 2,6-di(2-carboxy(4-pyridylcarboxylate ethyl ester))pyridine (dcpep) to allow for easier characterization and ultimately the carboxylic acid analog has caused no difficulty while the ester has caused numerous issues during the subsequent coordination reaction and characterization.

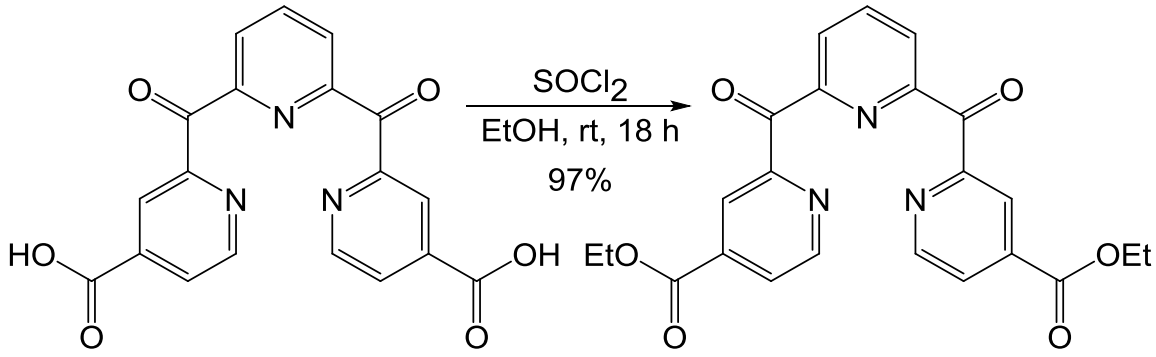

Scheme 5-3. Preparation of 2,6-di(2-carboxy(4-pyridylcarboxylate ethyl ester))pyridine (dcpep).

5.3.2 Preparation of $[Fe(dcpap)_2]^{2+}$ and $[Fe(dcpep)_2]^{2+}$

All attempts to crystalize the dcpep ligand have failed, therefore the oil product was dried in a vacuum dessicator and used as an oil in the coordination reaction. A variation of the standard coordination reaction was employed in which water was excluded, shown in Scheme 5-4. The dcpep oil was dissolved by gently warming in oxygen-free methanol and transferred to the iron(II) salt. The reaction does not appear to proceed as there is no darkening observed, even with prolonged stirring or heating. During the preparation of $[Fe(dcpp)_2]^{2+}$ the addition of NH_4PF_6 was found to drive the reaction forward, so NH_4PF_6 was added in hopes of completing the reaction with the esterified ligand. Again no color change was observed, but upon evaporation of the reaction mixture a dark oily film coated the flask. The brown oily residue was passed through an alumina column with acetonitrile and a small amount of blue/purple product was obtained in 6% yield.

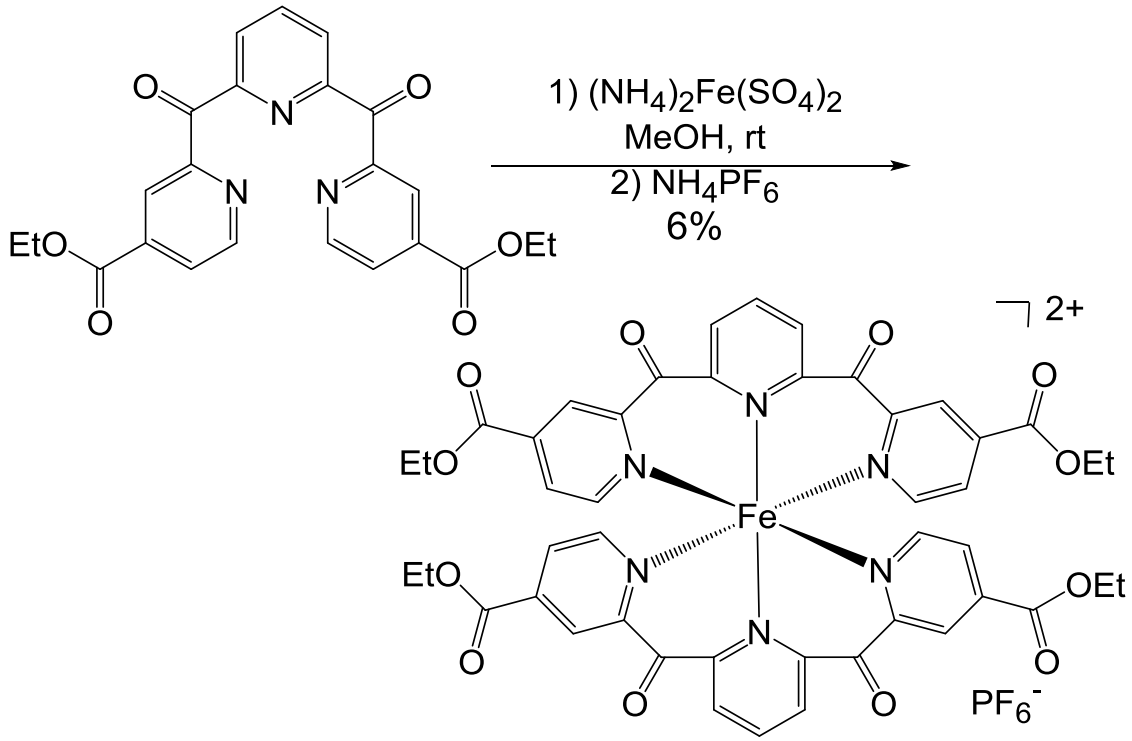

Scheme 5-4. Preparation of $[Fe(dcpep)_2]^{2+}$.

A few potential problems during the preparation of $[Fe(dcpep)_2]^{2+}$ that may be leading to the poor yield are as follows. Ferrous ammonium sulfate is acidic, which is usually beneficial in that when it is dissolved in solution the acidic conditions prevent immediate oxidation of iron(II) to iron(III). As an alternative $FeCl_2 \cdot 2H_2O$ was also employed, but did not produce better results. Though dry methanol was used in the reaction, the dcpep is hygroscopic and likely introduced water to the reaction and esters can readily undergo hydrolysis under acidic conditions. The NH_4PF_6 is also acidic which may be further detrimental to the ester functional groups. This could explain one aspect of the low yield, but could not be the reason that the ligand does not appear to be coordinating as is evident from the lack of color change. The ligand may not be coordinating well due to the presence of the highly electron withdrawing substituents which may induce the

following; 1) lowering the basicity of the pyridyl nitrogens making them less willing to donate the lone pair electrons to form the M-L bond, and 2) induce polarization making the carbonyl bridge carbon even more electropositive and susceptible to attack by the solvent, as was discussed in Chapter 2. Luckily, enough pure product was obtained to grow a few crystals and obtain the x-ray crystal structure shown in Figure 5-3. The crystallographic data is listed in table 5-1. The ethyl ester groups on the terminal pyridyl rings have not prevented the $[Fe(dcpep)_2]^{2+}$ from achieving the octahedral geometry as is evident in the selected geometric parameters listed in Tables 5-2 and 5-3.

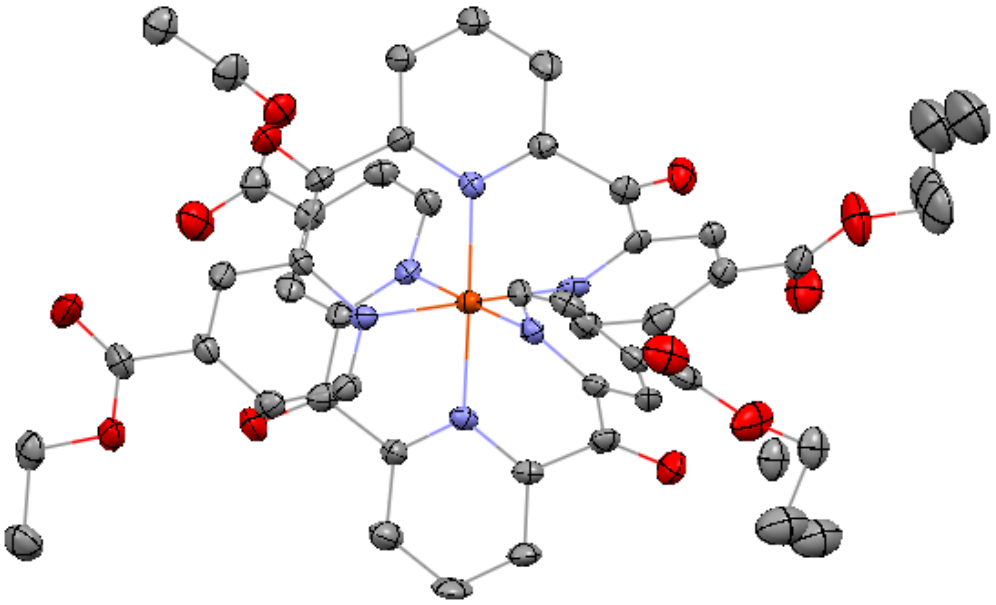

Figure 5-3: ORTEP Drawing of the cation of $[Fe(dcpep)_2]^{2+}$ obtained from single-crystal X-ray structure determination. Atoms are represented as 50% probability thermal ellipsoids. Hydrogen atoms and anions are omitted for clarity.

Table 5-1. Crystallographic data for $[Fe(dcpep)_2](PF_6)_2$.

$[Fe(dcpep)_2](PF_6)_2$ [a]			
Empirical formula	$C_{48}H_{41}F_{12}FeN_7O_{12}P_2$	ρ_{calc}mg/mm^3	1.631
Formula weight	1253.67	μ/mm^{-1}	0.473
Temperature/K	173.15	F(000)	2552
Crystal system	Monoclinic	2θ range	3.56° to 50.78°
Space group	$P2_{1/c}$	Reflections collected	40776
a/Å	15.948 (2)	Independent reflections	9374
b/Å	12.8826 (16)	*R*(int)	0.1129
c/Å	25.922 (3)	Final R indexes [I>=2σ (I)]	R_1 [b] = 0.0811 wR_2 [c] = 0.1854
Volume/Å^3	5104.6 (11)	Final R indexes [all data]	R_1 = 0.1434 wR_2 = 0.2136
Z	4	Goodness-of-fit on F^2	1.064

[a] Obtained with graphite monochromated Mo *K*α radiation (λ = 0.71073 Å) [b] $R_1 = \sum ||F_o| - |F_c|| / \sum |F_o|$. [c] $wR_2 = \{ \sum [w(F_o^2 - F_c^2)^2 / \sum [w(F_o^2)^2]\}^{1/2}$.

Table 5-2. Selected bond lengths from the x-ray crystal structure of $[Fe(dcpep)_2](PF_6)_2$.

Selected Bond Lengths (Å)	
Fe1—N1	1.980(5)
Fe1—N2	1.970(5)
Fe1—N3	1.990(5)
Fe1—N4	1.967(5)
Fe1—N5	1.957(5)
Fe1—N6	1.988(5)

Table 5-3. Selected bond angles from the x-ray crystal structure of $[Fe(dcpep)_2](PF_6)_2$.

Bond Angles (°)			
N1—Fe1—N3	179.8(2)	N4—Fe1—N6	178.9(2)
N1—Fe1—N6	88.6(2)	N5—Fe1—N1	91.1(2)
N2—Fe1—N1	90.0(2)	N5—Fe1—N2	178.7(2)
N2—Fe1—N3	90.2(2)	N5—Fe1—N3	88.7(2)
N2—Fe1—N6	89.9(2)	N5—Fe1—N4	90.8(2)
N4—Fe1—N1	90.3(2)	N5—Fe1—N6	89.6(2)
N4—Fe1—N2	89.7(2)	N6—Fe1—N3	91.4(2)
N4—Fe1—N3	89.7(2)		

In addition to the crystal structure, there was enough pure product to obtain a ^1H NMR spectrum, but the rest of the characterization proved to be problematic as the ester groups hydrolyze. To obtain a better overall picture, the iron(II) complex of the carboxylic acid functionalized ligand, $[Fe(dcpap)_2](PF_6)_2$, was prepared. The complex was synthesized by the standard method with slight modification, as shown in Scheme 5-5.

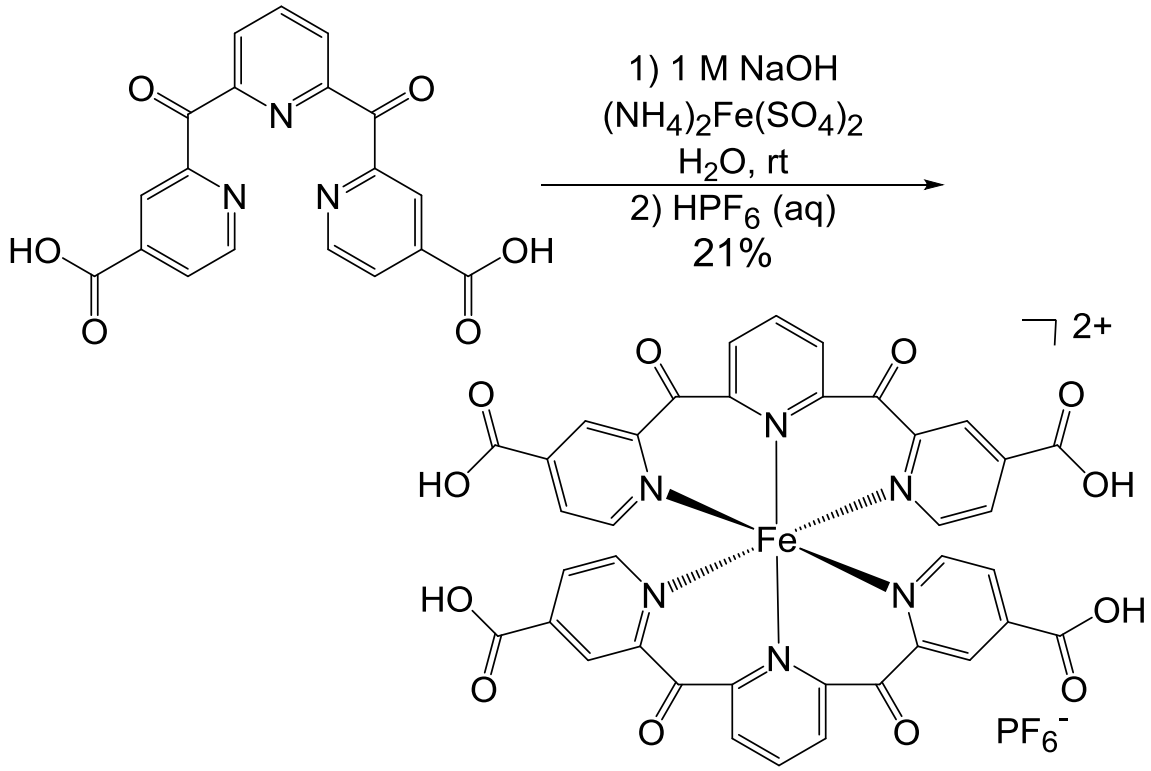

Scheme 5-5. Preparation of $[Fe(dcpap)_2]^{2+}$.

The dcpap ligand was suspended in water and the two acid groups deprotonated by the addition of two equivalents of NaOH in order to solubilize the ligand and the solution was degassed by bubbling with N_2. A solution of ferrous ammonium sulfate was added and the reaction mixture immediately darkened to a deep purple signifying formation of the iron(II) complex. HPF_6 was added to protonate the acid groups and obtain the desired complex. The product was obtained in 21% yield after 1 hour, but it is possible that if allowed to react longer the yield may be improved. For the first time, as opposed to all of the other complexes described in this dissertation, the complex was isolated by filtration with no evidence of byproducts. There was only evidence of the desired complex and unreacted ligand which was easily removed by dissolving the complex in methanol and filtering the insoluble ligand. The carboxylic acid analog proved to be more stable than the ethyl ester analog and the solubility of the complex in methanol allowed for thorough characterization.

Measuring the molar absorptivity of either $[Fe(dcpep)_2](PF_6)_2$ or $[Fe(dcpap)_2](PF_6)_2$ is complicated by the hygroscopic nature of the complexes. For the ethyl ester analog various attempts were made to obtain an extinction coefficient but a consistent ground state absorption spectrum could not be obtained as the ester groups hydrolyze over time. The acid analog is more stable but gains weight in air as it takes on water, therefore an accurate extinction coefficient could not be determined. The ground state absorption spectra of the two complexes are shown in Figure 5-4. The spectrum of $[Fe(dcpep)_2](PF_6)_2$ shows the normalized absorption of two samples where it is evident that the spectrum changes as hydrolysis of the ester groups occurs over time. The hydrolysis is apparent by eye as there is a color change from blue/purple to more red/purple.

The blue solid line was $[Fe(dcpep)_2](PF_6)_2$ taken as it was freshly obtained from the column following the reaction. The purple dashed line is an older sample that has clearly changed as a result of a different degree of protonation. The spectrum of $[Fe(dcpap)_2](PF_6)_2$ is shown on the right for comparison. A true comparison cannot be made as this spectrum was taken in methanol, but we can clearly see that the features are comparable to the hydrolyzed ester sample.

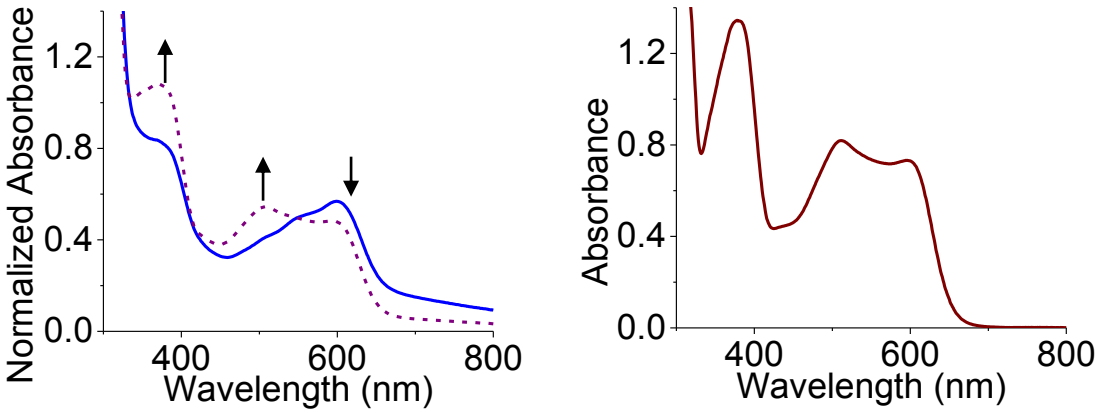

Figure 5-4. Ground state absorption spectra of $[Fe(dcpep)_2](PF_6)_2$ in acetonitrile (left) and $[Fe(dcpap)_2](PF_6)_2$ in methanol (right). The normalized absorption spectra of two crops of $[Fe(dcpep)_2](PF_6)_2$ clearly show that the spectrum changes as the ester groups on the complex undergo hydrolysis (—— $[Fe(dcpep)_2](PF_6)_2$) (- - - hydrolyzed $[Fe(dcpep)_2](PF_6)_2$).

A comparison of the optical properties of these analogs to the other complexes in this dissertation could provide useful information for our investigation of inductive effects. Unfortunately the integrity of $[Fe(dcpep)_2](PF_6)_2$ is in question, and $[Fe(dcpap)_2](PF_6)_2$ is insoluble in acetonitrile, consequently we cannot draw an accurate comparison.

Though the spectral features show a strong dependence on the degree of protonation, electrochemistry, may provide some insight. Sepehrifard et al. recently investigated a series of Ru(II)-terpy dyes in which carboxylic acid and ethyl ester analogs were prepared, and from the electrochemical data it appears that the difference in anchoring group, ester versus acid, has a minimal impact on the oxidation and reduction potential, showing only small variation of between 20-100 mV.[21] On the other hand, Ferrere has found a strong dependence of the electrochemical oxidation potential of [Fe(4,4-dicarboxylate-2,2'-bipyridine)$_2$(CN)$_2$] on the degree of protonation, with the acid being 300 mV more positive than the tetrabutylammonium salt.[22]

The electrochemical potentials of [Fe(dcpep)$_2$](PF$_6$)$_2$ were collected by cyclic voltammetry, and though the degree of protonation of the carboxylate groups are in question which increases the error of the experiment, we can use these values as approximations. The oxidation and first reduction potentials are listed in Table 5-4. It appears as though the inductive effect of the electron withdrawing carboxylate groups is shifting the oxidation potential and first reduction potential more positive compared to the unsubstituted dcpp. These values signify that there is stabilization of the HOMO t_{2g} levels of the metal and LUMO π^* levels of the ligand. Another notable feature of the electrochemistry of [Fe(dcpep)$_2$](PF$_6$)$_2$ is the presence of eight reversible reductions. The ability of the ligands to undergo four reductions each is attributed to the presence of the electron withdrawing functional groups: the four carbonyl bridges and four carboxylate groups.

Table 5-4. Electrochemical potentials for the oxidation and first reduction of $[Fe(dcpp)_2](PF_6)_2$ and $[Fe(dcpep)_2](PF_6)_2$, measured with Ag/AgCl reference with 0.1 M $TBAPF_6$ electrolyte in acetonitrile, externally referenced to ferrocene. *These values are approximations as hydrolysis may have occurred and the degree of protonation is unknown.

Compound	$E_{1/2}$ [ox]	$E_{1/2}$ [red]
$[Fe(dcpp)_2]^{2+}$	1.295 V	-0.965 V
$[Fe(dcpep)_2]^{2+}$	1.580 V*	-0.780 V*

Though the ester groups in $[Fe(dcpep)_2](PF_6)_2$ are susceptible to hydrolysis, the core structure seems to be quite stable, which is evident from the positive oxidation potential. The $[Fe(dcpap)_2](PF_6)_2$ analog appears to be stable as well as there is no change after days of standing in methanol solution in the presence of air. This is promising for application as a sensitizer in DSSCs, since dying the semiconductor requires soaking in an alcohol solution for at least 24 hours, also since DSSCs are commonly solution state cells in which there is an acetonitrile electrolyte solution. As for sensitization of TiO_2, the eight electron withdrawing groups have stabilized the orbitals to the extent that even the charge transfer excited states lies below the conduction band of TiO_2, making it unlikely that this complex could be a viable sensitizer (Figure 5-5). If we are able to effectively tune the excited states by the strategies described in Chapter 4, it may still be possible to develop a viable sensitizer.

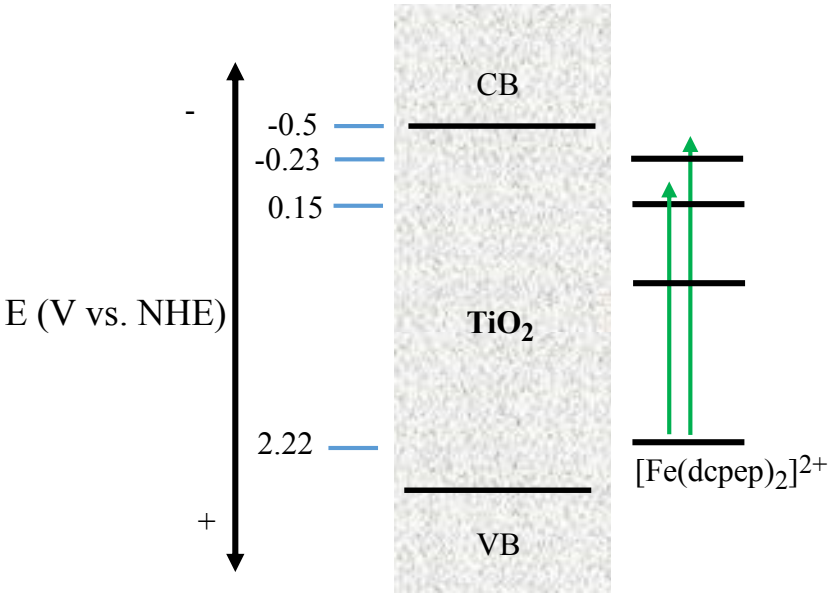

Figure 5-5: Band structure of TiO_2 compared to the energy level diagram of $[Fe(dcpep)_2](PF_6)_2$ showing that the MLCT excited states are lower that the conduction band of TiO_2.

5.3.3 Alternative Anchoring Groups for Dye-Sensitization

As mentioned in the introduction, the most widely employed anchor is the carboxylate functional group, as it has been shown to bind to TiO_2 with good stability and provide strong electronic communication. However, the ester linkages are only stable under anhydrous conditions and in the presence of water are susceptible to hydrolysis causing detachment of the dye from the oxide surface. Though the cells we are interested in utilize dry acetonitrile, long term stability may be improved by utilizing less reactive anchoring groups. The complications encountered during characterization of the ester analog described in the previous section, make it clear that the instability could present an issue.

We are looking into other options for anchoring groups and have found many possibilities in the literature which include catecholates,[8] boronates,[9] phosphonates,[10] malonates,[23] and isophthalates[24] (Figure 5-6). Two anchoring groups that stand out for their high stability on attachment to TiO_2 are acetylacetonate (acac) and hydroxamate.[4–6] In addition to their stability, the relative ease of installation of these groups make them a desirable alternative to the carboxylate group.

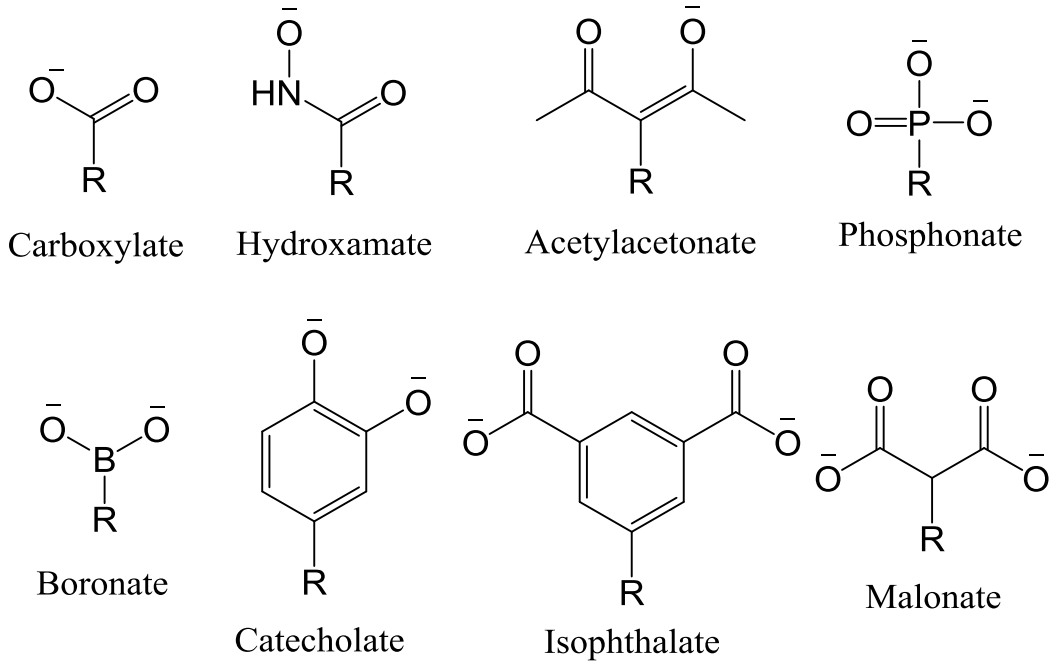

Figure 5-6: Functional groups that have been investigated for anchoring to a metal oxide substrate.

As with the carboxylic acid groups, the introduction of the anchoring groups requires a methyl group. The installation of methyl substitutents to the terminal rings has already been achieved, however we are also interested in functionalizing the central ring. The central pyridyl ring starting material is known in the literature and may be obtained through various procedures and once in hand, the standard method used to prepare all of the dcpp analogs described in this dissertation may be utilized.[25,26] The *p*-tolyl

stubstituent, on the dcptp ligand described in Chapter 4, will also allow for installation of anchoring groups, which will be attempted in due course.

The chemistry for the installation of acac should be fairly straightforward, as shown in Scheme 5-6. For simplicity, the reaction scheme shows the dcpp analog with only the central ring bearing a methyl substituent, but the procedure should be applicable to functionalization of all methyl or *p*-tolyl substituents on the various dcpp analogs. The proposed procedure is based on the known method of functionalization of 4-methylpyridine via low temperature coupling with acetyl chloride.[27,28] The acac group is known to be unstable and may undergo reverse Claisen condensation until bound by the TiO_2 substrate, therefore it should be freshly prepared and utilized quickly in order to maintain integrity. The hydroxamic acid group may be a better option for stability reasons.

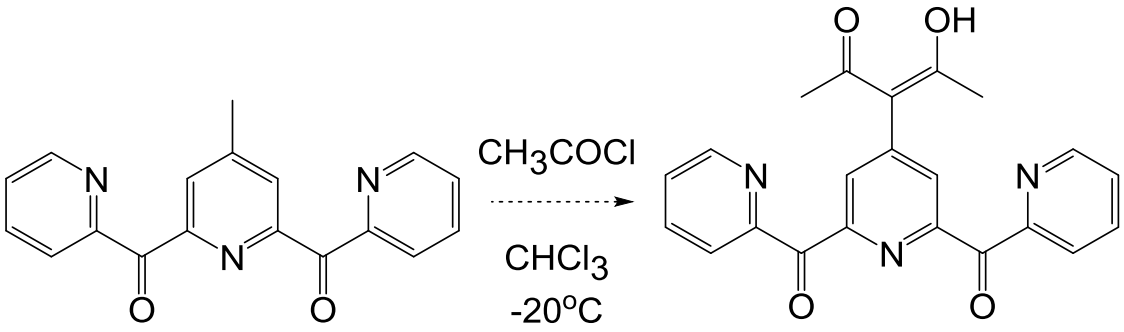

Scheme 5-6. Proposed installation of acetylacetonate (acac) anchoring group.

Hydroxamic acids possess a wide range of biological activities with antibacterial, antifungal, anti-inflammatory, and anti-asthmatic properties, therefore several methods have been developed for their preparation and they are well documented in the literature. Among the many methods, one stands out as a highly convenient synthesis involving the transformation of a carboxylic acid to a hydroxamic acid and is shown in Scheme 5-7.[29]

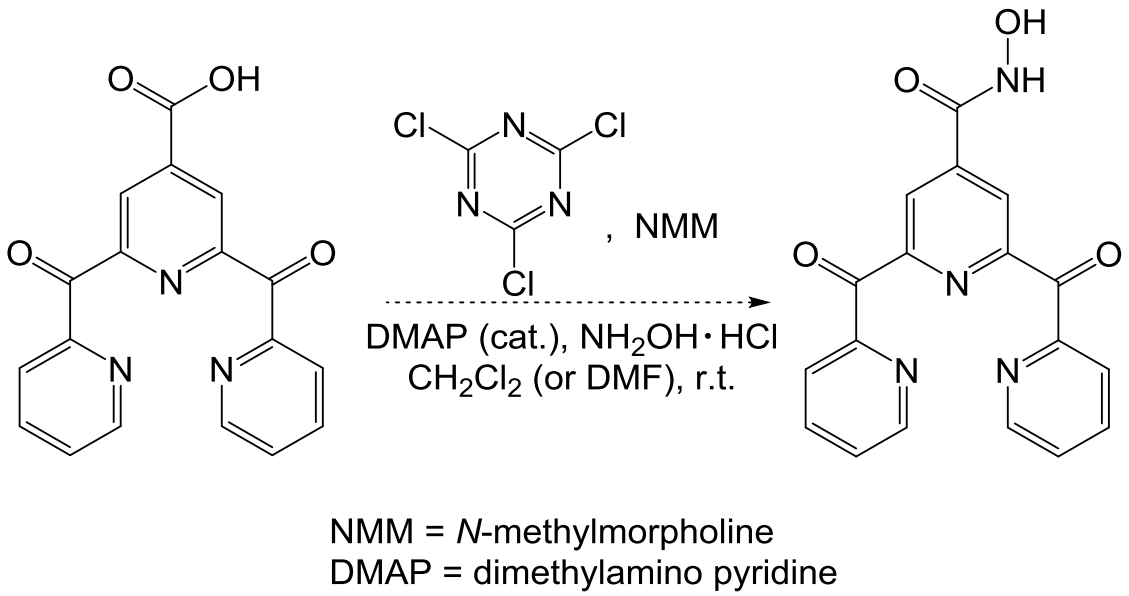

Scheme 5-7. Proposed installation of hydroxamic acid anchoring group.

This route is ideal, as the chemistry for the installation of carboxylic acid groups has already been worked out and the hydroxamic acid may be obtained in one step, under mild conditions in high yields. The method employs cyanuric chloride as a coupling agent, NMM base, and DMAP as a catalyst and complete conversion to the hydroxamic acid may be achieved by simply stirring at room temperature for up to 12 hours. Triazine byproducts may be simply removed by aqueous workup and the product obtained in pure form and high yield.

Experiment and theory both point to hydroxamate and acac anchoring groups having good binding and injection characteristics, even better than carboxylate groups.[4–6,11] With the culmination of the proposed syntheses we will be one step closer toward the development of a viable iron(II) sensitizer.

5.4 Concluding Comments

We have successfully prepared an analog of $[Fe(dcpp)_2]^{2+}$ that possesses the functionality required to bind to a semiconductor. The ester functionalized $[Fe(dcpep)_2]^{2+}$ is susceptible to hydrolysis, therefore the characterization was complicated; however, the acid functionalized $[Fe(dcpap)_2]^{2+}$ was also prepared and proved to be much more stable, and stability is key for the eventual use as a sensitizer in DSSCs. Synthetic efforts toward the development of alternative anchoring groups have been proposed and will also be pursued. With the ability to bind to the semiconductor we may begin a new branch of this research and investigate this new class of iron(II) chromophores on TiO_2 films.

APPENDIX

APPENDIX

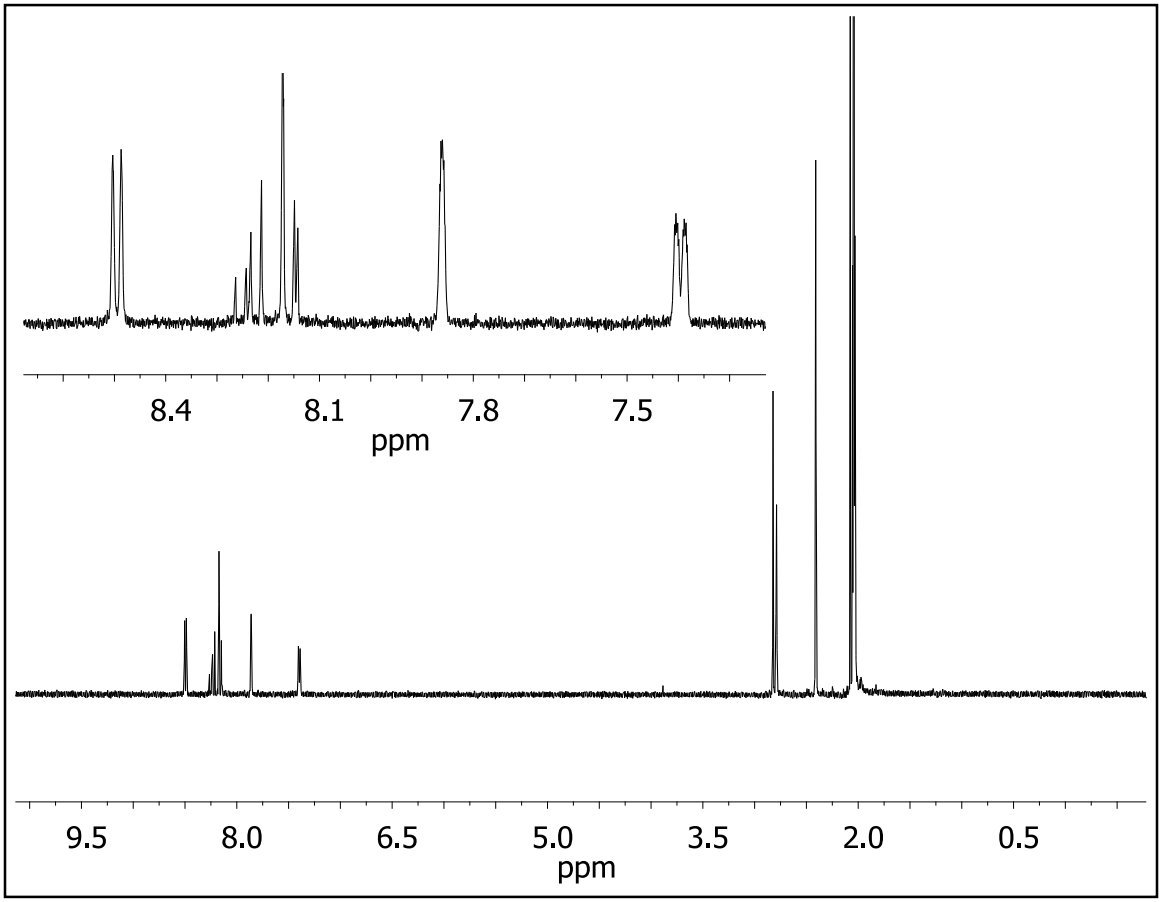

Figure 5-7. ^{1}H NMR of 2,6-di(2-carboxy(4-methylpyridyl))pyridine (dcmpp) in $(CD_3)_2CO$.

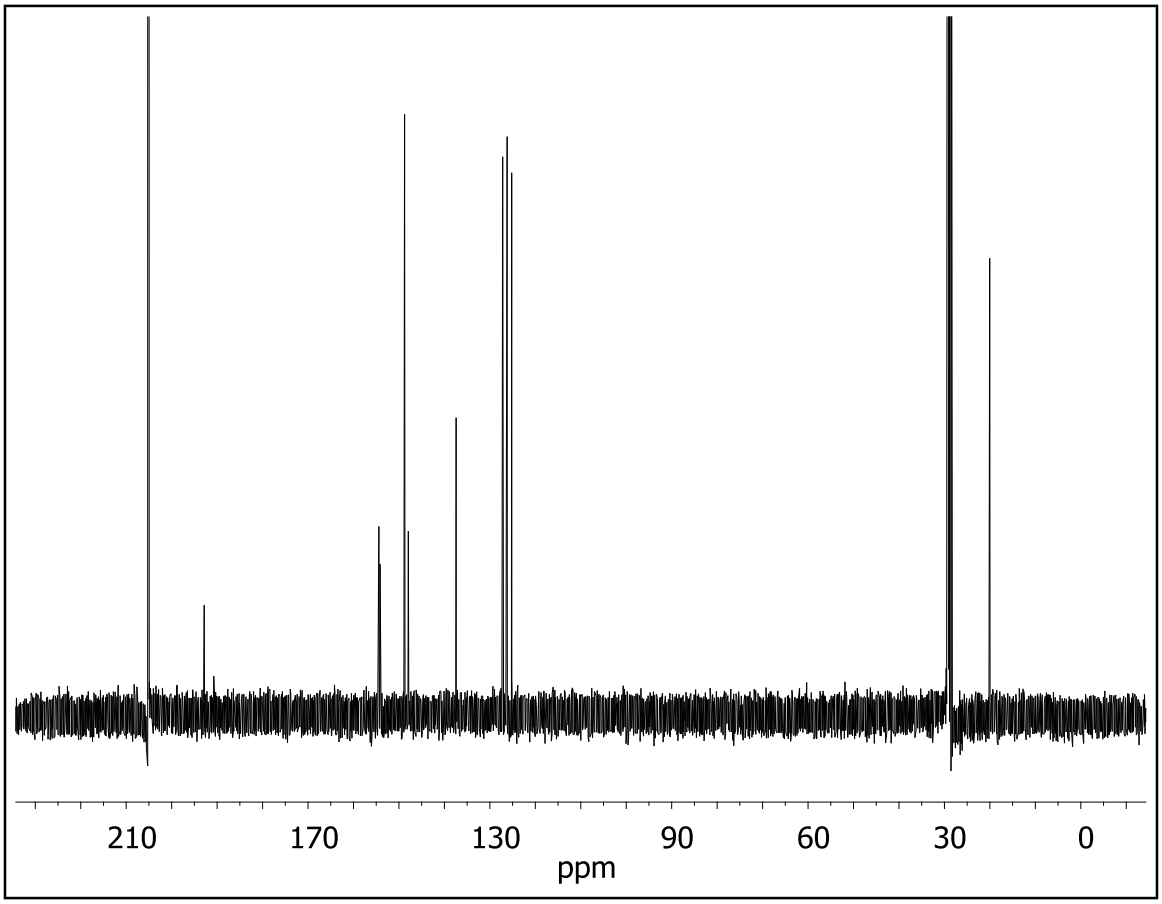

Figure 5-8. ^{13}C NMR 2,6-di(2-carboxy(4-methylpyridyl))pyridine (dcmpp) in $(CD_3)_2CO$.

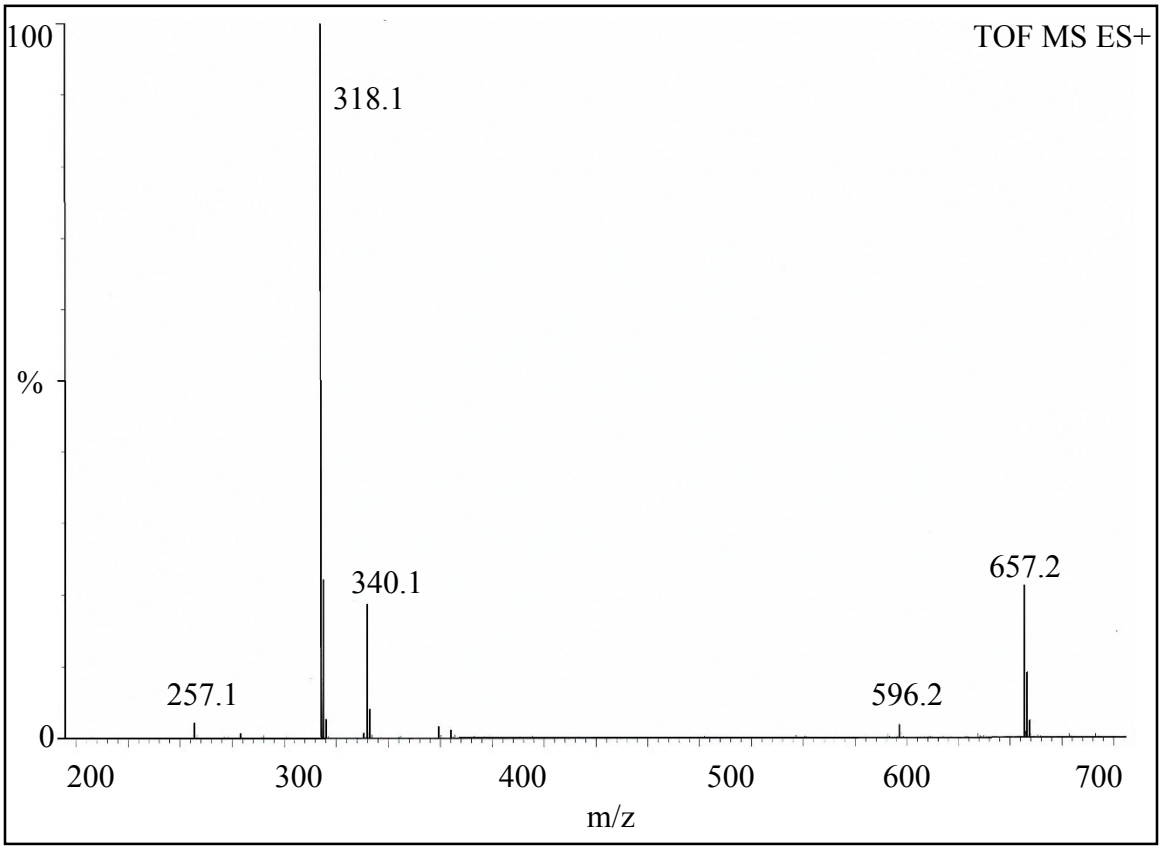

Figure 5-9. ESI-MS of 2,6-di(2-carboxy(4-methylpyridyl))pyridine (dcmpp).

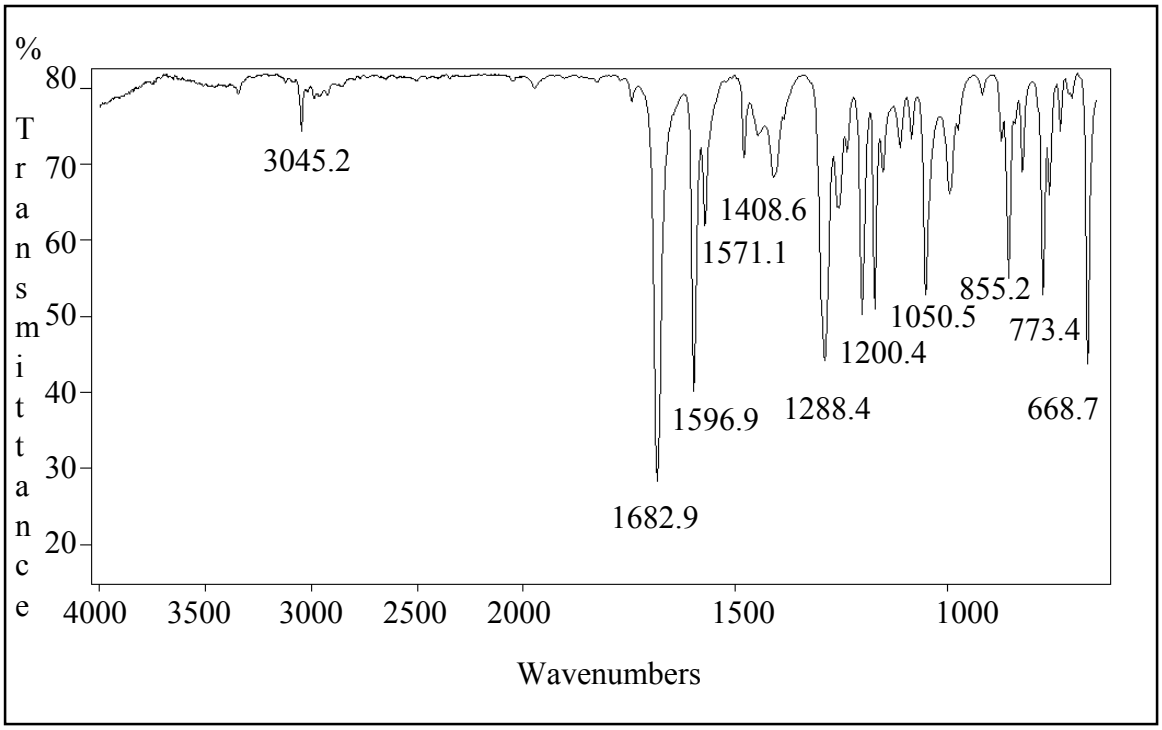

Figure 5-10. IR of 2,6-di(2-carboxy(4-methylpyridyl))pyridine (dcmpp)**.**

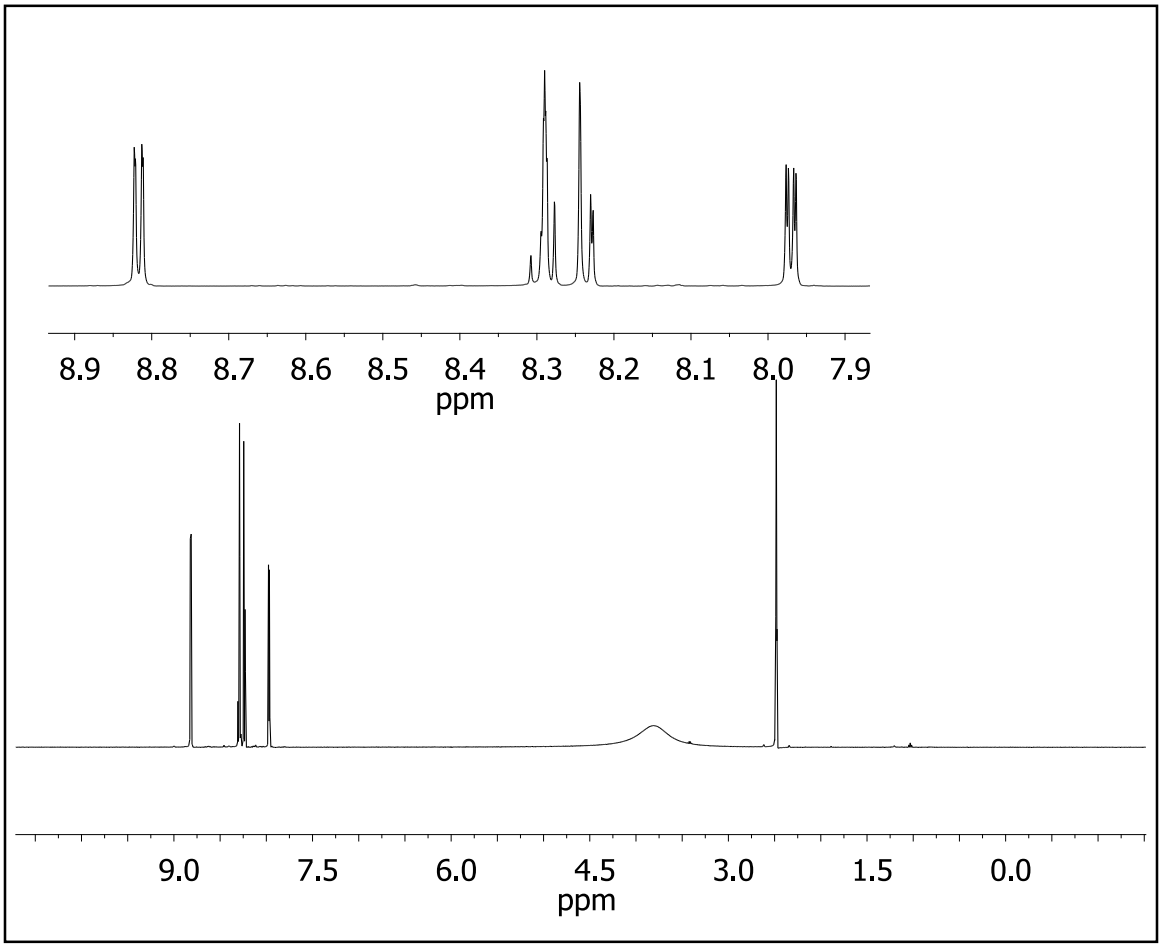

Figure 5-11. ^{1}H NMR of 2,6-di(2-carboxy(4-pyridylcarboxylicacid))pyridine (dcpap) in $(CD_3)_2SO$.

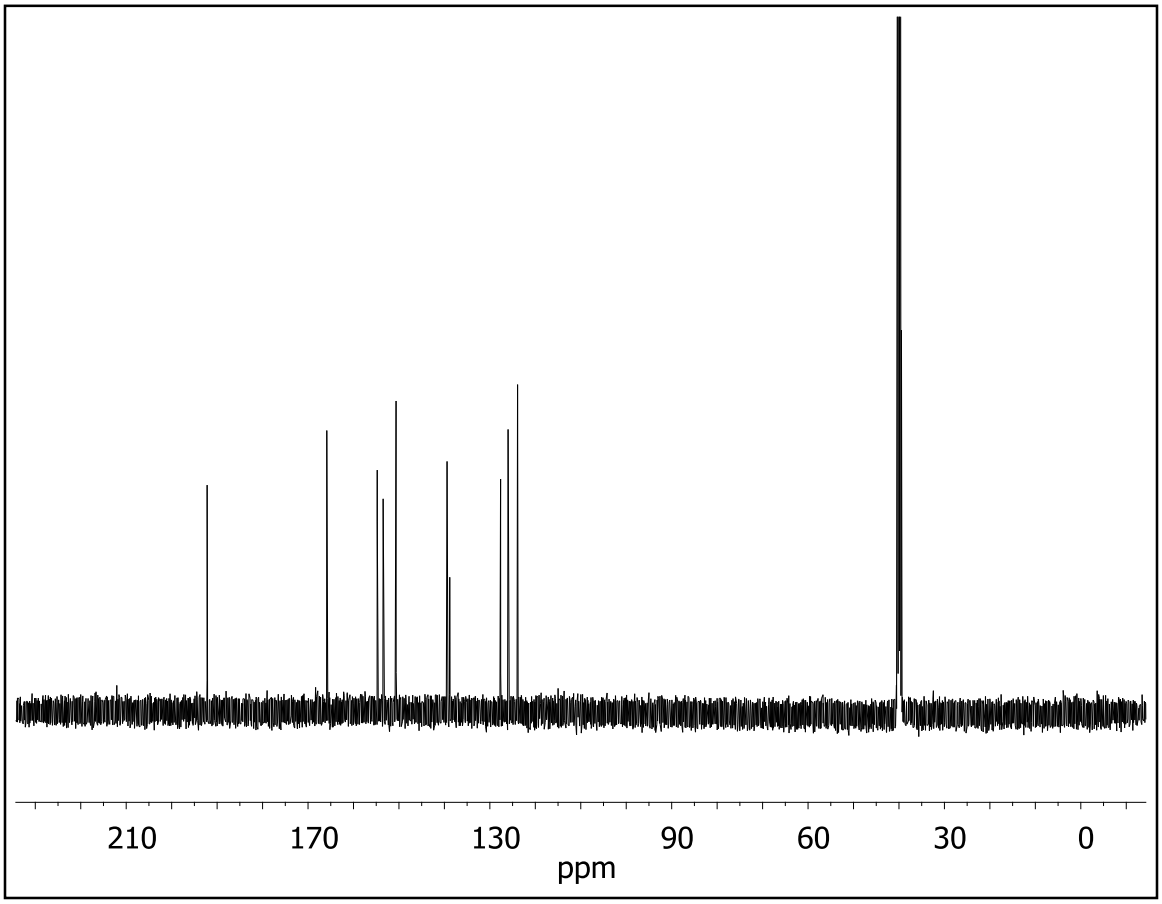

Figure 5-12. ^{13}C NMR of 2,6-di(2-carboxy(4-pyridylcarboxylicacid))pyridine (dcpap) in $(CD_3)_2SO$.

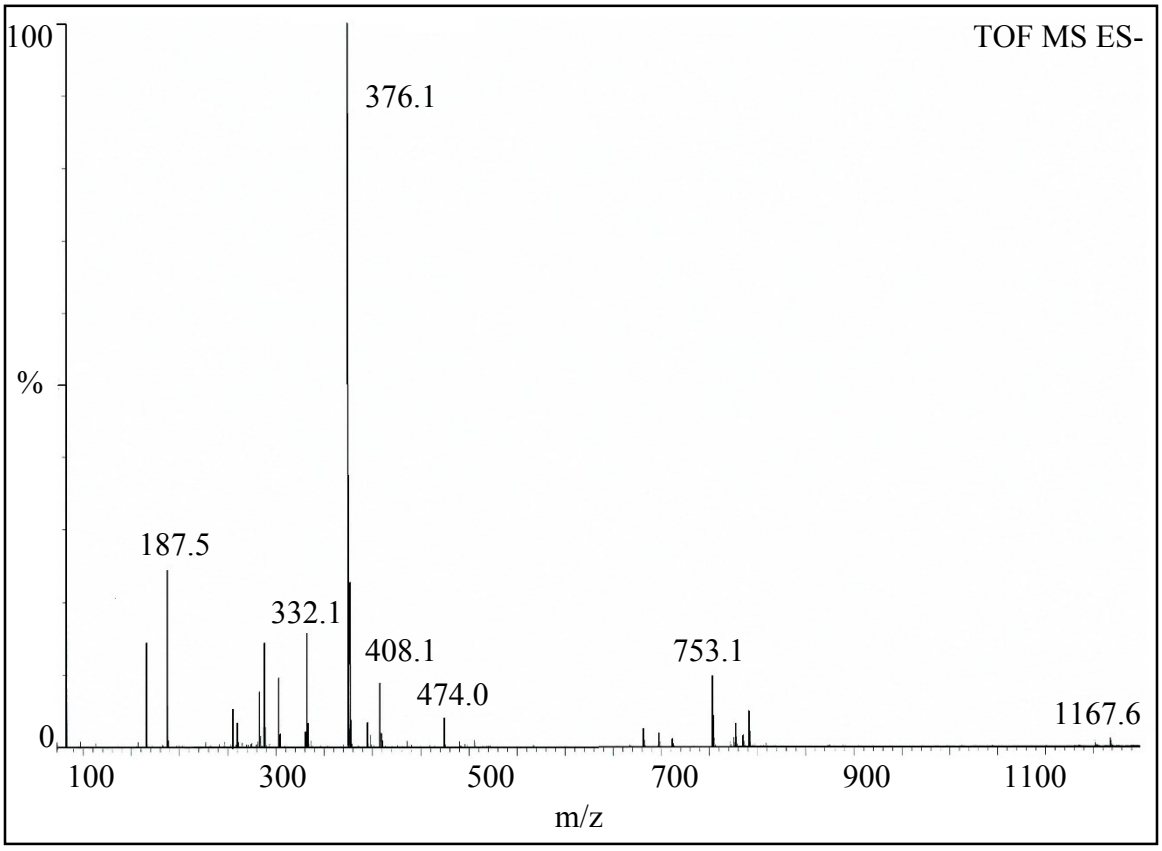

Figure 5-13. ESI-MS of 2,6-di(2-carboxy(4-pyridylcarboxylicacid))pyridine (dcpap).

.

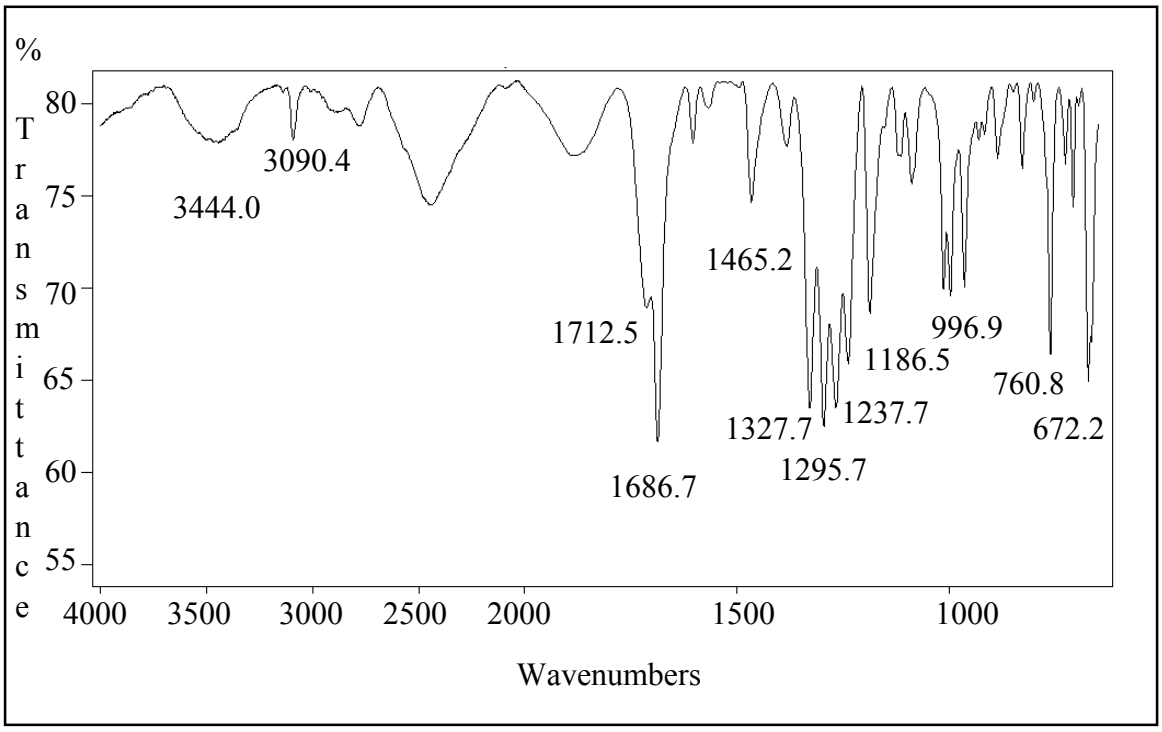

Figure 5-14. IR of 2,6-di(2-carboxy(4-pyridylcarboxylicacid))pyridine (dcpap)

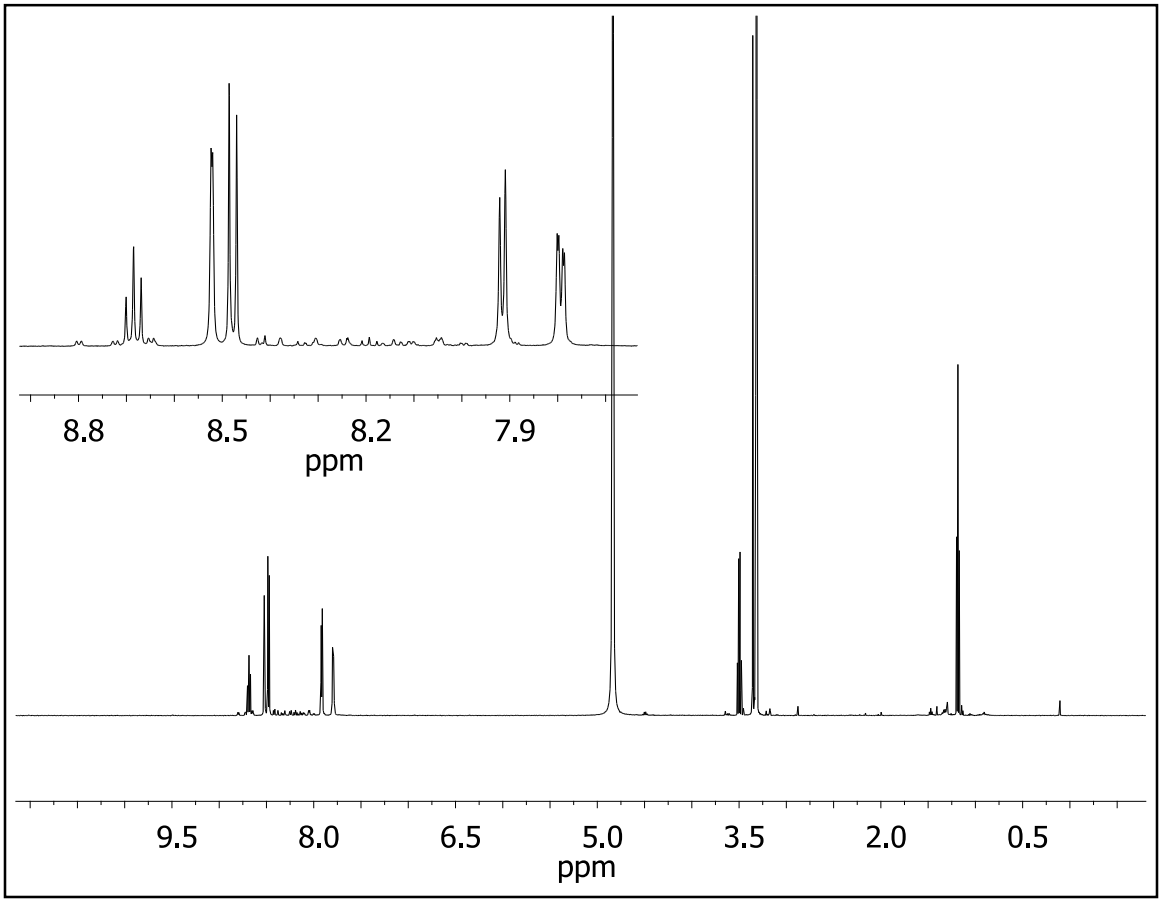

Figure 5-15. ^{1}H NMR of $[Fe(dcpap)_2](PF_6)_2$ in CD_3OD.

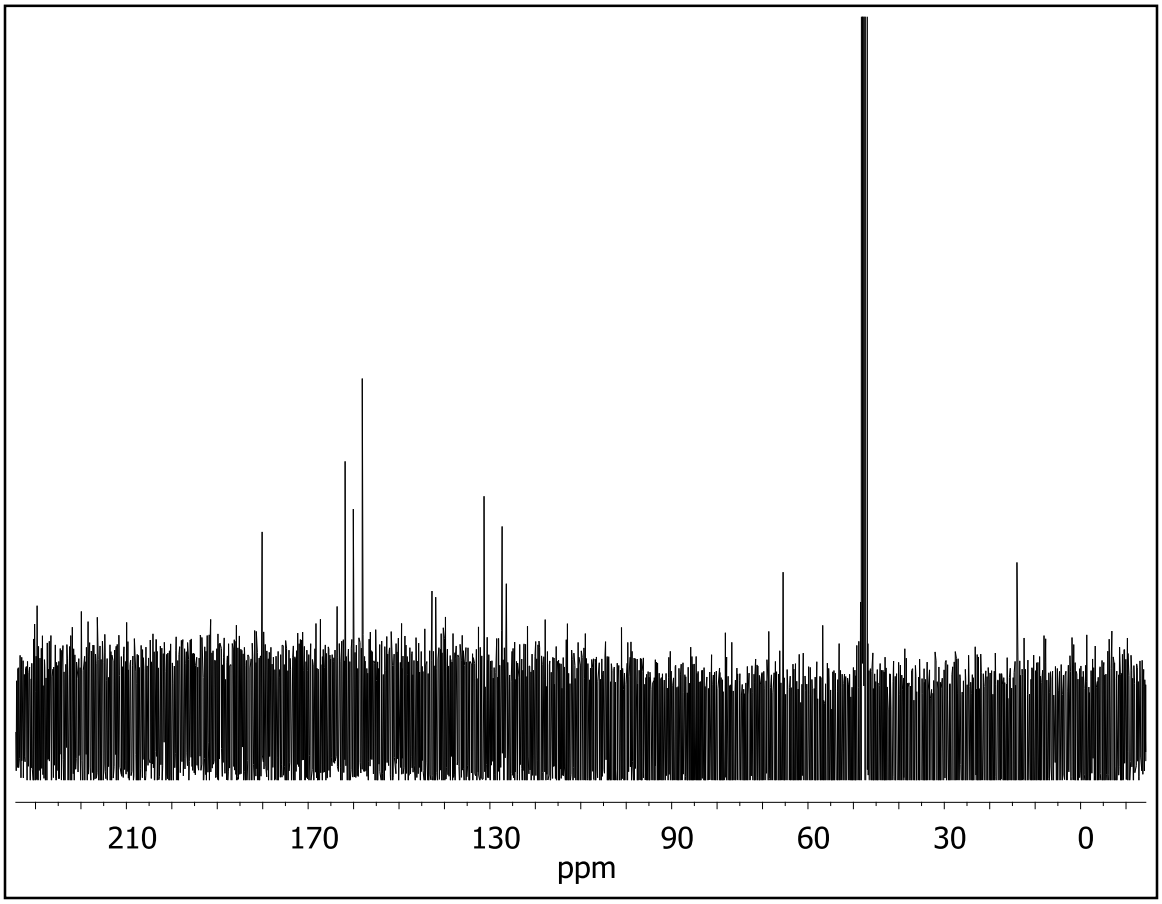

Figure 5-16. ^{13}C NMR of $[Fe(dcpap)_2](PF_6)_2$ in CD_3OD.

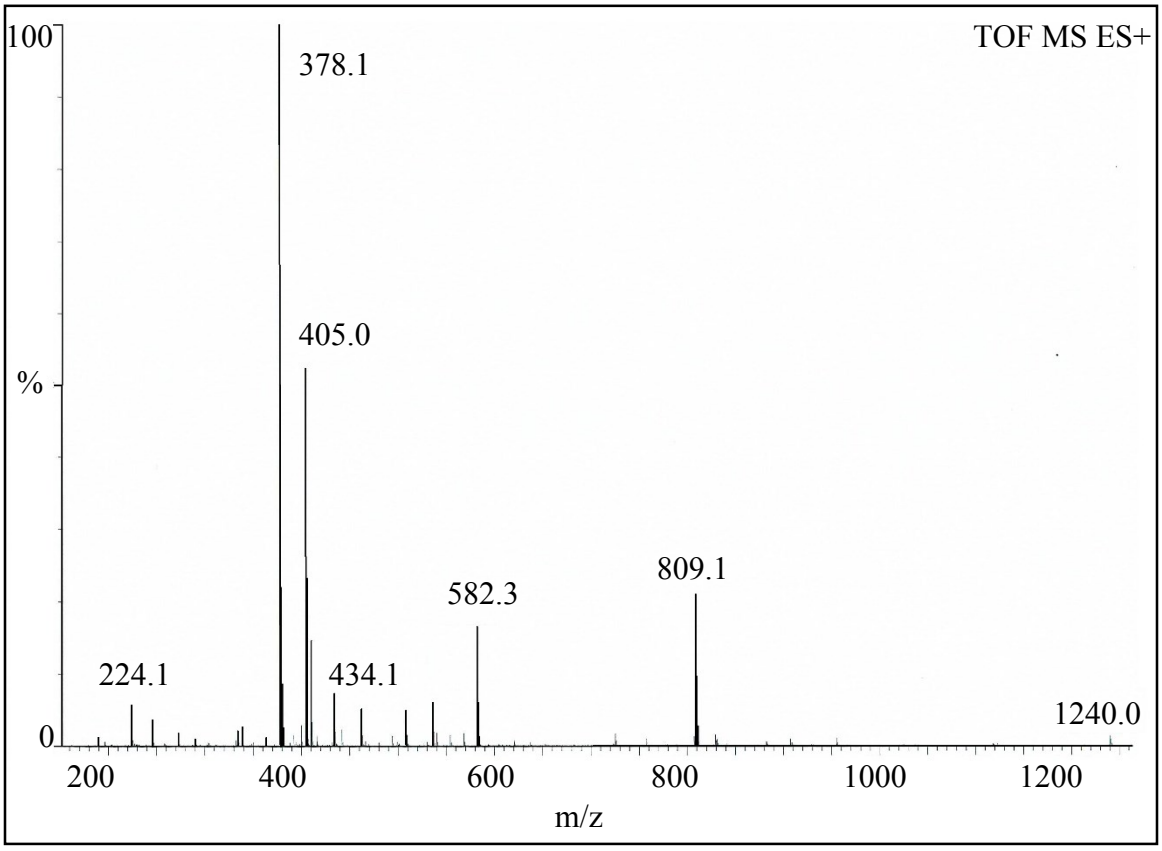

Figure 5-17. ESI-MS of $[Fe(dcpap)_2](PF_6)_2$.

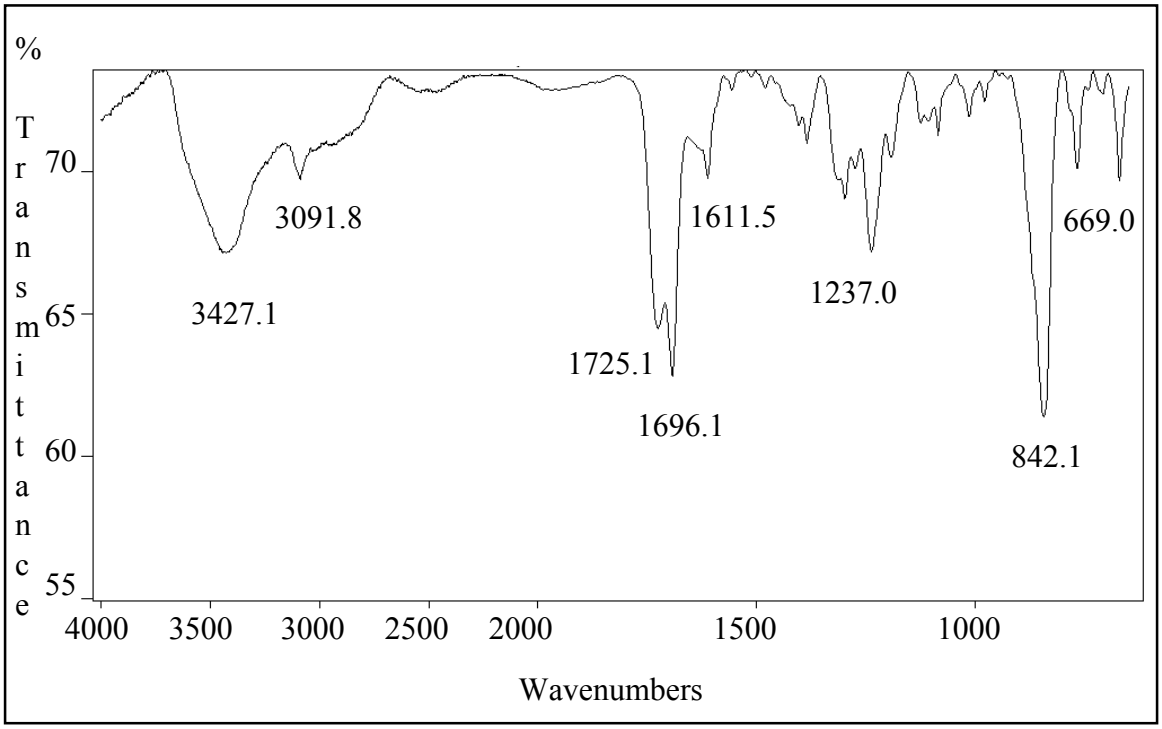

Figure 5-18. IR spectrum of $[Fe(dcpap)_2](PF_6)_2$.

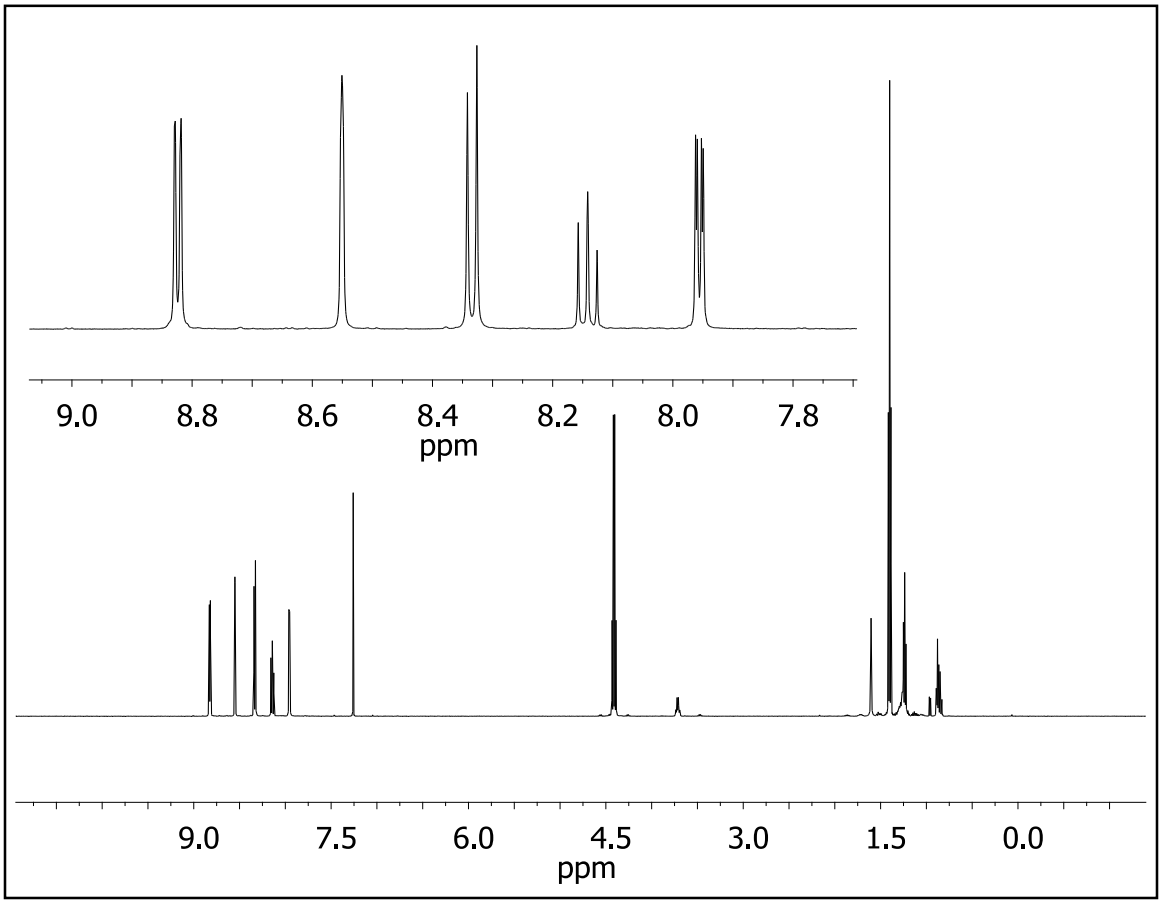

Figure 5-19. ^{1}H NMR of 2,6-di(2-carboxy(4-pyridylcarboxylate ethyl ester))pyridine (dcpep) in $CDCl_3$.

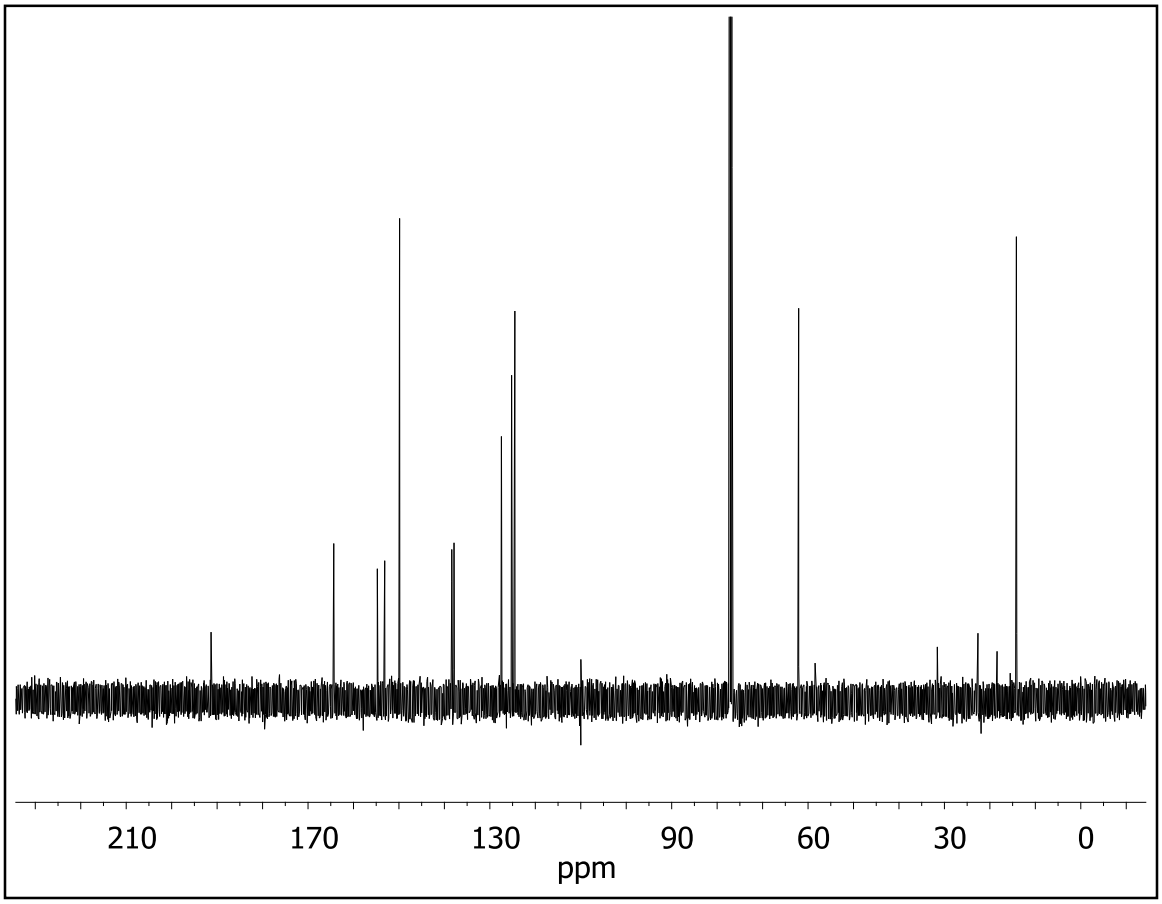

Figure 5-20. ^{13}C NMR of 2,6-di(2-carboxy(4-pyridylcarboxylate ethyl ester))pyridine (dcpep) in $CDCl_3$.

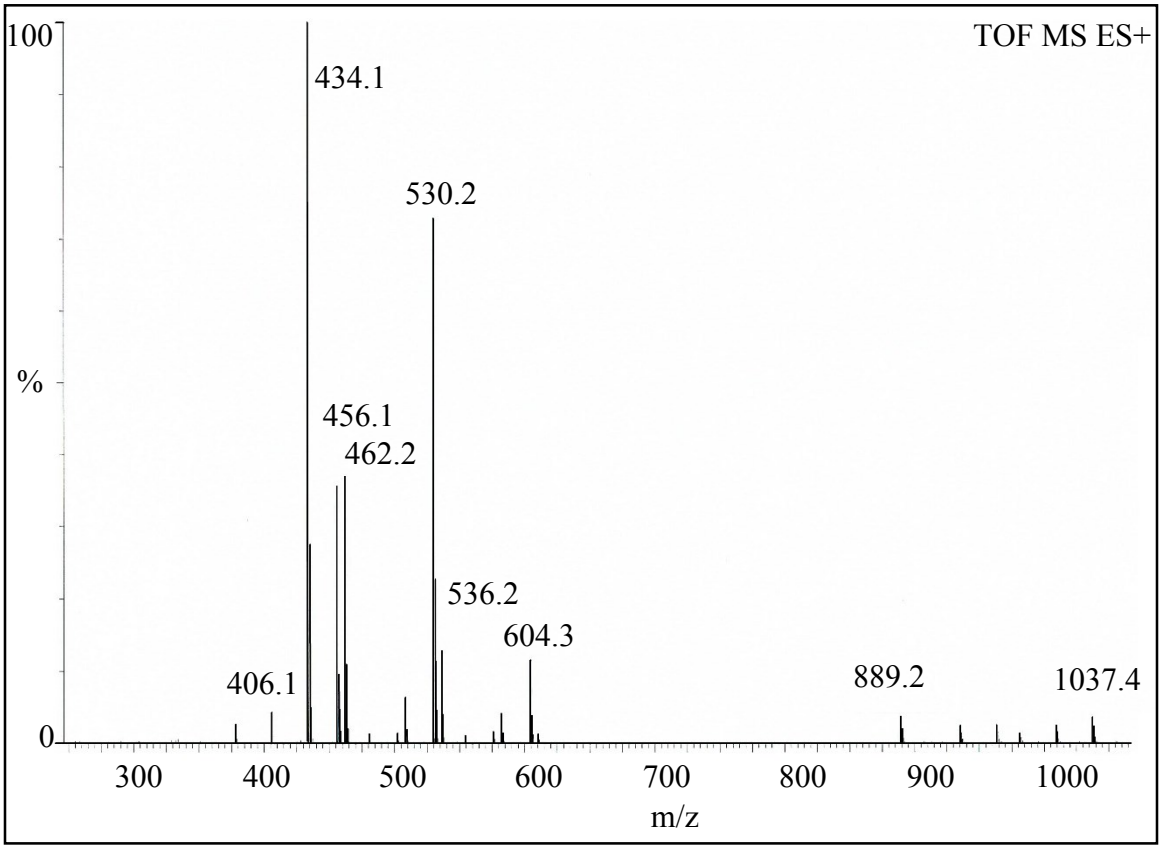

Figure 5-21. ESI-MS of 2,6-di(2-carboxy(4-pyridylcarboxylate ethyl ester))pyridine (dcpep).

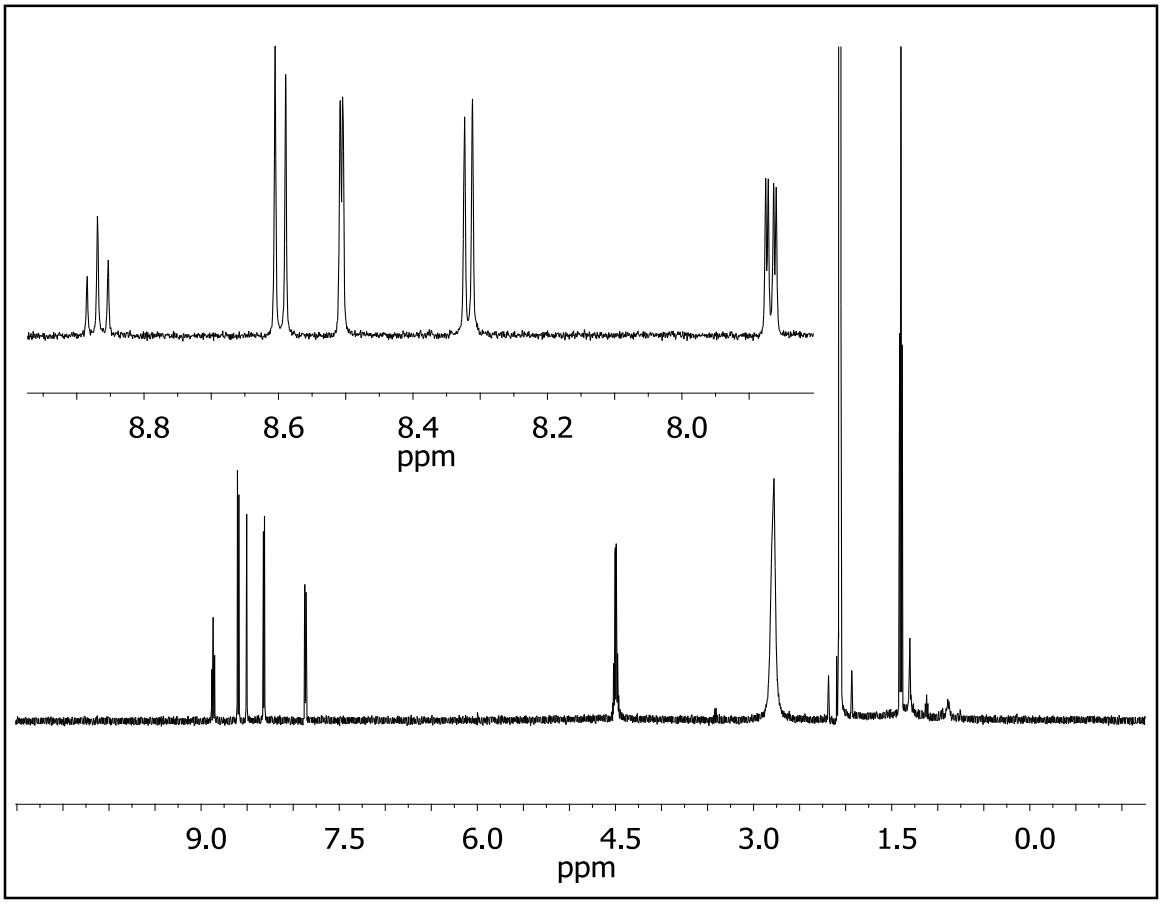

Figure 5-22. ^{1}H NMR of $[Fe(dcpep)_2](PF_6)_2$ in $(CD_3)_2CO$.

Table 5-5. Geometric parameters for the X-ray crystal structure of $[Fe(dcpep)_2](PF_6)_2$.

Bond Lengths (Å)					
Fe1	N1	1.980(5)	C11	C12	1.373(9)
Fe1	N2	1.970(5)	C12	C13	1.369(9)
Fe1	N3	1.990(5)	C13	C14	1.378(9)
Fe1	N4	1.967(5)	C14	C15	1.495(9)
Fe1	N5	1.957(5)	C15	C16	1.492(8)
Fe1	N6	1.988(5)	C16	C17	1.374(8)
O1	C6	1.305(8)	C17	C18	1.387(9)
O1	C7A	1.53(9)	C18	C19	1.384(9)
O1	C7B	1.42(9)	C18	C21	1.499(9)
O2	C6	1.207(8)	C19	C20	1.371(9)
O3	C9	1.215(7)	C22	C23	1.490(10)
O4	C15	1.208(7)	C24	C25	1.365(8)
O5	C21	1.321(8)	C24	C32	1.493(9)
O5	C22	1.460(7)	C25	C26	1.381(9)
O6	C21	1.192(8)	C26	C27	1.397(9)
O7	C29	1.340(9)	C26	C29	1.491(9)
O7	C30	1.449(11)	C27	C28	1.366(9)
O7	C30A	1.66(3)	C30	C31	1.49(2)
O8	C29	1.201(8)	C30A	C31A	1.49(5)
O9	C32	1.213(7)	C32	C33	1.505(9)
O10	C38	1.209(8)	C33	C34	1.364(8)
O11	C44	1.325(8)	C34	C35	1.389(9)
O11	C45	1.455(7)	C35	C36	1.386(9)
O12	C44	1.199(8)	C36	C37	1.383(9)
N1	C1	1.352(8)	C37	C38	1.507(9)
N1	C5	1.352(8)	C38	C39	1.482(9)
N2	C10	1.352(8)	C39	C40	1.386(9)
N2	C14	1.360(8)	C40	C41	1.389(9)
N3	C16	1.359(8)	C41	C42	1.384(9)
N3	C20	1.354(8)	C41	C44	1.501(9)
N4	C24	1.355(8)	C42	C43	1.384(9)
N4	C28	1.349(8)	C45	C46	1.475(10)
N5	C33	1.370(8)	P1	F1	1.513(6)
N5	C37	1.356(8)	P1	F2	1.501(6)
N6	C39	1.349(8)	P1	F3	1.568(6)
N6	C43	1.357(8)	P1	F4	1.507(6)
C1	C2	1.380(8)	P1	F5	1.553(6)
C1	C9	1.493(8)	P1	F6	1.585(7)

Table 5-5 (cont'd).

C2	C3	1.380(9)	P2	F7	1.582(5)
C3	C4	1.372(9)	P2	F8	1.587(5)
C3	C6	1.493(9)	P2	F9	1.583(5)
C4	C5	1.379(9)	P2	F10	1.578(5)
C7A	C8A	1.57(10)	P2	F11	1.602(5)
C7B	C8B	1.49(7)	P2	F12	1.606(5)
C9	C10	1.511(8)	N7	C48	1.130(12)
C10	C11	1.383(9)	C47	C48	1.460(15)

Bond Angles (o)

N1	Fe1	N3	179.8(2)	N3	C20	C19	123.0(6)
N1	Fe1	N6	88.6(2)	O5	C21	C18	111.5(6)
N2	Fe1	N1	90.0(2)	O6	C21	O5	125.7(6)
N2	Fe1	N3	90.2(2)	O6	C21	C18	122.8(6)
N2	Fe1	N6	89.9(2)	O5	C22	C23	106.8(6)
N4	Fe1	N1	90.3(2)	N4	C24	C25	123.5(6)
N4	Fe1	N2	89.7(2)	N4	C24	C32	118.9(5)
N4	Fe1	N3	89.7(2)	C25	C24	C32	117.3(5)
N4	Fe1	N6	178.9(2)	C24	C25	C26	119.5(6)
N5	Fe1	N1	91.1(2)	C25	C26	C27	118.2(6)
N5	Fe1	N2	178.7(2)	C25	C26	C29	122.1(6)
N5	Fe1	N3	88.7(2)	C27	C26	C29	119.6(6)
N5	Fe1	N4	90.8(2)	C28	C27	C26	118.4(6)
N5	Fe1	N6	89.6(2)	N4	C28	C27	124.4(6)
N6	Fe1	N3	91.4(2)	O7	C29	C26	110.2(6)
C6	O1	C7A	114(3)	O8	C29	O7	126.4(6)
C6	O1	C7B	121(4)	O8	C29	C26	123.4(7)
C7B	O1	C7A	16(5)	O7	C30	C31	106.9(11)
C21	O5	C22	115.2(5)	C31A	C30A	O7	102(3)
C29	O7	C30	123.1(7)	O9	C32	C24	121.2(6)
C29	O7	C30A	98.3(11)	O9	C32	C33	119.0(6)
C30	O7	C30A	30.9(9)	C24	C32	C33	119.2(5)
C44	O11	C45	117.0(5)	N5	C33	C32	118.8(5)
C1	N1	Fe1	122.6(4)	C34	C33	N5	123.4(6)
C5	N1	Fe1	120.9(4)	C34	C33	C32	117.7(6)
C5	N1	C1	116.5(5)	C33	C34	C35	120.0(6)
C10	N2	Fe1	122.3(4)	C36	C35	C34	117.7(6)
C10	N2	C14	116.5(5)	C37	C36	C35	119.7(6)
C14	N2	Fe1	121.1(4)	N5	C37	C36	123.2(6)
C16	N3	Fe1	120.6(4)	N5	C37	C38	120.1(5)
C20	N3	Fe1	122.4(4)	C36	C37	C38	116.6(6)
C20	N3	C16	116.5(5)	O10	C38	C37	119.4(6)
C24	N4	Fe1	121.4(4)	O10	C38	C39	120.7(6)
C28	N4	Fe1	122.5(4)	C39	C38	C37	119.4(6)

Table 5-5 (cont'd).

C28	N4	C24	115.9(5)	N6	C39	C38	119.7(5)
C33	N5	Fe1	122.0(4)	N6	C39	C40	122.1(6)
C37	N5	Fe1	121.9(4)	C40	C39	C38	117.9(6)
C37	N5	C33	116.0(5)	C39	C40	C41	119.5(6)
C39	N6	Fe1	121.6(4)	C40	C41	C44	120.0(6)
C39	N6	C43	118.2(5)	C42	C41	C40	118.4(6)
C43	N6	Fe1	119.9(4)	C42	C41	C44	121.6(6)
N1	C1	C2	123.0(6)	C41	C42	C43	119.5(6)
N1	C1	C9	118.9(5)	N6	C43	C42	122.1(6)
C2	C1	C9	118.0(5)	O11	C44	C41	111.3(6)
C3	C2	C1	119.4(6)	O12	C44	O11	125.9(6)
C2	C3	C6	122.4(6)	O12	C44	C41	122.8(6)
C4	C3	C2	118.4(6)	O11	C45	C46	110.8(6)
C4	C3	C6	119.2(6)	F1	P1	F3	88.8(5)
C3	C4	C5	119.5(6)	F1	P1	F5	86.0(5)
N1	C5	C4	123.2(6)	F1	P1	F6	91.1(6)
O1	C6	C3	112.8(6)	F2	P1	F1	91.6(5)
O2	C6	O1	125.4(6)	F2	P1	F3	92.5(4)
O2	C6	C3	121.7(7)	F2	P1	F4	97.5(5)
O1	C7A	C8A	104(6)	F2	P1	F5	91.6(4)
O1	C7B	C8B	106(6)	F2	P1	F6	176.1(5)
O3	C9	C1	120.9(6)	F3	P1	F6	90.3(4)
O3	C9	C10	119.7(6)	F4	P1	F1	170.3(5)
C1	C9	C10	118.7(5)	F4	P1	F3	87.8(5)
N2	C10	C9	119.3(5)	F4	P1	F5	96.7(5)
N2	C10	C11	123.4(6)	F4	P1	F6	79.9(5)
C11	C10	C9	117.3(6)	F5	P1	F3	173.5(5)
C12	C11	C10	118.7(6)	F5	P1	F6	85.8(4)
C13	C12	C11	119.1(6)	F7	P2	F8	90.4(3)
C12	C13	C14	119.8(6)	F7	P2	F9	92.5(3)
N2	C14	C13	122.5(6)	F7	P2	F11	89.7(3)
N2	C14	C15	119.7(5)	F7	P2	F12	178.9(3)
C13	C14	C15	117.7(6)	F8	P2	F11	89.4(3)
O4	C15	C14	119.6(6)	F8	P2	F12	89.6(3)
O4	C15	C16	121.0(6)	F9	P2	F8	90.3(3)
C16	C15	C14	118.9(5)	F9	P2	F11	177.8(3)
N3	C16	C15	118.6(5)	F9	P2	F12	88.6(3)
N3	C16	C17	123.3(6)	F10	P2	F7	91.5(3)
C17	C16	C15	117.9(6)	F10	P2	F8	177.7(3)
C16	C17	C18	119.2(6)	F10	P2	F9	90.9(3)
C17	C18	C21	117.9(6)	F10	P2	F11	89.3(3)
C19	C18	C17	118.0(6)	F10	P2	F12	88.5(3)
C19	C18	C21	124.1(6)	F11	P2	F12	89.2(3)
C20	C19	C18	119.9(6)	N7	C48	C47	178.3(12)

REFERENCES

REFERENCES

(1) Desilvestro, J.; Graetzel, M.; Kavan, L.; Moser, J.; Augustynski, J. *Journal of the American Chemical Society* **1985**, *107*, 2988–2990.

(2) Ardo, S.; Meyer, G. J. *Chemical Society Reviews* **2009**, *38*, 115–64.

(3) Nazeeruddin, M. K.; Grätzel, M. *Struct. Bond.* **2007**, *123*, 113.

(4) McNamara, W. R.; Milot, R. L.; Song, H.; Snoeberger III, R. C.; Batista, V. S.; Schmuttenmaer, C. a.; Brudvig, G. W.; Crabtree, R. H. *Energy & Environmental Science* **2010**, *3*, 917.

(5) McNamara, W. R.; Snoeberger, R. C.; Li, G.; Schleicher, J. M.; Cady, C. W.; Poyatos, M.; Schmuttenmaer, C. a; Crabtree, R. H.; Brudvig, G. W.; Batista, V. S. *Journal of the American Chemical Society* **2008**, *130*, 14329–38.

(6) McNamara, W. R.; Snoeberger III, R. C.; Li, G.; Richter, C.; Allen, L. J.; Milot, R. L.; Schmuttenmaer, C. a.; Crabtree, R. H.; Brudvig, G. W.; Batista, V. S. *Energy & Environmental Science* **2009**, *2*, 1173.

(7) Xiao, D.; Martini, L. a; Snoeberger, R. C.; Crabtree, R. H.; Batista, V. S. *Journal of the American Chemical Society* **2011**, *133*, 9014–22.

(8) Abuabara, S. G.; Cady, C. W.; Baxter, J. B.; Schmuttenmaer, C. A.; Crabtree, R. H.; Brudvig, G. W.; Batista, V. S. *Journal of Physical Chemistry C* **2007**, *111*, 11982–11990.

(9) Altobello, S.; Bignozzi, C. .; Caramori, S.; Larramona, G.; Quici, S.; Marzanni, G.; Lakhmiri, R. *Journal of Photochemistry and Photobiology A: Chemistry* **2004**, *166*, 91–98.

(10) Zakeeruddin, S. M.; Nazeeruddin, M. K.; Pechy, P.; Rotzinger, F. P.; Humphry-Baker, R.; Kalyanasundaram, K.; Grätzel, M.; Shklover, V.; Haibach, T. *Inorganic Chemistry* **1997**, *36*, 5937–5946.

(11) Ambrosio, F.; Martsinovich, N.; Troisi, A. *The Journal of Physical Chemistry Letters* **2012**, *3*, 1531–1535.

(12) Pal, S. K.; Sundström, V.; Galoppini, E.; Persson, P. *Dalton Transactions (Cambridge, England : 2003)* **2009**, 10021–31.

(13) Thavasi, V.; Renugopalakrishnan, V.; Jose, R.; Ramakrishna, S. *Materials Science and Engineering: R: Reports* **2009**, *63*, 81–99.

(14) Wang, D.; Mendelsohn, R.; Galoppini, E.; Hoertz, P. G.; Carlisle, R. A.; Meyer, G. J. *The Journal of Physical Chemistry B* **2004**, *108*, 16642–16653.

(15) Perrin, D. D.; Armarego, W. L. F. *Purification of Laboratory Chemicals, 3rd ed.*; Pergamon Press: New York, 1988.

(16) Goldsmith, C. R.; Stack, T. D. P. *Inorganic Chemistry* **2006**, *45*, 6048–55.

(17) Garelli, N.; Vierling, P. *The Journal of Organic Chemistry* **1992**, *57*, 3046–3051.

(18) SPARTAN 5.0 ed.; Wavefunction Inc.: Irvine, CA, **1997**.

(19) Frisch, M. J.; Trucks, G. W.; Schlegel, H. B.; Scuseria, G. E.; Robb, M. A.; Cheeseman, J. R.; J. A. Montgomery, J.; Vreven, T.; Kudin, K. N.; Burant, J. C.; Millam, J. M.; Iyengar, S. S.; Tomasi, J.; Barone, V.; Mennucci, B.; Cossi, M.; Scalmani, G.; Rega, N.; Petersson, G. A.; Nakatsuji, H.; Hada, M.; Ehara, M.; Toyota, K.; Fukuda, R.; Hasegawa, J.; Ishida, M.; Nakajima, T.; Honda, Y.; Kitao, O.; Nakai, H.; Klene, M.; Li, X.; Knox, J. E.; Hratchian, H. P.; Cross, J. B.; Adamo, C.; Jaramillo, J.; Gomperts, R.; Stratmann, R. E.; Yazyev, O.; Austin, A. J.; Cammi, R.; Pomelli, C.; Ochterski, J. W.; Ayala, P. Y.; Morokuma, K.; Voth, G. A.; Salvador, P.; Dannenberg, J. J.; Zakrzewski, V. G.; Dapprich, S.; Daniels, A. D.; Strain, M. C.; Farkas, O.; Malick, D. K.; Rabuck, A. D.; Raghavachari, K.; Foresman, J. B.; Ortiz, J. V; Cui, Q.; Baboul, A. G.; Clifford, S.; Cioslowski, J.; Stefanov, B. B.; Liu, G.; Liashenko, A.; Piskorz, P.; Komaromi, I.; Martin, R. L.; Fox, D. J.; Keith, T.; Al-Laham, M. A.; Peng, C. Y.; Nanayakkara, A.; Challacombe, M.; Gill, P. M. W.; Chen, B. J. W.; Wong, M. W.; Gonzalez, C.; Pople, J. A. Gaussian 03, Revision D.01 **2004**.

(20) Schubert, U. S.; Eschbaumer, C.; Hochwimmer, G. *Synthesis* **1999**, 779–782.

(21) Sepehrifard, A.; Chen, S.; Stublla, A.; Potvin, P. G.; Morin, S. *Electrochimica Acta* **2013**, *87*, 236–244.

(22) Ferrere, S. *Inorganica Chimica Acta* **2002**, *329*, 79–92.

(23) He, J.; Lindström, H.; Hagfeldt, A.; Lindquist, S. *Solar Energy Materials and Solar Cells* **2000**, *62*, 265–273.

(24) Xia, H.-L.; Ardo, S.; Narducci Sarjeant, A. a; Huang, S.; Meyer, G. J. *Langmuir : The ACS Journal of Surfaces and Colloids* **2009**, *25*, 13641–52.

(25) Chavarot, M.; Socquet, S.; Kotera, M.; Lhomme, J. *Tetrahedron* **1997**, *53*, 13749–13756.

(26) Yu, X.; Yang, T.; Wang, S.; Xu, H.; Gong, H. *Organic Letters* **2011**, *13*, 2138–41.

(27) Mackay, L. G.; Anderson, H. L.; Sanders, J. K. M. *Journal of the Chemical Society, Perkin Transactions 1* **1995**, 2269.

(28) Olivier, J.-H.; Harrowfield, J.; Ziessel, R. *Chemical Communications (Cambridge, England)* **2011**, *47*, 11176–88.

(29) Giacomelli, G.; Porcheddu, A.; Salaris, M. *Organic Letters* **2003**, *5*, 2715–7.

Chapter 6. Concluding Comments and Future Directions

6.1 Concluding Comments

The overall goal of this research project is the development of low cost sensitizers for DSSCs by moving to first row transition metal-based chromophores, specifically iron(II) polypyridyl complexes. To be an effective sensitizer the MLCT state of a chromophore must be sufficiently long lived for injection into the semiconductor to occur. Unfortunately, iron(II) polypyridyl complexes intrinsically have short lived MLCT states due to ultrafast deactivation to lower lying ligand field states. The research has been developed to gain more understanding of the fundamental causes underlying the ultrafast processes.

Iron(II) polypyridyl complexes commonly possess a strained coordination environment through which orbital degeneracy is removed. The dense ligand field manifold that arises from the deviation from octahedral symmetry may be mediating the charge transfer to ligand field excited state deactivation. To investigate this theory, we set out to develop a highly symmetric iron(II) chromophore. The first efforts yielded a complex with a nearly perfect octahedral coordination environment that exhibits some exciting properties. Though the charge transfer state lifetime has not been extended, it may have introduced a strong enough ligand field to achieve inversion of the lowest energy excited state. The study was then redirected toward unraveling the sources of the seemingly unique characteristics. The development of a control molecule is crucial, but despite our best efforts, has yet to be attained and still ongoing.

An isostructural iron(II) analog was developed to investigate the impact of the carbonyl bridging groups within the ligands. The desired symmetry was achieved with a

vinylidene analog, but the characteristics were vastly different, therefore it appears that the properties are driven by inductive effects from the bridging groups. Since the inductive effects are seemingly enhanced by the symmetrical environment we propose to take advantage of that to further modulate the energetics of the excited states. We have just begun to investigate the possibilities and are setting out to systematically introduce substituents to the periphery of the ligands in an effort to induce stabilization of the charge transfer state and destabilization of the ligand field states. With the first analog, in which an extended π-system has been introduced, it appears that we are on the right track. If further functionalization has the desired effect, an iron(II) complex with a redox active ^{3}MLCT excited state as the lowest energy excited state could be realized, which would have major impact toward application in DSSCs. Though a viable sensitizer has yet to be developed, the first step has been taken toward implementing the new symmetric iron(II) chromophores in a DSSCs by installing carboxylate anchoring groups. Work is ongoing along this front and methods have been proposed to introduce alternative anchoring groups.

The synthetic efforts presented here provide a nice starting point to investigate fundamental aspects of iron(II) chromophores. Though the goal of this research is highly focused, it has presented the opportunity to sample from all areas of chemistry to develop the synthetic methods. There is much work left to be done, as was proposed throughout each chapter, but the molecules that have been realized have laid the foundation for further analysis.

6.2 Future Directions

The research presented in this dissertation evolved from the observation of the exciting properties of the symmetric iron(II) chromophore that was developed; however,

work has been ongoing from the original investigation of the role that torsional modes may play in the ultrafast dynamics. As mentioned in Chapter 1, and discussed in detail in my Masters Thesis, we set out to investigate the extent to which a torsional coordinate might modulate MLCT to ligand field kinetics by introducing steric bulk to the terminal rings of terpy and preparing the bis-tridentate iron(II) complexes.[1] The terpy series yielded a lot of information on the correlation between charge transfer deactivation and ground state recovery, but did not slow the charge transfer deactivation.[2] The next approach involves fixed ligand cage structures, introducing a rigid environment that would restrict motion along any torsional coordinate. We set out to prepare the two cryptand ligands that were developed by Lehn and coworkers, shown in Figure 6-1.[3,4]

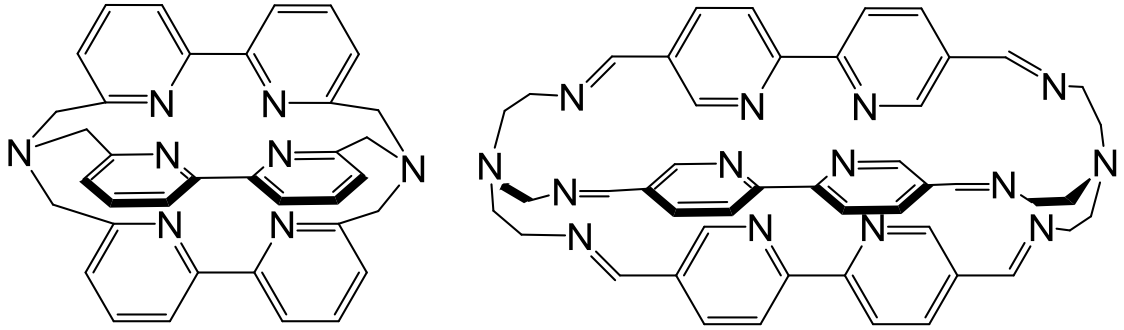

Figure 6-1. Cryptand ligand structures.

The structure of [bpy.bpy.bpy] that is linked through the 6-position of the bpy rings may make an ideal ligand to introduce the desired rigidity, but does raise a point of concern. It is well established that substitution at the ortho position of polypyridines leads to the stabilization of the high spin form when bound to iron(II).[5] The iron-nitrogen bond lengths in high spin iron(II) complexes are longer than in low spin complexes due to the population

of the antibonding orbitals. If the cage structure is able to bind to iron(II), it is our hope that the compound is rigid enough to force the low spin ground state upon binding. If this is the case, then the rigidity of the molecule may destabilize the high spin excited state, thereby interfering with the rate of relaxation from the charge transfer to the ligand field states. The ligand synthesis is quite time consuming, but progress has been made; however efforts were turned toward the analog that is linked through the 5-position as its prospects may be more exciting, and is much more synthetically accessible.

The Lehn cryptand is readily obtained through well established chemistry. The method involves a straightforward Schiff base condensation of two equivalents of tris(2-aminoethyl)amine (tren) and three equivalents of 5,5-diformyl-2,2'-bipyridine (dfbpy), which may be prepared through many known methods from 5,5'-dimethyl-2,2'-bipyridine (dmb).[6–8] While 4,4'-dfbpy may be simply prepared by direct oxidation from 4,4'-dmb with selenium dioxide, the 5-position is much less reactive and another route is necessary.[9] 5,5'-dmb may be oxidized to the carboxylic acid via Jones oxidation and converted to the ethyl ester through Fisher esterification.[10,11] The ester may be readily reduced to the hydroxymethyl derivative with sodium borohydride, which can then be converted to dfbpy through Swern oxidation.[6,12]

The tren capped 5-position bpy cage ligand was successfully prepared from the method described by Lehn.[4] The reaction was stirred at room temperature, in dry acetonitrile for four days and the reaction progress monitored by eye since the orange Schiff base product precipitates from the reaction as it forms. The ligand is simply filtered recrystallized from methanol. The imine functional groups appear to be unstable toward

hydrolysis during the subsequent reaction to prepare the iron(II) complex, which has been unsuccessful. All is not lost yet as there is an alternate plan for this structure.

The cryptand was originally designed for its complexation ability to bind to metals through the tren caps and bpy ligands and trinuclear-silver(I) and binuclear-copper(I) complexes are known.[4] The Cu(I) ions showed selectivity to the four coordinate tren position and left the bpy ligands free. As iron(II) has a high propensity for six coordination we should be able to achieve a mixed metal trinuclear complex with Fe(II) selectively coordinating to the bpys and Cu(I) coordinating to the imine groups. This could be quite interesting as it would contain an iron(II) chromophore in the center flanked by two Cu(I) species. We intend to explore this molecule for potentially interesting redox properties, as the presence of the Cu(I) centers could provide a remote site for electron transfer regeneration, specifically we are looking into the possibility of reductive quenching of the MLCT state of Fe(II) by Cu(I). This would be highly desirable for application in DSSCs as upon photoexcitation, a bpy radical is created by the MLCT from Fe(II) to bpy leaving Fe(III), if Cu(I) could effectively reduce Fe(III) prior to relaxation it could drive electron transfer into the semiconductor.

The tri-nuclear complex was readily obtained, as shown in Scheme 6-1, through a simple one pot procedure of dissolving the ligand in dichloromethane and adding acetonitrile solutions of Fe(II) and Cu(I) salts and excess NH_4PF_6. The complexation occurred quickly, as it turned blue from the addition of Fe(II) and turned red as Cu(I) was added and it began to precipitate immediately upon the addition of NH_4PF_6, yielding a dark purple/maroon solid. It is interesting to note that the coordination is highly selective as the reaction was carried out in an inert atmosphere dry box creating much difficulty in

weighing out the desired quantities to ensure one equivalent of Fe(II) and two equivalents of Cu(I). Due to the small scale it was nearly impossible to obtain the desired amounts and excess Fe(II) and Cu(I) were added, however this did not appear to affect the outcome of the reaction.

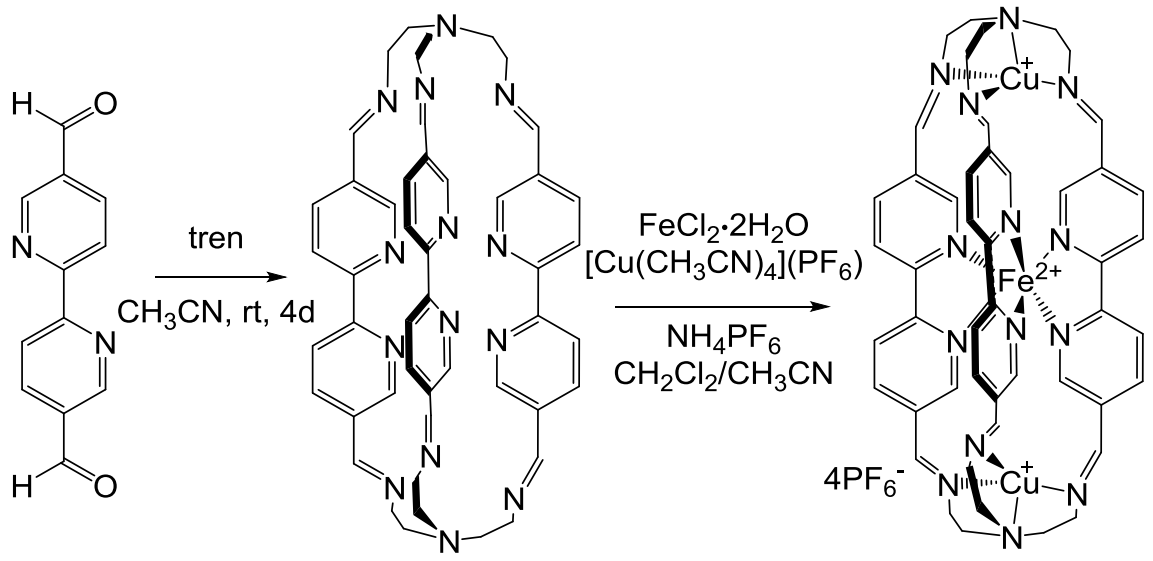

Scheme 6-1. Preparation of the iron(II) dicopper(I) Lehn cryptand trinuclear complex $[Cu_2Fe(5\text{-Lehn-cryptand})]^{4+}$.

The characterization of this complex is just beginning and the reaction conditions yet to be optimized, as it was only prepared once as a test reaction. It is present by ESI-MS, however the purity is difficult to ascertain at this point. Luckily, crystals suitable for X-ray crystallography were grown by ether diffusion into an acetonitrile solution of the compound, and the structure is in the process of being solved. Disorder from solvent molecules has complicated the process, however it is clear that selective coordination of the Fe(II) and Cu(I) in the desired positions has been achieved, as shown in Figure 6-2. Another critical piece of evidence ascertained from the crystal structure is that a low spin

iron(II) center has been achieved, which is evident in the Fe—N bond lengths, listed in Table 6-1.

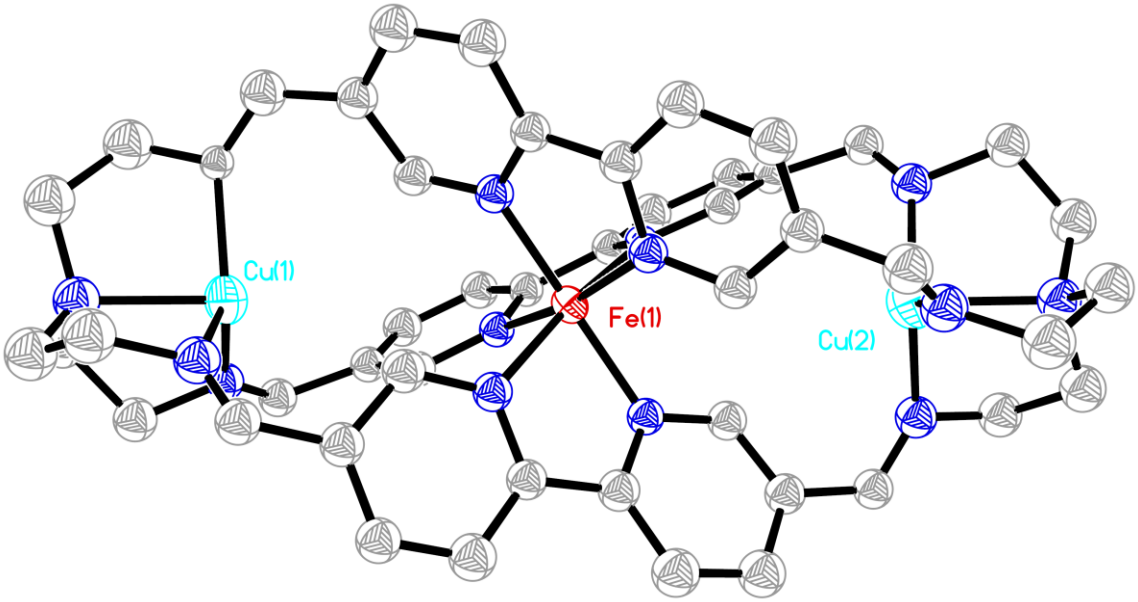

Figure 6-2. ORTEP Drawing of the cation of $[Cu_2Fe(5\text{-Lehn-cryptand})]^{4+}$ obtained from single-crystal x-ray structure determination (in progress). Hydrogen atoms and anions are omitted for clarity.

Table 6-1. Selected bond lengths from the x-ray crystal structure of the tri-nuclear cryptand $[Cu_2Fe(5\text{-Lehn-cryptand})]^{4+}$.

Selected Bond Lengths (Å)	
Fe1—N1	1.975(7)
Fe1—N2	1.978(7)
Fe1—N3	1.977(7)
Fe1—N4	1.974(6)
Fe1—N12	1.986(7)
Fe1—N13	1.980(7)

Whether this cryptand can be employed as a redox relay type system will depend on numerous factors which will be assessed in due course, with electrochemical and spectroelectrochemical measurements, fluorescence upconversion measurements, time-

resolved spectroscopy, etc. Analysis of the electrochemistry of the intricate tri-nuclear cryptand has just begun, however it is proving to be highly complicated and without further characterization we cannot draw any conclusions just yet. In mononuclear iron(II) polypyridyl complexes the electrochemistry is fairly straightforward in that there is one oxidation that may be attributed to the oxidation of metal center, and multiple reductions that are attributed to the ligand. In multinuclear systems with similar cryptand ligands the electrochemistry is much more complicated, and a few details about the known systems will be outlined here in order to guide future efforts with this complex system.[13–15]

From the standard redox potentials of iron and copper, where Fe(III) + e- → Fe(II) is 0.77 V and Cu(II) + e- →Cu(I) is 0.159 V vs. SHE, it is apparent that copper is more easily oxidized than iron.[16] However, the ligand environment and presence of other metal centers will influence the redox chemistry. A comparison of a known di-copper cryptand with analogous hetero-nuclear Cu(I) M(II) cryptands (M(II) = Fe(II), Ni(II), Co(II) Mn(II)) has provided evidence of an electrostatic influence on the oxidation potential of Cu(I).[15] There is a correlation of the oxidation potential of Cu(I) with proximity to a divalent cation, becoming harder to oxidize the closer it is to the divalent cation. The influence of the Cu(I) center on the oxidation potential of the other metal is unclear as the researchers were unable to distinguish the metal oxidation from a feature attributed to the oxidation of the ligand. This raises concern with this system since the cryptand ligand is similar, and the possibility of ligand oxidation will complicate the identification of features in the electrochemistry.

A second complication can arise from the relative ease of reduction of Cu(I) and Cu(II), as it has been noted in various sources that sweeping negative can result in stripping/deposition of copper on the electrode anywhere past around -0.9 to -1.1 V vs.

ferrocene (Fc).[13,15] Evidence of the copper deposition can be observed with the appearance of a wave at -0.49 V and the oxidation of the copper can then result in the presence of $[Cu(CH_3CN)_4]^+$ giving rise to an oxidation feature at +0.55 V vs. Fc, therefore a small scan window must be utilized to prevent degradation of the complex.[14] As it stands we cannot gain any conclusive information from the electrochemistry that was taken as the scan window was too large; the electrochemical data must be recollected and a bulk electrolysis experiment should also be done.

The development of analogs of the cryptand system may provide useful information to unravel the complicated electrochemistry. To date, the attempted isolation of the cryptand with iron(II) alone has failed, however the di-copper(I) analog of this cryptand could be useful. It is quite possible that instead of clarifying it could complicate the picture even further as the environment would be vastly different; nevertheless it should provide evidence involving the electrostatic influence of neighboring metal centers. Overall, this is the first system of this type that we have set out to investigate and it appears to be quite complex, and without further characterization it is unclear where this may lead. Keeping in line with the running theme of this entire research project, we set out on the path toward the investigation of ultrafast dynamics of iron(II)-polypyridyls and it appears to be ever evolving in a new direction.

In closing, there are so many avenues that one may take from here, from all the syntheses proposed throughout this dissertation to this new path presented here. As outlined in the introduction, there are two approaches we could take toward developing a viable iron(II) sensitizer: 1) speed up the electron injection process, or 2) slow down the relaxation process. This research has been developed to tackle the second approach and

has diverged along two distinct paths, in which there is much left to be done along both fronts. The investigation of torsional modes that was introduced in my Masters Thesis can be pursued further with the development of rigid 6-position Lehn cryptand structure shown in Figure 6-1. The syntheses proposed throughout chapters 2-4 can be carried out to further investigate means to tune the electronic structure of iron(II) polypyridyl chromophores through enhanced symmetry and inductive effects. The approach of speeding up the electron transfer process has yet to be targeted, however the installation of alternative anchoring groups that was proposed in Chapter 5 may be taken on as a first step. Finally, the investigation into the trinuclear cryptand system presented here is just getting underway and may present a nice starting point to a whole new area of research. Overall, the prospects are wide open.

APPENDIX

APPENDIX

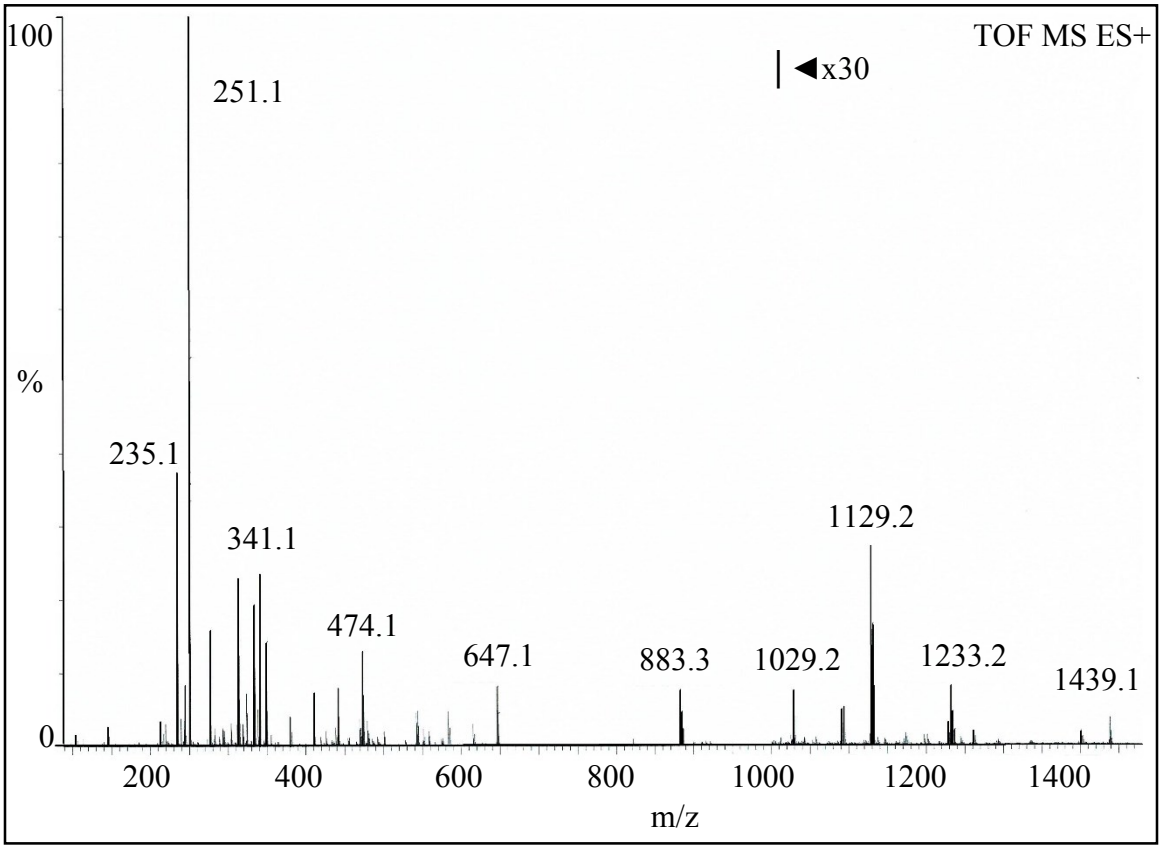

Figure 6-3. ESI-MS of $[Cu_2Fe(5\text{-Lehn-cryptand})]^{4+}$. $[C_{48}H_{48}Cu_2F_{24}FeN_{14}P_4]^{4+}$ m/z = 251.1; $[C_{48}H_{48}Cu_2F_{24}FeN_{14}P_4](PF_6)_2\}^{2+}$ m/z = 647.1; $[C_{48}H_{48}Cu_2F_{24}FeN_{14}P_4](PF_6)_3\}^{+}$ m/z = 1439.1.

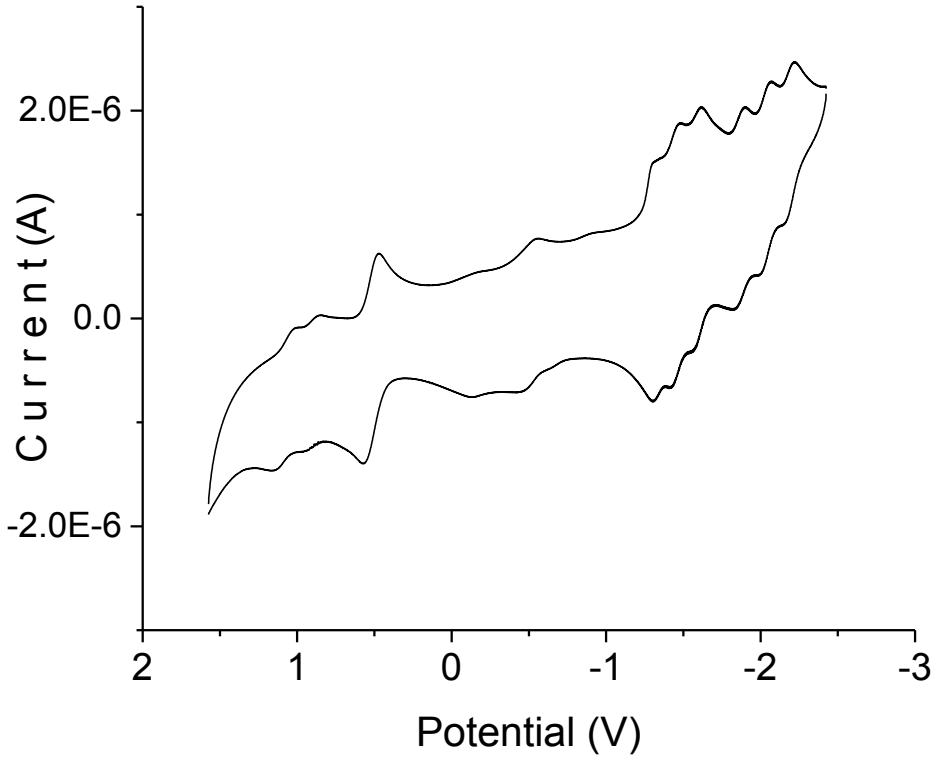

Figure 6-4. Cyclic voltammogram of $[Cu_2Fe(5\text{-Lehn-cryptand})]^{4+}$ measured with a Ag/AgCl reference with 0.1 M $TBAPF_6$ electrolyte in acetonitrile (50 mV/s), referenced to ferrocene. The presence of the feature at -0.49 V is attributed to stripping/deposition of copper, therefore the complex degrades under the present conditions and must be recollected.

REFERENCES

REFERENCES

(1) Jamula, L. L. Masters Thesis, Michigan State University, 2010.

(2) Brown, A. M. PhD Dissertation, Michigan State University, 2011.

(3) Rodriguez-Ubis, J.-C.; Alpha, B.; Plancherel, D.; Lehn, J.-M. *Helv. Chim. Acta* **1984**, *67*, 2264.

(4) De Mendoza, J.; Mesa, E.; Rodríguez-Ubis, J.-C.; Vázquez, P.; Vögtle, F.; Windscheif, P.-M.; Rissanen, K.; Lehn, J.-M.; Lilienbaum, D.; Ziessel, R. *Angewandte Chemie International Edition in English* **1991**, *30*, 1331–1333.

(5) Halcrow, M. a. *Polyhedron* **2007**, *26*, 3523–3576.

(6) El-ghayoury, A.; Ziessel, R. *The Journal of Organic Chemistry* **2000**, *65*, 7757–7763.

(7) Narayan, K. S.; Geetha, K. V.; Nakmanovich, G.; Ehrenfreund, E.; Eichen, Y. *The Journal of Physical Chemistry B* **2001**, *105*, 7671–7677.

(8) Hodacová, J.; Budesínský, M. *Organic Letters* **2007**, *9*, 5641–3.

(9) Sasaki, I.; Daran, J. C.; Balavoine, G. G. A. *Synthesis* **1999**, 815–820.

(10) Szeto, K. C.; Kongshaug, K. O.; Jakobsen, S.; Tilset, M.; Lillerud, K. P. *Dalton Transactions* **2008**, 2054–60.

(11) Yu, S. C.; Hou, S.; Chan, W. K. *Macromolecules* **2000**, *33*, 3259–3273.

(12) Telfer, S. G.; Bernardinelli, G.; Williams, A. F. *Dalton Transactions* **2003**, 435–440.

(13) Brooker, S.; Ewing, J. D.; Ronson, T. K.; Harding, C. J.; Nelson, J.; Speed, D. J. *Inorganic Chemistry* **2003**, *42*, 2764–73.

(14) Coyle, J.; Downard, A. J.; Nelson, J.; McKee, V.; Harding, C. J.; Herbst-Irmer, R. *Dalton Transactions* **2004**, 2357–63.

(15) Ronson, T. K.; Nelson, J.; Jameson, G. B.; Jeffery, J. C.; Brooker, S. *European Journal of Inorganic Chemistry* **2004**, 2570–2584.

(16) Douglas, B.; McDaniel, D.; Alexander, J. *Concepts and Models of Inorganic Chemistry*; Third Edit.; John Wiley & Sons, Inc.: New York, 1994.